Transorbital Skull Base Surgery;

Exploratory Quantitative Assessment of the Microscopic and Endoscopic Surgical Corridor

by

Lena Mary Houlihan

A Dissertation Presented in Partial Fulfillment
of the Requirements for the Degree
Doctor of Philosophy

Approved September 2021 by the
Graduate Supervisory Committee:

Mark C. Preul, Co-Chair
Brent Vernon, Co-Chair
Michael T Lawton
Griffin Santarelli
Michael O' Sullivan
Brian Smith

ARIZONA STATE UNIVERSITY

December 2021

ABSTRACT

Transorbital surgery has gained recent notoriety due to its incorporation into endoscopic skull base surgery. The body of published literature on the field is cadaveric and observation. The pre-clinical studies are focused on the use of the endoscope only. Furthermore the methodology utilised in the published literature is inconsistent and does not embody the optimal principles of scientific experimentation. This body of work evaluates a minimally invasive novel surgical corridor - the transorbital approach - its validity in neurosurgical practice, as well as both qualitatively and quantitatively assessing available technological advances in a robust experimental fashion. While the endoscope is an established means of visualisation used in clinical transorbital surgery, the microscope has never been assessed with respect to the transorbital approach. This question is investigated here and the anatomical and surgical benefits and limitations of microscopic visualisation demonstrated. The comparative studies provide increased knowledge on specifics pertinent to neurosurgeons and other skull base specialists when planning pre-operatively, such as pathology location, involved anatomical structures, instrument maneuvrability and the advantages and disadvantages of the distinct visualisation technologies. This is all with the intention of selecting the most suitable surgical approach and technology, specific to the patient, pathology and anatomy, so as to perform the best surgical procedure. The research findings illustrated in this body of work are diverse, reproducible and applicable. The transorbital surgical corridor has substantive potential for access to the anterior cranial fossa and specific surgical target structures. The neuroquantitative metrics investigated confirm the utility and benefits

specific to the respective visualisation technologies i.e. the endoscope and microscope. The most appropriate setting wherein the approach should be used is also discussed. The transorbital corridor has impressive potential, can utilise all available technological advances, promotes multi-disciplinary co-operation and learning amongst clinicians and ultimately, is a means of improving operative patient care.

DEDICATION

To my parents, Michael and Eileen Houlihan; without whom I would not be here. They have been my lifelong support and unconditional love. I owe my whole life to them and thank God every day that I am their daughter.

To my husband David; without whom there would be significantly less chapters in this body of work. His engineering knowledge and insight has substantially enhanced this translation research and its clinical applicability, as well as the robustness of the scientific method. I try every day to be as outstanding as him and am a better person because of him.

Finally to Professor O' Sullivan, Dr. Preul and Dr. Lawton; without whom there would be no PhD, no phenomenal opportunities, no accomplishments. Thank you all for putting your trust in me, making me a better doctor and a better person. I hope I have made you all proud and will continue to do so. Thank you all for my achievements.

ACKNOWLEDGMENTS

Such work is not completed alone. It absolutely takes a village. I would like to acknowledge the contributions of so many people on different levels for the mentorship, teaching, assistance and support throughout this endeavour.

I would like to thank my committee. Dr. Preul, Dr. Lawton, and Professor O'Sullivan gave me this fantastic opportunity and have continued to invest in my professional progression, which I am so appreciative of. You all are my inspiration to continuously improve and be the best person I can be for the betterment of the care we provide to our patients. Thank you all.

I would like to thank Dr. Santarelli for inspiring me with this captivating area of evolving skull base research. It was because of his excellent presentation at Barrow Neurological Institute Grand Rounds that I became interested in transorbital surgery and am very happy that my degree is rooted in surgically applicable translational research.

I greatly appreciate the expertise and input of Dr. Vernon, who co-chaired my committee and helped validate and advance the translational bioengineering aspects of the projects.

I would like to thank Dr. Smith for supervising all facets of the project who ensured the data and results produced were of the highest robust level of scientific standards. I hold Dr. Smith's opinion in high esteem and value his investment in my studies. Thank you for driving me to produce the best research possible.

Thank you also to Dr. Sattler co-director of the ASU-BNI IGPN for bringing me into the Neuroscience programme. The ASU and BNI faculty are outstanding. I am a better clinician, researcher and academic because of this world class course.

I am indebted to those who facilitated my studies and provided me with such incredible resources. I would like to thank all the staff of the Loyal and Edith Davis Neurosurgical Research Laboratory, especially William Bichard, and the Barrow Neurological Institute Neuroscience Publications for showing me the highest quality of academic writing. I also want to thank Melissa Kovacs for her statistical tuition and guidance. Thank you for teaching me and improving the quality of my analysis. I am so appreciative of Barrow Neurological Foundation for their financial support, as well as that provided by Dr. Preul, the Newsome Family Endowed Chair of Neurosurgery Research, Director of Neurosurgery Research.

Without the assistance of so many colleagues and new friends, none of this would be possible. I wish to extend a huge thank you to Mohammed Labib, Thanapong Loymak, David Naughton, Irakliy Abramov, Jubran Jubran, Ann Staudinger Knoll, Dara Farhadi, Xiaochun Zhao, Evgenii Belykh, Jacob T. Howshar, Chelsea Tran and Ryan Pevey. I have worked as a project leader and team player with each of these phenomenal people who I feel very blessed to have met. Thank you for your teaching, support, assistance and your comradery.

DISCLOSURES

The author has no personal, financial, or institutional interest in any of the drugs, materials, or devices described in this body of work.

FINANCIAL SUPPORT

This study was supported by funds from the Newsome Chair of Neurosurgery Research held by Dr. Mark Preul and from the Barrow Neurological Foundation award grant (4550003033296).

TABLE OF CONTENTS

Page

LIST OF TABLES x

LIST OF FIGURES xi

ABBREVIATIONS xvi

CHAPTER

1 INTRODUCTION 1

2 FROM KRÖNLEIN, THROUGH MADNESS, TO A USEFUL MODERN SURGERY: THE JOURNEY OF THE TRANSORBITAL CORRIDOR TO ENTER THE NEUROSURGICAL 9

3 TRANSORBITAL NEUROENDOSCOPIC SURGERY AS A MAINSTREAM NEUROSURGICAL CORRIDOR: A SYSTEMATIC REVIEW 32

4 TRANSORBITAL MICROSURGERY: A MINIMALLY INVASIVE CORRIDOR TO THE ANTERIOR CRANIAL FOSSA AND PARAMEDIAN STRUCTURES 73

5 VOLUME OF SURGICAL FREEDOM: THE MOST APPLICABLE ANATOMICAL MEASUREMENT FOR SURGICAL ASSESSMENT AND 3-DIMENSIONAL MODELING 106

CHAPTER Page

6 OPTIMAL ANTERO-LATERAL ACCESS CORRIDORS TO THE ANTERIOR SKULL BASE AND PARAMEDIAN VASCULATURE: QUANTITATIVE ANALYSIS OF UNILATERAL SUPRAORBITAL, TRANSORBITAL MICROSCOPIC AND TRANSORBITAL ENDOSCOPIC APPROACHES 166

7 EXPLORATORY ANALYSIS OF THE BIPORTAL TRANSORBITAL APPROACH; QUANTITATIVE COMPARISON OF ANTERIOR SUBFRONTAL CRANIOTOMY VERSUS BILATERAL TRANSORBITAL ENDOSCOPIC AND MICROSCOPIC APPROACHES TO THE ANTERIOR CRANIAL FOSSA AND PARAMEDIAN VASCULATURE 198

8 DISCUSSION 229

REFERENCES 245

APPENDIX

A LIST OF PUBLICATIONS 259

B CHAPTER 3 SEARCH PROTOCOL 262

C CHAPTER 3 DATABASE SEARCH STRATEGY……..……..……... 279

D CHAPTER 6 DETAILED STATISTICAL ANALYSIS……... 281

E CHAPTER 7 DETAILED STATISTICAL ANALYSIS……... 296

LIST OF TABLES

Table Page

3.1 Characteristics of 23 Studies Involving Transorbital Neuroendoscopic Surgery …...44

3.2 Demographic and Clinical Data Reported in Selected Studies Involving Transorbital Neuroendoscopic Surgery, by Type of Pathology Treated ……...51

3.3 Complications Reported in Selected Studies Involving Transorbital Neuroendoscopic Surgery ……..57

5.1 Comparative Volumetric Results of the VSF for Measuring Instrument Maneuverability Specific to the Surgical Target Structure and Approach……. 141

6.1 Analysis of Variance of Accessible Length of Intracranial Structures Specific to the Surgical Approach ……..180

7.1 Analysis of Variance of Accessible Length of Intracranial Structures Specific to the Surgical Approach ……..212

LIST OF FIGURES

Figure Page

2.1 Rudolf Krönlein ……. 14

2.2 Walter Dandy ……..... 19

3.1 Flow Chart Showing the Selection Process for Studies Included in This Systematic Review ……..40

3.2 Number of Articles Detailing the Transorbital Approach Published per Year, January 1, 2010, Through September 5, 2020 …….....49

3.3 Flowchart of Tones Complications with Respect to a, Conservative and B, Surgical Treatment ……..59

3.4 Graphic Representation of the Transient Postoperative Neurological Sequelae in Relation to the Selected Operative Incision …….....61

3.5 Graphic Representation of Postoperative Diplopia, V2 Numbness, and Ptosis with Respect to the Approach Used ……..62

3.6 Bar Chart Comparing the Number of Patients With Preoperative Deficits and Postoperative Deficits …….....63

4.1 Illustration Depicts the Positioning of the Patient, Microscope, and Surgeon for Access to Particular Anatomical Structures from a Right-sided Superior Lid Crease Approach …….. 80

4.2 Incision Marking and Superficial Dissection ……..82

Figure Page

4.3 Cutaneous Dissection, Identification of the Lateral Boundaries, and Subperiosteal Dissection Toward the Superior Orbital Fissure ……...84

4.4 Microscopic View of the Medial Subperiosteal Dissection That Permits Full Mobilization of the Globe …….86

4.5 Boundaries of the Transorbital Microsurgery Craniectomy ……...88

4.6 Microscopic Extradural and Intradural Views of the Floor of the Anterior Cranial Fossa upon Completion of the Craniectomy Performed Using Transorbital Microsurgery ……... 90

4.7 Microscopic View of the Neurovascular Structures Visible and Accessible Through the Transorbital Microsurgery Craniectomy …… 96

5.1 Illustration of the Neuronavigation System in the Surgical Setup Commonly Used to Localize Both Pathologic and Anatomically Pertinent Structures Using Stereotaxis …114

5.2 Examples of a Pterional and Supraorbital Transcranial Approach ……..119

5.3 Axial View Illustration of the Skull Base Showing the Primary Vasculature Supplying the Brain ……... 122

5.4 Illustrative Depiction of the Data Collection Process ……..…….124

5.5 3d Modeling of the Steps of the Volume of Surgical Freedom Methodology ….....129

5.6 Illustration Depicting 3d Modeling of the Surgical Corridor to the Paraclinoid Internal Carotid Artery from a Pterional and Supraorbital Approach ……....143

5.7 Illustration Depicting 3d Modeling of the Surgical Corridor to the Terminal Internal Carotid Artery from a Pterional Approach and Supraorbital Approach ……144

Figure Page

5.8 Illustration Depicting 3d Modeling of the Surgical Corridor to the Anterior Communicating Artery from a Pterional Approach and Supraorbital Approach ...…...145

5.9 Plot of the Average Probe Length of Each Set of Measurement Data …….....147

5.10 Illustration Depicting a Limitation of Using Heron's Formula to Calculate the Area of an Irregular Closed Shape …….. 153

5.11 Surgical Maneuverability of an Instrument Using a Transcranial Pterional Approach Compared with a Transnasal Transplanum-cavernous Approach to the Paraclinoid Internal Carotid Artery ……... 161

6.1 Percentage of Surgical Target Structures That Were Inaccessible with the Supraorbital, Transorbital Microscopic, and Transorbital Endoscopic Approaches 178

6.2 Percentage of Surgical Target Structures in Which Assessment of Angle of Attack and Volume of Surgical Freedom Was Not Possible Due to Impaired Instrument Maneuverability ……. 179

6.3 Quantitative Comparison of the Mediolateral and Craniocaudal Angles of Attack with Use of the Supraorbital, Transorbital Microscopic, and Transorbital Neuroendoscopic Surgery Approaches ……..……. 182

6.4 Quantitative Comparison of the Volume of Surgical Freedom with the Supraorbital, Transorbital Microscopic, and Transorbital Neuroendoscopic Surgery Approaches ….185

6.5 Illustration Depicting 3-dimensional Modelling of the Surgical Corridor to the Terminal Internal Carotid Artery from Supraorbital, Transorbital Microscopic, and Transorbital Neuroendoscopic Surgery Approaches ……. 190

Figure Page

6.6. Illustration Depicting 3-dimensional Modelling of the Surgical Corridor to the Paraclinoid Internal Carotid Artery from a Supraorbital, Transorbital Microscopic, and Transorbital Neuroendoscopic Surgery Approach ……..…... 193

6.7. Illustration Depicting 3-dimensional Modelling of the Surgical Corridor to the Anterior Communicating Artery from a Supraorbital, Transorbital Microscopic, and Transorbital Neuroendoscopic Surgery Approach ……. 194

7.1 Percentage of Surgical Target Structures in 10 Cadaveric Heads That Were Inaccessible with the Anterior Subfrontal, Bilateral Transorbital Microscopic, and Bilateral Transorbital Endoscopic Approaches ……. 210

7.2. Percentage of Surgical Target Structures in 10 Cadaveric Heads with the Anterior Subfrontal, Bilateral Transorbital Microscopic, and Bilateral Transorbital Endoscopic Approaches in Which Assessment of Angle of Attack and Volume of Surgical Freedom Was Not Possible Due to Impaired Instrument Maneuverability …….. 211

7.3. Quantitative Comparison of the Mediolateral and Craniocaudal Angles of Attack with Use of the Anterior Subfrontal, Bilateral Transorbital Microscopic, and Figure Page Bilateral Transorbital Neuroendoscopic Surgery Approaches, Respectively ……..... 214

7.4 Quantitative Comparison of the Volume of Surgical Freedom with Use of the Anterior Subfrontal, Bilateral Transorbital Microscopic, and Bilateral Transorbital Neuroendoscopic Surgery Approaches, Respectively ……... 217

Figure Page

7.5 Illustration Depicting 3-dimensional Modelling of the Surgical Corridor to the Right Paraclinoid Internal Carotid Artery from an Anterior Subfrontal, Bilateral Transorbital Microscopic, and Bilateral Transorbital Neuroendoscopic Surgery Approach …… 219

7.6 Illustration Depicting 3-dimensional Modelling of the Surgical Corridor to the Right Terminal Internal Carotid Artery from an Anterior Subfrontal, Bilateral Transorbital Microscopic, and Bilateral Transorbital Neuroendoscopic Surgery Approach …… 220

7.7 Illustration Depicting 3-dimensional Modelling of the Surgical Corridor to the Anterior Communicating Artery from an Anterior Subfrontal, Bilateral Transorbital Microscopic, and Bilateral Transorbital Neuroendoscopic Surgery Approach …… 221

ABBREVIATIONS

- ACF: anterior cranial fossa
- ACoA: anterior communicating artery
- AOA: angle of attack
- AOE: area of exposure
- A.Sub: anterior subfrontal craniotomy
- BTM: bilateral transorbital microsurgery
- BTE: bilateral transorbital neuroendoscopic surgery
- CN: cranial nerve
- CT: computed tomography
- CSF: cerebrospinal fluid
- SD: standard deviation
- EOM: extraocular movement
- ICA: internal carotid artery
- IQR: interquartile range
- LOS: length of stay
- MCA: middle cerebral artery
- MCF: middle cranial fossa
- NV: normalised volume
- PRISMA: preferred reporting items for systematic reviews and meta-analyses
- SLC: superior lid crease

- SOC: supraorbital craniotomy
- STS: surgical target structure
- TMS: transorbital microsurgery
- TONES: transorbital neuroendoscopic surgery
- VSF: volume of surgical freedom
- 2D: 2-dimensional
- 3D: 3-dimensional

CHAPTER 1

INTRODUCTION

Significance

Transorbital surgery has gained recent notoriety due to its incorporation into endoscopic skull base surgery. However use of this surgical corridor has pervaded throughout the 20th century, utilised by multiple disciplines for both clinical and experimental purposes to great success, although its historical origin is both medico-ethically controversial and chequered. From Knapp's original introduction of the experimental orbital surgical technique in 1874 and Kronlein's procedure in 1889, to Freeman's controversial legacy, the evolution of modern technology and microsurgery has resulted in the incorporation of orbital surgery into the neurosurgeon's armamentarium. This has been a necessary entity of skull base surgical progression.

Intracranial endoscopy revolutionised the skull base field by improving illumination, magnification and visualisation, as well as its ability to enter previously obscure microscopic surgical corridors (Balakrishnan & Moe, 2011; Fries & Perneczky, 1998; Perneczky & Fries, 1998). Despite the substantial progress established by endoscopic skull base surgery it was not without its obstacles. Transnasal endoscopy for intracranial access to the anterior and middle cranial fossae was restricted by the orbital roof curvature and neurovascular structures surrounding the supraorbital fissure and optic canal. This limited the endonasal approach's generalisability for skull base lesions which extended laterally, or encompassed broader intracranial parameters. Endonasal anatomy and geometrical relations to the skull base limited working angles and visualization of

certain intracranial structures, particularly for lesions that crossed neurovascular bundles or were situated in far-lateral areas (Stippler et al., 2009).

The reignition of interest in the transorbital surgical corridor came to the fore within the last 10 years due to the invention of transorbital neuroendoscopic surgery (TONES). This approach allows for substantial access for visualisation, assessment and management of multiple intracranial, intraparenchymal and complex skull base/facial lesions, which under previous circumstances, would have warranted large, morbid, disfiguring operative interventions. It provides the surgeon with profound minimally invasive broad access to deep structures of the anterior and middle cranial fossa opening this technique's utility to trauma, vascular, functional and oncological subspecialties.

The idea of endoscopic orbital access aimed to achieve equal visibility, surpass the anatomical limitations of the endonasal approach and in turn, decrease the overall invasiveness and complications associated with open skull base surgery (Choi, Jang, & Abi Hachem, 2018; Dallan, Castelnuovo, et al., 2015; K. S. Moe, Bergeron, & Ellenbogen, 2010). It is for this reason that the structure which originally hindered neuroendoscopy evolved to become, to date, the most minimally invasive access corridor at the neurosurgeon's disposal (Abdel Aziz et al., 2011; Andaluz et al., 2008).

The concept of TONES was first introduced by Kris Moe at the Pacific Coast Otolaryngology-Ophthalmology Society Annual Meeting in June 2007 (K. Moe, 2007) and then in print, 'Transorbital Neuroendoscopic Surgery' in 2010 (K. S. Moe et al., 2010). This paper detailed 20 TONES procedures for anterior skull base pathology, including CSF leaks, optic nerve decompression, repair of skull base fractures, and

removal of 3 skull base tumours. This research group proposed TONES as a new skull base operative corridor with incorporation of improved instrumentation for visualisation and refined surgical technique via keyhole endoscopy. It aimed to provide a coplanar endoscopic surgical pathway that coursed through the orbit, traversing a craniotomy created through one of the four orbital walls aiming to provide optimal visualisation and magnification (K. S. Moe et al., 2011). Transorbital surgery was divided into four approaches to facilitate specific accessible compartments;

1. Precaruncular
2. Superior eyelid crease
3. Lateral retrocanthal
4. Preseptal lower eyelid (for access to the infratemporal fossa and pterygopalatine fossa)

Use of such an approach introduced the idea of the sino-orbito-cranial interface, an anatomical area of interest and surgical complexity. The modern remodelling of this surgical corridor has opened a new realm of innovation and experimentation in skull base surgery.

Historical analysis of present aspirational goals in modern skull base surgery echoes principles established through an approach first described almost 150 years ago; minimally invasive, minimal morbidity, with priority of patient satisfaction. This approach has opened new possibilities for maximally beneficial, minimally invasive skull base surgery, but further systematic analysis of the technique's merits and risks warrants examination. Given the substantial technological and robotic advances, it is necessary to

investigate the optimal means to augment this corridor's surgical success and provide an evidence-based assessment of neurosurgical targets best tackled by this approach.

Aim of work

This body of work aimed to establish key surgical determinants as to transorbital corridor's surgical abilities and establish the technology of best use within this access corridor.

Gaps in the Literature

TONES has proved to be a significant development in transorbital skull base surgery. However there still remains a paucity of data and clinical studies likely due to the juvenile nature of this modern approach. Apart from in expert centres, comprehensive robust comparative analysis and increasing use and generalisability of this technique in skull base surgery is still awaited. The dialogue on technical and operative superiority is premature, because the body of evidence on the efficacy of this approach is yet to be established. Budding attempts have been made at comparative analysis, an example of which is TONES versus endoscopic extended mini-pterional craniotomy which has been published showing comparable results. (Noiphithak et al., 2019). The ability and insight necessary to evaluate this operative approach amongst the international neurosurgical community is still developing.

The orbit gives us access to the frontal and middle cranial fossae, a pathway not limited by the carotid vessels and cranial nerves as the transnasal approach is laterally. This approach has evolved due to the concurrent advances of many surgical specialities; otorhinolaryngology, ophthalmoplastics and maxillofacial. Transorbital intracranial

access was not first conceived by neurosurgeons, but with the advance of microsurgical and endoscopic technique this keyhole port to the skull base is a novel and appealing corridor which neurosurgeons are keen to explore. It encompasses the modern requirements of a proficient surgical technique; minimising morbidity, minimally invasive, aesthetically satisfactory and decreasing hospital length of stay (Castelnuovo et al., 2013; Dallan, Castelnuovo, et al., 2015).

The published clinical data on TONES predominantly describes extra parenchymal procedures. Attempts have been made to increase the body of literature on parenchymal and cerebrovascular TONES feasibility. In 2017 Almeda et al completed cadaveric studies assessing whether the transorbital approach was a reasonable pathway to the anterior circulation (Almeida et al., 2017). They felt the exposure via the eyelid incision with drilling of the posterior wall of the orbit and lesser sphenoidal wing, allowed for successful exposure of the sphenoidal portion of the sylvian fissure and M1/2 segments of the middle cerebral artery. Angled endoscopes provided visualization of the mesial temporal lobe and crural cistern.

Again, clinical applicability studies were recommended. Neurosurgical access to the incisural space via TONES have also been anatomically evaluated (Lin et al., 2019).

Chen et al in 2014 completed a feasibility study examining this minimally invasive surgical option for amygdalohippocampectomy (Chen, Bohman, Loevner, & Lucas, 2014). This neurosurgical group established that a 97% hippocampal resection was possible. Following on from this two patients underwent transorbital amygdalohippocampectomy in 2015 for complex seizures (Chen et al., 2015). Both

patients had successful clinical outcomes with complete surgical resection. In June 2018 Dallan et al provided a perfect surgical multi-disciplinary model, combining the skull base expertise of otorhinolaryngology and neurosurgery to perform their first in vivo transorbital endoscopic approach to the temporal lobe (Dallan et al., 2018). They successfully completed a partial anterior temporal lobectomy and debulking of a recurrent multi-compartmental sphenoid ridge meningioma via the superior lid crease exposure.

Ho and Hwang reported a retrospective review completed in Singapore in 2014 on ruptured intracranial aneurysms where a small fronto-temporal craniotomy with lateral orbitotomy was completed (Ho & Hwang, 2015). They used the endoscope to inspect the aneurysm and its surrounding anatomy before clipping, subsequently verifying the completeness of the aneurysm clipping after, as well as the patency of the adjacent neurovascular structures. Similarly Reisch et al. documented transorbital endoscopic assistance for anterior circulation aneurysmal surgery (Reisch et al., 2014). The endoscope provided important visual information in the vicinity of the aneurysm, resulting if necessary, in subsequent clip repositioning.

Skull base surgery has in recent years adopted mainstream technologies to guide, improve and minimise the surgical morbidity associated with the field. Endoscopy has been used as a neurosurgical instrument since its ‘neuro’genesis by Guiot in 1963 (Guiot et al., 1963), but its neurosurgical popularity cannot compare to that of microsurgery. This is potentially attributable to either the exceptional development of microscopic skull base surgical technique from the 1970s onwards (Delashaw et al., 1992; MG Yasargil,

1975; Yasargil et al., 1976; Yasargil et al., 1977), or the neurosurgeon's proficiency at the orbitotomy in overcoming the 'orbital obstacle'. Even presently, the new capabilities of the robotic microscope allows for new levels of optical and digital visual modalities, as well as surgeon-controlled robotics easing the neurosurgeon's mainstream microscopic technique towards a more technologically advanced era. Whether this advance will result in a pure transorbital microsurgical approach to intracranial skull base pathologies is yet examined.

Composition of the Thesis

This dissertation is composed of 8 chapters: Chapter 1 serves as an introduction. Chapters 2-7 examine the in depth review and central hypotheses of the work. Chapter 2 is dedicated to the complex historical evolution of the transorbital corridor and details the influence that specific prominent medical individuals and socio-ethical stigma played in its progression. Chapter 3 evaluates the body of literature published on transorbital neuroendoscopic surgery and highlights the most common pathologies, operative nuances and surgical pitfalls identified thus far in the approach. Chapter 4 answers the first hypothesis driven question of this body of work; is the microscope a feasible method of visualisation when using a minimally invasive transorbital approach. Chapter 5 adds an extra component to the research's architecture and, in combination with bioengineering expertise, establishes a new neuroquantitative metric – the volume of surgical freedom - which is the first spatial and 3-dimensional means of assessing surgical instrument maneuvrability. In chapter 6 for the first time comprehensive analysis of the transorbital

access corridor with an equivalent open craniotomy (the supraorbital craniotomy) was completed. Comparison of the utility and instrument maneuvrability of the endoscope and microscope with respect to the transorbital corridor was also investigated. Chapter 7 continues along this vein and produces robust neuroquantitative metrics assessing the biportal bilateral transorbital approach's feasibility, as well as determining whether a biportal bilateral transorbital approach is anatomically and clinically practical for appropriate surgical pathologies, with respect to the visualisation technologies and a comparable open craniotomy. Finally, chapter 8 is a discussion section encompassing the innovative and novel elements of the body of research, as well as detailing future projects generated from this dissertation.

Publications

A complete list of peer-reviewed manuscripts describing the work performed on this dissertation project is presented in appendix A.

CHAPTER 2

The following chapter has been published in the Journal of Neurosurgery.

(doi: 10.3171/2020.8.JNS201251)

Dr. Lena Mary Houlihan was awarded the 2020 Vesalius Prize from the American Association of Neurological Surgeons Section on History of Neurological Surgery for this study.

CHAPTER 2

FROM KRÖNLEIN, THROUGH MADNESS, TO A USEFUL MODERN SURGERY: THE JOURNEY OF THE TRANSORBITAL CORRIDOR TO ENTER THE NEUROSURGICAL ARMAMENTARIUM

Houlihan L.M., Belykh E., Zhao X., O'Sullivan M.G.J., Preul M.C.

Abstract

Transorbital surgery has gained recent notoriety because of its incorporation into endoscopic skull base surgery. The use of this surgical corridor has been pervasive throughout the 20th century. It has been utilized by multiple disciplines for both clinical and experimental purposes, although its historical origin is medically and ethically controversial. Hermann Knapp first introduced the orbital surgical technique in 1874, and Rudolf Krönlein introduced his procedure in 1889. Rivalry between Walter Dandy in neurosurgery and Raynold Berke in ophthalmology further influenced methods of tackling intracranial and intraorbital pathologies. In 1946, Walter Freeman revolutionized psychosurgery by completing seemingly successful transorbital leucotomies and promoting their minimally invasive and benign surgical characteristics. However, as Freeman's legacy came into disrepute, so did the transorbital brain-access corridor, again resulting in its stunted evolution.

Microsurgery and endoscopy further influenced the use, or lack thereof, of the transorbital corridor in neurosurgical approaches. Historical analysis of present goals in

modern skull base surgery echoes the principles established through an approach described almost 150 years ago: minimal invasion, minimal morbidity, and priority of patient satisfaction. The progression of the transorbital approach not only reflects psychosocial influences on medical therapy, as well as the competition of surgical pioneers for supremacy, but also describes the diversification of skull base techniques, the impact of microsurgical mastery on circumferential neurosurgical corridors, the influence of technology on modernizing skull base surgery, and the advancing trend of multidisciplinary surgical excellence.

Introduction

Transorbital surgery has gained recent notoriety because of its incorporation into endoscopic skull base surgery. However, the genesis and evolution of the approach long predate this resurgence. The use of this surgical corridor has been pervasive throughout the 20th century. It has been used in multiple disciplines for clinical and experimental purposes to great success, although its historical involvement in neurosurgery suffered significant medico-ethical controversy. The exploration of the transorbital surgical corridor began in earnest nearly 150 years ago, providing insight and therapeutic interventions for diverse pathologies and portraying the evolution of surgical technique, specifically neurosurgical practice, in skull base surgery. A historical evaluation of transorbital surgery reflects the temporal medical trends in therapy, the diversification of skull base surgical skills, and the influence of advancing technology on neurosurgical evolution.

Although the transorbital surgical corridor has undergone a renewal over the last 10 years, the definition of what constitutes a transorbital approach remains variable. The rigid description is that it entails access to the skull base via the orbital bone without the removal of the orbital rim, thereby preserving its structural integrity. (Benedict, 1949; Moe, Bergeron, & Ellenbogen, 2010) This interpretation narrows the breadth and expanse of surgical procedure and the medico-historical developments attributable to the orbital approach.

An open surgical technique was the original gateway to the intracranial compartment and was the path extensively nurtured by the founders of modern neurosurgical practice. As imaging, stereotaxis, surgical skill, and technology improved, so too did our awareness of the damage caused by open operative intervention. Despite the progress with microsurgical technique and skull base approaches, the deep midline structures were notoriously known as difficult targets, with treacherous access corridors and multiple vascular and neural networks vulnerable to injury. The movement toward minimally invasive and minimally intrusive surgery became a key neurosurgical goal. (Hakuba, Tanaka, Suzuki, & Nishimura, 1989)

The aspirations of modern skull base surgery echo principles established through an approach first described almost two centuries ago: minimal invasion, minimal morbidity, and priority of patient satisfaction. This manuscript analyses the historical journey of the transorbital approach, providing a unique and fascinating opportunity to explore the development, evolution, and adoption of a neurosurgical operative technique. The evolution of this approach throughout the years reflects psychosocial influences on

medical therapy, the impact of microsurgical mastery on circumferential alternative neurosurgical techniques, the influence of technology on modernizing skull base surgery, and the advancing trend of the multidisciplinary approach toward surgical excellence.

The Ophthalmologist's Influence

Since the late 1800s, the development of ophthalmological surgery has allowed more refined and expansive procedures, such as the orbitotomy, a procedure recognized to provide minimally invasive access and satisfactory surgical outcomes. These methods evolved from earlier procedures, such as globe removals and orbital exenterations for massive and destructive orbital tumors, performed by surgeons and "oculists" for centuries. In 1874, Hermann Knapp, (Knapp, 1874) a German ophthalmologist who emigrated to New York, introduced an experimental operative orbital technique. He described the anterior orbitotomy for optic sheath carcinoma, a procedure designed for the resection of lesions through a superior eyelid/eyebrow or transconjunctival/inferior eyelid incision. The procedure only gained significant notoriety more than 70 years later because of its use by William Benedict to resect lesions of the anterior two-thirds of the orbit. Interestingly, Benedict was of the opinion that it was the neurosurgical community that, at the time, was pushing the boundaries of interconnected cranial and orbital pathology. Benedict wrote: "*Neurosurgeons, however, have accepted no such limitations to their field of activity. Late comers to the field as they are, nevertheless, their progress has been remarkable in the field of Ophthalmology." (Benedict, 1949)*

In many respects, Benedict's opinion was correct in that it was early surgeons performing neurosurgical procedures who sought improved routes with improved exposures to confront destructive pathologies involving the posterior orbit. The lateral orbitotomy, or classic "Krönlein operation," a technique of unknown magnitude at its time, was proposed in 1889. (Kronlein, 1889) In 1886, Swiss surgeon Rudolf Krönlein, also famous for neurosurgical interventions, devised the removal of the lateral or exterior orbital wall for excision of orbital dermoid cysts without excision of the eye, and this technique was subsequently used for the treatment of retrobulbar tumors (Figure 2.1).

A

Figure 2.1. (A) Portrait of Rudolf Krönlein; (B) the skin and bone incision color plates for his lateral orbitotomy; and (C and D) Krönlein's instruments. Otto Haab, (Haab, 1905) the Swiss ophthalmologist and a colleague of Krönlein, provided a detailed description (better than Krönlein's communications) of his friend's surgical method in his 1905 ophthalmological textbook and commented on its significance:

Up to the time until Knapp (1874), *and especially Krön*lein (1889), *described their methods of operation, retrobulbar tumors, with few exceptions, were treated by enucleation of the globe. . . .* [Krönlein's operation] *represents a distinct advance in orbital surgery. . . . It possesses the immense advantage that the operative field, the retrobulbar space, is much more freely exposed, so that the surgeon can see what he is doing, and is therefore able to operate without doing so much harm.*

Figure 2A is in the public domain.

There is no evidence, however, that Krönlein used his surgical method to enter completely through the posterior orbital wall for surgery of pathologies involving the brain or intracranial structures. Raynold Berke, a prominent figure in the evolution of ophthalmological surgery, modified and modernized the approach in 1954. (Berke, 1954) He proposed a simplified procedure that improved cosmesis, increased surgical exposure, and incorporated more advanced instruments to facilitate the surgical steps.

The medial transconjunctival orbitotomy was developed by James Galbraith and John Sullivan in 1973, almost 100 years following the original orbitotomy. (Galbraith & Sullivan, 1973) This approach, originally designed for optic nerve decompression of the

periorbital meninges for the relief of papilledema, was also applied to resection of anterior and medial intraconal lesions. It was clinically successful and safe.

Clash of surgical titans and the incorporation of the orbit into the modern craniotomy

Neurosurgeons had reasons to question the benefit of the purely transorbital approach as an access corridor to the intracranial compartments, given narrow dimensions of the skull base opening, crudeness of instrumentation, poor visualization and magnification, and concern over ocular injury and eyelid function. Ophthalmologists had no such anxiety, given their competence and insight into the orbital construct, dissipating any preconceptions about injury as they teased out and overcame clinical and operative issues throughout the 1900s. (Norris & Cleasby, 1981) The structural relationship between intracranial, intracanalicular, and intraorbital anatomy could not be ignored, and thus incorporation of the orbit into the cranial approach developed early in the evolution of skull base surgical technique. This train of thought, however, was not always widely accepted.

Neurosurgery assumed an open approach to the intracranial compartment, philosophically consistent with early neurosurgical practice. Although open surgical technique allowed for situation-specific superior exposure, trends developed in attempting to minimize retraction injury, incision sites, cosmetic defects, and surgical recovery time. In 1913, Charles Frazier, already well known for surgery of the cranial nerves and unsatisfied with current approaches to the hypophysis, described a craniotomy

involving the orbit using the supraorbital ridge in an attempt to provide access to the sella turcica region. (Frazier, 1913) Frazier noted:

I am very much in doubt whether eventually the transphenoidal [sic] *route will be the operation of choice, and although there are some conditions in which this method will have to be resorted to, I believe in the future preference will be given to the intracranial route through the anterior cranial fossa . . . . I have endeavored to elaborate a technic which will make the exposure of the hypohysis* [sic] *as feasible as the exposure of other basal structures, such as the Gasserian ganglion. The procedure, which I resorted to lately, seems to me the safest and most rational that has come to my notice. The operation consists essentially in the reflection of an osteoplastic flap from the right frontal region, in the removal en bloc of the supra-orbital ridge . . . with a portion of the roof of the orbit, later to be replaced, and in rongeuring away what remains of the roof of the orbit down to the optic foramen. With the elevation of the frontal lobe and the depression of the orbital contents, a free and adequate exposure is secured, and there remains only to make a short incision in the dura to lay bare the cavity of the sella turcica.* (Frazier, 1913)

In 1922, Walter Dandy addressed opinions on the ophthalmological-transorbital versus the neurosurgical-cranial method of treating pathologies that crossed both intracranial and intraorbital compartments. His opinion would evolve to become more definitive over the next 20 years. In 1922, he wrote:

The intracranial operation is advocated for all tumors in which an intracranial optic nerve growth is known to be present. I am not yet prepared to say how far this procedure should be adopted in intraorbital tumors of the optic nerve. It must depend upon a more careful report of the pathology of optic nerve tumors, i.e., exactly what proportion of these tumors have intracranial extension of the growth. If it is found . . . that most orbital tumors enter the cranium, then this intracranial operation (which combines the intraorbital also) will be found the safest procedure in the beginning, rather than to await the verdict of the operator who has done a local removal of the orbital tumor. (Dandy, 1922)

When considering surgery to attack intracranial extensions of intraorbital pathology or when severing the optic nerve, Dandy was concerned with surgical technique and an appropriately sterile route to the brain:

The reports . . . of the terrific mortality from meningitis following the removal of intraorbital tumors, reflects the bad treatment of these tumors in the past. There is now, of course, little excuse for any procedure which will permit meningitis. No operation should be performed thru a field which cannot be sterilized and protected. For this reason, operations thru the palpebral fissure and conjunctiva cannot be too strongly condemned. . . . Krönlein's operation seems the best and safest of the local procedures; it gives the best exposure, and the operator can work thru an aseptic field. (Dandy, 1922)

By the early 1940s, Dandy had become an authority on the neurosurgical approach to orbital tumors, as evidenced by his book *Orbital Tumors*. (Dandy, 1942) He proposed that orbital tumors were best confronted from a transcranial approach only,

claiming superiority in localization, surgical exposure, and operative technique (Figure 2.4).

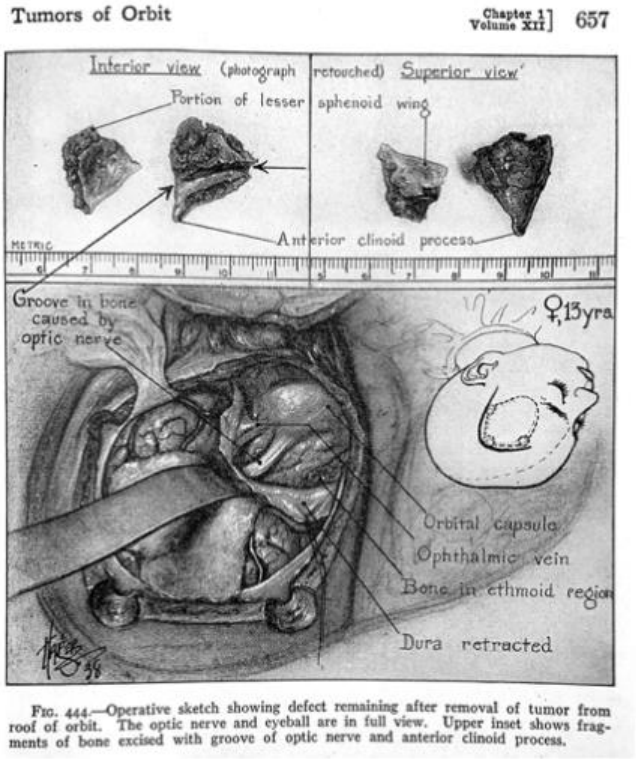

Figure 2.2. A sketch from Dandy's surgical manual illustrating many of his operations, showing a craniotomy to remove a tumor involving the orbit. (Dandy, 1942). Given his vast surgical experience by the 1940s, Dandy had become the authority on the transcranial versus transorbital route:

It is rarely possible before operation to be certain whether or not a tumor lies within the cranial cavity. . . . Even for tumors confined to the orbit alone, this approach has been found far superior to those hitherto used by ophthalmologists. . . . Most orbital tumors are now in the field of neurosurgery, the transcranial approach being used, the frontal

lobe being retracted and the roof of the orbit removed. This attack was originally suggested because a very high percentage of tumors of the orbit extended into the cranial chamber or those primarily intracranial broke through into the orbit. To reach them through the conventional orbital approaches used by ophthalmologists meant that the intracranial portion of the tumor remained and continued to grow. By the transcranial attack the entire intraorbital and intracranial parts of the tumors can be removed at the same operation .(Dandy, 1945)

Dandy referenced studies noting that:

75 to 80 per cent of all orbital tumors had intracranial extensions which subsequently caused death. . . . It has since been shown that any tumor back of the eyeball and confined to the orbit can be attacked transcranially far more effectively than by any orbital approach, including the Krönlein route which is probably the one most generally used. After removing the orbital roof the whole cavity is exposed so well. . . . With the Krönlein approach the view is restricted and blind dissection is necessary. . . . [F]*or all tumors back of the globe the transcranial approach is the only rational procedure. The only safe attack is the transcranial one in the beginning when the entire tumor, both cranial and orbital, can be removed completely at the same operation.* (Dandy, 1945)

Figure is in the public domain.

Berke, advocating for the ophthalmological artistry of the transorbital approach, which he believed to be "*ingenious*," (Berke, 1954) and Dandy, claiming neurosurgical superiority, had conflicting opinions on the usefulness of the orbitotomy. Harvey Cushing

took a more measured approach to assess surgical feasibility and success. After generally poor outcomes in patients treated transcranially for optic nerve and chiasmal gliomas, Paul Martin and Cushing concluded that Dandy was "*over-enthusiastic regarding the operability of the gliomas*" that are intraorbital optic nerve tumors involving the intracranial structures. (Martin & Cushing, 1923) Both fields evolved in a separate, yet parallel, manner, attempting to tackle similar surgical conditions.

From an ophthalmological perspective, anatomical insight and operative finesse within the orbit had been established. However, given the contention between Berke and Dandy, the transorbital corridor was limited to eye-related pathologies. The use of this approach for any other anatomical domain was avoided. Furthermore, disease that crossed the bony parameters of the orbit resulted in divided opinions among ophthalmologists throughout the 20th century. As the orbitotomy was popularized by Howard Naffziger, Berke, and Benedict, so was the defiant idea that the surgery could be used beyond the parameters of the orbit. For over a decade, Hyla Stallard staunchly advocated the use of orbitotomies for tumors that crossed orbital and intracranial fields. (Stallard, 1947, 1960) Conversely, Joseph Maroon and John Kennerdell, pioneers of ophthalmic microsurgery, professed that any orbital lesion with intracranial extension required a transcranial approach. (Maroon & Kennerdel, 1976)

Freeman's transorbital leucotomy affects the development of a transorbital brain route

The benefits attributable to this surgical approach and the reason behind its present state of prominence among neurosurgeons are strikingly similar to what resulted in the transorbital approach gaining significant notoriety among the medical community in the 1930s. Amarro Fiamberti, a prominent psychiatrist in Northern Italy, is credited with the original transorbital prefrontal lobotomy in 1937. (Fiamberti, 1937) This technique was introduced as a minimally invasive procedure for patients with schizophrenia and psychosis as an adjunct or alternative to electroconvulsive shock therapy to avoid undesirable personality changes. In the United States, Walter Freeman and James Watts completed substantial work in leucotomy surgery, initially adopting the transcranial approach of Egas Moniz. (El-Hai, 2005; Moniz) In 1948, further developing Fiamberti's work, Freeman published research on the transorbital (leucotomy) lobotomy, with subsequent significant popularization of the technique within the psychiatric community. (Freeman, 1948a, 1948b)

Freeman believed that the transorbital route was simple, safe, and quick and that it did not warrant a neurosurgeon for completion. He demonstrated that the orbital plate could be easily perforated and an orbitoclast used to sever the connection with the frontal lobe tissue without endangering the structures within the orbit and without encountering large intracranial blood vessels. (El-Hai, 2005)

He believed the procedure was well tolerated compared to large-scale prefrontal lobotomies, and he noted rapid recovery in the patient cohort. (Freeman, 1948b) Freeman adapted the procedure to a point where he believed Watt's neurosurgical expertise was no longer necessary. Watts, a neurosurgeon, had pronounced reservations about the validity,

safety, and sterility of this transorbital procedure. He also had reservations about the removal of key surgical principles from a major neurosurgical procedure. This led to a contentious difference of opinion and a pugnacious cessation of their multidisciplinary collaboration. (El-Hai, 2005)

Following these positive reports, transorbital leucotomy became popular and widely accepted as an optimal treatment for thousands in the psychiatric community of the United States and Europe. Some years following the incorporation of this procedure into the psychiatrist's compendium, medicolegal, psychosocial, and ethical issues associated with the overuse of lobotomies cast a negative view on the operative intervention, decimating Freeman's professional standing. (Caruso & Sheehan, 2017) The demise of both the psychosurgical intervention and Freeman's career has been extensively described, noting not only the paucity of evidence to support the intervention but also the societal, political, media-driven, and medical negativity that resulted in the expulsion of Freeman and the transorbital intervention from practice. (Caruso & Sheehan, 2017) Understandably, the development of this corridor for brain access was stunted.

Pneumoventriculography and vascular surgical access

In 1951, the transorbital route was proposed for pneumoventriculography. (Wada & Toyota, 1951) With patients initially supine, Toyoji Wada and Masateru Toyota established that a standard needle puncture aimed at the anterior angle of the ipsilateral ventricle at approximately 30.5 degrees toward the inion resulted in optimal ventricular access. (Wada & Toyota, 1951) The investigators commented on the ease with which this

surgical technique was completed and how well it was tolerated by patients. They noted how rapid the recovery was and reported no postoperative complications. Despite the limited results of the pneumoventriculography itself, Wada and Toyota astutely appreciated the potential of this operative approach and proposed this route as an option for tumor resection. Arguably, because of the nuances of procedure convenience that hearkened to Freeman's procedure, the transorbital pneumoventriculographic technique never gained significant notoriety or acceptance.

Although dispelled at this point from clinical practice, the use of the transorbital approach was not deterred experimentally, given its utility as a direct-access portal to the skull base, integral intracranial neurovascular structures, and ventricular system. In 1970, occlusion tests of the intracranial vasculature confirmed a superior model for middle cerebral artery (MCA) occlusion animal experiments, given the preservation of the cranial compartments and the exclusion of a craniotomy. (Hudgins & Garcia, 1970) Transorbital craniectomy was used to access the MCA in monkeys for occlusion tests in 1976. (de la Torre & Surgeon, 1976) The investigators observed minimal bleeding with this approach, and following transorbital craniectomy, they noted easy identification, manipulation, and clipping of the MCA. Huang et al., still promoted transorbital occlusion tests in the year 2000 as the experimental method of preference to access the internal carotid artery in baboons and to assess ischemia time and reperfusion injury. (Huang et al., 2000)

One may have believed that the next logical surgical development, given the difficulties faced by both fields, would have led to a communal effort to face these pathologies. Unfortunately, combined neurosurgical/ophthalmological practice did not gain momentum, and separate methods of surgical treatment remained the status quo among ophthalmologists and neurosurgeons. In the 1970s, the growth of what is now considered to be the modern craniotomy technique became aligned with the development of technology, such as the operating microscope and microinstrumentation. Surgical preference developed toward minimally invasive techniques with maximal intracranial exposure. Donald Wilson, (Wilson, 1971) Gazi Yaşargil, (Yasargil, Fox, & Ray, 1975) and Mario Brock and Hermann Dietz (Brock & Dietz, 1978) all developed skull base approaches attempting to minimize invasive methods for cerebral vasculature exposure, limit blood loss and vasogenic edema, preserve tissue integrity, and optimize cosmesis.

Despite these operative advances, the anatomical boundaries of the orbit remained a challenge in the treatment of skull base pathologies of the anterior and middle cranial fossae. The orbit encompasses up to 80% of the anterior cranial fossa floor, and its convexity impedes surgical visualization, necessitating either awkward operative angles, increased parenchymal retraction, or larger craniotomies. (Moe, Kim, & Bergeron, 2011) Nevertheless, the incorporation of the orbit into neurosurgical operative standard practice was necessary for the expansion of skull base approaches. The supraorbital approach, described in 1982 by Jane et al., allowed access to skull base supraorbital lesions. (J. A. Jane, Park, Pobereskin, Winn, & Butler, 1982)

As the microscopic technique developed, so did the variety of neurosurgical skull base approaches striving to reach deeper neurovascular structures. (Delashaw, Tedeschi, & Rhoton, 1992; Jho, 1997; van Lindert, Perneczky, Fries, & Pierangeli, 1998) The supraorbital approach did not overcome all the challenges that the orbit presented. To overcome these obstacles, Akira Hakuba and coworkers developed the orbitozygomatic infratemporal approach in 1986. (Hakuba et al., 1986) They believed that lesions in the parasellar region and interpeduncular fossa, including medial-third sphenoid wing meningiomas, petroclival meningiomas, trigeminal neuromas, and basilar tip aneurysms, were best visualized by this extended craniotomy, thus minimizing brain retraction, achieving excellent exposure, and allowing for safer brain manipulation. Almost exactly a century later, this conceivably represented neurosurgery's first attempt to incorporate Krönlein's lateral orbital osteotomy with the frontotemporal craniotomy for the management of intracranial lesions.

From that time on, neurosurgical nuances of skull base surgery adopted the amalgamation of the orbitotomy and the craniotomy. This amalgamation inspired innumerable attempts to optimize the surgical corridor. (Beretta et al., 2010; Jho, 1997) The expansion of the microsurgical technique broadened the utility of craniotomies for orbit-adjacent areas, allowing for a more minimally invasive skull base access corridor. The subsequent 20 years, to the present day, have been spent detailing and quantifying operative modifications to these combined, minimally invasive fronto-orbito-temporo-zygomatic approaches. The perfection of the neurosurgical orbital keyhole approach meant that surgical competence in orbital osteotomies became an integral skill in the

skull base surgeon's arsenal. (Dare, Landi, Lopes, & Grand, 2001; Mariniello et al., 2010)

Transorbital neuroendoscopic surgery

Intracranial endoscopy revolutionized the surgical field by improving illumination, magnification, and visualization and by entering previously obscure microscopic surgical corridors. (Perneczky & Fries, 1998) Gerard Guiot first published a neurosurgical trial of skull base endoscopy in 1963. (Guiot et al., 1963) The first reported case of endoscopic-assisted orbital surgery was by John Norris and Gilbert Cleasby in 1981 for the removal of orbital foreign bodies and the excisional biopsy of orbital tumors. (Norris & Cleasby, 1981) With this method, they further confirmed that temporary retraction of the eyeball was possible, permitting direct access to the sphenoid bone, orbital apex, and anterior and middle cranial fossae.

It is important to appreciate that otorhinolaryngologists developed early proficiency in cranial endoscopy, using its illumination and visualization advantages to explore the sinus, paranasal, and extracranial fossae. (Draf, 1983) As neurosurgeons mastered the endoscope for midline intracranial interventions and otorhinolaryngologists excelled in the extracranial skull base, the natural progression was toward transnasal endoscopic approaches to the anterior, middle, and parasellar regions. This collaboration of neurosurgeons and otorhinolaryngologists opened endless possibilities for advancing skull base surgical technique by successfully reaching anatomical targets, which had previously been problematic through the open transcranial approach, and opened up a

new operative subspecialty, endoscopic skull base surgery. (Kassam, Gardner, Snyderman, Mintz, & Carrau, 2005) This subspecialty encompassed a myriad of endoscopic endonasal approaches developed in the early 2000s, including transsphenoidal, transmaxillary, and transclival, to name a few.

The spread and acceptance of transnasal endoscopy proved beneficial in propagating the benefits of these skull base approaches, encouraging companies to develop endoscopes that provided better visualization, as well as instrumentation that could function at depth within a narrow surgical corridor. It is with these advances that the use of the modern transorbital pathway as an access point to the skull base became an attainable possibility.

Endonasal endoscopic skull base surgery became popular as an operative technique, but it was only feasible along a narrow midline corridor. Endonasal anatomy, orbital roof curvature, the supraorbital fissure, and optic canal, in addition to the geometrical relations to the skull base, limited working angles and the visualization of certain intracranial structures, particularly for lesions that crossed neurovascular bundles. (Stippler et al., 2009) These features limited the generalizability of the endonasal approach to skull base lesions that extended laterally or that encompassed broader intracranial parameters. The original modern concept behind endoscopic transorbital surgery was to overcome the limitations presented by endonasal skull base surgery. The idea of endoscopic orbital access aimed to achieve equal visibility, surpass the anatomical limitations of the endonasal approach, and, in turn, decrease the overall invasiveness and complications associated with open skull base surgery. (Dallan, Castelnuovo, et al., 2015;

Moe et al., 2010) It is for this reason that the structure that originally hindered both open transcranial and endoscopic transnasal operative approaches evolved to become, to date, the most minimally invasive access corridor at the neurosurgeon's disposal, with new degrees of surgical depth.

The concept of transorbital neuroendoscopic surgery (TONES) was first introduced by Kris Moe at the Pacific Coast Otolaryngology-Ophthalmology Society Annual Meeting in 2007. (K. S. Moe, 2007) Moe et al., detailed 20 TONES procedures for anterior skull base pathology, including cerebrospinal fluid (CSF) leaks (which were the most common), optic nerve decompression, the repair of skull base fractures, and the removal of three skull base tumors. (Moe et al., 2010) TONES was proposed as a new skull base operative corridor with the incorporation of improved instrumentation for visualization and refined surgical technique via keyhole endoscopy. This technologically amplified procedure sought to provide a coplanar endoscopic surgical pathway that coursed through the orbit and traversed a craniotomy created through one of the four orbital walls to achieve optimal visualization and magnification of the pathology. (Moe et al., 2011) The use of such an approach introduced the idea of the sino-orbito-cranial interface, an anatomical area of interest and surgical complexity.

The largest study of TONES procedures to date in the clinical setting was reported by Ramarkrishna and colleagues in 2016 in which 45 surgical cases, specifically using the neuroendoscopic approach, were detailed. "*The advantages of expanding the indications for TONES procedures are many and include increased working angles, increased ease of four handed operating, an absence of a cranial incision, limited or*

absent brain retraction, and similar outcomes from more traditional open approaches." (Ramakrishna, Kim, Bly, Moe, & Ferreira, 2016) Documented pathologies predominantly included CSF leakage, inflammatory and tumor interventions, fracture, meningoencephalocele, abscess, and hematoma.

The transorbital approach also garnered notoriety in Europe. Alqahtani et al., members of an Italian otorhinolaryngology group, had previously proposed the concept of "the 4-hand technique," allowing for the optimization of human and instrument resources. (Alqahtani et al., 2015) They took further strides toward actualizing the practical aspects of the transorbital technique (Figure 2.7). Any practical boundaries to this minimally invasive procedure became surmountable as exposure and visualization became the responsibility of additional surgeons, and the procedure was established as best practice in endoscopic transorbital surgery. In 2015, Dallan and coworkers reported the clinical use of the multicompartmental approach, highlighting its ability to offer a multi-perspective view of the intracranial spaces, producing a galvanized, polished procedure. (Dallan, Castelnuovo, et al., 2015) These cases now call for the combined expertise of a multifaceted, integrative surgical team.

Conclusion

The performance becomes progressively simplified by the combined suggestion and experience of many.

Harvey Cushing (Cushing, 1912)

During the 20th century, various medical, surgical, and experimental specialties took advantage of the transorbital surgical corridor. Minimally invasive interventions were completed by the psychiatric and ophthalmological communities with rudimentary instrumentation, but neurosurgery's path was checkered. Conflicting opinions of the respective neurosurgical and ophthalmological experts did not allow for the early maturation of an integrative approach. Dandy felt that a transcranial route was absolutely necessary for pathologies of intracranial and intraorbital locations, but he could not foresee that the addition of the orbitotomy would revolutionize skull base neurosurgery more than 60 years later. Although separated for over 125 years by differences in surgical and anatomic territorial perceptions by the three specialties, the key to the minimally invasive surgical technique with extensive visualization is a multiple-surgeon, multiportal approach. Ironically, this technique encompasses nearly the same objectives and requirements that were sought in the late 1800s: proficient surgical technique, minimal morbidity, minimal invasion, aesthetic satisfaction, and relatively short hospital length of stay. (Dallan, Castelnuovo, et al., 2015)

The intriguing history and evolution of transorbital surgery reflect the diversity, proficiency, and collaborative expertise necessary for competency, not only in skull base surgery but also for progress in surgery in general. Whether the transorbital surgical corridor becomes a cardinal pillar of skull base surgical practice and arguably takes its rightful place in the neurosurgeon's armamentarium after years of stigma and controversy, is yet to be seen.

CHAPTER 3

The following chapter has been published in the journal World Neurosurgery and featured as World Neurosurgery Editor's Choice Article for August 2021.

(doi: 10.1016/j.wneu.2021.04.104)

CHAPTER 3

TRANSORBITAL NEUROENDOSCOPIC SURGERY AS A MAINSTREAM NEUROSURGICAL CORRIDOR: A SYSTEMATIC REVIEW

Houlihan L.M., Staudinger Knoll A.J., Kakodkar P., Zhao X., O'Sullivan M.G.J., Lawton M.T, Preul M.C.

Abstract

Background: Transorbital neuroendoscopic surgery (TONES) offers a new level of minimally invasive, minimally disfiguring skull base surgery with maximal surgical visualization.

Methods: This review systematically assesses the body of published anatomical (cadaveric) and clinical evidence for the approach. PubMed, Cochrane Library, Ovid MEDLINE, and EMBASE were systematically searched for publications where the TONES surgical technique was used in an anatomical, clinical, or combined study. The outcomes of interest included identification of the pathologies, operative outcomes, and complication rates.

Results: Twenty-three papers were selected for this systematic review: 10 were purely anatomical, 10 were clinical, and 3 had both clinical and cadaveric components. The papers reported on 69 patients undergoing transorbital or combined transorbital and transnasal intervention. A total of 30 cases of cerebrospinal fluid leak were documented; of these, 28 (93%) had successful resolution, 2 (7%) had recurrence, and 5 (15%)

experienced complications. A total of 31 tumors were biopsied (n=1), resected (n=22), or debulked (n=8). Meningiomas were the most common lesion managed via TONES, with 5 of 7 patients with meningioma who reported preoperative neurological deficits experiencing an improvement in extraocular movement impairment, visual acuity, proptosis, and ptosis. Transient postoperative clinical sequelae, including diplopia and ptosis, were increasingly associated with the superior lid crease incision and the sole transorbital approach.

Conclusion: TONES is a significant development in transorbital skull base surgery. However, comprehensive, robust, comparative analyses and increasing use and generalizability of this technique in skull base surgery are awaited.

Introduction

Transorbital Neuroendoscopic Surgery

As imaging, stereotaxis, surgical skill, and technology have improved, so too has awareness of the damage associated with open operative interventions. Large incisions, breach of normal brain parenchyma, brain retraction, trauma to neurovascular structures and cranial nerves, and longer postoperative recovery are realistic risks associated with attempts to improve neurosurgical performance. This is especially pertinent when dealing with large complex lesions for which surgical intervention would previously not have been considered, where there is a certain accepted level of relative risk. The morbidity of these immense operative procedures has increased the interest in more minimally invasive approaches.

The original concept behind endoscopic transorbital surgery was to overcome the limitations presented by endonasal skull base surgery. Endoscopic orbital access aimed to achieve equal visibility, surpass the anatomical limitations of the endonasal approach, and decrease the overall invasiveness and complications associated with open skull base surgery. (Choi, Jang, & Abi Hachem, 2018; Dallan, Castelnuovo, et al., 2015; Moe et al., 2010) It is for these reasons that the orbit, the structure that originally hindered both open transcranial and endoscopic transnasal operative approaches, evolved to become, to date, the most minimally invasive access corridor at the neurosurgeon's disposal, with new degrees of surgical depth. (Abdel Aziz et al., 2011; Andaluz, Romano, Reddy, & Zuccarello, 2008)

The concept of transorbital neuroendoscopic surgery (TONES) was introduced by Kris Moe at the Pacific Coast Otolaryngology-Ophthalmology Society Annual Meeting in June 2007(K. Moe, 2007) and appeared in print in 2010. (Moe et al., 2010) TONES was proposed as a new skull base operative corridor that incorporates improved instrumentation for visualization and refined surgical technique via keyhole endoscopy. It provides a coplanar endoscopic surgical pathway that courses through the orbit, traversing a craniotomy created through one of the four orbital walls, affording optimal visualization, illumination, and magnification. (Moe et al., 2011) The use of such an approach introduced the idea of the sino-orbito-cranial interface, an anatomical area of interest and surgical complexity.

Historical analysis detailing the evolution of the transorbital approach has been evaluated and published. (Houlihan, Belykh, Zhao, O'Sullivan, & Preul, 2021) This

surgical corridor's development illustrates the various factors that influence our perception and use of an approach, ranging from influential, enigmatic individuals and societal stigma to technological developments and a trend toward multidisciplinary collaboration. It has been approximately 10 years since this surgical corridor, along with a combination of long-standing surgical principles and modern medical technology, was acknowledged as a feasible endoscopic technique. However, the approach has yet to achieve mainstream practice in neurosurgery. This study formally appraises the quantity and quality of the literature on the transorbital approach.

Methods

Electronic Literature Search

A systematic review was performed using the Preferred Reporting Items for Systematic Reviews and Meta-Analyses (PRISMA) guidelines. (Moher, Liberati, Tetzlaff, & Altman, 2009) This study was registered with PROSPERO international prospective register of systematic reviews, registration number CRD42020158756. The PubMed, Cochrane Library, Ovid MEDLINE, and EMBASE electronic databases were searched for the period from inception through September 5, 2020. The search strategy was developed in conjunction with a health sciences librarian specializing in systematic review searching. A medical subject headings term and keyword search of each database was performed using the Boolean operators OR and AND. Keywords included "trans orbital" or "transorbital," "endoscopic," "neuroendoscopic," "open," "trans cranial" or "transcranial," "transnasal," "superior lid crease" (SLC), "precaruncular," "lateral

retrocanthal," "approach," "skull base," "anterior cranial fossa," and "middle cranial fossa." The complete search protocol is available as Appendix B and search strategy in Appendix C.

Study Definitions

Definitions of key variables used in determining what studies were included in and excluded from this review are noted below.

- Transorbital surgery: an endoscopic surgical intervention through the orbital roof to gain access to the intracranial compartments with the preservation of the orbital rim and lateral orbital ridge. Patients who had a lateral orbitotomy or any form of open cranial access in addition to a TONES approach were excluded. TONES combined with an endoscopic endonasal approach was included, given the similarities in the technological fundamentals.
- Intracranial compartment: fossa within the cranial vault containing brain parenchyma and neuronal tissue.
- Anatomical and cadaveric studies: publications that describe research completed in a laboratory environment on human cadavers for anatomical exploration and analysis.
- Clinical studies: publications that describe research completed in the clinical setting where patients constitute the study population.

- First surgical intervention: the first attempt to treat the pathological condition (e.g., cerebrospinal fluid [CSF] leak or tumor).
- Redo surgical intervention: at least the second attempt to treat the pathological condition (e.g., CSF leak or tumor).

Study Selection

Inclusion criteria were as follows: all clinical and anatomical studies published from all institutions; studies involving human participants and including both men and women; studies with patient age greater than 18 years; studies involving patients who had undergone transorbital surgical intervention, where transorbital surgery is defined as an intracranial endoscopic surgical intervention with the preservation of the orbital rim; studies involving patients who had undergone combined transorbital and transnasal operative intervention; articles published in English or articles for which there were English translations available; available full-text publications; and studies found on the PubMed, Cochrane Library, Ovid MEDLINE, and EMBASE databases.

Three authors with neurosurgical training (LMH, ASK, PK) independently evaluated the titles and abstracts of all retrieved publications to determine their relevance. Articles with titles and abstracts that met the inclusion criteria were selected for further review, with all duplicates accounted for at this point and removed. Full reports were

obtained for all studies that met the inclusion criteria. Following this step, the same 3 authors independently screened articles to assess the full text on the basis of the predetermined inclusion criteria. Any disagreements between the 3 authors were resolved by discussion and percent agreement, and where necessary, a final decision was determined by the principal investigator (MCP). The reasons for the exclusion of full-text articles were recorded. The reviewers were not blind to the journal titles, study authors, or institutions. At all steps throughout the process, a supervisory assessment of the selection decisions was reviewed by the lead author (LMH). The PRISMA chart outlines the study's short-listing and selection process (Figure 3.1). (Moher et al., 2009)

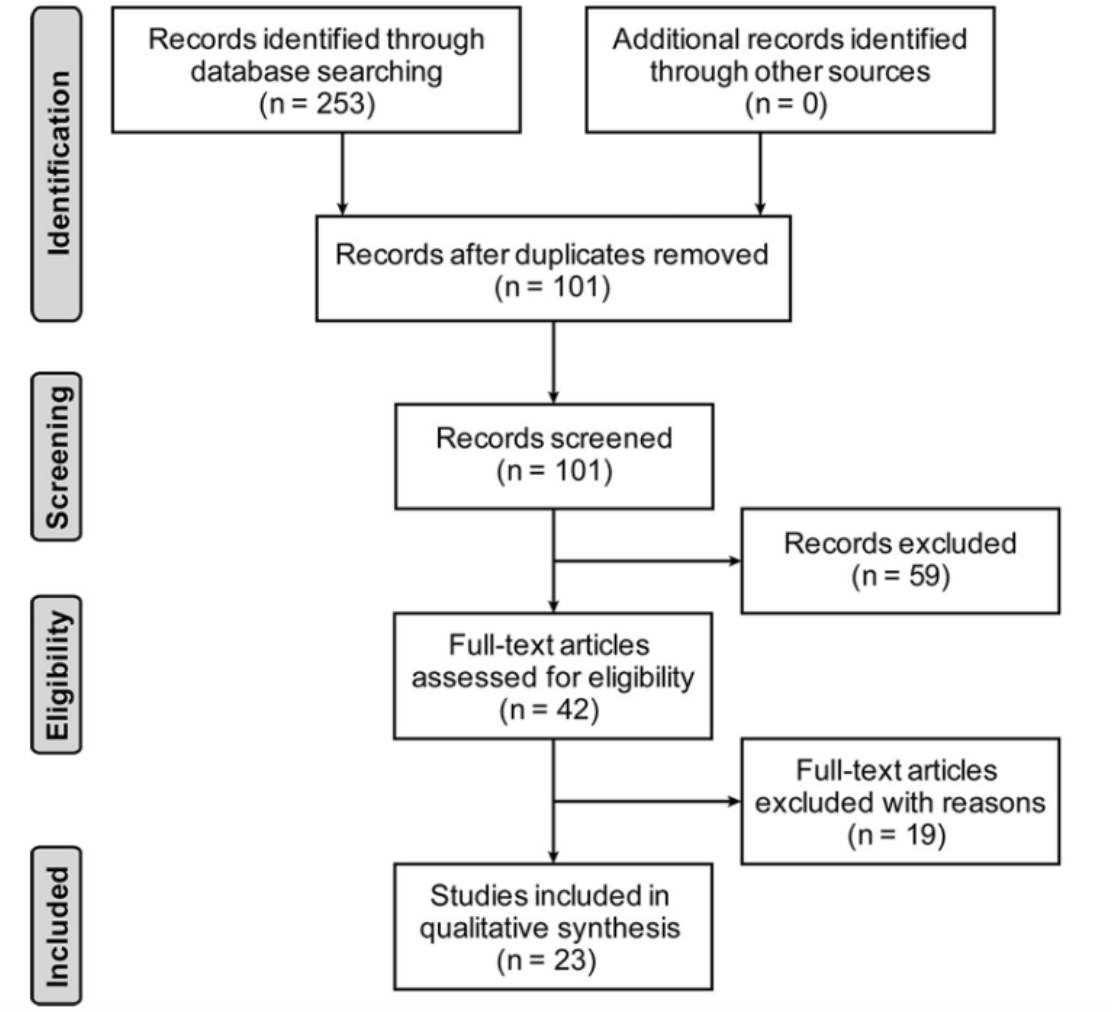

Figure 3.1. Flow chart showing the selection process for studies included in this systematic review. Used with permission from Barrow Neurological Institute, Phoenix, Arizona.

Data Extraction

The data extracted were first divided into 3 categories based on the study design: 1) anatomical, 2) clinical, and 3) combined anatomical and clinical studies. To increase the robustness and accuracy of the selection method, 4 authors (LMH, ASK, PK, XZ) independently cataloged the data in a protocol spreadsheet to account for overlapping patient populations described in multiple papers. Metadata attached to papers were also assessed. Each patient within the selected papers was reviewed individually to ensure consistency with the inclusion criteria for the cumulative patient cohort. Spreadsheets, once completed, were assessed for interrater variability. Any dispute was resolved by discussion, and, where needed, the decision was finalized by the principal investigator. These data included 1) publication year, 2) number of participants, 3) study design, 4) surgical specialty, 5) research level of evidence (based on the criteria published by the Centre for Evidence-Based Medicine), (P. Burns, Rohrich, & Chung, 2011) 6) cranial fossa accessed, 7) approach used, 8) number of patients, 9) country of research, 10) pathology addressed, 11) age range, 12) sex, 13) hospital length of stay (LOS), 14) length of follow-up, 15) outcome, 16) procedural complications, and 17) type of incision used.

Data Synthesis and Quality Assessment

The primary outcomes of interest were the pathologies and the outcomes for which this approach was most commonly used specific to the pathology addressed. For CSF leak this was defined as:

- Success : resolution of CSF leak

- Failure: recurrence of CSF leak

In tumor pathologies surgical outcomes were defined as:

- Biopsy
- Debulking
- Resection

Secondary outcomes included complication rates. Descriptive statistics were used to calculate the rates and means for each study. A meta-analysis could not be performed, because all included studies were of an evidence level of IV or less. There was marked heterogeneity of surgical rationale and outcome measures among the publications. A risk bias assessment was not completed because all included studies were observational. (Moher et al., 2009)

Results

Study Selection

The database search yielded 253 studies (Ovid MEDLINE, 58; Ovid Embase, 67; PubMed, 128; and Cochrane Library, 0). After the removal of duplicates, 101 articles remained. A total of 59 publications were excluded on the basis of title and abstract, and 42 full-text articles were assessed for inclusion. Of these, 19 were excluded, and 23 publications met all criteria for inclusion in this systematic review (Figure 3.1).

Study Characteristics

Table 3.1 describes the details of the selected articles.

Table 3.1. Characteristics of 23 studies involving transorbital neuroendoscopic surgery

Clinical, anatomical, or Both	Study	Year	Country of origin	Journal	Type of study	Surgical specialty	Level of evidence	Cranial fossa accessed	Surgical incision	Endoscopic approach: transorbital or transorbital plus transnasal	No. of pt.
Clinical	Schaberg et al.(Schaberg, Murchison, Rosen, Evans, & Bilyk, 2011)	2011	US	*The Orbit*	Case report	Otolaryngology	IV	Anterior	Precaruncular	Transorbital plus transnasal	1
Clinical	Raza et al.(Raza, Quinones-Hinojosa, Lim, & Boahene, 2013)	2013	US	*World Neurosurgery*	Case series	Neurosurgery	IV	Anterior	Precaruncular	Transorbital plus transnasal	5
Clinical	Chen et al.(Chen et al., 2015)	2015	US	*Journal of Oto-rhino-laryngology and its Related Specialties*	Case series	Neurosurgery, ophthalmology	IV	Middle	Lateral	Transorbital	1
Clinical	Dallan et al.(Dallan, Locatelli, et al., 2015)	2015	Italy	*European Archive of Oto-Rhino-Laryngology*	Case report	Otolaryngology, neurosurgery	IV	Middle	SLC	Transorbital	1
Clinical	Tham et al.(Tham	2015	US	*Journal of Neurological Surgery Reports*	Case report	Otolaryngology, neurosurgery	IV	Anterior	SLC	Transorbital plus transnasal	1

	et al., 2015)										
Clinical	Ramakrishna et al.(Ramakrishna et al., 2016)	2016	US	*Journal of Clinical Neuroscience*	Case series	Neurosurgery	IV	Anterior	Lateral + precaruncular	Transorbital	28
Clinical	Almeida et al.(Almeida et al., 2018)	2018	US	*Journal of Neurosurgery*	Case series	Neurosurgery, ophthalmology, otolaryngology	IV	Middle	SLC	Transorbital plus transnasal	2
Clinical	Park et al.(Park et al., 2019)	2019	Korea	*Journal of Neurosurgery*	Case series	Neurosurgery, ophthalmology, otolaryngology	IV	Middle and Posterior	SLC	Transorbital	9
Clinical	Di Somma et al.(Di Somma et al., 2020)	2020	Spain/ Italy	*Journal of Neurosurgery*	Case report	Neurosurgery, ophthalmology, otolaryngology	IV	Middle	SLC	Transorbital plus transnasal	1
Clinical	Park et al.(Park, Yoo, Yun, & Hong, 2020)	2020	Korea	*World Neurosurgery*	Case series	Neurosurgery, ophthalmology, otolaryngology	IV	Middle	SLC	Transorbital	7
Anatomical	Ciporen et al.(Ciporen et al., 2010)	2010	US	*World Neurosurgery*	Cadaveric	Neurosurgery	VI	Middle	Precaruncular	Transorbital	NA
Anatomical	Bly et al.(Bly, Ramakrishna, Ferreira,	2014	US	*Journal of Neurological Surgery–Skull Base Part B*	Cadaveric	Otolaryngology, neurosurgery	VI	Middle	Lateral	Transorbital	NA

	& Moe, 2014)										
Anatomical	Chen et al.(Chen, Bohman, Loevner, & Lucas, 2014)	2014	US	*Journal of Neurosurgery*	Cadaveric	Neurosurgery	VI	Middle	Lateral	Transorbital	NA
Anatomical	Alqahtani et al.(Alqahtani et al., 2015)	2015	Italy	*Acta Otorhinolaryngologica Italica*	Cadaveric	Otolaryngology	VI	Anterior and Middle	SLC	Transorbital	NA
Anatomical	Ferrari et al.(Ferrari et al., 2016)	2016	Italy	*World Neurosurgery*	Cadaveric	Otolaryngology, neurosurgery	VI	Middle	Inferior lid crease	Transorbital	NA
Anatomical	Almeida et al.(Almeida et al., 2017)	2017	US	*Acta Neurochirurgica*	Cadaveric	Otolaryngology, neurosurgery	VI	Middle	SLC	Transorbital	NA
Anatomical	Di Somma et al.(Di Somma et al., 2018)	2018	Spain/ Italy	*Operative Neurosurgery*	Cadaveric	Neurosurgery	VI	Middle	SLC	Transorbital	NA
Anatomical	Saraceno et al.(Saraceno et al., 2019)	2019	Italy	*World Neurosurgery*	Cadaveric	Neurosurgery	VI	Middle	SLC + lateral	Transorbital	NA
Anatomical	Lima et al.(L. R.	2020	US	*World Neurosurgery*	Cadaveric	Otolaryngology, neurosurgery	VI	Middle	SLC	Transorbital	NA

	Lima et al., 2020)										
Anatomical	Topczewski et al.(Topczewski et al., 2020)	2020	Italy/Spain	*Acta Neurochirurgica*	Cadaveric	Otolaryngology, neurosurgery	VI	Posterior	SLC	Transorbital plus transnasal	NA
Both	Moe et al.(Moe et al., 2010)	2010	US	*Neurosurgery*	Case series	Facial plastic and reconstructive surgery	IV	Anterior	SLC + Lateral + precaruncular	Transorbital	4 (all duplicate patients)
Both	Moe et al.(Moe et al., 2011)	2011	US	*Laryngoscope*	Case series	Facial plastic and reconstructive surgery	IV	Anterior	SLC + precaruncular	Transorbital	10
Both	Dallan et al.(Dallan, Castelnuovo, et al., 2015)	2015	Italy	*World Neurosurgery*	Case series	Otolaryngology, neurosurgery	IV	Middle	SLC	Transorbital plus transnasal	4

Abbreviations: NA, not available; SLC, superior lid crease.

Of the 23 publications, 10 were clinical, (Almeida et al., 2018; Chen et al., 2015; Dallan, Locatelli, et al., 2015; Di Somma et al., 2020; Park et al., 2019; Park et al., 2020; Ramakrishna et al., 2016; Raza et al., 2013; Schaberg et al., 2011; Tham et al., 2015) 10 were anatomical, (Almeida et al., 2017; Alqahtani et al., 2015; Bly et al., 2014; Chen et al., 2014; Ciporen et al., 2010; Di Somma et al., 2018; Ferrari et al., 2016; L. R. Lima et al., 2020; Saraceno et al., 2019; Topczewski et al., 2020) and 3 included a combination of both cadaveric description and case examples. (Dallan, Castelnuovo, et al., 2015; Moe et al., 2010; Moe et al., 2011) The earliest study was published in 2010, and the most recent study was published in 2020. Figure 3.2 illustrates the number of articles detailing the purely transorbital approach per year.

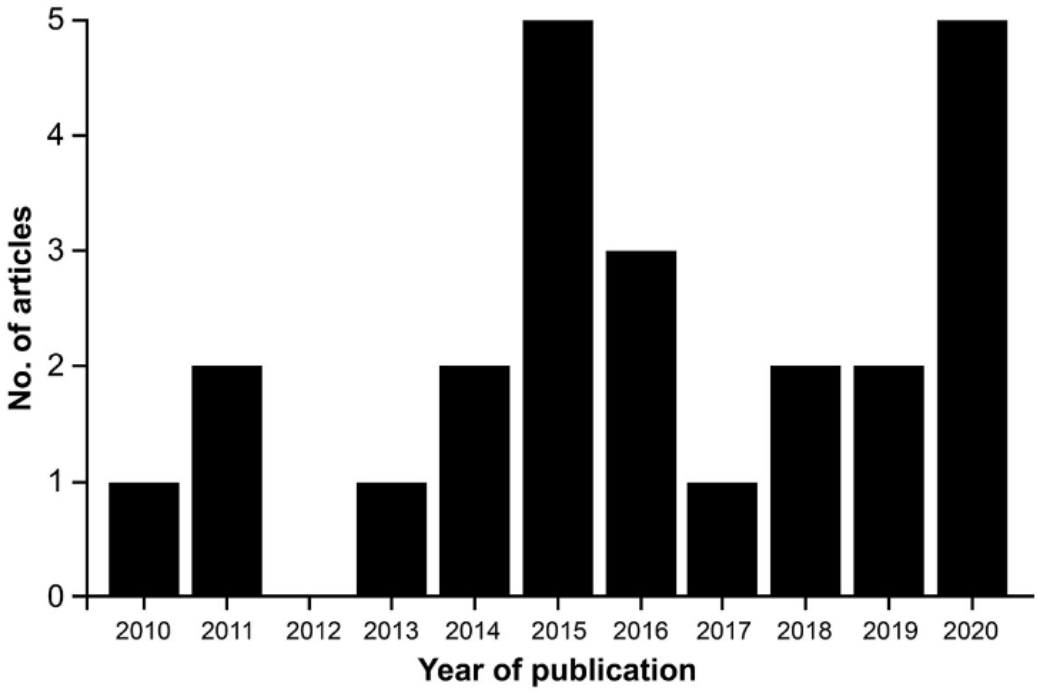

Figure 3.2. Number of articles detailing the transorbital approach published per year, January 1, 2010, through September 5, 2020. Used with permission from Barrow Neurological Institute, Phoenix, Arizona

The United States (13 publications), Italy and Spain (8 publications), and Korea (2 publications) are the countries of origin of the 23 publications. The highest level of evidence identified was level IV, with case series being the most common type of study design used. Among the 23 papers, 19 involved neurosurgical specialists, 14 involved otolaryngology specialists, 5 involved ophthalmology specialists, and 2 involved facial plastic and reconstructive surgery specialists. Sixteen publications described the use of

the SLC incision. Both the lateral and precaruncular incisions were reported in 6 papers each, and 1 paper reported the inferior lid crease incision to access the intracranial vault. Sixteen publications described access to the middle cranial fossa, and 7 of those publications were clinical articles. Seven papers reported the endoscopic transorbital route to access the anterior cranial fossa, and 6 of those papers involved clinical cases. In clinical research, 7 articles reported the transorbital approach to access the cranial compartment, whereas 6 reported a combined transorbital and transnasal approach.

Clinical Cohort

In the literature, a cumulative total of 69 patients were reported to have undergone transorbital neuroendoscopic surgical intervention (Table 3.2).

Table 3.2. Demographic and clinical data reported in selected studies involving transorbital neuroendoscopic surgery, by type of pathology treated

Type of pathology, study	Total no. of patients	Specific pathology, no. of patients	Cause or intervention, no. of patients	Sex, no. of patients	No. of patients age <40 years; age ≥40 years	Mean length of stay (days)	Mean length of follow-up (months)	First vs redo intervention, no. of patients	Fossa accessed, no. of patients	Approach used, no. of patients	Endoscopic approach distribution, no. of patients
CSF leak											
Raza et al.(Raza et al., 2013)	3	CSF leak, 3	Iatrogenic, 3	F, 2; M, 1	2; 1	4.3	6	First, 3	Anterior, 3	Precaruncular, 3	Transorbital plus transnasal, 3
Schaberg et al.(Schaberg et al., 2011)	1	CSF leak, 1	Iatrogenic, 1	F, 1	0; 1	NA	5	First, 1	Anterior, 1	Precaruncular, 1	Transorbital plus transnasal, 1
Moe et al.(Moe et al., 2011)	10	CSF leak, 10	Trauma, 4; iatrogenic, 6	F, 7; M, 3	4; 6	13[a]	7.6	First, 4; redo, 6	Anterior, 10	Precaruncular, 4; SLC, 6	Transorbital, 10
Ramakrishna et al.(Ramakrishna et al., 2016)	16	CSF leak, 16	Trauma, 7; iatrogenic, 3; congenital, 6	F, 8; M, 8	4; 12	19.4[b]	7.5[c]	First, 16	Anterior, 13; middle, 3	Precaruncular, 4; SLC, 10; lateral, 2	Transorbital, 13; transorbital plus transnasal, 3
CSF overall	30	CSF leak, 30	Trauma, 11; iatrogenic, 13; congenital, 6	F, 18; M, 12	10; 20	12.2	6.5	First, 24; redo, 6	Anterior, 27; middle, 3	Precaruncular, 12; SLC, 16; lateral, 2	Transorbital, 23; transorbital plus transnasal, 7
Tumor											
Chen at al.(Chen et al., 2015)	1	Glioma, 1	Biopsy, 1	M, 1	0; 1	NA	12	First, 1	Middle, 1	Lateral, 1	Transorbital, 1
Dallan et al.(Dallan, Castelnuovo, et al., 2015)	4	Malignant schwannoma, 1; meningioma, 3	Resection, 3; debulking, 1	F, 3; M, 1	0; 4	4.8	8.2	First, 3; redo, 1	Middle, 4	SLC, 3; inferior lid crease, 1	Transorbital plus transnasal, 4

Raza et al.(Raza et al., 2013)	1	Esthesioneuroblastoma, 1	Resection, 1	M, 1	0; 1	4	6	First, 1	Anterior, 1	Precaruncular, 1	Transorbital plus transnasal, 1
Almeida et al.(Almeida et al., 2018)	2	Meningioma, 2	Debulking, 2	F, 2	0; 2	2	2	First, 1; redo, 1	Middle, 2	SLC, 2	Transorbital plus transnasal, 2
Ramakrishna et al.(Ramakrishna et al., 2016)	6	Adenocarcinoma, 1; osteoma, 1; osteoblastoma, 1; neuroesthesioblastoma, 1; squamous cell carcinoma, 1; meningioma, 1	Debulking, 2; resection, 4	M, 4; F, 2	1; 5	6.5	24 [d]	First, 4; redo, 2	Anterior, 5; middle, 1	Precaruncular, 5; lateral, 1	Transorbital, 2; transorbital plus transnasal, 4
Di Somma et al.(Di Somma et al., 2020)	1	Meckel's cave schwannoma, 1	Resection, 1	M, 1	0; 1	3	NA	First, 1	Middle, 1	SLC, 1	Transorbital plus transnasal, 1
Park et al.(Park et al., 2019)	9	Trigeminal schwannoma, 9	Debulking, 2; resection, 7	F, 6; M, 3	2; 7	NA	NA	NA	Middle, 9	SLC, 9	Transorbital, 9
Park et al.(Park et al., 2020)	7	Sphenoid wing meningioma, 7	Debulking, 1; resection, 6	F, 6; M, 1	2; 5	NA	NA	NA	Middle, 7	SLC, 7	Transorbital, 7
Overall	31	Glioma, 1; schwannoma, 11; meningioma, 13; neuroesthesioblastoma, 2; adenocarcinoma, 1; osteoma, 1; osterblastoma, 1; squamous	Biopsy, 1; debulking, 8; resection, 22	F, 19; M, 12	5; 26	3.25	10.45	First, 22; redo, 8	Anterior, 6; middle, 25	Precaruncular, 6; SLC, 22; lateral, 2; inferior lid crease, 1	Transorbital, 19; transorbital plus transnasal, 12

		cell carcinoma, 1									
Vascular											
Dallan et al.(Dallan, Locatelli, et al., 2015)	1	Hemangioma, 1	Congenital, 1	F, 1	NA	3	12	First, 1	Middle, 1	SLC, 1	Transorbital, 1
Infection											
Ramakrishna et al.(Ramakrishna et al., 2016)	2	Intraorbital/epidural abscess, 1; frontal abscess (iatrogenic), 1		F, 1; M, 1	1; 1	26.5	NA	First, 2	Anterior, 2	SLC, 2	Transorbital, 2
Other											
Ramakrishna et al.(Ramakrishna et al., 2016)	3	Frontal mucocele, 1; fibrous dysplasia, 1; fibroxanthoma, 1	Debulking, 1; resection, 2	M, 3	2; 1	2 [e]	12[d]	First, 3	Anterior, 3	SLC, 2; precaruncular, 1	Transorbital, 2; transorbital plus transnasal, 1
Tham et al.(Tham et al., 2015)	1	Fibrous dysplasia, 1	Debulking, 1	M, 1	1; 0	5	NA	First, 1	Anterior, 1	SLC, 1	Transorbital plus transnasal, 1
Raza et al.(Raza et al., 2013)	1	Paget's disease, 1	Resection, 1	F, 1	0; 1	3	6	First, 1	Anterior, 1	Precaruncular, 1	Transorbital, 1

Abbreviations: CSF, cerebrospinal fluid; F, female; M, male; NA, not available; SLC, superior lid crease.

[a]Five of 10 patients had length of stay data recorded, 1 of whom had posttrauma hospitalization of 40 days.

[b]Two trauma patients were hospitalized more than 60 days.

[c]Only 4 patients had follow-up data.

[d]Only 2 patients had follow-up data.

[e]One patient was readmitted for 10 days because of a complication.

Four papers described the use of either endoscopic transorbital approaches or combined transorbital and transnasal approaches for CSF leakage. Thirty patients (18 women and 12 men) underwent operative intervention for CSF leaks. Two-thirds of the patients (20 of 30 patients) were older than 40 years. Additionally, 13 (43%) of 30 CSF leaks were iatrogenic in origin. The mean hospital LOS was 12.2 days (range, 4.5-19.5 days); however, this result is skewed by both omissions of data and inclusion of long-term polytrauma patients who had multiple medical conditions. Patients were monitored for a mean of 6.5 months (range, 5-7.5 months). Among the 30 patients with CSF leaks, the defect was located in the anterior cranial fossa in 27 patients, and 24 patients underwent first operations. The SLC incision was commonly used (16 of 30 patients; 53%). CSF leaks were managed via the transorbital endoscopic approach in 23 of 30 patients. Thirty-one patients underwent an endoscopic transorbital intervention for a tumor, and 22 of the 31 lesions (71%) were completely resected. Meningiomas were the most common tumor managed via the transorbital or combined transorbital and transnasal routes, accounting for 13 (42%) of 31 tumors, followed by middle cranial fossa schwannomas (11 of 31 tumors). The SLC incision was used in 71% of cases. The overall mean LOS was 3.25 days (range, 2-6.5 days), with mean follow-up time by the neurosurgical team of 10.4 months (range, 2-24 months).

The sole transorbital approach was the preferred route of operative access for tumor resection, used in 19 of 31 cases (61%). A combined transorbital and transnasal approach was used in 12 of 31 cases (39%).

Of the meningioma cohort, 7 cases were managed with a sole transorbital approach, whereas 6 were managed through a combined transorbital and transnasal approach. Twelve patients underwent an SLC incision, and the remaining patient underwent a precaruncular incision. Nine of the meningiomas were completely resected, and the other 4 were debulked. For 2 patients, the operation was the second intervention for further surgical debulking. Neither of these operations achieved gross-total resection.

Schwannomas of the middle cranial fossa accounted for the second largest tumor cohort treated via a transorbital approach. Two of these cases were managed with a combined transorbital and transnasal approach. One patient underwent an inferior lid crease incision to access the middle cranial fossa, whereas all other patients had an SLC incision. Nine of 11 schwannoma cases achieved a gross total resection.

There was only 1 case of vascular pathology noted in this review. A hemangioma extended intracranially via the superior orbital fissure and was accessed through an SLC incision into the middle cranial fossa.

There were 2 cases of infection treated: 1 epidural abscess extending from the intraorbital compartment intracranially and 1 postoperative frontal lobe abscess. Both cases were treated solely through an endoscopic transorbital approach via an SLC incision. Their LOS was notably longer compared to that of the other subgroups, which was likely attributable to the prolonged need for intravenous antibiotic therapy. Other novel cases noted were fibrous dysplasia in 2 patients and 1 case each of frontal mucocele, fibroxanthoma, and Paget's disease. All of these cases involved the anterior cranial fossa.

Procedural Complications

Procedural complications were noted in 9 of 69 patients, for a complication rate of 13% for transorbital surgery, with 5 complications occurring in patients with CSF leak repairs. All complications were transient or resolved following an adjunct operative intervention, except in 1 patient who had permanent proptosis following debulking of a fibrous dysplastic tumor. The length of follow-up was not recorded in the article.

Six complications were reported in 5 patients who underwent transorbital endoscopic management of CSF leaks (Table 3.3 and Figure 3.3).

Table 3.3. Complications reported in selected studies involving transorbital neuroendoscopic surgery

Pathology, patient no.	Study	Complication	Treatment	Resolution of complication	Fossa accessed	Incision	Endoscopic approach
CSF leak							
1	Moe et al.(Moe et al., 2011)	CSF leak on postoperative day 7	Lumbar drain	Yes	Anterior	SLC	Transorbital
2	Ramakrishna et al.(Ramakrishna et al., 2016)	Levator muscle dysfunction	None	Yes	Anterior	SLC	Transorbital
3	Ramakrishna et al.(Ramakrishna et al., 2016)	Meningitis	Antimicrobial therapy	Yes	Anterior	Precaruncular	Transorbital + transnasal
4	Ramakrishna et al.(Ramakrishna et al., 2016)	Periorbital hematoma; CSF leak 1 month later	Bedside needle aspiration; lumbar drain	Yes	Anterior	SLC	Transorbital
5	Ramakrishna et al.(Ramakrishna et al., 2016)	Epiphora	Conjunctival dacryocystorhinostomy	Yes	Anterior	Precaruncular	Transorbital
Tumor							
6	Chen et al.(Chen et al., 2015)	Orbital pseudomeningocele	Ventriculoperitoneal shunt	Yes	Middle	Lateral	Transorbital
7	Park et al.(Park et al., 2019)	Surgical site infection	Antimicrobial therapy	Yes	Middle	SLC	Transorbital

Frontal mucocele							
8	Ramakrishna et al.(Ramakrishna et al., 2016)	CSF leak	Endoscopic reexploration and CSF leak repair	Yes	Anterior	SLC	Transorbital
Fibrous dysplasia							
9	Tham et al.(Tham et al., 2015)	Proptosis	None	No	Anterior	SLC	Transorbital plus transnasal

Abbreviations: CSF, cerebrospinal fluid; SLC, superior lid crease.
*The total procedural complication rate for these studies was 13% (9/69).

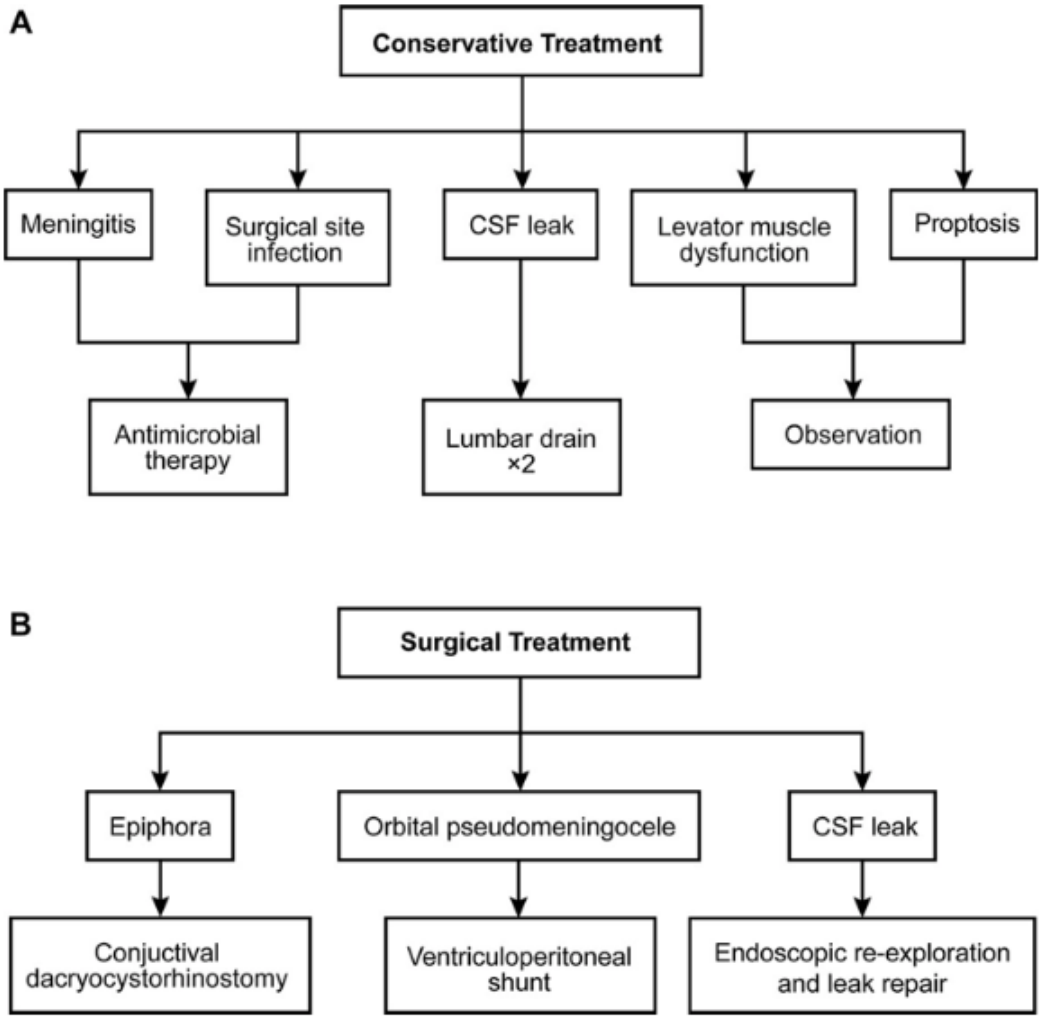

Figure 3.3. Flowchart of TONES complications with respect to A, conservative and B, surgical treatment. Used with permission from Barrow Neurological Institute, Phoenix, Arizona.

Recurrent CSF leaks managed by lumbar drain placement accounted for 2 complications associated with CSF repair; the remaining complications were 1 case each of levator muscle dysfunction, meningitis, periorbital hematoma, and epiphora. There were 2 complications associated with tumor-related transorbital interventions: a superficial surgical site infection, which resolved with antimicrobial therapy, and an orbital pseudomeningocele, which occurred in a patient who underwent biopsy for a mesiotemporal lobe glioma. The publication reports that the patient was offered a ventriculoperitoneal shunt, and the patient chose this option. Another significant complication was noted in a 33-year-old man who underwent transorbital access for a frontal mucocele. He developed a postoperative CSF leak that warranted endoscopic reexploration and CSF leak repair. Following his second operative intervention, the patient reported temporary diplopia and ptosis, which eventually resolved.

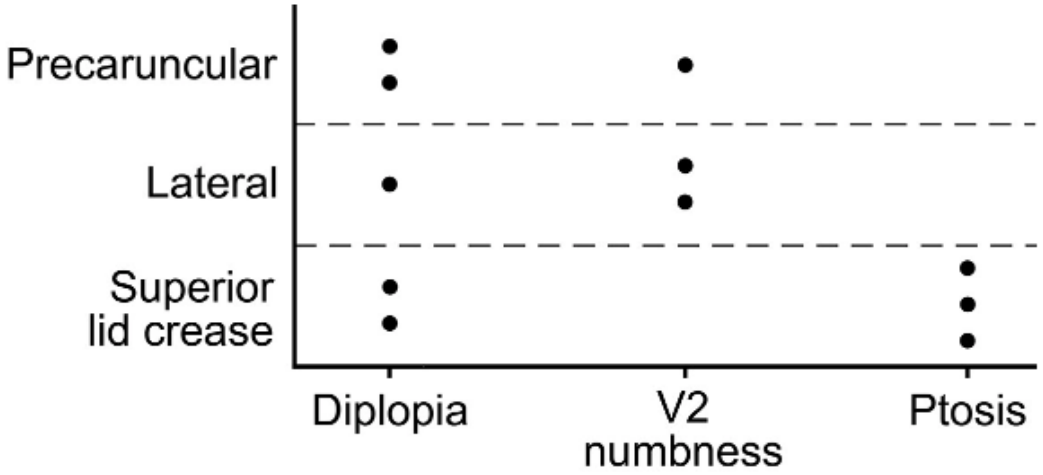

Figure 3.4. Graphic representation of the transient postoperative neurological sequelae in relation to the selected operative incision. Diplopia, n = 5; V2 numbness, n = 3; ptosis n = 3. Used with permission from Barrow Neurological Institute, Phoenix, Arizona.

Figure 3.4 shows the temporary procedural neurological deficits related to the incision made. Transient postoperative sequelae included diplopia in 5 patients, V2 numbness in 3 patients, and ptosis in 3 patients. Of the 3 patients with V2 numbness, 2 patients underwent a lateral approach, which accounted for half of the 4 patients who underwent a lateral incision within the whole patient cohort. Ptosis occurred solely in patients who had an SLC incision, accounting for 7% of the patients who underwent an approach through this soft-tissue corridor (3 of 44 patients).

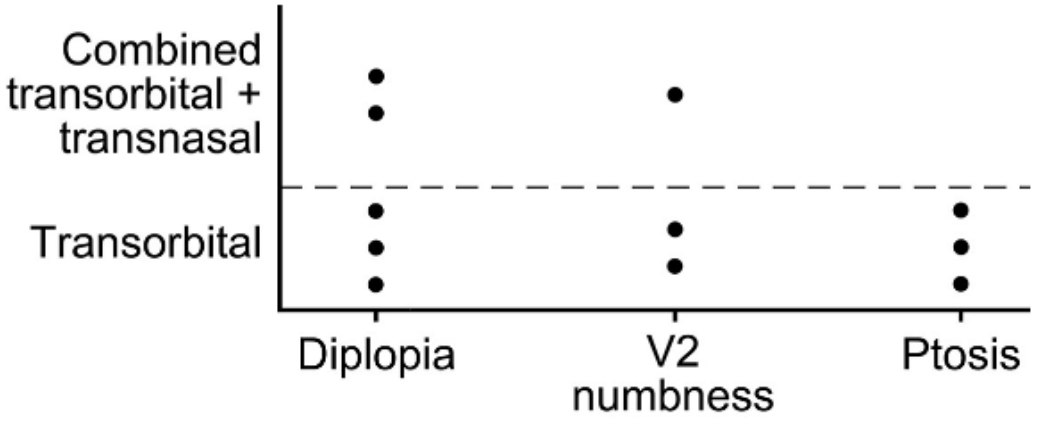

Figure 3.5. Graphic representation of postoperative diplopia, V2 numbness, and ptosis with respect to the approach used. Diplopia, n = 5; V2 numbness, n = 3; ptosis n = 3. Used with permission from Barrow Neurological Institute, Phoenix, Arizona.

Of the 5 patients who had postoperative diplopia, 3 patients had a solely transorbital intervention (Figure 3.5). The rates of diplopia, V2 numbness, and ptosis in the transorbital approach cohort were 6%, 5%, and 6%, respectively. The diplopia and V2 numbness rates in the combined transorbital and transnasal approach group were 10% and 5%, respectively.

Resolution of Neurological Deficits

Regarding patients with tumors, notable improvement occurred in some neurological deficits that were present preoperatively. Figure 3.6 depicts the resolution or improvement of neurological deficits within the symptomatic cohort.

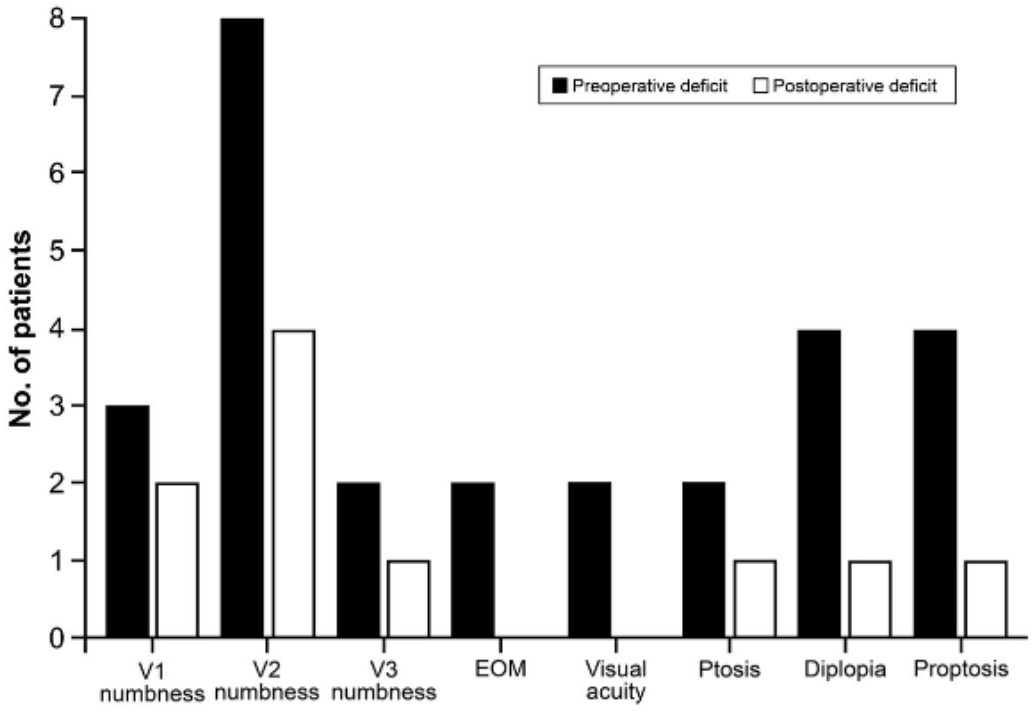

Figure 3.6. Bar chart comparing the number of patients with preoperative deficits and postoperative deficits. EOM, extraocular movement. Used with permission from Barrow Neurological Institute, Phoenix, Arizona.

Main preoperative symptoms included V1, V2, and V3 numbness; extraocular movement (EOM) and visual acuity impairment; ptosis; proptosis; and diplopia. Operative intervention showed a reduction in all categories, most notably in EOMs and visual acuity, both of which returned to baseline for symptomatic patients.

Discussion

This is the first systematic review of the neuroendoscopic transorbital and combined transorbital and transnasal approaches that provides a calculated insight into the body of evidence available on this minimally invasive surgical technique. Since the advent of the TONES technique almost 10 years ago, most papers have had an anatomical focus aimed at proving the surgical feasibility and merits of this approach. These publications represent a small selection of authors who are predominantly responsible for the body of data on the topic. This situation suggests that a core group of specialists are promoting and investigating the advantages of this technique.

Body of Evidence

We applied clear definitions, inclusion criteria, and exclusion criteria in our search because “transorbital” and “transorbital endoscopic” surgeries have various meanings for different research groups. We sought to identify the clinical and anatomical data on transorbital neuroendoscopic surgery to establish the highest level of evidence available and the breadth of research completed on this surgical technique.

Although the TONES technique was originally published 10 years ago, the quantity of publications is small. Our original literature search identified only 253 results, including duplicates. The final study count for the quantitative synthesis was 23 papers, of which 10 were exclusively cadaveric studies. The most robust studies that we identified still provided only level IV evidence (case series). Furthermore, due to heterogeneity in the reported cases, meta-analysis and cumulative statistical assessment were not possible. Although the cadaveric studies are promising, there are no publications of any substantial level of evidence to unequivocally convince the neurosurgical community that transorbital neuroendoscopy techniques should be firmly adopted into the neurosurgeon's armamentarium. We suggest that if this approach is going to grow and develop, large-volume prospective clinical studies with meticulous data collection must be completed.

Although physicians in the facial and reconstructive specialty (Moe et al., 2010) originally proposed and promoted transorbital neuroendoscopy, the majority of published cases are from neurosurgical departments or have neurosurgical input. What is evident is that evolution and advancement of this surgical intervention requires a multidisciplinary team that incorporates neurosurgeons, ophthalmologists, and otolaryngologists is preferred.

Cerebrospinal Fluid Leaks managed with TONES

The pathology of CSF leaks had the largest collective cohort and arguably has the strongest evidence with regard to TONES. The causes of the CSF leaks were identified as

posttraumatic, iatrogenic (postoperative), or congenital (presence of an encephalocele). Almost all of these cases involved the anterior cranial fossa, and the majority were managed solely via the transorbital route.

Five of the 30 patients with CSF leaks had a postoperative complication. CSF leakage recurred in 2 of the patients; the first patient, as noted in the article, was not adhering to medical advice, and the second patient was already recovering from a postoperative periorbital hematoma. Both complications resolved with the placement of a lumbar drain. These findings suggest that the rate of success (defined as resolution of the CSF leak) for an endoscopic transorbital repair of a CSF leak is 28 of 30 cases (93%), with 6 of the 30 successful cases being redo surgeries where a repair had already been attempted via an alternative technique.

The success rates for endoscopic endonasal CSF leak repairs varied in the literature from 83% to 100% (6 studies; n = 142 total patients). (J. A. Burns, Dodson, & Gross, 1996; Janakiram, Subramaniam, & Parekh, 2015; Tosun et al., 2003; Wax, Ramadan, Ortiz, & Wetmore, 1997; Wormald & McDonogh, 1997; Zweig et al., 2000) Regarding craniotomy for CSF leak repair, some studies report a success rate as low as 70%–80%, (McMains, Gross, & Kountakis, 2004) with potential risks including anosmia, memory deficits, seizures, osteomyelitis, and recurrence. (Ismail, Costantino, & Sen, 2007; Nyquist, Anand, Mehra, Kacker, & Schwartz, 2010) There are few cases where comparative analysis of the TONES technique has data comparable to a craniotomy counterpart. (Noiphithak et al., 2019) The international neurosurgical community is still developing the ability and insight necessary to evaluate this operative approach. Given that this report is the largest and only

cumulative cohort describing transorbital CSF leak repairs, a recurrence rate of 7% (2 of 30 cases) and a cumulative complication rate for transorbital interventions of 13% (9 of 69 cases) compare favorably with the present surgical alternatives.

Transorbital Tumor Surgery

Several histological types of tumors were managed via either the transorbital or the transorbital and transnasal routes. Of the 31 patients with tumors, the meningioma cohort was the largest, with a modest success rate associated with gross total resection, which was achieved in almost 70% of cases. Among the 7 patients with meningioma who reported preoperative neurological deficits, 5 had improvement in EOM impairment, visual acuity, proptosis, and ptosis. Two of these cases were for the treatment of recurrent meningioma. A combined transorbital and transnasal approach was used for 6 patients, whereas 7 patients were managed with a transorbital route only. Given the notable improvement in patient symptoms, the lack of complications, and the minimally invasive surgical approach, both the combined transorbital and transnasal route and transorbital-only route for managing skull base meningiomas of the anterior and middle cranial fossae have significant potential and warrant further clinical investigation.

Of note, in June 2020, a case series was published by Kong et al. comparing TONES and TONES plus lateral orbitotomy over a 3-year period, in which 41 patients were treated for spheno-orbital meningiomas. (Kong, Kim, & Hong, 2020) Nineteen of these patients were treated with TONES alone, but the patient-specific details were not reported in the published article or supplementary data and were thus not included in our

study's cumulative cohort. The research group surmised that gross total resection for spheno-orbital meningiomas was best achieved when combined with a lateral orbital rim osteotomy. The publication of this study and its impressive patient numbers illustrate how the use of this approach in neurosurgical practice is increasing and appears to be specifically suitable for the management of spheno-orbital meningiomas.

Few complications were noted in the tumor cohort. One patient with a tumor developed an orbital pseudomeningocele and underwent placement of a ventriculoperitoneal shunt. This case involved a biopsy of an intradural, mesiotemporal lobe lesion via a lateral incision through a transorbital approach. A second patient experienced a superficial surgical site infection, which had an uncomplicated resolution with antibiotic treatment.

Surgical Length of Stay

Endoscopic approaches promote rapid recovery by minimizing postoperative complications and discomfort and decreasing hospital LOS. (Shimanskaya et al., 2018) The transorbital approach has been identified to have favorable hospital LOS. (Castelnuovo et al., 2013) The mean LOS for patients treated transorbitally for CSF leakage was 12.2 days (range, 4.5-19.5 days). For transorbital tumor resection, the mean was 3.25 days (range, 2-6.5 days). Within the infection cohort, the mean LOS was 26.5 days (range, 21-32 days). Among the other transorbital surgical interventions, the mean LOS was 5 days (range, 2-5 days). These results show a vast spectrum of hospital admission periods. However, these data do not accurately represent the true LOS among a

cohort of patients treated via the TONES approach. Although attempts were made to account for all patient information, there were missing data regarding patient LOS. Additionally, there is significant skewness in the means for each pathology. Within the CSF leak cohort, 10 of the 30 patients were inpatients for over 7 days, likely secondary to adjunct injuries following their original trauma. In the 2 patients treated for intracranial infection, both stayed in the hospital for over 20 days, most likely because they were treated with intravenous antimicrobial therapy. The mean LOS identified for tumor surgery of 3.25 days (range, 2-6.5 days) is probably closer to reality for LOS for transorbital interventions.

Transient Postoperative Sequelae

The type of incision selected was at the discretion of the surgeon, whose decision was based on the site of the targeted pathology and the surgeon's confidence and competency with the incision. We describe the transient postoperative clinical effects of specific incisions on complications. The precaruncular approach has never been associated with complications. (Moe, 2003; Vijayalakshmi, 2007) Nonetheless, 2 cases of diplopia and 1 case of V2 numbness were noted after precaruncular intervention (Figure 3.4). Concerning a lateral incision, 2 cases of V2 numbness and 1 case of diplopia are reported. The SLC incision appears to cause the most clinical sequelae, with 2 cases of diplopia and 3 cases of ptosis reported. The duration of these effects was not reported in the articles, but all cases were noted to be temporary. This is true apart from a case where a patient underwent transorbital debulking of fibrous dysplasia via an SLC incision,

which resulted in permanent proptosis. The length of follow-up was not recorded in this case.

Transorbital surgical intervention was markedly associated with diplopia, V2 numbness, and ptosis postoperatively. In contrast, the combined transorbital and transnasal approach was less likely to result in diplopia and V2 numbness, with no cases of ptosis documented. This finding may echo the surgical principals of the multicompartmental approach promoted by Dallan et al and Castelnuovo et al, (Castelnuovo et al., 2013; Dallan, Castelnuovo, et al., 2015) who believed that the key to minimally invasive surgical techniques with extensive visualization and improved surgical access is a multi-surgeon, multiport approach. It is possible that attempting to insert both an endoscope and instrumentation through a single periorbital incision traumatizes the surrounding structures more than in cases where a proportion of the surgical instruments enter the cranial vault via an additional keyhole opening.

It is reasonable to expect these postoperative sequelae, given the skin incisions and proximity to the orbital contents. It may be argued that these are acceptable surgical effects, especially given the fact that these effects are temporary in the majority of cases. One author commented that the ptosis was noted by the surgical team and not by the patient. (Moe et al., 2011) Regardless, when selecting the appropriate incision for the patient, it is important to be aware of these postoperative effects to minimize any factors that may increase the patient's hospital LOS and hinder the patient's rehabilitation.

The paucity of clinical data and the gaps in patient data hindered the potential reach of this review and prevented a meta-analysis from being completed. The surgical rationale behind the selection of the sole transorbital or combined transorbital and transnasal route could not be established. Therefore, it is not possible to assess the respective surgical corridors used for the different pathologies.

The only anatomical variable we could establish throughout the entire body of literature was whether the pathology and surgical route focused on the anterior or middle fossa. Better anatomical data would have helped elucidate the decision-making process for selecting a transorbital or combined transorbital and transnasal approach. The lack of anatomical data could have accounted for some factors not being considered when calculating complication rates. This situation limited the comparisons that could be extrapolated from the published data.

All interventions and complications were reported by the authors without an objective reporting system. We found vast heterogeneity in the nomenclature and definitions used by the authors. This phenomenon is an unfortunate result of pooled data from multiple articles.

The published clinical data on TONES predominantly describe extra-parenchymal procedures. The increase in the number of cadaveric publications detailing complex parenchymal and neuronal structures appears promising for further clinical research.

Conclusion

TONES is an innovative development for approaching pathology in transorbital skull base surgery. However, there are few clinical studies, likely due to the relatively recent development of this approach and inconsistent, subjective means of data recording. Apart from the use of TONES at centers of excellence in skull base surgery, comprehensive and robust comparative analyses and generalizability, along with increased use of this technique in skull base surgery, are awaited. The dialogue on technical and operative superiority is premature. At present, given the body of data available, it is difficult to appreciate the applicability of the approach, although the transorbital route has had a long legacy of interest within neurosurgical, ophthalmological, and craniofacial surgical disciplines. We propose that this technique has merit and should be incorporated as a mainstream minimally invasive, minimally morbid surgical option, especially in the management of middle cranial fossa skull base meningiomas and schwannomas. However, further prospective studies are warranted. Whether a relatively minimally invasive, transorbital surgical corridor becomes a cardinal pillar of skull base surgical practice is yet to be seen, but such a corridor would seem to possess significant advantages.

CHAPTER 4

This following chapter is in preparation for submission to the Journal of Neurosurgery.

CHAPTER 4

TRANSORBITAL MICROSURGERY: A MINIMALLY INVASIVE CORRIDOR TO THE ANTERIOR CRANIAL FOSSA AND PARAMEDIAN STRUCTURES

Houlihan L.M., Loymak T., Abramov I., Labib M.A., O'Sullivan M.G.J., Lawton M.T., Preul M.C.

Abstract

Objective: The aim of endoscopic orbital access is to achieve equal visibility, surpass anatomical limitations of the endonasal approach, and decrease overall invasiveness and complications of open skull base surgery. Transorbital neuroendoscopic surgery (TONES) has ignited increasing interest in the transorbital access corridor, increasing its use as single and multi-portal skull base interventions. However, the capabilities of the endoscope are limited. Crowding of an already small corridor and 2-dimensional viewing restrict the benefits of this access portal. Studies have yet to prove the feasibility of the microscope for transorbital microsurgery (TMS).

Methods: Dissection of six cadaveric specimens was systematically completed using TMS to the anterior cranial fossa and paramedian structures. Dissection steps and instrumentation were recorded to ensure homogeneous methodology. Anatomical parameters of the TMS craniectomy were established, and the visible and accessible neuroanatomy was highlighted. Each orbital roof craniectomy was measured to determine mean size.

Results: A superior lid crease incision achieved essential orbital rim exposure and preseptal dissection. Deep dissection along the medial wall led to the optic nerve, where it exits the optic canal. The orbital roof craniectomy is defined by three boundaries: (1) frontozygomatic suture to the frontosphenoid suture, (2) frontal sinus and cribriform plate, and (3) frontal sinus and orbital rim. The mean (standard deviation) craniectomy was 440 mm^2 (78 mm^2). Exposure of the ipsilateral optic nerve and internal carotid artery obviates the need for frontal lobe retraction to identify the A1-M1 bifurcation. The complete length of the ipsilateral A1 is visible and accessible. Minimal manipulation of frontal and temporal lobes is necessary to produce nearly complete visualization of the M1 artery. Although the anterior communicating artery is evident, visualization and instrument maneuverability are obstructed by the lateral orbital rim, inhibiting the ability to operate.

Conclusion: TMS is a feasible corridor for intracranial access. Mobilization of orbital contents is imperative for maximal intracranial access and protection of the globe. TMS enables access to the frontal lobe base, ipsilateral optic nerve, and most of the ipsilateral anterior circulation. The orbital rim acts as the superior and lateral boundaries, limiting instrument freedom and impairing midline visualization. This cosmetically satisfactory approach causes minimal destruction of the anterior skull base with maximal exposure of the anterior cranial fossa floor without sinus invasion.

Introduction

Transorbital neuroendoscopic surgery (TONES) is an advanced minimally invasive, minimally disfiguring type of skull base surgery that maximizes surgical visualization. (Dallan, Castelnuovo, et al., 2015) Previously, the term *transorbital* had diverse meanings, and the approach usually included variations of the lateral orbitotomy or zygoma-sphenotomy. (Ulutas et al., 2019) Increased use of the TONES access corridor has also increased recognition of the transorbital approach. The drive toward minimally invasive surgical interventions has helped identify an operative corridor to the skull base through the orbital bone without removing the orbital rim, thereby preserving structural integrity. (Benedict, 1949; Moe et al., 2010)

Introduced in 2010, TONES has been documented for use treating multiple anterior skull base pathologies, including cerebrospinal fluid (CSF) leaks, meningoencephaloceles, optic nerve decompression, skull base fractures, inflammatory intraorbital lesions, intracranial abscesses, and skull base tumors. (Moe et al., 2010; Moe et al., 2011; Ramakrishna et al., 2016) Despite its technological advances, TONES has weaknesses and advantages that require elucidation. This minimally invasive skull base approach seeks to maximize surgical efficiency while minimizing exposure and manipulation of neurovascular structures and resultant morbidity. Disadvantages associated with TONES include a paucity of evidence (level IV, at best), the lack of adequate orbital instrumentation appropriate to surgical depth, and surgical corridor crowding. (Priddy et al., 2017) Inserting both an endoscope and standard instrumentation through a periorbital incision may injure surrounding structures more than when some of the surgical instruments enter the cranial vault through a larger opening or an additional

keyhole. Furthermore, pioneers in the field remain cautious and advocate maintaining the ability to convert swiftly to an open craniotomy in an emergency, which has not yet been necessary. (Castelnuovo et al., 2013; K. Moe, 2007) Such concerns highlight potential weaknesses of TONES, specifically regarding its instrumentation and visualization methods, and raise questions about how best to minimize intraportal instrumentation when using the transorbital corridor. The feasibility and advantages of transorbital microsurgery (TMS) have yet to be investigated. Therefore, we sought to identify the optimal transorbital craniectomy, an approach with maximal exposure and minimal destruction of the skull base, and to identify the accessible intracranial structures most appropriate to this surgical corridor. Our research aim is to elucidate the merits of the microscopic visualization method.

Methods

The study was conducted in the surgical neuroanatomy laboratory at Barrow Neurological Institute, Phoenix, Arizona. Six cadaveric heads embalmed in an alcohol-formalin-based solution were dissected, and arteries and veins were injected with red and blue silicone. The transorbital approach to the anterior cranial fossa (ACF) and paramedian structures was systematically completed and visualized using a clinical neurosurgery operating microscope (OPMI Pentero, Carl Zeiss Meditec AG, Oberkochen, Germany). Dissection steps and instrumentation were recorded to ensure a homogeneous approach methodology. High-definition (HD) 3-dimensional (3D) video images were

obtained using the Trenion 3D HD system (Carl Zeiss Meditec) and displayed on an HD LED monitor.

The orbital roof craniectomy was measured 3 times in all 6 specimens by different neurosurgeons to account for interrater and interrater variability and to obtain the mean size, thereby ensuring standardized and feasible technical replication. Repeated measurements facilitate the estimation of variability and improve the power of the analysis. Measurements were performed using a clinical neurosurgery navigation system (StealthStation, Medtronic plc, Dublin, Ireland). Every point was regarded as a spatial point with three coordinates (*x, y,* and *z*), with units in mm. This method of visualization enabled us to establish the anatomical parameters of the TMS craniectomy and the visible and accessible neuroanatomy specific to this access corridor.

Statistical Analysis

Statistical analysis of our measurements was performed using open-source statistical software: R.app (GUI 1.72 [7847 Catalina build], S. Urbanek & H.-J. Bibiko, R Foundation for Statistical Computing, Vienna, Austria, 2020) and RStudio (1.3.1073, RStudio, PBC, Boston, MA, 2020). Data are reported as means with ranges and standard deviations.

TMS Superior Lid Crease Approach: Surgical Technique

Step 1: Positioning - Tailor to Surgical Situation

The head is positioned supine with a shoulder roll. Subtle extension produces the optimal angle for review of the frontal lobe base, especially anteriorly, and for access to deeper neurovascular structures (Figure 4.1).

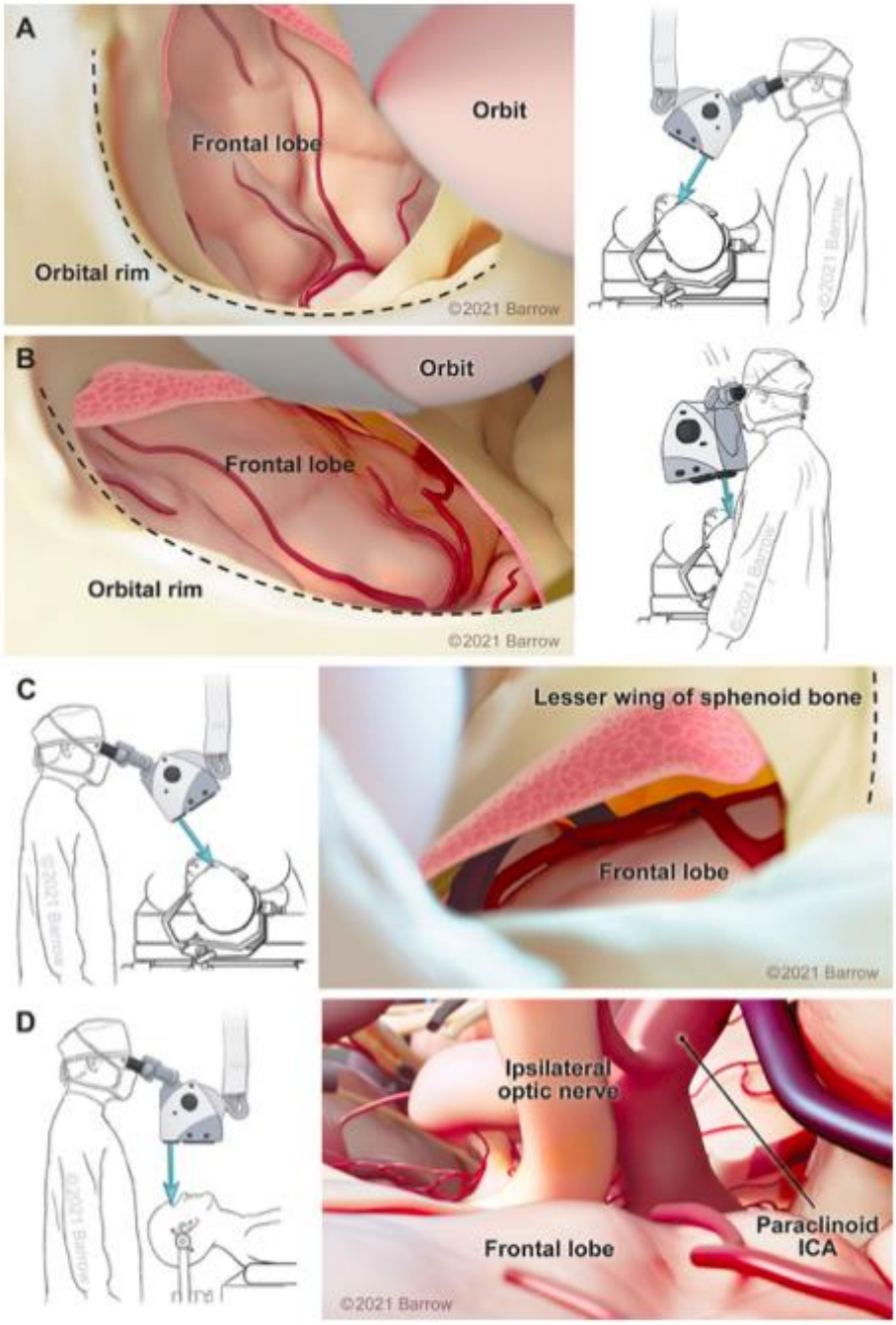

Figure 4.1. Illustration depicts the positioning of the patient, microscope, and surgeon for access to particular anatomical structures from a right-sided superior lid crease approach.

(A) Medial view of the frontal lobe base with the microscope tilted superomedially. The surgeon is positioned parallel to the patient's ipsilateral shoulder. (B) Positioning needed to achieve the most superior-anterior view of the frontal lobe base, with the microscope tilted superiorly along the axis of the mid-pupillary line. The surgeon and microscope are positioned at a 45° angle to the patient's ipsilateral shoulder. (C) Positioning needed for the most lateral view of the frontal lobe base, with the microscope tilted superolaterally. The surgeon is positioned on the patient's contralateral side either parallel to or along the axis of the patient's shoulder. (D) Positioning for evaluation of deep neurovascular structures. The surgeon is positioned at the patient's head, with the microscope directed straight down through the transorbital incision. This positioning of the microscope provides a coplanar view of the intracranial paramedian components at the level of the orbital roof. Used with permission from Barrow Neurological Institute, Phoenix, Arizona.

The head is fixed with a 3-pin holder and rotated from 0° to 45° contralaterally. Optimal positioning and rotation are based on the surgical target of interest. For the accessible portion of the ipsilateral middle cerebral artery, rotation is not necessary. Rotation from 10° to 30° is optimal for review of the ipsilateral internal carotid artery (ICA) and up to 45° for viewing the anterior communicating artery and circumferential midline region.

Step 2: Superior Lid Crease Incision

A lubricated corneal protector is placed over the orbit. The supraorbital notch and exit point of the supraorbital nerve are identified (Figure 4.2).

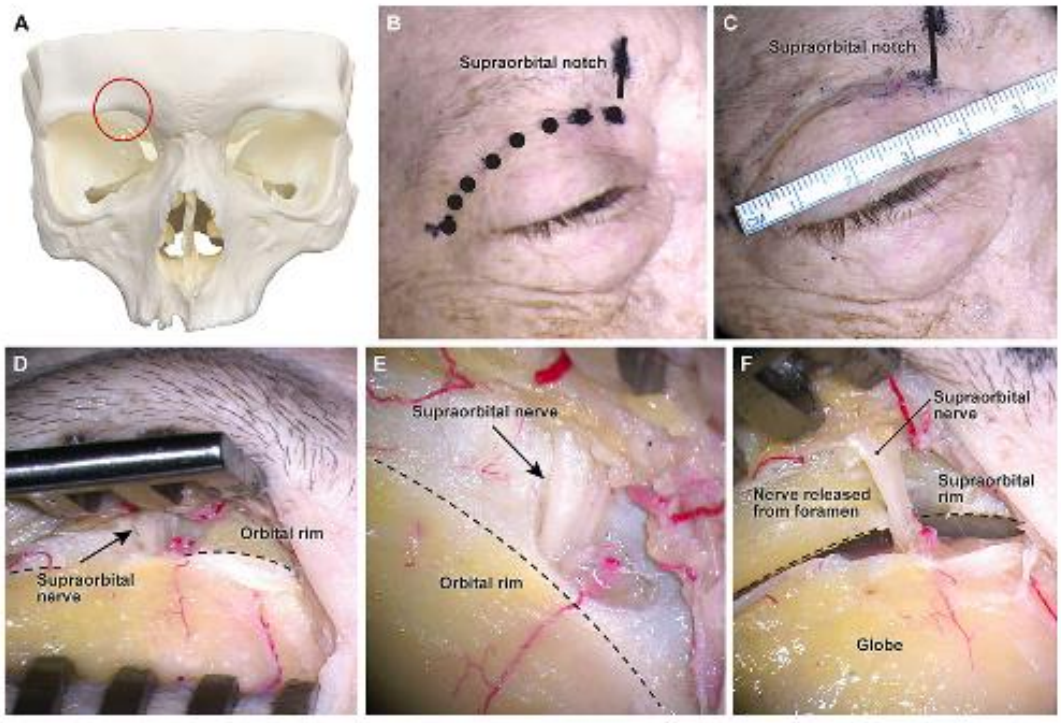

Figure 4.2. Incision marking and superficial dissection. (A) Depiction of the photographic marker of the region of interest (supraorbital nerve) with anatomical annotator (circle) for orientation. (B) Marking for the superior lid crease (SLC) incision, with identification of the supraorbital notch (vertical line). (C) The SLC incision measures approximately 4-5 cm. Vertical line representing the palpation point of the supraorbital notch. (D) Undermining of the subcutaneous tissues to expose the orbital rim and supraorbital nerve. (E) Exit of the supraorbital nerve from the supraorbital foramen. (F) Release of the

supraorbital nerve from the supraorbital foramen to allow increased mobilization and manipulation. Used with permission from Barrow Neurological Institute, Phoenix, Arizona.

The natural crease in the upper eyelid is used to plan a 4 to 5 cm incision. The orbital rim must be identified for direct dissection along that trajectory. Eyebrow skin is elevated and undermined to ensure full visualization. Sharp dissection through the orbicularis oculi muscle is completed along the preseptal plane to identify the superior orbital rim. Injury of the levator aponeurosis leading to ptosis is avoided by exposing the orbital rim superficial to the fat pad. The supraorbital nerve is identified and preserved, if possible. For maximal mobilization, the nerve is released from the supraorbital canal. The periosteum is incised to enable subperiosteal dissection. The frontozygomatic suture is identified along the lateral orbital rim (Figure 4.3). The suture represents the lateral and inferior boundary of the ACF.

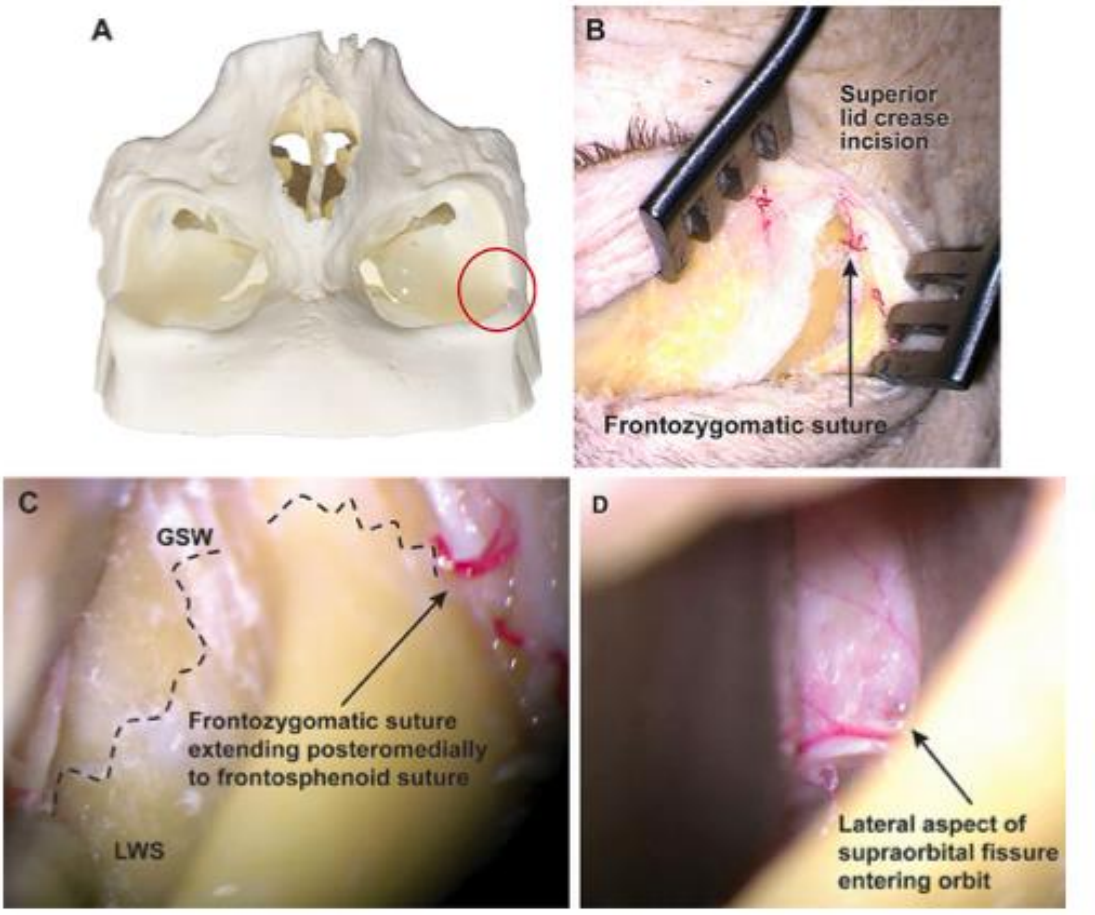

Figure 4.3. Cutaneous dissection, identification of the lateral boundaries, and subperiosteal dissection toward the superior orbital fissure. (A) Microscope trajectory of images viewed for orientation. The frontozygomatic suture (circle) marks the lateral and most inferior boundary of the anterior cranial fossa (ACF) and delineates the ACF and the middle cranial fossa (MCF) as the frontozygomatic suture extends posteromedially. (B) Lateral orbital rim with exposure of the frontozygomatic suture as it extends posteromedially and intersects with the frontosphenoid suture. (C) Microscopic deep view of the lateral orbital wall following the frontosphenoidal suture line to the lateral

margin of the superior orbital fissure. GWS, greater wing of the sphenoid; LWS, lesser wing of the sphenoid. (D) Lateral aspect of the supraorbital fissure entering the orbit. Used with permission from Barrow Neurological Institute, Phoenix, Arizona.

Step 3: Periorbital Dissection

After the periosteum is incised at the orbital rim, a window is opened for subperiosteal dissection along the intraorbital roof. A dissector is first used to gently sweep laterally to release the lateral orbital contents before sweeping medially and posteriorly to the supraorbital nerve while avoiding retraction of the nerve. A periosteal window is then incised medial to the supraorbital nerve, and the subperiosteal dissection is advanced medially. The anterior ethmoidal artery is identified, cauterized, and cut along the side of the periorbita (Figure 4.4).

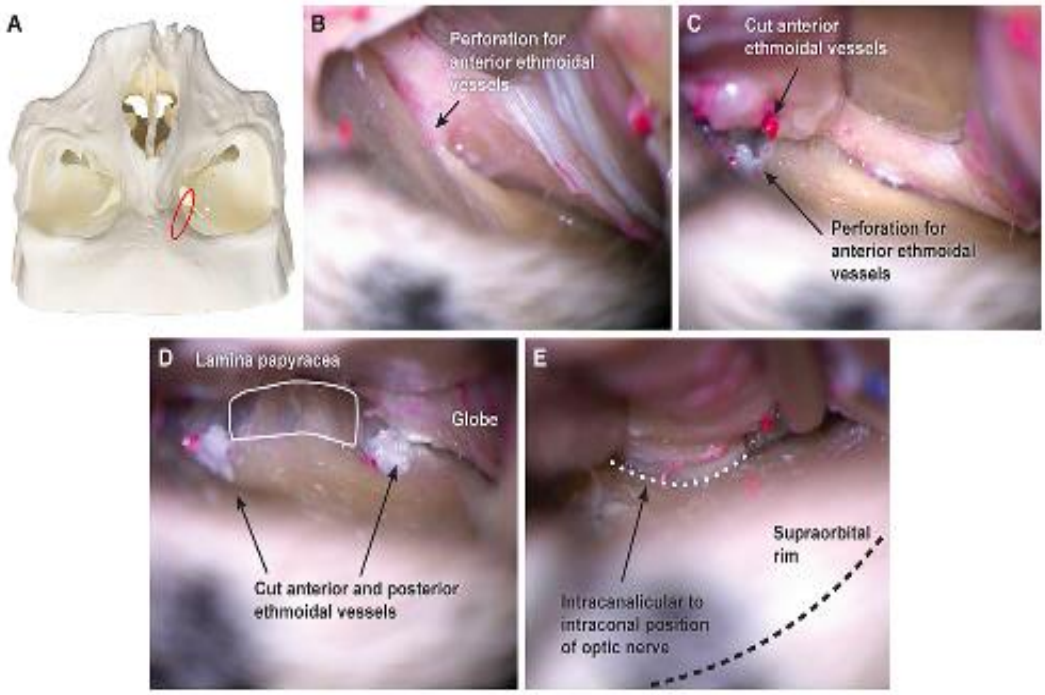

Figure 4.4. Microscopic view of the medial subperiosteal dissection that permits full mobilization of the globe. (A) Microscope trajectory (circle) of subsequent images viewed for orientation. (B) The first medial structure is the perforation of the lamina papyracea for the anterior ethmoidal vessels. (C) Transection of the anterior ethmoidal vessels permits further mobilization of the orbital contents. This mobilization allows deeper dissection and exposure of the posterior ethmoidal vessels along the same plane. (D) Transection of the anterior and posterior ethmoidal vessels for full medial exposure of the optic canal. (E) Medial disconnection of the ethmoidal vessels and content mobilization enables deep microscopic intraorbital visualization. Dynamic retraction during extracranial dissection minimizes the need for long periods of fixed globe retraction. Used with permission from Barrow Neurological Institute, Phoenix, Arizona.

The vessel is not cut along the ethmoidal canal border to avoid retraction of an inadequately cauterized vessel, resulting in inaccessible hemorrhage. The bony region medio-inferiorly corresponds with the lamina papyracea. Subperiosteal dissection posteromedially is continued using a periosteal dissector. The posterior ethmoidal artery along the same plane is cauterized and cut. Just superior to the anterior and posterior ethmoidal arteries is the frontoethmoidal suture, which continues anteriorly as the frontolacrimal suture. Deep dissection farther along the medial wall leads to the optic nerve, where it exits the optic canal. Laterally, the optic strut, which projects posteromedially, separates the optic canal from the superior orbital fissure. The frontosphenoid suture lies at the superolateral apex of the superior orbital fissure (Figure 4.3). Drilling superior to it leads to the ACF, which is inferior to the MCF. The bone superior to the optic canal represents the most posterior, most medial, and deepest angle of the TMS craniectomy. This point also represents the axial plane (the optic canal roof) along which intraparenchymal structures are identified.

Adequate subperiosteal dissection ensures that the globe is mobile, that satisfactory space exists for a safe craniectomy, and that the surgical corridor is maximized for intracranial work and instrument access. Ample mobilization of orbital contents maximizes the access corridor and minimizes aggressive retraction.

During completion of the cutaneous and subperiosteal dissection, the dissector and suction are used as dynamic retractors. This dual-purpose usage avoids the need for constant, fixed retraction and maximizes a small, potentially crowded, surgical corridor.

Both dynamic and fixed retraction using malleable ribbon retractors is used to complete the craniectomy. A fixed retractor can be used during intracranial manipulation and dissection. During retraction, the retractor is placed along the natural curve of the globe; ventral pulling is avoided to prevent injury to intracranial structures. A key component of any transorbital approach is awareness of the pressure applied to the globe during intraorbital and intraparenchymal dissection. All instruments should be removed from the orbit every 15- 20 minutes, at which point the pupils are checked for symmetry.

Step 4: Orbital Roof Craniectomy

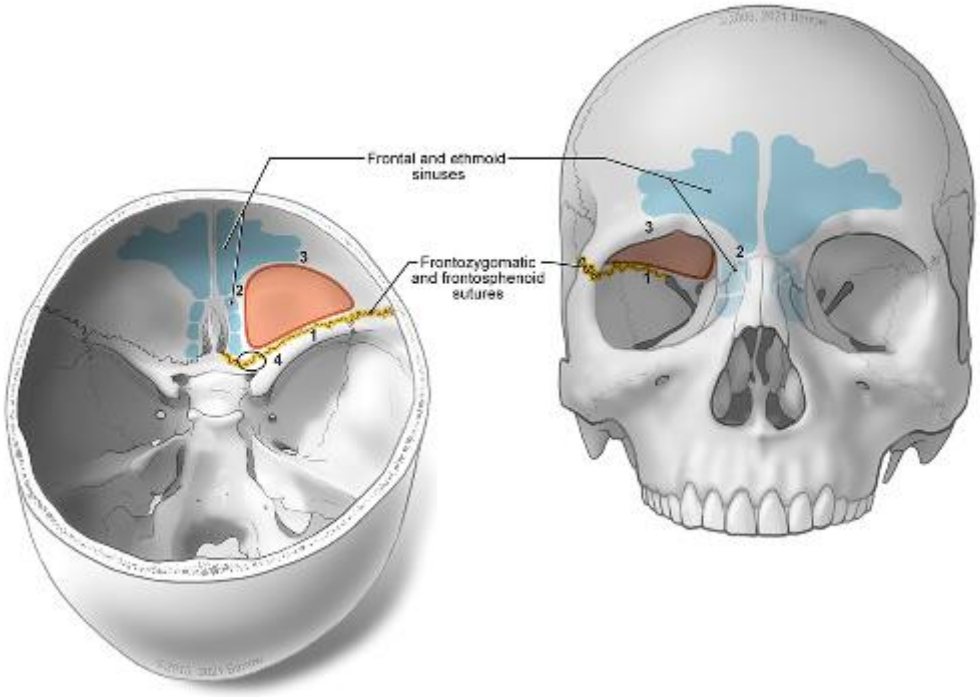

Figure 4.5. Boundaries of the transorbital microsurgery (TMS) craniectomy. (A) Anterior view of critical structures that dictate the extent of the craniectomy, with the orbit retracted inferiorly, including the frontal and ethmoidal sinuses medially and the frontozygomatic suture to the frontosphenoid suture laterally. (B) Axial illustration delineating the boundaries of the craniectomy established using TMS: (1) medial boundary: frontal sinus and junction of the frontal bone and cribriform plate of ethmoid bone; (2) anterior boundary: frontal sinus medially and orbital rim laterally; and (3) lateral boundary: frontozygomatic suture to frontosphenoid suture leading back to the roof of the optic canal. Used with permission from Barrow Neurological Institute, Phoenix, Arizona.

The transorbital craniectomy has three boundaries: (Figure 4.5):

(1) Lateral boundary: Frontozygomatic suture to frontosphenoid suture leading back to the roof of the optic canal
(2) Medial boundary: Frontal sinus anteriorly and the junction of the frontal bone and cribriform plate of the ethmoid bone
(3) Anterior boundary: Frontal sinus medially and orbital rim laterally

In this study, the craniectomy was completed using a high-speed bone-cutting and removal system (Midas Rex Legend, Medtronic) with a telescoping tube attachment (T12BA20) and upcutting rongeurs (1 mm). The aim was to complete a maximal craniectomy for feasible exposure and access to the ACF and paramedian contents. The

TMS craniectomy was completed sequentially. All drilling was completed lateral to the supraorbital nerve (Figure 4.6). Dissection of medial soft tissue was only to allow maximal mobilization of the globe.

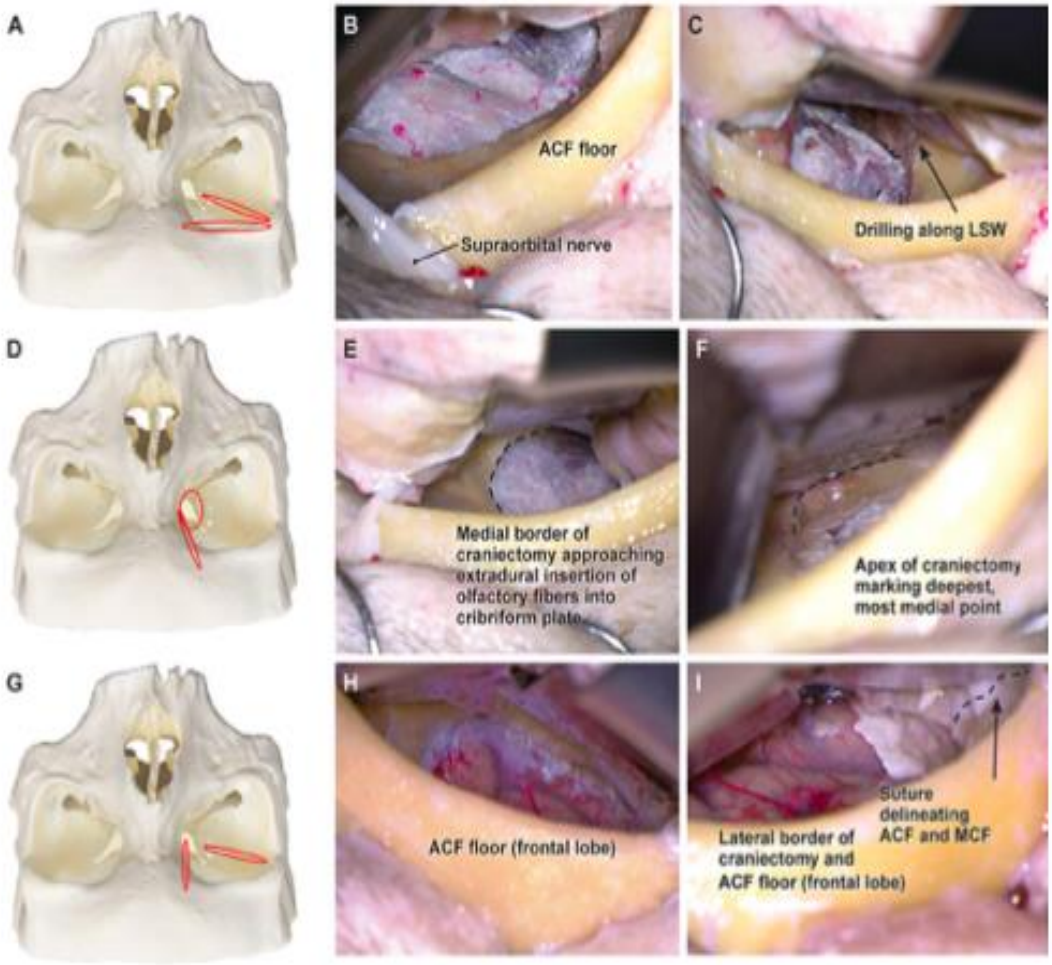

Figure 4.6. Microscopic extradural and intradural views of the floor of the anterior cranial fossa (ACF) upon completion of the craniectomy performed using transorbital microsurgery (TMS). (A) Microscope trajectory (circles) of subsequent images viewed

for orientation. (B) Anterosuperior view of the ACF floor, which has more medially preserved bone as evidenced by the presence of the frontal sinus and preservation of the supraorbital nerve. (C) Anterolateral view of the extradural exposure, where the lesser sphenoid wing (LSW) has been drilled to extend the craniectomy posteriorly. (D) Microscope trajectory (circles) of subsequent images viewed for orientation. (E) Microscopic view of the medial boundary at the junction of the frontal bone and the cribriform plate of the ethmoid bone. (F) Apex of the craniectomy, where the flat level of the roof of the intracranial optic canal, which represents the lowest accessible plane of this approach, can be palpated extradurally. (G) Microscope trajectory (circles) of subsequent images viewed for orientation. (H) Medial microscopic view of the ACF floor (frontal lobe) and parenchyma. (I) Lateral microscopic view of the ACF floor (frontal lobe) parenchyma. Note that the full extent of the TMS craniectomy cannot be visualized in only one view because of the curvature of the orbital rim. MCF, middle cranial fossa. Used with permission from Barrow Neurological Institute, Phoenix, Arizona.

A safe, advantageous point to commence the craniectomy (after identifying and avoiding the frontal sinus) is approximately 1 cm lateral to the lateral margin of the supraorbital nerve and 1.5 cm posterior to the orbital rim. This region usually contains thin shell-like bone that is accessible to drill, enabling quick extradural infiltration of the cranium. After the dura has been identified and a craniectomy window established, the dura is preserved as long as possible during craniectomy enlargement to protect the frontal lobe parenchyma. After a defect is created, a blunt dissector is used to sweep the

dura from the fossa floor. Undermining the dura is important for better dural repair later in the operative intervention. Drilling and upcutting rongeurs are used while advancing anteriorly, laterally, and medially. In thin regions, the orbital roof can be down-fractured. Extradural insertion of olfactory fibers entering the cribriform perforations can be appreciated as the dura is detached along the medial boundary. Palpation of these perforations is an additional intraoperative means to identify the medial boundary of the TMS craniectomy.

The thick lateral border of the craniectomy superior to the frontozygomatic suture and frontosphenoid suture warrants using a drill instead of a bone punch on the lesser wing of the sphenoid bone to extend the craniectomy. The frontosphenoid suture, which projects posteromedially, represents the most lateral boundary of the craniectomy. Drilling above this suture retains the procedure in the ACF, whereas drilling below it results in entry into the MCF. A dissector is used to palpate the extradural inner table of the lesser sphenoid wing, and the deep lateral extent can be appreciated when the ridge dividing the ACF and MCF is visualized. Drilling progresses medially until the medial and lateral craniectomy boundaries converge at a deep apex, i.e., the roof of the optic canal.

A deeper extension can be achieved by careful drilling with a telescoping tube attachment. The deepest extension of the craniectomy is determined either by visualization of bone quality changing from cortical to cancellous at the root of the anterior clinoid process or by palpation of the flat level of the intracranial optic canal roof medial to it that represents the lowest accessible plane of this approach. The roof of the

optic canal can be removed and the optic nerve decompressed, but doing so will not increase craniocaudal exposure and may increase the risk of injury to the ophthalmic artery as it transverses the canal along the inferomedial surface of the nerve.

Discretionary anterior drilling of the orbital roof is limited by the extent of the frontal sinus. For frontal lobe pathology, the anterior craniectomy boundary should be maximized to the orbital rim. Interventions focused on paramedian and neurovascular structures do not require anterior exposure. However, greater maneuverability and access to medial structures can be achieved by continuing the craniectomy to the most lateral boundary.

High-resolution computed tomography (CT) is essential for preoperative planning. Intraoperative neuronavigation aids identification of the borders of sinuses and further delineates the superomedial and medial craniectomy boundaries. The frontal and ethmoidal sinuses are key structures that influence the anatomical breadth and boundaries of this approach. Without CT, the surgeon may inadvertently enter the frontal sinus and blindly extend the craniectomy anteromedially. Drilling inferior to the foramina of the anterior and posterior ethmoidal vessels results in fracture of the lamina papyracea and invasion of the ethmoid ostium. Although entry into the ethmoid sinus can be completed for a more medial approach or may be appropriate for lesions invading the sinus, doing so requires repair of an additional defect. Thus, every attempt should be made to preserve the lamina papyracea. Although the junction of the frontal bone and cribriform plate is not appreciable through an intraorbital view because of the curvature of the ethmoidal sinus, neuronavigation can facilitate its identification. Alternatively, when the original

defect has been made in the orbital roof, systematic lateral to medial bone removal can also delineate this junction extradurally.

Step 5: Dural Opening

The shape of the dural incision is based on the site where access is warranted. For frontal lobe lesions, the dura is incised in a cruciate fashion, with the reflection of the leaflets inferiorly from the field of interest. This incision substantially assists with dural closure. For access to the deep neurovascular structures, the dura is incised proximal to the anteromedial boundaries of the craniectomy. For increased mobilization, this incision can be extended around the anterolateral curvature of the craniectomy. After the incision reaches the deep apex at the roof of the optic canal, the single dural leaflet is reflected laterally for maximal medial exposure. A fixed retractor can be used from this point onward.

Results

Qualitative Analysis

Accessible Brain Parenchyma

The base of the frontal lobe is easily accessible through the craniectomy defect (Figure 4.6). Complete visualization is not possible with the operating microscope. Thus,

different angular views are used to appreciate the full extent of the exposure. Given the preservation of the cribriform plate, visualization of the gyrus rectus is not obvious.

Neurovascular Elements

The first appreciable deep structure is the ipsilateral optic nerve, as it follows the trajectory of the optic canal medially (Figure 4.7).

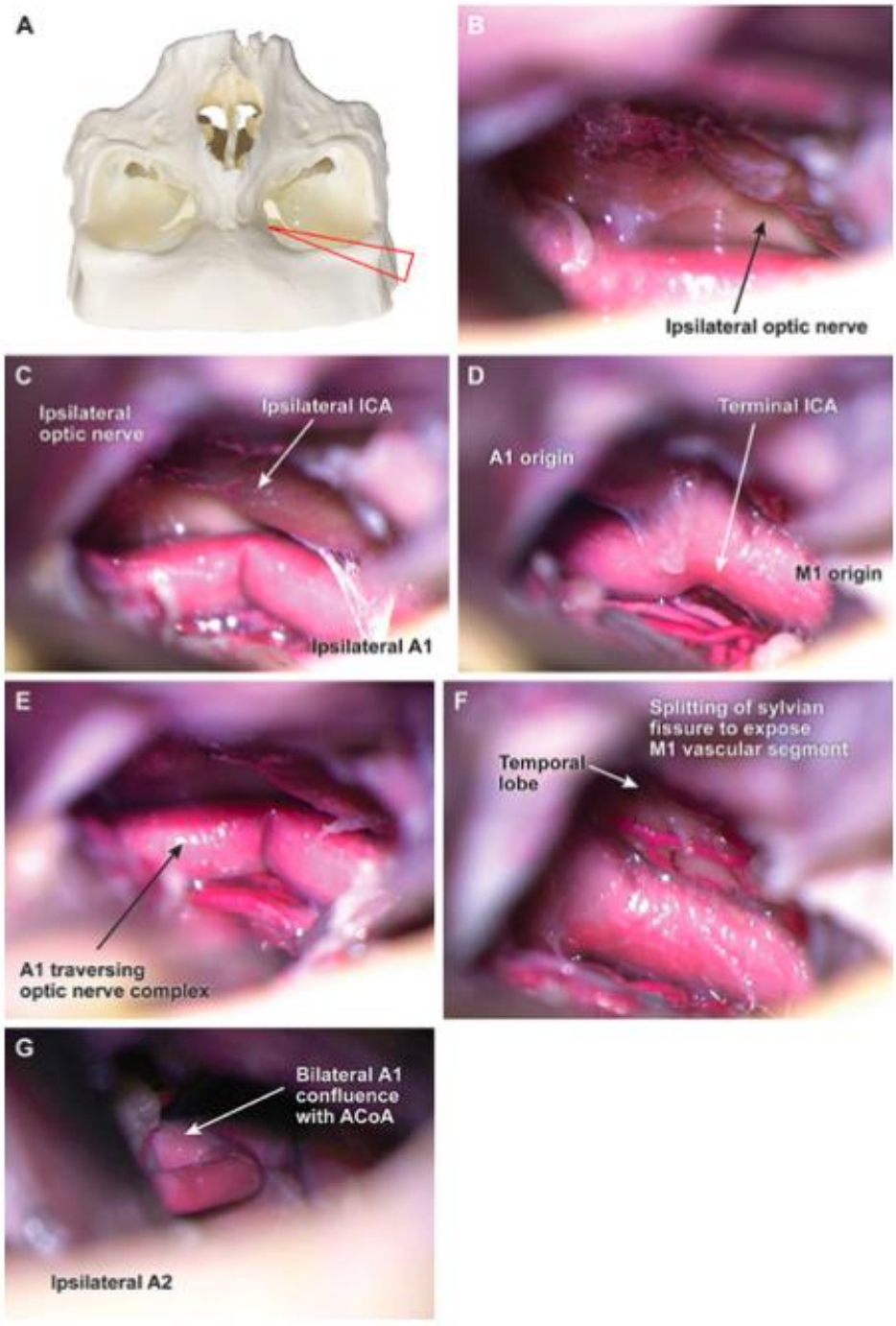

Figure 4.7. Microscopic view of the neurovascular structures visible and accessible through the transorbital microsurgery (TMS) craniectomy. (A) Microscope trajectory of

subsequent images viewed (triangle) for orientation. (B) The first identifiable structure is the ipsilateral optic nerve. (C) Full exposure of the ipsilateral internal carotid artery (ICA) from paraclinoid section to terminus. (D) Full exposure of the ICA terminus and the origins of the ipsilateral A1 and M1. (E) The complete length of the ipsilateral A1 is visible and accessible. (F) Gentle arachnoid dissection allows atraumatic splitting of the sylvian fissure and impressive exposure of the proximal M1 artery. (G) Deep visualization of the confluence of the bilateral A1 vessels with the anterior communicating artery (ACoA). Instrumentation use is hindered by the orbital rim. Used with permission from Barrow Neurological Institute, Phoenix, Arizona.

Lateral to the ipsilateral optic nerve, the paraclinoid ICA can be visualized. The full length of the intracranial ICA to the A1-M1 bifurcation is accessible without parenchymal retraction. Gentle arachnoid dissection medially allows atraumatic splitting of the sylvian fissure and impressive exposure of the proximal M1 artery. Following the ICA terminus medially reveals the complete length ipsilateral A1 artery as it traverses across the optic chiasm toward the anterior communicating artery complex. As the vasculature is followed medially, microscopic visualization and instrumentation maneuverability are limited by the lateral orbital rim. The confluence of the bilateral A1 vessels is evident, but no form of manipulation is possible because of the restricted instrument freedom (Figure 4.7F).

Size of TMS Craniectomy

The size of the craniectomies in the 6 cadaver specimens ranged from 337.07 to 572.34 mm^2. The mean (standard deviation) size was 440.53 mm^2 (78 mm^2). The size of the defect does not include the natural curvature of the orbital roof, as it would increase the reported area of exposure.

Discussion

TMS vs TONES

TONES is a clinically significant development in skull base surgery. It encompasses the modern requirements of a proficient surgical technique, minimizing morbidity, being minimally invasive, producing aesthetically satisfactory results, and decreasing hospital length of stay. (Castelnuovo et al., 2013; Dallan, Castelnuovo, et al., 2015) The aim of orbital access is to achieve equal visibility, surpass the anatomical limitations of the endonasal approach, and thereby decrease the overall invasiveness and complications of open skull base surgery. (Choi et al., 2018; Dallan, Castelnuovo, et al., 2015; Moe et al., 2010)

Both the microscope and the endoscope provide different technical and surgical benefits and disadvantages. The microscope was the first means for the visualization of minutiae, and it resulted in the advent of the microsurgery technique. Conversely, midline interventions require deep open dissection, and visualization attempts increase the risk of injury to superficial structures. The endoscope overcomes these obstacles, producing impressive midline illumination and panoramic views while avoiding the crossing of neurovascular structures. The endoscope is not without drawbacks, especially in

minimally invasive approaches. Unlike the microscope, which offers a 3D view and sophisticated proprioceptive awareness, the endoscope is 2-dimensional.

Crowding of the surgical corridor is a key limitation of the TONES visualization technique. Clinical sequelae of TONES include transient diplopia, V2 numbness, and ptosis. (Houlihan, Staudinger Knoll, et al., 2021b) In contrast, the combined transorbital-transnasal approach has a reduced rate of these adverse events. Inserting both an endoscope and instrumentation through a single periorbital incision may injure surrounding structures more so than in cases where some of the surgical instruments enter the cranial vault through an additional keyhole. Various reports in the neurosurgery literature have documented attempts to develop multiportal access in interventions that can still be considered minimally invasive. Multiportal endoscopic skull base approaches have evolved to maximize transorbital-transnasal and transorbital-open working angles to anatomical targets with multiple compartments. (Castelnuovo et al., 2013; Ciporen et al., 2010; Lim et al., 2020) Quantitative measurements of different parameters support the superiority of these approaches. The ultimate addition of a second working port will provide better visualization of structures and easier dissection because it will facilitate a two-handed technique. In contrast, a technical weakness of TONES is that it requires so much intraportal instrumentation. However, TMS, which is also a 2-handed technique, does not require an additional port.

TMS Considerations

Differences between the 2 approaches are inherent within the nuance of the operative technique. The TMS craniectomy provides a minimally invasive skull base–sparing corridor to the intracranial regions. Unlike TONES, TMS provides clearly defined anatomical parameters for maximal parenchymal and neurovascular exposure while preserving the structural and functional integrity of the skull base.

Lesions on the ACF floor may require large cosmetically unsatisfactory incisions, (Reinard et al., 2015) but, even more worryingly, they harbor an increased risk of serious complications. The SLC incision used in the current study is the most frequently reported cutaneous approach. (Houlihan, Staudinger Knoll, et al., 2021a) This incision provides wide medial and lateral access, allows for the maximal mobilization of the globe, and produces optimal maneuverability for accessing the ACF. It is also frequently used to access the MCF. (Park et al., 2020)

Previous anatomical reports detailing TONES used the anterior and posterior ethmoidal vessels as the medial boundary of the orbital roof craniectomy (Moe et al., 2010). However, extending the craniectomy medially this far inevitably results in an invasion of the ethmoidal sinus. Breaching the ethmoidal sinus should be considered an adverse event unless the target is pathology in the ethmoidal sinus or a biportal, transorbital transnasal approach is being used. In contrast, TMS provides a safe medial boundary that ensures preservation of the sinuses. It also protects the olfactory fibers perforating the cribriform plate.

Although no reports have documented postoperative visual deficits after the use of TONES, this possibility is a consideration of any transorbital approach. Vision should be

assessed both preoperatively and postoperatively, and intraoperative efforts should focus on minimizing retraction injury. The use of dynamic retraction during cutaneous and periosteal dissection minimizes fixed retraction of the globe throughout the procedure.

Published reports on TONES mention the use of fixed retractors only. (Balakrishnan & Moe, 2011) However, in TMS, surgical instrumentation and suction are used for dynamic retraction only during the preliminary steps of the operation, thus minimizing the risk of injury. Increased intraocular pressure is caused by direct compression of the optic nerve or its vasculature. (V. Lima et al., 2009; Winterton, Patel, & Mizen, 2007) The ophthalmic artery should also be protected. It enters the optic canal at the inferomedial aspect of the nerve and then courses laterally as it enters the orbit. The artery lies inferolateral to the nerve in 81% of patients and inferior to the nerve in 19%. (Li et al., 2008) When the globe contents are retracted while drilling superiorly, an awareness of these vascular structures at the apex is pivotal.

Another advantage of the transorbital access corridor is the low rate of CSF leaks, both iatrogenically and after defect repair. Neurosurgeons are adept not only at large open craniotomies to access the ACF but also at exclusive transnasal approaches. Craniotomies for the repair of CSF leaks have a low (70-80%) success rate (McMains et al., 2004), with potential risks of anosmia, memory deficits, seizures, osteomyelitis, and recurrence. (Ismail et al., 2007; Nyquist et al., 2010) The CSF recurrence rate after TONES repair is 7%. A CSF pseudomeningocele has been reported in only one patient after tumor resection. (Chen et al., 2015; Houlihan, Staudinger Knoll, et al., 2021a) These TONES results are comparable, if not superior, to those for open and transnasal interventions. It

has been hypothesized that these impressive outcomes regarding CSF leaks are due to the intraorbital pressure exerted by the globe's contents on the orbital roof defect. (Moe et al., 2010) Since normal intraocular pressure is approximately 15 mm Hg, (Knoop KJ, 2014) the idea that this pressure gradient facilitates superior dural defect closure and improved repair is noteworthy, albeit not scientifically assessed.

Indications for TMS

Lesions appropriate for TMS predominant depend on select factors, including anatomical site and positioning of the frontal and ethmoidal sinuses:

(1) Anatomical site: Two-handed functional instrumentation is possible in this surgical corridor when the microscope is used for visualization. ACF base meningiomas and low intraparenchymal lesions can be efficiently approached because of low skull base access. The ipsilateral anterior circulation can be manipulated with little or no lobar retraction and, when necessary, easy and rapid proximal control can be obtained at the level of the paraclinoid ICA. The cerebrovascular value of a transorbital approach has been reported previously. Drilling the posterior wall of the orbit and the lesser sphenoid wing exposes the sphenoidal portion of the sylvian fissure and the M1 and M2 segments of the middle cerebral artery. No published reports document the use of the transorbital approach for the clinical management of aneurysms, arteriovenous malformations, or cavernomas. The application of this corridor to neurovascular surgery will depend on instrument maneuverability and

proximal control. Determinants include the degree of the attacking angle in specific axes, satisfactory visualization for vessel interrogation, and surgical freedom. Preservation of the lateral orbital rim precludes the use of the TMS approach for visualization and access to more midline structures, including midline or contralateral vasculature.

(2) Position of the frontal and ethmoid sinuses: With frontal craniotomies, invasion of the frontal sinus or inadequate dural repair results in a 41% risk of CSF leak after craniotomy. (Imola, Sciarretta, & Schramm, 2003) Thus, minimally invasive methods like TMS for accessing the ACF and the ACF floor are pivotal to minimizing morbidity and mortality. The frontal and ethmoid sinuses are anatomically significant factors to consider when assessing whether TMS is an appropriate surgical corridor for a specific lesion. These structures may represent the entire anteromedial boundary for the craniectomy. If the aim is to tackle a low frontal anterior lesion, special attention should be paid to the extent of the frontal sinus. The transorbital craniectomy would be substantially restricted along the anterior boundary, making an invasion of the frontal sinus more likely during drilling. Therefore, in patients with a large frontal sinus, the use of TMS for these conditions is not recommended.

Study Limitations

Our recommendation of TMS as an operative intervention is limited in that it is based on a cadaveric dissection study. Brain tissue of cadaveric specimens is more rigid than live brain parenchyma. Thus, our findings may not be predictive of outcomes for TMS in clinical cases. Furthermore, this report is the first in the literature on the use of the operating microscope as the method of visualization while using a sole transorbital access corridor. In this preclinical study, the endoscope is the only instrument used to date in the clinical setting. The next step in the assessment of TMS is its use in surgical practice, which requires a surgeon who is competent in the anatomy, access corridor, and both methods of visualization. Given that transorbital intracranial surgery has yet to reach the mainstream of neurosurgical practice, such experience would likely occur only in a high-level center of excellence, where the approach is already standard practice and where sufficient cases are completed to ensure competent surgical expertise.

Conclusion

This study is the first report of the TMS route used to complete skull base surgery in 6 cadavers. We have detailed the integral components of TMS, the anatomical and clinically essential considerations, and the related surgical contraindications. Our aim is to emphasize its merits for visualization through the transorbital access corridor and to identify select pathologies for which it can be used safely and effectively rather than to proclaim that TMS is better than TONES. Although the use of the microscope for visualization is limited with respect to its midline accessibility, this method of visualization promotes certain aspects of operative and technical superiority over those of

the endoscope. This selective craniectomy has impressive intracranial access, considering the size of the skull base defect, and it facilitates efforts to preserve normal skull base anatomy. This study provides the first anatomical description of the TMS craniectomy to the ACF and neurovascular structures. The use of this approach in clinical practice is warranted to test its efficacy and to evaluate its proposed merits as the most minimally invasive, minimally destructive skull base corridor.

CHAPTER 5

The following chapter has been published in the journal Frontiers in Bioengineering and Biotechnology.

(doi: 10.3389/fbioe.2021.628797)

CHAPTER 5

VOLUME OF SURGICAL FREEDOM: THE MOST APPLICABLE ANATOMICAL MEASUREMENT FOR SURGICAL ASSESSMENT AND 3-DIMENSIONAL MODELING

Houlihan L.M., Naughton D., Preul M.C.

Abstract

Surgical freedom is the most important metric at the disposal of the surgeon. The volume of surgical freedom (VSF) is a new methodology that produces an optimal qualitative and quantitative representation of an access corridor and provides the surgeon with an anatomical, spatially accurate, and clinically applicable metric. In this study, illustrative dissection examples were completed using two of the most common surgical approaches, the pterional craniotomy and the supraorbital craniotomy. The VSF methodology models the surgical corridor as a cone with an irregular base. The measurement data are fitted to the cone model, and from these fitted data, the volume of the cone is calculated as a volumetric measurement of the surgical corridor. A normalized VSF compensates for inaccurate measurements that may occur as a result of dependence on probe length during data acquisition and provides a fixed reference metric that is applicable across studies. The VSF compensates for multiple inaccuracies in the practical and mathematical methods currently used for quantitative assessment, thereby enabling

the production of 3-dimensional models of the surgical corridor. The VSF is therefore an improved standard for assessment of surgical freedom.

Introduction

Importance of Quantitative Anatomy

Anatomy is the foundation of medical understanding. Medical practice has evolved through the continual scrutiny of biological structure and physiologic function. (Acar, Naderi, Guvencer, Ture, & Arda, 2005; Arraez-Aybar, Navia-Alvarez, Fuentes-Redondo, & Bueno-Lopez, 2015; Elhadi et al., 2012) As the merits of anatomical scrutiny in disease therapy were elucidated, the drive to be able to discriminate between "normal" and "abnormal" biological arrangement increased. This development resulted in the advent of quantitative anatomical research, the objective of which was to measure the complexity of human architecture.

Biological variability is an accepted reality (Higdon, 2013; Kreutz & Timmer, 2009) and a key aspect of managing pathologic processes. The aim of quantifying anatomy has been to identify the most reproducible homogenous model of specific organ systems, thereby establishing principles in biological structure and physiology. The establishment of these principles allowed for the appreciation of abnormal morphology and pathologic processes. The criteria for what now constitutes the so-called normal anatomy has been used in every aspect of medical education, investigation, translational research, and treatment development. (Iaizzo, Anderson, & Hill, 2013)

Anatomical competency is of the utmost importance in surgical practice. (Aziz & Mansor, 2006; Burgess & Ramsey-Stewart, 2015) It is the cardinal infrastructure upon which the knowledge base for all surgeons is founded and subsequently evolves. (Selcuk, Tatar, & Huri, 2019) The surgeon must be aware of standardized structures and their spatial positioning, associated variations, and physiologic sequelae. The efforts and discoveries of anatomists have spurred pivotal breakthroughs in surgical and medical treatment (Iorio-Morin & Mathieu, 2020; Melly, Torregrossa, Lee, Jansens, & Puskas, 2018) as well as in the development of basic scientific progression and understanding of the disease process. (Barth & Ray, 2019)

Quantitation of Surgical Feasibility

Quantitative anatomy is the method the surgeon uses to assess the surgical benefits and disadvantages of different surgical approaches. Studying quantitative anatomy improves the techniques of neurosurgery and other related surgery disciplines. This process allows the surgeon and related personnel to assess, plan, and select the optimal intervention or surgical approach specific to the pathology, thereby improving surgical outcomes for patients. Neuroanatomy is especially relevant and critical because the structural, functional, and physiologic components are often small in dimensional relation and are particularly intertwined. There is little room for error in neurosurgery; all system components represent a significant function, usually reflected in their structural integrity. The intricacy of preserving structural eloquence in the nervous system is further echoed in the surgical parameters the neurosurgeon must use. Dr. Albert Rhoton Jr.

revolutionized the field of neuroanatomy making neurosurgery "*more accurate, gentle and safe*," (Matsushima et al., 2018) not only by establishing key concepts in microsurgical anatomy but also by extrapolating the findings to a surgical approach-specific setting. This innovation enhanced the relevance of anatomy in surgical planning and led to the development of integral concepts that surgeons now use to determine the efficacy of the surgical approach.

The ability to manipulate surgical instruments is an important criterion in comparing surgical approaches and selecting the optimal one. Freedom of movement is especially relevant in neurosurgery, where surgical access through the cranium and into the deep areas of the brain is often restricted. When accessing the most extreme limitations of a surgical corridor, the neurosurgeon encounters parenchymal, bony, musculocutaneous, and neurovascular structures that define the boundaries. The degree of manipulation within these parameters is specific to the approach and delicacy of the structure, the appreciation of which is only possible with extensive knowledge of the circumferential anatomy. An appreciation of these anatomical confines is second nature for the trained neurosurgeon; nonetheless, the mapping of surgical corridors specific to these structures has not yet been robustly completed.

When neurosurgery is performed using an operating microscope for magnification, the movement of surgical instruments to work on pathoanatomical structures may be in increments of millimeters. Small surgical corridors, microscopic anatomy, surgical depth, and impaired visualization all impose limitations on neurosurgical interventions. These are the principal surgical criteria that influence the

neurosurgical decision-making process. Technological advances have broadened the available visualization options, with the microscope, endoscope, and exoscope all possessing specific benefits and disadvantages. This additional component must be assimilated into the surgical decision-making process. (Belykh et al., 2018; Herlan, Marquardt, Hirt, Tatagiba, & Ebner, 2019; J. A. Jane, Jr., 2013) Only through quantitative anatomical assessment specific to these surgical parameters can neurosurgeons increase their insight and proficiency in neurosurgical techniques and operative interventions.

Analysis of the surgical corridor is critical to assessing the validity of any surgical approach. From a neurosurgical perspective, the ideal corridor to the structure of interest should be minimally invasive, with minimal morbidity and mortality, and it should be cosmetically satisfactory. (Castelnuovo et al., 2013) Conceptually, the best surgical corridor combines the maximal room for instrument maneuverability and maximal visualization with the shortest distance to the target of interest. Instrument maneuverability and visualization are primary concerns; thus, a means is required for quantitatively assessing the spatial and morphometric advantages of the surgical corridor, in addition to considering the distance to the surgical target structure (STS). This metric enables consideration of the influence of neuroanatomical structures on the feasibility of the corridor, as well as the ability of the neurosurgeon to function and complete the specific intervention. How well the neurosurgeon can operate and manipulate instruments with respect to the surgical approach directly influences the patient's outcome.

The measurement by which instrument maneuverability is quantified is termed "surgical freedom." The first description of surgical freedom was noted in 2000. (Horgan et al., 2000; Spektor et al., 2000) Stereotactic data gathered using a frameless stereotactic navigation device was used to produce a quantitative measurement of the area available for instrument maneuverability. The 3D coordinate data of the region were used to calculate the area by the summation of triangular areas. Twenty years later, this method remains the crux of neuroanatomical quantitation and a key determinant of the feasibility of any surgical approach. (Elhadi et al., 2014; Elhadi et al., 2015; Pillai, Baig, Karas, & Ammirati, 2009)

Surgical Freedom

Surgical freedom is presently defined in the medical literature as the maximum allowable working area at the proximal end of a probe with the distal end on the target structure. (Horgan et al., 2000; Noiphithak et al., 2018; Spektor et al., 2000) The goal of this procedure is to assess the maneuverability of an instrument and provide the operator with insight into how realistic and appropriate it is to use a specific access corridor while also allowing for the comparison of surgical approaches.

Neuroanatomists and neurosurgeons use specific methods to measure surgical freedom:

- The cadaveric head specimen is fixed in a rigid head holder.

- A stereotactic navigation system (Figure 5.1) is used to acquire the 3D coordinates of the target points for each surgical approach being analyzed, specific to the intracranial structure or region of interest.
- The distal end of the surgical instrument is placed on the target structure.
- For a quadrangular area measurement, the surgical instrument is moved as far mediocranially, mediocaudally, laterocranially, and laterocaudally as possible for four or more points to represent the most extreme limits of the surgical corridor specific to the approach. At all times, the distal end of the probe is not moved from the target structure.
- The coordinates of the surgical instrument's proximal tip are obtained with the navigation probe when the tip of the instrument is at the most extreme position.
- The area bounded by the coordinate data points from the probe's proximal tip at the extreme limits is calculated by dividing the bounded area into triangles in which the data points form the triangle vertices, then calculating the sum of the areas of all the triangles using Heron's formula. (Erid W. Weisstein)
- The result is represented in either square millimeters or square centimeters.

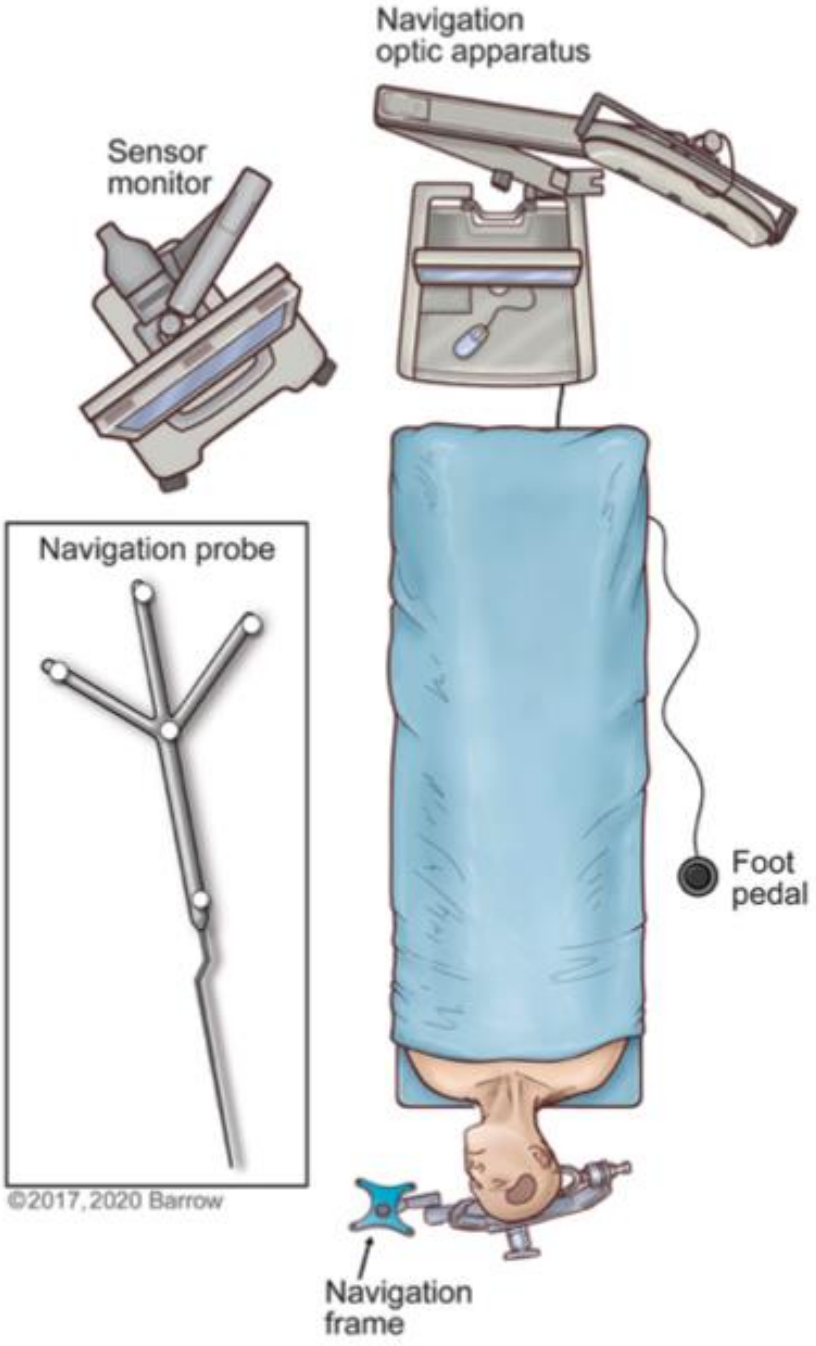
Navigation
optic apparatus
Sensor
monitor
Navigation probe
Foot
pedal
©2017, 2020 Barrow
Navigation
frame

Figure 5.1. Illustration of the neuronavigation system in the surgical setup commonly used to localize both pathologic and anatomically pertinent structures using stereotaxis. Used with permission from Barrow Neurological Institute, Phoenix, Arizona.

This method produces an area that is used as a metric for surgical freedom. The standard process is to collect four, but occasionally six, data points. The distribution of these points, as dictated by the measuring researcher, is usually along the extrema of the surgical corridor, which does not necessarily take into account any structural components, or the lack thereof, between the points. Previous methods have tended to impose regular, symmetrical shapes on the measurement data to simplify the shape of the access corridor. In reality, however, the borders of any surgical corridor are never symmetrical, and they are never a perfect shape that can be represented by conventional shapes.

This method aims to quantitatively portray the range of motion of an instrument during a surgical intervention to illustrate the feasibility and functionality of the surgical approach and the surgical corridor specific to the target structure. However, multiple inaccuracies are associated with this calculation method from a practical, mathematical, and application perspective: (1) The measured data points are not coplanar, which distorts the perceived area of surgical freedom. (2) The surgical freedom metric is dependent on the length of the probe that is used to capture data. This variation across the literature precludes interstudy comparisons, which weakens the scientific robustness of such studies and impairs reproducibility. (3) Measurement inaccuracy can result in substantial variation in the measured area. (4) Surgical corridors are irregular and cannot be fully

expressed using simple shapes. (5) A 2-dimensional (2D) shape does not allow for visualization of a 3D surgical corridor.

In terms of visualization, the area of surgical freedom is not an optimal representational concept of the surgical approach corridor because the area is a 2D measurement and neurosurgical approaches and corridors are volumetric, or 3D, shapes. Surgical freedom is arguably the most important technical parameter dictating the surgical approach and selection process specific to an anatomical target. Quantitatively analyzing surgical freedom allows the neurosurgeon to proceed in a more informed fashion by comparing the numerical values with those of different approaches to the same anatomical target. What is not taken into consideration by this method is the fact that surgical instruments are not deployed in a 2D area but rather in an irregularly shaped 3D corridor.

Due to the nature of the surgical site, the surgical corridor transitions from a region of large maneuverability at the surgical entry point to an apex of minimal freedom at the target structure. At present, an instrument's maneuverability within the surgical corridor is estimated by the angle formed at the apex of the corridor (the angle of attack) in one or two planes, usually vertical or horizontal. The angle of attack is another anatomical metric neurosurgeons use to evaluate an instrument's maximal working ability in one or more planes where the instrument will be most frequently deployed. This information gives specific insight regarding the instrument's operational freedom, which may not be evident when assessing the numerical value produced by the present method

of calculating surgical freedom. However, this method produces a limited representation of the 3D shape of the surgical corridor.

The deficits in estimating this surgical principle are exemplified by the illustrations published in the neurosurgery literature. These illustrations broadly represent the surgical corridors, denoting general shapes and trajectories garnered from the neurosurgeon's experience, but they lack anatomical, spatial, and surgical accuracy. Surgical freedom should be defined by the whole expanse of the surgical corridor and should not be limited to its 2D infrastructure. For all these reasons, we have endeavored to improve upon the imprecision in presently accepted methodology for this crucial method of quantitative surgical anatomy.

Volume of Surgical Freedom

The volume of surgical freedom (VSF) is defined as the maximal available working volume with respect to a specific surgical corridor and target structure. VSF is a new methodology that produces the optimal qualitative and quantitative representation of an access corridor and provides the neurosurgeon with an anatomical, spatially accurate, and clinically applicable metric. From this representation, 3D visualization of the surgical corridor is possible.

The VSF metric uses a normalized calculation to reduce error and allow for direct comparison among measurements. This calculation is achieved by measuring the volume of the irregular-based cone model of the surgical corridor, with the irregular base of the cone at a fixed distance from the apex. This report details a novel approach for surgical

anatomy quantitation, the anatomical experiment used to investigate its validity, and the key steps in producing a mathematically and spatially superior model of the approach corridor.

Materials and Methods

Anatomical Specimen Preparation

Cranial dissections of 14 cadaveric specimens were completed to investigate the data-collection process and for logistical and surgical representation. The cadaveric heads were fixed with a customized alcohol-based solution as a preservative. Colored silicone was incrementally injected into the cerebral vasculature, with the arteries represented by red and the veins represented by blue. This differentiation allowed for clearer interrogation of the intracranial structures and STSs. Each head was rigidly fixed in a head holder while measurements were obtained.

Dissections were completed by the first author, a neurosurgery resident competent in the two selected approaches. Dissection was completed using a clinical-grade neurosurgical operating microscope (Zeiss OPMI Pentero, Carl Zeiss Meditec AG, Oberkochen, Germany). The two open transcranial neurosurgical approaches selected to model this quantitative methodology were the standard pterional craniotomy and the supraorbital craniotomy (Figure 5.2).

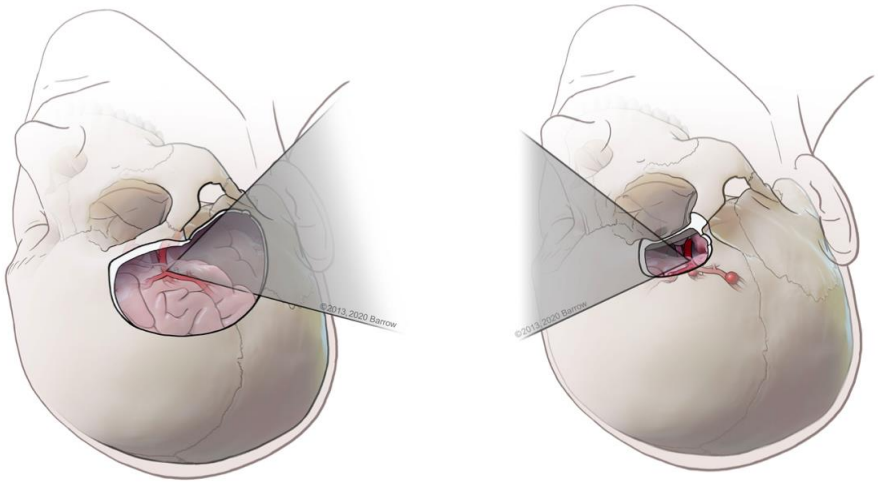

Figure 5.2. (A) Example of a pterional transcranial approach, in which the surgeon uses a lateral trajectory that usually traverses the natural fissures of the brain to access complex paramedian regions. (B) Example of a supraorbital approach, with an incision made along the eyebrow approaching the skull base from a more anterolateral perspective, tracking medially along the bone of the anterior cranial fossa that represents the roof of the orbit. Used with permission from Barrow Neurological Institute, Phoenix, Arizona.

These approaches are two of the most common neurosurgical corridors used to access deep paramedian structures and regions of surgical complexity. These anatomical areas are of particular interest in the context of anatomical quantitation because of the need to avoid injury to critical neurovascular structures.

Neuronavigation System

A neuronavigation system (StealthStation S7 Surgical Navigation System; Medtronic, Dublin, Ireland) was used to acquire predetermined data points. Neuronavigation uses the principle of stereotaxis. The neuronavigation system uses Cartesian coordinates to divide the geometric volume of the brain into three imaginary intersecting spatial planes (axial, sagittal, and coronal) that are orthogonal to each other. Any point within the brain can be specified by measuring its distance along these three intersecting planes. Neuronavigation uses the reference of this coordinate system in parallel with 3D images of the brain displayed on the console of the computer workstation to provide guidance to the corresponding anatomical locations using medical images. (Seyit Kagan Başarslan, 2014)

Institutional review board approval was not required for this cadaveric laboratory investigation.

Methodology Calculator and 3D Modeling Software

The methodology described herein was implemented as a calculation tool in Excel for Office 365 (Microsoft, Redmond, WA, USA). An Excel spreadsheet was used to carry out all of the calculation steps described in this paper, apart from the calculation of the best-fit plane. The generalized reduced gradient nonlinear engine of Microsoft Excel Solver was used to calculate the least-squares best-fit plane for the data points. The Excel spreadsheet calculation tool was used to calculate the normalized volume of the surgical corridor (normalized VSF), using the measurement data as an input. In addition to

calculating the VSF metric using Excel, the VSF data were modeled using a student license for the 3D modeling software Solidworks 2020 (Dassault Systèmes, Vélizy-Villacoublay, France). The modeling software was used to create 3D renderings of the surgical corridors from the measurement data to visualize the surgical corridor for each dataset. The 3D models were also superimposed onto microscope images of anatomical approaches to illustrate the surgical corridor to the structure of interest.

Methods

Data Collection

A pterional craniotomy was conducted on seven cadaveric specimens, and a supraorbital craniotomy was conducted on seven cadaveric specimens. Predetermined STSs were selected by the first author. To illustrate the methodology, three surgical targets (Figure 5.3) were identified that are common to both approaches: (1) paraclinoid internal carotid artery (ICA), (2) terminal ICA, and (3) anterior communicating artery (ACoA) complex.

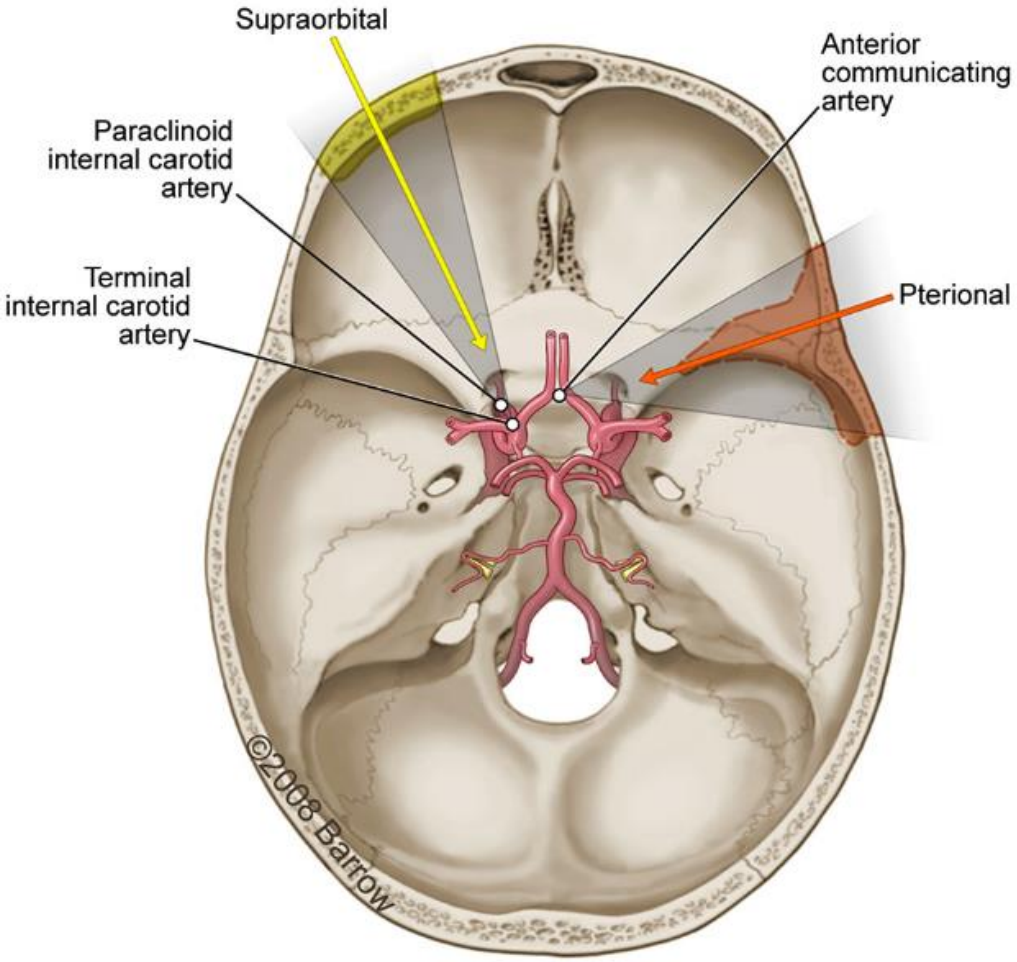

Figure 5.3. Axial view illustration of the skull base showing the primary vasculature supplying the brain. The three surgical structures of interest accessible using either a pterional craniotomy (orange arrow and shading; dashed line) or supraorbital craniotomy (yellow arrow and shading; solid line) are the paraclinoid internal carotid artery (ICA), the terminal ICA, and the anterior communicating artery. Used with permission from Barrow Neurological Institute, Phoenix, Arizona.

The data points required to calculate the VSF and produce a spatially and anatomically accurate model were collected for each STS and both the pterional and supraorbital surgical approaches. Figure 5.4 depicts the collection process for all data points.

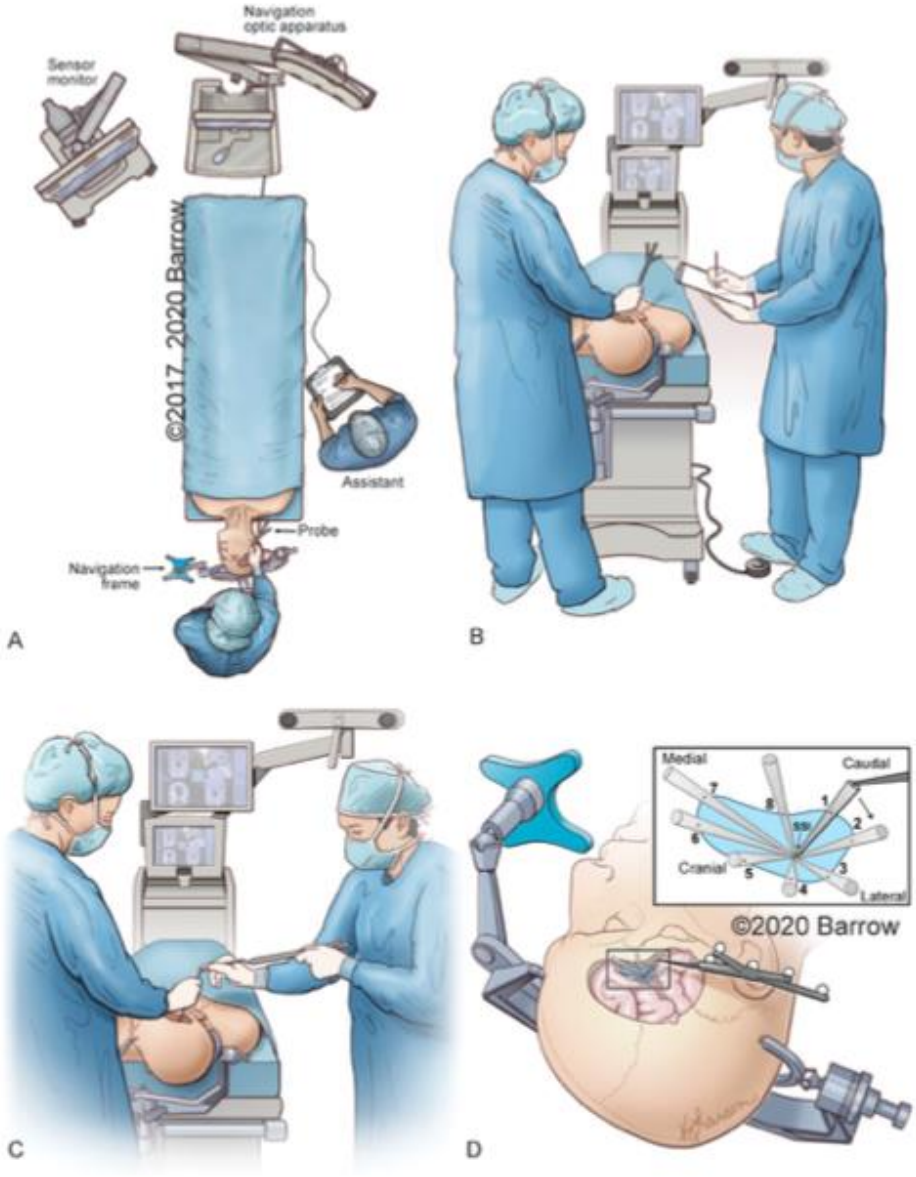

Figure 5.4. Illustrative depiction of the data collection process. (A) Position of the neuronavigation system, the cadaver, the neurosurgeon with probe, and the assistant recording data. (B) The neurosurgeon obtains coordinates of the surgical target structure with the tip of the neuronavigation probe on the surgical target structure. The coordinates,

as depicted on the monitor, are recorded by the assistant. (C) While the surgeon holds an instrument with its distal end on the surgical target structure, the assistant holds the neuronavigation probe and places its distal tip on the proximal end of the surgeon's instrument to obtain the 3D coordinates of the instrument's proximal end in space. (D) Eight data points are sequentially collected that represent the maximal allowable parameters of the surgical corridor. The data points are obtained by placing the tip of the navigation probe on the proximal end of the surgical instrument in the position marking a specific boundary point. Points 1 and 5 represent the craniocaudal maximal angle of attack, whereas points 3 and 7 can be used to represent the mediolateral angle of attack. STS, surgical target structure. Used with permission from Barrow Neurological Institute, Phoenix, Arizona.

Interrater and intrarater variability were accounted for by recording the STS VSF for each specimen and approach a minimum of three times by multiple qualified neurosurgery residents. This replication ensured reproducibility of the method, as well as a larger pool of measurements to assess our methodology's advantages and limitations. VSF results are reported as cubic millimeters, and each result was normalized to a height of 10 mm from the STS.

Mathematical Methodology

The VSF was calculated by modeling the surgical corridor as a cone with an irregular base. The STS is the apex of the cone, and the points measured at the extrema of

the maneuverability of the instrument compose the base of the cone. For this study, we measured eight extrema points around the base of the cone, but the calculation methodology is equally applicable to more or less than 8 points. The 3D coordinate data from the measurements were used to calculate the volume of the irregular-based cone. This method can be summarized as follows:

(1) Calculate a best-fit plane to the extrema data points, which best represents the plane of the base of the cone.

(2) Translate the best-fit plane in 3D space to a fixed perpendicular distance from the apex point (normalized height), maintaining the slope of the plane.

(3) Translate the extrema data points onto the best-fit plane, along the line between the measured point and the apex point.

(4) Convert the 3D coordinates of the data points to a 2D coordinate system on the best-fit plane.

(5) Use the 2D coordinates to calculate the area of the irregular polygon enclosed by the data points.

(6) Calculate the perpendicular height from the best-fit plane to the apex point.

(7) Calculate the volume of the irregular-based cone from the area and the perpendicular height.

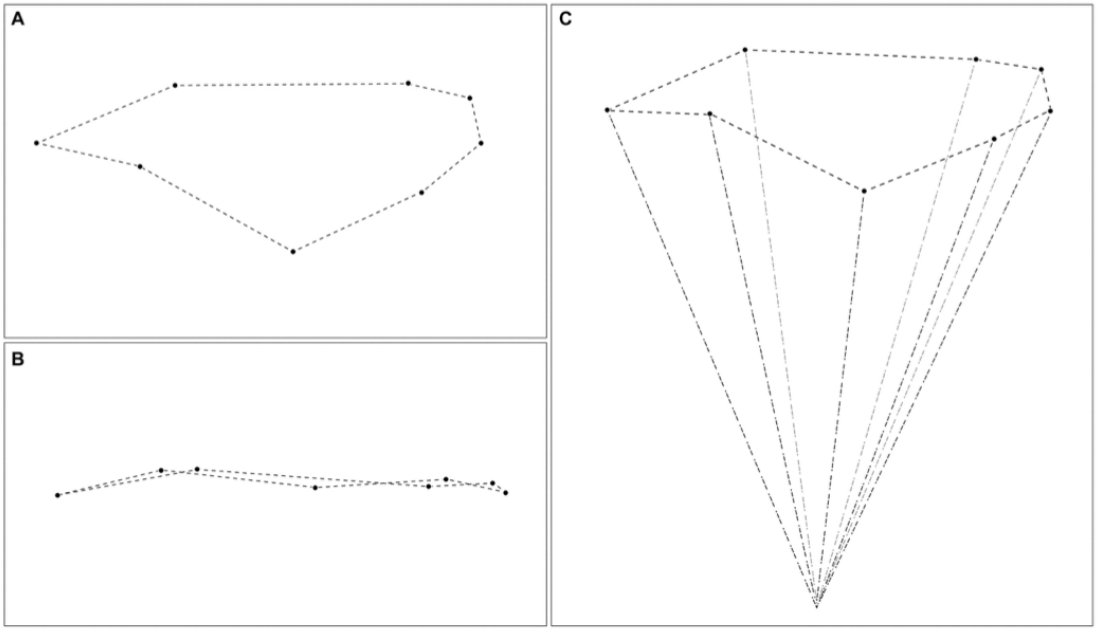
A
B
C

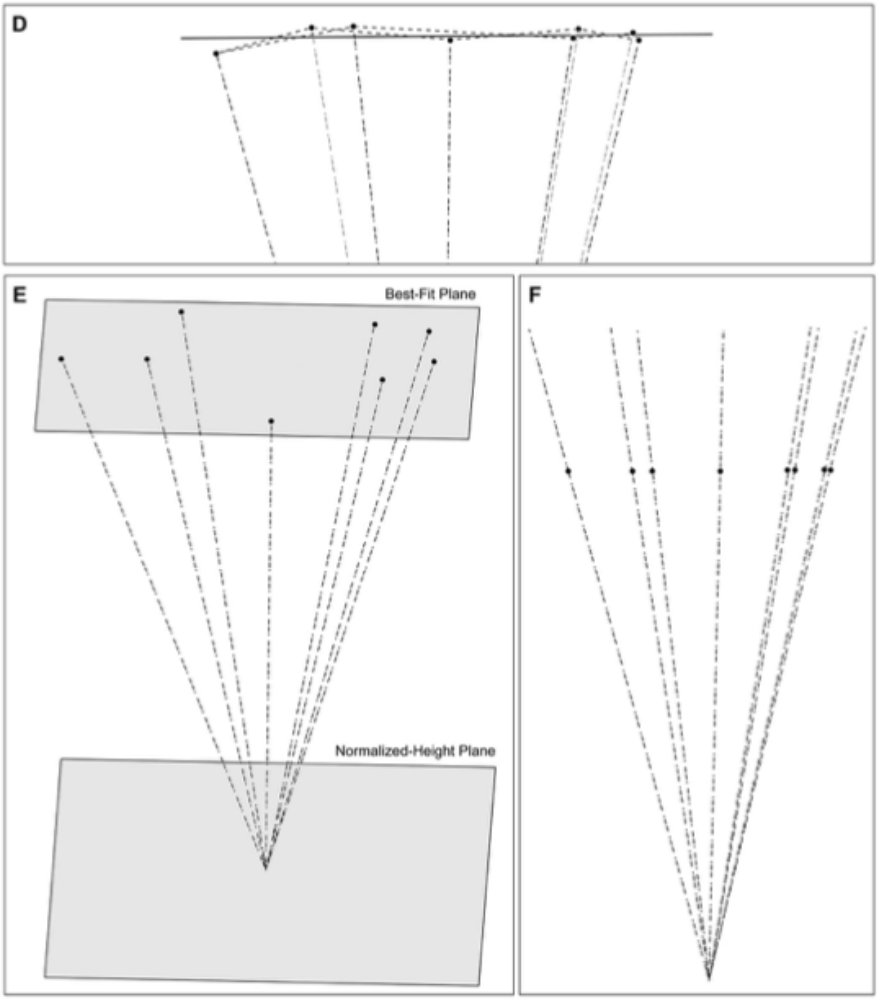
D
E
Best-Fit Plane
Normalized-Height Plane
F

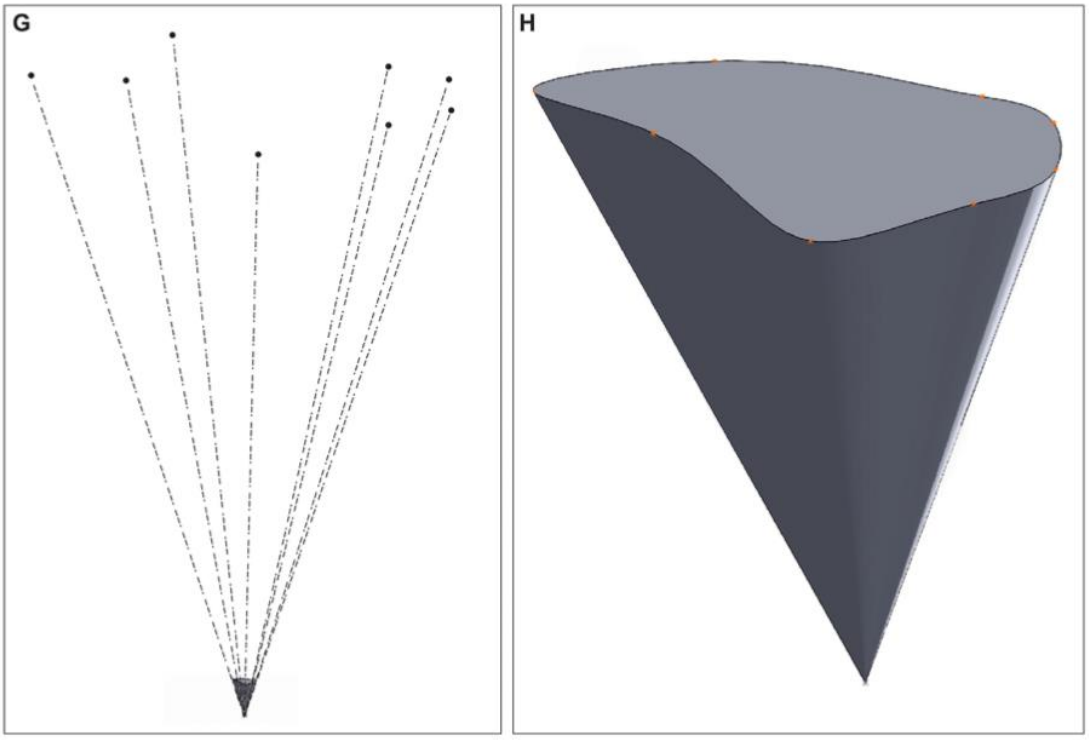

Figure 5.5. 3D modeling of the steps of the volume of surgical freedom methodology. (A) A plan view of the data points in 3D space. (B) An elevation view of the points, illustrating that they are not on a single plane. (C) A view of the data points and apex point in space. (D) The best plane fitted to the data points. (E) An elevation view of the data points before and after translating them to the best-fit plane. (F) The two sets of data points and the best-fit plane. (G and H) The 3D representation of the shape of the surgical corridor (G), with smooth lines connecting the data points (H). 3D, 3-dimensional. Used with permission from Barrow Neurological Institute, Phoenix, Arizona.

This methodology calculates a normalized volume by calculating the volume of the cone with an irregular base, modeling the surgical corridor at a fixed height from the

apex point (Figure 5.5). This methodology was conceived to reduce the effects of measurement inaccuracy and measurement probe length on the calculated VSF value.

Calculation of Best-Fit Plane

The best-fit plane was fitted to the data points using the least-squares method. The best-fit plane was considered to be the plane that results in the minimum sum of the squares of the perpendicular distances between each data point and the plane.

The problem is nonlinear, so a nonlinear solver was used to optimize the best-fit plane. An average plane was first calculated to use as an initial condition in the solver. The plane intersecting each subset of three points was calculated using various combinations of three data points from the set of extrema data points. The average plane equation coefficients of all the calculated planes were used as the coefficients of the average for the initial condition in the solver.

Calculating a Plane from Three Points

The general equation of a plane can be expressed as follows:

$$Ax + By + Cz + D = 0,$$

where *A, B,* and *C* are the coefficients of the slope in the directions of the *x, y,* and *z* axes, respectively, and *D* is the coefficient representing the distance from the plane to the origin.

Calculating a plane from three points $P_1 = (x_1, y_1, z_1)$, $P_2 = (x_2, y_2, z_2)$, and $P_3 = (x_3, y_3, z_3)$ first requires calculating the two vectors between the three points:

$$\overrightarrow{P_1P_2} = P_2 - P_1,$$

$$\overrightarrow{P_1P_3} = P_3 - P_1.$$

The *A, B,* and *C* coefficients of the plane can then be calculated from the cross-product of the two vectors:

$$[A\ B\ C\ ] = \overrightarrow{P_1P_2} \times \overrightarrow{P_1P_3}.$$

The coefficient *D* can then be calculated from the plane equation by using one of the points (P_1):

$$D = -(Ax_1 + By_1 + Cz_1)$$

Calculating the Average Plane

After the plane equation of *n* planes has been calculated, the average plane can be calculated from the average coefficients:

$$A_{\text{average}}x + B_{\text{average}}y + C_{\text{average}}z + D_{\text{average}} = 0,$$

where

$$A_{\text{average}} = \frac{A_1 + A_2 + \cdots + A_n}{n},$$

$$B_{\text{average}} = \frac{B_1 + B_2 + \cdots + B_n}{56},$$

$$C_{\text{average}} = \frac{C_1 + C_2 + \cdots + C_n}{n}, \text{ and}$$

$$D_{\text{average}} = \frac{D_1 + D_2 + \cdots + D_n}{n}.$$

Running the Excel Solver to Calculate the Least-Squares Best-Fit Plane

Because the least-squares calculation of the best-fit plane is a nonlinear problem, a nonlinear solver was used to calculate the coefficients of the least-squares fitting plane. The coefficients A_{average}, B_{average}, C_{average}, and D_{average} were used as the initial conditions for the solver. The distance *d* between each point $P = (x, y, z)$ and the plane $Ax + By + Cz + D = 0$ is obtained by

$$d = \frac{|Ax + By + Cz + D|}{\sqrt{A^2 + B^2 + C^2}}.$$

The nonlinear solver then solved for the coefficients *A*, *B*, *C*, and *D*, which minimized the expression

$$\sum_{p=1}^{n}\left(\frac{Ax_p+By_p+Cz_p+D}{\sqrt{A^2+B^2+C^2}}\right)^2,$$

where *n* is the number of data points to which the plane is being fitted.

Normalizing the Best-Fit Plane

Calculating the cone's cross-sectional area at a fixed distance from the apex required a new normalized-height plane, which is parallel to the cone's base, at the required distance from the apex point. After the best-fit plane $Ax + By + Cz + D = 0$ is calculated using the nonlinear solver, this plane is translated into 3D space so that the perpendicular distance between the apex point and the plane is the required normalized height of the cone.

Because the plane is parallel to the base of the cone (i.e., the calculated best-fit plane for the data points), the *A*, *B*, and *C* plane coefficients will be the same for both planes. Given this constraint, the formula for the perpendicular distance between the normalized-height plane $Ax + By + Cz + D_{\text{norm}} = 0$ and the apex point $P_a = (x_a, y_a, z_a)$ can be rearranged to give the following:

$$D_{\text{norm}} = h_{\text{norm}}\left(\sqrt{A^2 + B^2 + C^2}\right) - (Ax_a + By_a + Cz_a).$$

The least-squares best-fit plane was used as the plane for the base of the cone model.

Translating the Points to the Best-Fit Plane

After the normalized-height plane is calculated, the points must be translated onto this plane to calculate the area of the base of the cone model. Maintaining the shape of the cone requires the points to be translated onto the normalized-height plane along the line between each point and the apex. This method ensures that the cross-section profile of the shape of the cone is unaltered when the points are translated.

The vector between each data point $P = (x, y, z)$ and the apex point $P_a = (x_a, y_a, z_a)$ is given by the following:

$$\overrightarrow{PP_a} = P_a - P.$$

A multiplication factor, *t*, representing the distance between the point and the best-fit plane $Ax + By + Cz + D_{\text{norm}} = 0$ is calculated as follows:

$$t = \frac{-(Ax_a + By_a + Cz_a + D_{\text{norm}})}{Ax_0 + By_0 + Cz_0}.$$

The coordinates of the point after translation onto the best-fit plane are then calculated by

$$P' = [x'\ y'\ z'\ ] = [tx\ ty\ tz\ ].$$

The translation was performed for all *n* data points to obtain the translated points $P_1', P_2' \ldots P_n'$.

Calculating the Area Enclosed by the Translated Points

The shoelace formula (Eric W. Weisstein) was used to calculate the area of the base of the cone model. This formula calculates the enclosed area of an irregular polygon from the 2D coordinates of the vertices of the polygon. Calculating the area using this method required mapping the translated 3D points to a 2D coordinate system on the normalized-height plane.

The choice of the origin was arbitrary, so the 2D plots of the data points were simplified by taking the centroid of the data points as the new origin. The centroid is calculated by taking average *x*, *y*, and *z* coordinates of all data points as follows:

$$\text{Centroid } O = [x_O \quad y_O \quad z_O] = \left[\frac{x_1+x_2+\cdots+x_n}{n} \quad \frac{y_1+y_2+\cdots+y_n}{n} \quad \frac{z_1+z_2+\cdots+z_n}{n}\right].$$

Two perpendicular axes on the plane were created by defining two vectors on the normalized-height plane using the centroid *O*, and two of the translated points P_1' and P_2':

$$\vec{v} = P_1' - O,$$

$$\vec{u} = P_2' - O.$$

A vector $\vec{w}$ is calculated that is perpendicular to both $\vec{u}$ and $\vec{v}$:

$$\vec{w} = \vec{u} \times \vec{v}.$$

A new vector, $\overrightarrow{u'}$, is then calculated perpendicular to both $\vec{v}$ and $\vec{w}$:

$$\overrightarrow{u'} = \vec{v} \times \vec{w}.$$

The unit vectors $\hat{v}$ and $\widehat{u'}$ are then calculated:

$$\hat{v} = \frac{v}{|v|}, \ \widehat{u'} = \frac{u'}{|u'|}.$$

This series of calculations results in two perpendicular vectors on the normalized-height plane that are then used as the axes for the 2D coordinate system. Each 3D data point P' is converted to a 2D point P_{2D} by calculating the dot product of each axis vector with the vector between the origin and the point $\overrightarrow{OP'}$:

$$P_{2D} = (x_{2D}\ y_{2D}) = \left(\widehat{u'}.\overrightarrow{OP'}\ \hat{v}.\overrightarrow{OP'}\right).$$

With the data points mapped to a 2D coordinate system, the area of the shape enclosed by the points is calculated using the shoestring formula:

$$A = \frac{1}{2}(|x_1\ x_2\ y_1\ y_2\ | + |x_2\ x_3\ y_2\ y_3\ | + \cdots + |x_n\ x_1\ y_n\ y_1\ |),$$

where $|x_n\ x_{n+1}\ y_n\ y_{n+1}\ |$ is the determinant of the matrix, given by

$$|x_n\ x_{n+1}\ y_n\ y_{n+1}\ | = x_n y_{n+1} - y_n x_{n+1}.$$

Calculating the Perpendicular Height of the Cone Shape

The perpendicular height of the cone shape, *h*, is simply the perpendicular distance between the best-fit plane $Ax + By + Cz + D = 0$ and the apex point $P_a = (x_a, y_a, z_a)$:

$$h = \frac{|Ax_a + By_a + Cz_a + D|}{\sqrt{A^2 + B^2 + C^2}}.$$

Calculating the Volume of the Cone Shape

The volume of the cone shape can be calculated from the area enclosed by the points on the best-fit plane (*A*) and the perpendicular height of the cone shape (*h*):

$$\text{Volume} = \frac{1}{3} \times A \times h \, .$$

This volume is reported as cubic millimeters.

Normalized Volume of Surgical Freedom

The volume calculation depends on the length of the probe used to obtain the point data because the length of the probe determines the height of the cone shape. If this factor is removed from the calculation, then the resulting VSF values will be directly comparable to all other calculations using this spreadsheet or methodology, regardless of the length of the probe used to take the measurements.

Modeling Methodology

The 3D models of the surgical corridors were generated from the coordinates of the extrema points after translation onto the normalized-height plane and from the coordinates of the apex point. Although the mathematical calculation of the area assumes straight lines between each of the extrema data points when calculating the enclosed area of the base of the cone, the 3D model of the surgical corridor used curved splines between each of the extrema points to better visualize the shape of the surgical corridor observed in the specimen.

Measurement Inaccuracy Analysis

Because the original measurement data points were not coplanar, we investigated their effect on the calculation of the area bounded by the points. For an illustrative data set, the area bounded by the measured data points was calculated using Heron's formula. The data points were then translated onto the best-fit plane, and the area bounded by these translated points was calculated using the same method.

As of this writing, 174 individual VSF measurements have been completed in the neurosurgical research laboratory to explore multiple neurosurgical approaches. A 190-mm probe was used for all measurements. For each set of measurement data, the average probe length was calculated by averaging the calculated distance from each of the eight coordinates to the apex coordinate. The average minimum and maximum probe lengths with standard deviations (SDs) were identified for the 174 measurement samples.

Analysis of the effect of the probe length on the calculated volume of the surgical corridor required the calculation of the volume of a cone from the best-fit plane of the measurement data points to the apex point. The cone shape was maintained while the cone height was increased by 5 mm, and the data points were translated onto the plane 5 mm farther away from the apex. This translation created a new data set representing the same surgical corridor as that measured by a longer probe. The volume of the cone was then calculated again from the best-fit plane to the new data set representing a longer probe. Data analysis was completed in Microsoft Excel.

Results

Quantitation and Modeling

This methodology generated two useful products: a mathematically robust quantitation of the surgical freedom of a neurosurgery instrument and a 3D spatially accurate model of the surgical corridor that takes into account irregular neuroanatomical parameters. This process gives direct quantitative information to allow for the comparison of surgical approaches. VSF is expressed in cubic millimeters. By default, the VSF also produces the craniocaudal and mediolateral angles of attack. The spatially accurate model obtained with the VSF provides a visual representation of this information, elucidating the breadth of maneuverability specific to all planes.

Table 5.1 depicts the comparative quantitative results of a set of measurements for specific anatomical STSs and pterional and supraorbital approaches.

Table 5.1. Comparative volumetric results of the VSF for measuring instrument maneuverability specific to the surgical target structure and approach*

Surgical Target Structure	VSF, mm^3 NU		Craniocaudal Angle of Attack, degrees		Mediolateral Angle of Attack, degrees	
	Pterional	Supraorbital	Pterional	Supraorbital	Pterional	Supraorbital
Paraclinoid ICA	165.88	43.83	36.72	20.86	50.55	37.40
Terminal ICA	50.69	31.01	22.63	16.29	27.59	31.62
ACoA complex	38.34	15.66	12.64	14.50	31.69	17.44

Abbreviations: ACoA, anterior communicating artery; ICA, internal carotid artery; NU, normalized unit; VSF, volume of surgical freedom.

*Craniocaudal and mediolateral angles of attack were also produced using this measurement system.

These illustrative examples show that the pterional craniotomy provides a larger VSF for all three STSs than the VSF provided by the supraorbital craniotomy. Thus, if any of these structures must be accessed, the pterional craniotomy would be the superior corridor because it provides an increased VSF and an increased angle of attack in both the craniocaudal and mediolateral dimensions.

Figures 5.6, 5.7, and 5.8 demonstrate the 3D models of the surgical corridors available for deployment of neurosurgery instruments, specific to the pterional and supraorbital approaches and the STSs. This methodology provides an increased body of quantitative and visual information on surgical approach metrics to aid the neurosurgeon in the decision-making process.

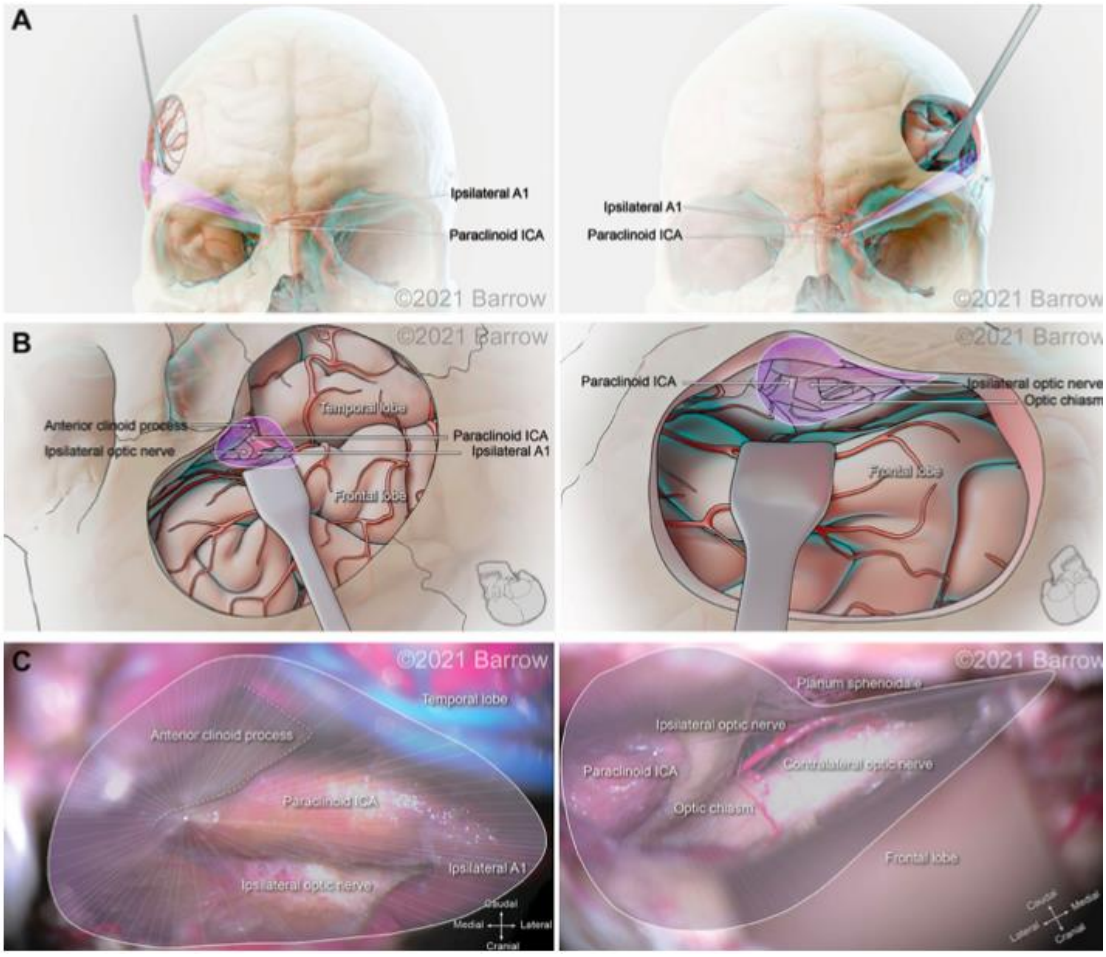

Figure 5.6. Illustration depicting 3D modeling of the surgical corridor to the paraclinoid internal carotid artery (ICA) from a pterional approach (left) and a supraorbital approach (right). (A) The anterior of the surgical corridor. (B) The surgical anatomy as visualized specific to the surgical corridor model. (C) The surgical view of the cadaveric anatomy, which is in continuity with the surgical corridor model parameters (pterional: VSF = 165.88 mm^3, craniocaudal angle of attack = 36.72°, mediolateral angle of attack = 50.55°; supraorbital: VSF = 43.83 mm^3, craniocaudal angle of attack = 20.86°, mediolateral angle

of attack = 30.40°). VSF, volume of surgical freedom; 3D, 3-dimensional. Used with permission from Barrow Neurological Institute, Phoenix, Arizona.

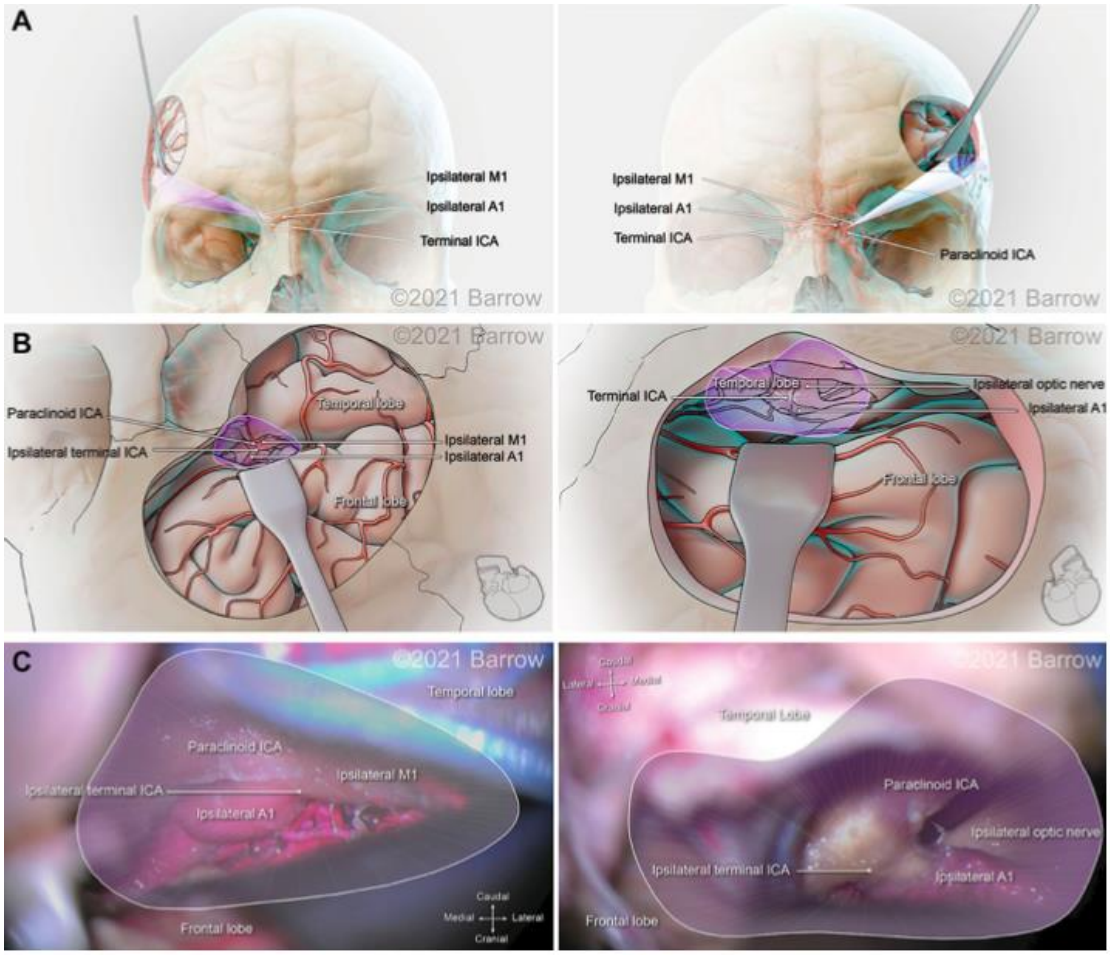

Figure 5.7. Illustration depicting 3D modeling of the surgical corridor to the terminal internal carotid artery (ICA) from a pterional approach (left) and a supraorbital approach (right). (A) The anterior of the surgical corridor. (B) An illustration of the surgical anatomy as visualized specific to the surgical corridor model. (C) The surgical view of the cadaveric anatomy, which is in continuity with the surgical corridor model parameters

(pterional: VSF = 50.69 mm^3, craniocaudal angle of attack = 22.63°, mediolateral angle of attack = 27.59°; supraorbital: VSF = 31.01 mm^3, craniocaudal angle of attack = 16.29°, mediolateral angle of attack = 31.62°). ACoA, anterior communicating artery; VSF, volume of surgical freedom; 3D, 3-dimensional. Used with permission from Barrow Neurological Institute, Phoenix, Arizona.

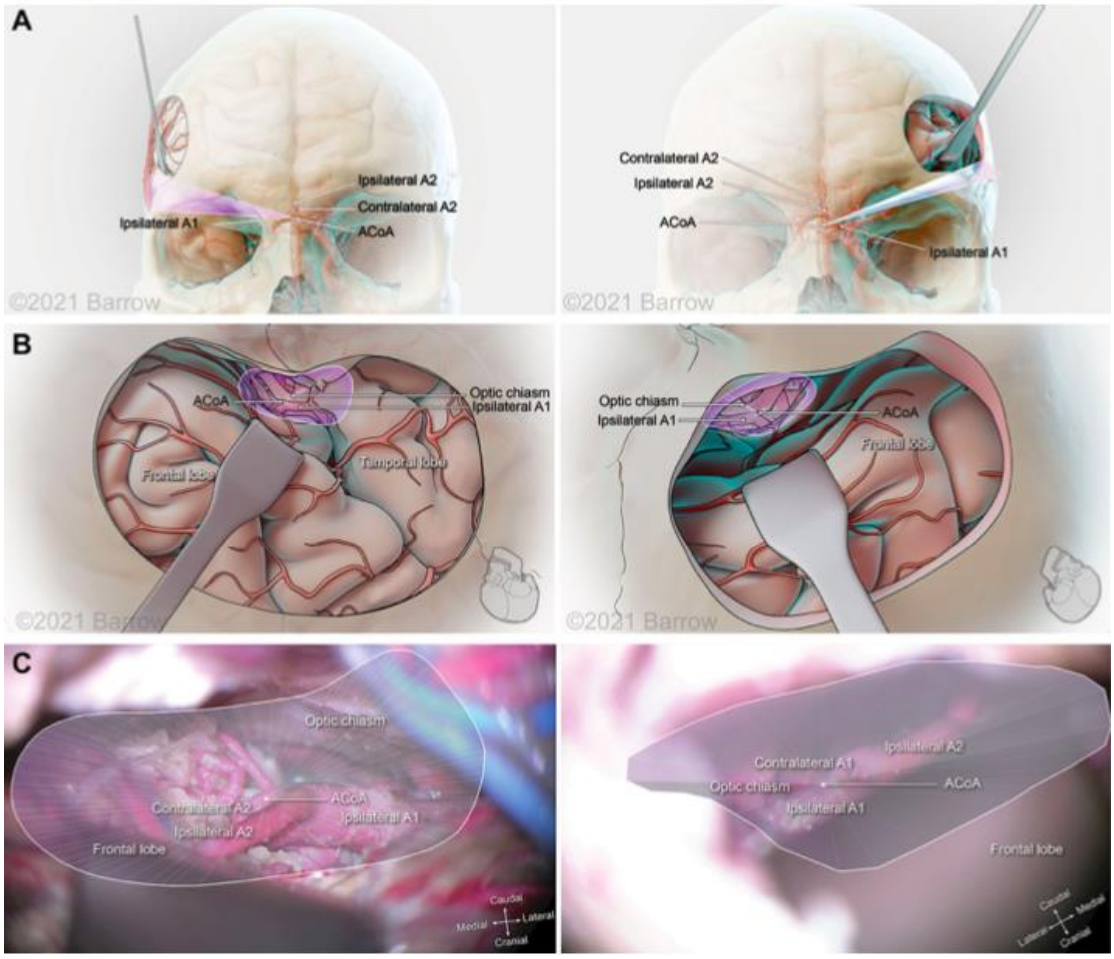

Figure 5.8. Illustration depicting 3D modeling of the surgical corridor to the anterior communicating artery (ACoA) from a pterional approach (left) and a supraorbital

approach (right). (A) The anterior of the surgical corridor. (B) The surgical anatomy as visualized specific to the surgical corridor model. (C) The surgical view of the cadaveric anatomy, which is in continuity with the surgical corridor model parameters (pterional: VSF = 38.34 mm^3, craniocaudal angle of attack = 12.64°, mediolateral angle of attack = 31.69°; supraorbital: VSF = 15.66 mm^3, craniocaudal angle of attack = 14.50°, mediolateral angle of attack = 17.44°). ICA, internal carotid artery; VSF, volume of surgical freedom; 3D, 3-dimensional. Used with permission from Barrow Neurological Institute, Phoenix, Arizona.

Measurement Inaccuracy

The illustrative data set for Figure 5.5 was used to compare the calculated area bounded by the original measurement data points to the calculated area bounded by the points after translation onto the best-fit plane. The sample data set comprised measurements for a supraorbital craniotomy surgical corridor to the anterior communicating artery. It represented the area calculated by the previous surgical freedom method (Heron's Formula) and the area after translation onto the best-fit plane. The calculation of the area bounded by this sample set of data point measurements was 1489 mm^2, and the calculation of the area bounded by the data points after translation onto the best-fit plane for the data set was 1418 mm^2. To illustrate the effect of probe length on the calculated volume, we used this same data set to calculate the volume from the best-fit plane of the measured data points to the apex. A cone height of 183.6 mm gave a

volume of 119,386 mm^3. The points representing data of the same corridor as measured were then translated to a plane 5 mm farther away from the apex. This 5-mm increase in the height of the same cone shape, to 188.6 mm, gave a cone volume of 129,448 mm^3.

Figure 5.9 shows the frequency distribution of the probe lengths of the 8 data points for the 174 sets of measurements. The mean (SD) probe length was 190.4 (5.0) mm, with a minimum of 168.3 mm and a maximum of 212.0 mm.

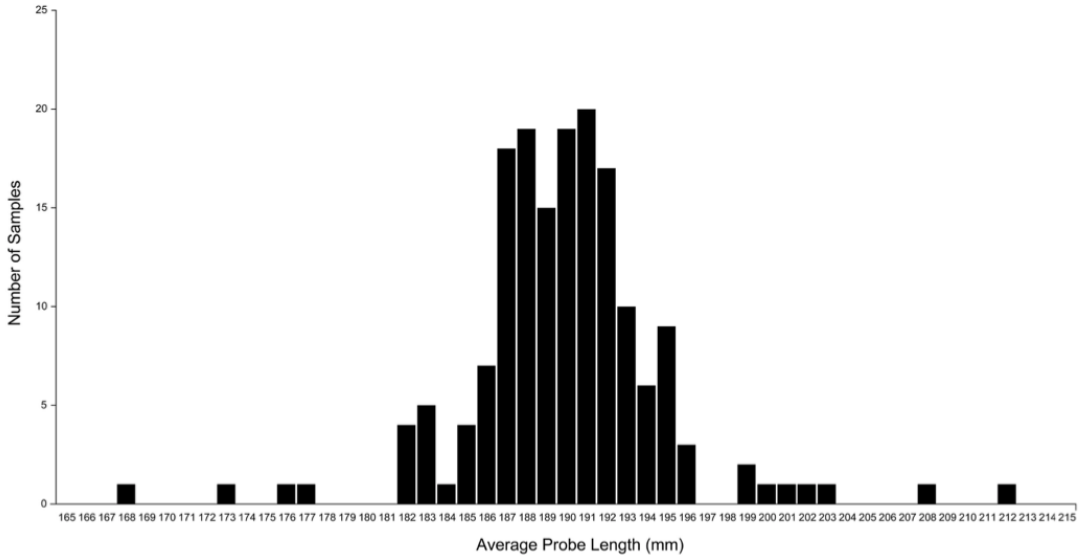

Figure 5.9. A plot of the average probe length of each set of measurement data. Probe length was calculated as the distance between the coordinates of each extrema point and the apex point. The plot shows considerable variation in the calculated probe length, although the same fixed-length probe was used in all measurements. This variation is caused by measurement error that can be mitigated by using the normalized volume of

surgical freedom metric. Used with permission from Barrow Neurological Institute, Phoenix, Arizona.

Discussion

Surgical Application Advantages of the VSF

The VSF compensates for multiple defects in the established method of producing a quantitative result to assess surgical instrument freedom. The process incorporates various spatial, anatomical, and technical components pertinent for the accurate and insightful analysis of a surgical corridor. This quantitative approach resolves issues in assessing this surgically imperative parameter that are cause by multiple planes, irregularly shaped access corridors, procedural variability, and mathematical inaccuracies.

This methodology comprises the various embodiments of a system and an associated mathematical method to determine a 3D VSF before operating on neurosurgical structures. The system characterizes, assesses, and models a 3D volumetric measurement of the maneuverability of a surgical instrument within a surgical corridor with respect to STS access, thereby providing new insight into the accessibility of an intracranial structure via a specific approach. It is explicitly advantageous to medical specialties, such as neurosurgery, that deal with microanatomical structure and require competency in microsurgical techniques. Dealing with small structures that have

definitive targets is inherent in the microsurgery of STSs that lie at a depth from the surgical entry point.

Neurosurgeons try to maximize the potential physiologic space at their disposal to minimize circumferential damage. The VSF is a metric that enables a more accurate assessment of the freedom of this physiologic space in conjunction with specific surgical maneuvers. Anatomically, this concept and the basis behind neurosurgical corridor modeling can be characterized by examining the pathologic processes encountered by the neurosurgeon. For example, vascular aneurysms are abnormal protrusions or weaknesses in the wall of a blood vessel. Obliteration of these weaknesses is imperative to prevent intracranial hemorrhage and potential morbidity and mortality. Minimizing the degree of brain retraction is an important factor in decision-making when selecting a surgical approach. With the VSF, the degree of retraction can be quantitatively measured with respect to each approach and each STS. Another example is the midline tumor, such as the pituitary lesion, which often produces complex surgical conditions because of the need to cross neurovascular structures and overcome difficult angles of attack produced by the anatomy. As with vascular lesions, the VSF can provide a more accurate quantitative assessment of midline tumors and better anatomical visualization of the different surgical corridors to reach this region of interest. Finally, a third example is the abnormal lesion of the nerves, such as an acoustic neuroma growing at the deep apex of the cerebellopontine angle of the skull base, the trajectory of which naturally follows the

conical structure of our model when the potential physiologic space is created by brain retraction and the release of cisternal cerebrospinal fluid.

Given that neurovascular structures tend to traverse the fossae floors along their pathway, the use of this surgical corridor modeling method is particularly relevant in surgical interventions of the skull base, where the STSs are usually bounded inferiorly by the skull base. Skull base surgery usually entails both anatomical and technical obstacles: deep STSs, multiple eloquent structure boundaries, dural tethering, and skull base canal insertion. These influential factors substantially limit maneuverability, which is extremely precious. The VSF is a valuable tool for evaluating surgical corridors that allow only restricted movement and therefore is a particularly useful metric for the assessment of skull base surgical approaches.

This methodology generates the first spatially accurate model of an irregular surgical corridor that also considers actual anatomical boundaries. Furthermore, it allows the influence of the different visualization techniques used in surgical intervention to be examined. For example, the operating microscope, although limited in image expanse and illuminating capabilities, does not function within the approach corridor. In contrast, the endoscope is used within the surgical corridor, where, as an extra instrument or a space-occupying entity, it will impede the freedom of other instrumentation. Experimental scrutiny of this variable has not been completed, although it is common knowledge among endoscopic surgical specialists who have proposed multiportal endoscopic approaches to combat instrument crowding or “swording.” (Dallan, Castelnuovo, et al.,

2015; Lim et al., 2020) The VSF not only provides a numerical representation of the effect of the endoscope on instrument freedom but also creates a 3D representation of this influence. Notably, the endoscope is dynamic and can be moved out of the trajectory of attack as dictated by the operating surgeon, but the numeric change in the VSF caused by its presence remains valid. Given the dynamic nature of the endoscope, mapping its optimal position in the context of different STSs and angles of attack could pose a useful predictive model for improving the efficiency of surgical movement and minimizing exposure.

The system and the associated method provide the surgeon with a volumetric metric to determine the appropriateness and utility of a surgical approach to access a specific pathology. It would, therefore, potentially allow the neurosurgeon to select approaches and define a safe access corridor for guidance during both the planning and the conduct of surgery. This metric can also elucidate the appropriateness of surgically attainable targets specific to an approach. Like all attempts at neuroanatomical quantitation, the VSF functions as a quantifiable metric for assessing the likelihood of surgical risk and injury to anatomical STSs, but it achieves this with substantially superior accuracy and volumetric spatial computation.

Procedural Superiority of the VSF

The VSF methodology includes the calculation of the area bounded by the surgical corridor extrema coordinate points. Perpendicular to the central axis of the

surgical corridor, this area is bounded by the surgical corridor extrema points that are measured.

Previous methods also measured the bounded area and used this area calculation as the metric of surgical freedom. These methods used Heron's formula to calculate the area, which involved subdividing the bounded area into triangles, with the measured points as the vertices of the triangles. With the coordinates of each vertex known, the lengths of the three sides of each triangle were calculated using Heron's formula, and the areas were summed to give the total bounded area.

In our proposed VSF methodology, the bounded area is used in calculating the VSF because the base of the cone shape is formed by the bounded area and the area value is used to calculate the volume of the cone shape. The VSF methodology uses a different method—the shoelace formula—to calculate the area. The shoelace formula was used instead of Heron's formula because it can calculate the area of irregular shapes more accurately. Heron's formula inherently requires choosing how to divide the area into triangles, which is important, as illustrated in Figure 5.10.

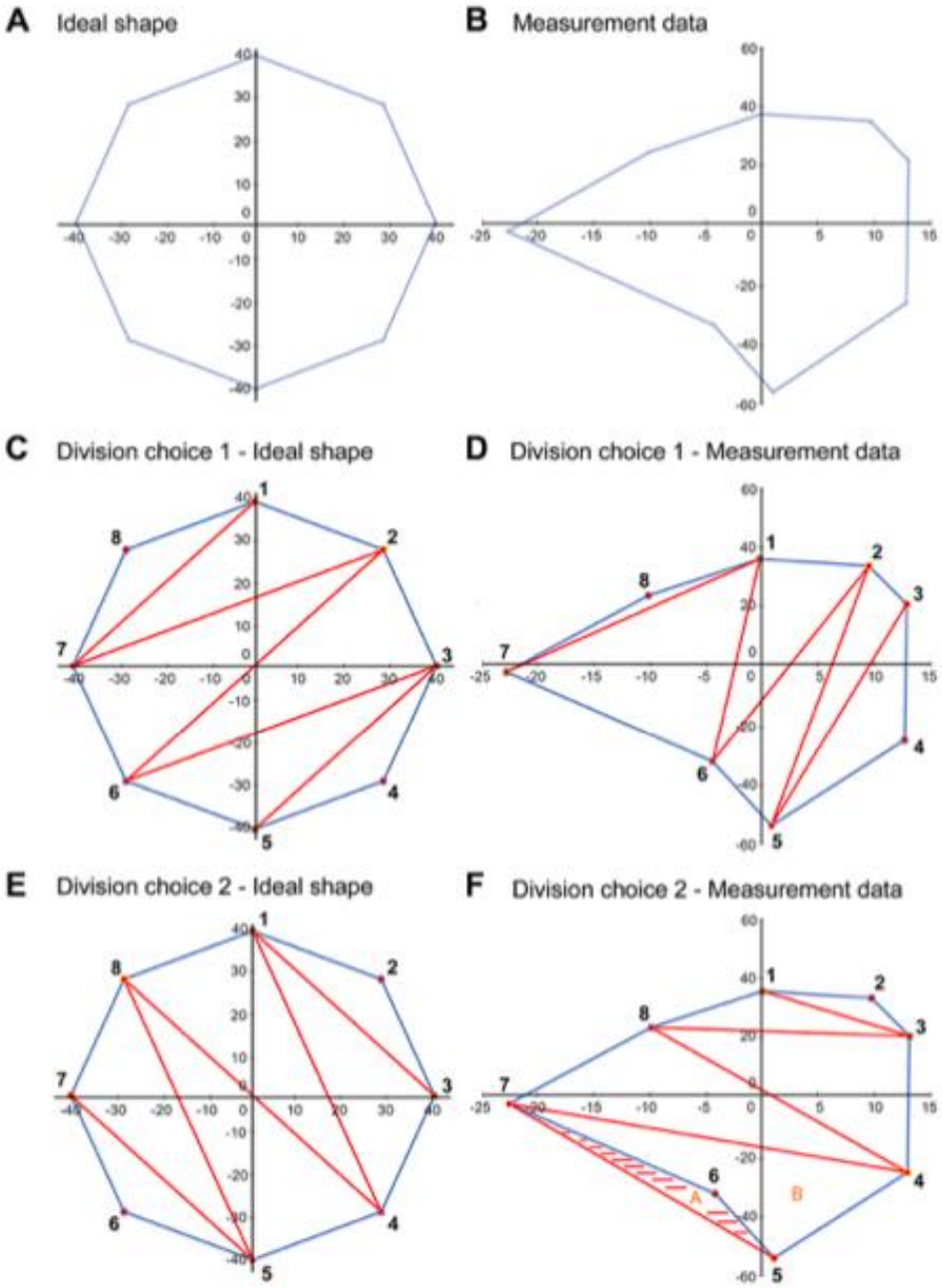

Figure 5.10. Illustration depicting a limitation of using Heron's formula to calculate the area of an irregular closed shape. (A) An idealized shape made up of eight data points. (B) A shape plotted from a sample measurement, also with eight data points. (C) An

example of a choice of division of the area into component triangles for application of Heron's formula. (D) This division choice applied to the sample data. In this case, using Heron's formula on each of the triangles results in a correct calculation of the total area. (E) Another example of a choice of division of the area into component triangles. (F) This division choice applied to the sample data. In this case, using Heron's formula on each of the triangles results in an overestimation of the bounded area, as the shaded area is included twice in the calculated area, as part of triangles A (5-6-7) and B (4-5-7), although it is outside the area bounded by the data points. Used with permission from Barrow Neurological Institute, Phoenix, Arizona.

This figure illustrates two methods of dividing an ideal shape and a shape determined from measurement data into triangles. The first choice of division of the shape results in an accurate calculation of the bounded area of each shape. However, the second choice of division, while calculating the area of the ideal shape correctly, overestimates the area of the shape from the measurement data and results in an area outside the bounds of the shape being included in the calculation.

A method that requires a choice, or the validation of a choice, for each set of data is not conducive to creating a calculator that will give repeatable and accurate results because each calculation requires user input to review and determine how the shape will be divided into triangles. To avoid this dilemma, we selected the shoelace formula to use in calculating the area for the VSF methodology. This formula uses coordinate data of the

vertices of a closed, irregular shape to calculate the enclosed area. This method accounts for irregular shapes and does not overestimate the area, as the Heron's formula method does. Because the VSF method includes the identification of a normalized-height plane for the base of the cone, and the measured points are translated onto this plane, the points can be converted into a 2D coordinate system on the normalized-height plane, and the 2D shoelace formula can be used. Converting the 3D coordinates to 2D coordinates has the advantage of allowing the creation of 2D plots of the cone base that can be used to verify the measurement data.

Translating the original measurement points onto a plane and calculating the area using the translated points also increases the accuracy of the calculated area over a calculation using the original 3D measurement points. The area of interest is the area of the surgical corridor perpendicular to the central axis of the surgical corridor, which is the truest representation of the accessibility of the surgical approach. Because the best-fit plane is perpendicular to the central axis of the surgical corridor, the area bounded by the translated points is perpendicular to the axis of the surgical corridor and thus represents a true cross-section of the surgical corridor. As noted previously, the 3D coordinate data that are measured are not in a single plane because of inaccuracies in measurement, meaning that the triangles formed for measuring the bounded area using Heron's formula are not perpendicular to the central axis of the surgical corridor. As a result, calculating the total area by summing the areas of the triangles would be an overestimation. The sample data set of Figure 5 illustrates this as the area calculated using Heron's formula on

the original measurement data points (1489 mm^2) was 5% higher than the perpendicular area measured from the data points after translation onto the best-fit plane (1418 mm^2).

Benefits of Using Normalized Height

Although the concept of volumetric quantification of surgical freedom is novel, we further refined the concept to a normalized volumetric quantification of surgical freedom to compensate for several inaccuracies inherent in the measurement process. The measurement process involves measuring the coordinate data points for the extrema of the surgical corridor at the end of a surgical instrument of fixed length (Figure 5.4). Doing so resulted in the coordinate data being measured outside the cadaveric specimen, such that the area being measured was not a measurement of the surgical entrance but rather an abstract measurement of surgical freedom that could only be compared to other measurements that used a surgical instrument of equal length. Measuring with a shorter probe would result in a smaller measurement of surgical freedom for the same surgical corridor because of the conical shape of the surgical corridor, whereas measuring with a longer probe would result in a larger measurement of surgical freedom because the length of the probe defines the vertical height of the cone shape from base to apex.

The depth of the structure from the surgical entry point is of secondary importance to the degree of freedom of the instruments within the surgical corridor, which is why this method of measurement can be used at the end of a fixed probe. With the use of this method, surgical corridors and their quantitative measurements with

respect to STSs can be directly compared only if the probe length is exactly equal across studies. This limitation raises questions about the scientific validity of these studies and restricts replication of results and large-scale analysis of anatomical surgical corridor data. The limitation is equally applicable to a volumetric measurement of surgical freedom; for the same surgical corridor, a shorter probe results in a smaller volume measurement, and a longer probe results in a larger volume measurement. Measuring the volume of the surgical corridor up to a fixed distance from the apex (a normalized height) can mitigate this issue. The measurement data from any length of probe can be used to calculate the VSF at a fixed distance from the apex, so the normalized VSF calculation allows the direct comparison of VSF data from any measurement that uses this method.

This decoupling of cone height from probe length also improves the accuracy of the VSF measurement. In our experimental data, human error in collecting coordinate data led to variation in the distance between the apex point and each of the extrema data points of the surgical corridor. This inaccuracy in the data existed in all three dimensions, and there is little that can be done in processing the data to improve the accuracy in the two dimensions on the plane of the base of the cone. However, the normalized VSF measurement, by defining a fixed distance from the apex to the base of the cone, can reduce the inaccuracy in the third dimension along the axis of the cone. The inaccuracy in this dimension has a large effect on resultant calculations. The SD of the average probe length data for all measurement data sets was identified as 5 mm from the plot (Figure 5.9). The effect of this variation on the calculated volume can be seen in our sample data

set analysis. In this case, the height of the cone shape increased from 183.6 mm to 188.6 mm, for an increase of 5 mm (2.7%). The resultant calculation of the cone volume increased by 8.4%. This outcome demonstrates how errors in probe length measurements can be exaggerated in the calculated surgical freedom metric, and thus may translate to important surgical implications. The use of a normalized cone height eliminates this variation in the calculated volume and leads to a more consistent result that can be compared to other normalized VSF data with a much higher degree of confidence.

3D Modeling of the Operative Corridor

Visualization is a critical skill. From the surgeon's perspective, being able to orient and envision the structures and any restrictions and obstacles in the surgical corridor is imperative to selecting the most appropriate approach and planning specifically for the selected surgical strategy. As previously noted, neuroanatomy has been extensively analyzed and neurosurgeons have a well-established knowledge base about anatomical sites and the sizes and arrangements of specialized regions. Less explicitly defined are the physiologic and surgical corridors created by operators, the architecture of these potential or created spaces, and how the circumferential anatomy affects these crucial aspects in surgical decision-making.

The novel design of the VSF results in an improved concept constructing a configuration that embodies the actual geometry of the surgical approach corridor, which is illustrated by our models. When incorporated with the clinical, anatomical, and

surgical application, this volumetric model yields better assessment and prediction of the ability to manipulate surgical instruments, while providing spatially and anatomically accurate representation that can aid the surgeon in decision-making. These images accentuate the importance of not only anatomical considerations but also the critical principles of microsurgery: technique, instrument maneuverability, and the predicted primary instrument axis. The VSF methodology provides an anatomically and spatially accurate 3D depiction illustrating all these key surgical ideals, which proves its substantial clinical applicability.

Limitations

Ideally, this quantitative analysis and modeling should be conducted in vivo in human patients rather than in cadaveric specimens because the brain parenchyma can harden in cadavers with fixed tissue, resulting in decreased surgical maneuverability. However, cadaveric brain tissue is the best model available; although it may not be exactly representative, the quantitative results are proportionate. Although the surgical corridor may be larger in vivo, the anatomical parameters are the same, and the 3D models of the surgical corridor are therefore still reflective of real-time surgical views.

Ideally, the VSF measurements should be made in relation to pathologic processes, such as a vascular weakness like an aneurysm or an intracranial mass lesion, which was not possible in the current study. We therefore could not take into account the potential mass effect influence of intracranial pathology on surrounding brain

parenchyma and structures, nor could we predict the pathologic decrease in intracranial potential space. Again, this limitation is inherent in all cadaveric modeling because the accessible anatomy is generally physiologically normal. The reproducible STSs are reasonable representations of delicate neurovascular components of high priority to the neurosurgeon who must select the optimal approach on the basis of quantitative metrics that are critical to the decision-making process. What can be extrapolated from our analysis is the predictable numeric value and anatomical shape of surgical access corridors used to reach the pathologic target. In addition, the VSF quantitatively and visually allows for the comparison of approaches, and it ultimately provides increased multifaceted information for surgical decision-making that is comparable to other available metrics.

The VSF methodology is based on the assumption that the surgical corridor traverses from a region of large freedom and maneuverability to an apex or an STS. This assumption produces the cone shape that supports the mathematical and modeling structure of this system. This is the accepted surgical trajectory of transcranial surgical interventions and potentially that of other surgical interventions, where instruments proceed from areas of large surgical freedom to small, confined regions necessitating microsurgical technique. However, this model is not applicable for comparison with all approaches. The caveat of this quantitative and visual estimator is the assumption of the surgical apex; the corridor ends at the point represented by the STS. For quantitatively and spatially comparable results, the comparison of different surgical approaches is

possible only when both approaches abide by this assumption. For example, the comparison of a transcranial pterional approach and an endonasal transplanum-cavernous approach to the paraclinoid internal carotid artery is not an equivalent assessment, because an endonasal approach creates a large amount of deep surgical exposure, and its parameters do not converge to an apex as in a transcranial approach (Figure 5.11).

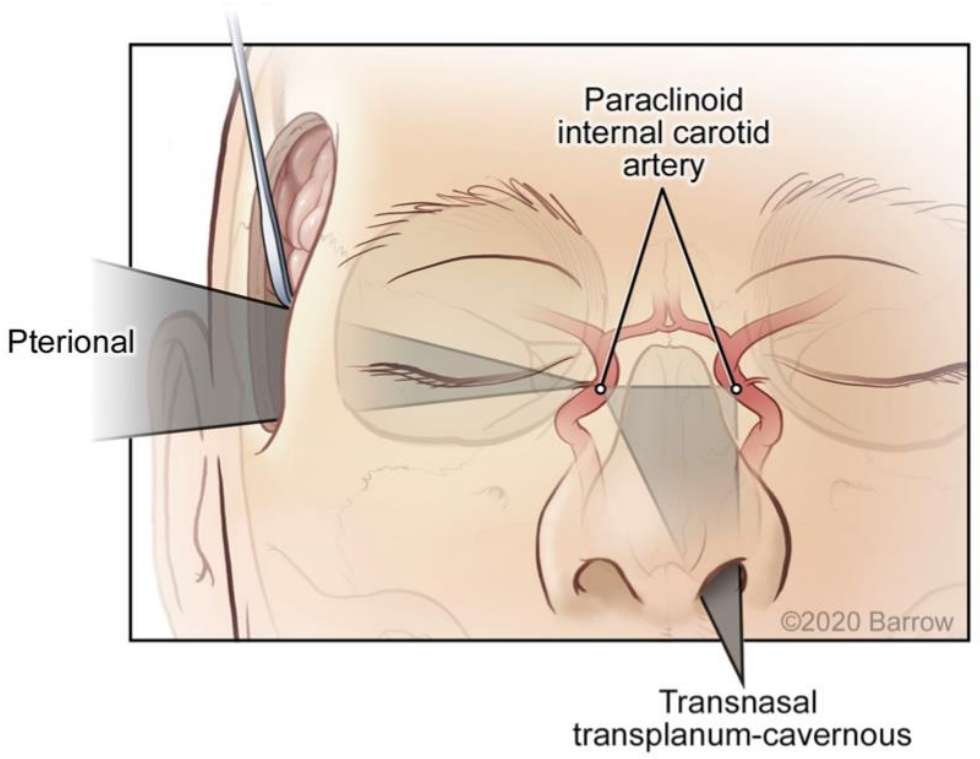

Figure 5.11. Surgical maneuverability of an instrument using a transcranial pterional approach compared with a transnasal transplanum-cavernous approach to the paraclinoid internal carotid artery. In the transcranial approach, the surgical corridor progresses from a superficial region of large maneuverability to a small deep apex, whereas in the transnasal approach, a significant amount of deep volume is created by traversing the

ethmoid and sphenoid sinuses. Used with permission from Barrow Neurological Institute, Phoenix, Arizona.

Conversely, it is acceptable to quantify and model specific to an STS if both approaches have the same surgical boundaries (i.e., both use a deep transsphenoidal approach) and if an assumption has been established that the STS represents the conical apex. For example, a comparison of a transnasal approach and a transmaxillary approach is possible because both produce the same deep surgical exposure, although they are restricted more superficially by different anatomical structures at the surgical entrance. In this scenario, the VSF is a useful metric and a helpful surgical corridor modeling tool for visualizing these restrictions.

Future Directions

This report describes in detail an improved and more representational mathematical and modeling methodology for quantitatively assessing surgical freedom. Our rationale was to produce a robust, multifaceted tool that neurosurgeons can use to estimate the benefits and disadvantages of different surgical approaches specific to various STSs.

Although we have illustrated quantitatively and visually how the various constituents of this novel design are superior to the previous method, comparative analysis has yet to be completed. Our next step in proving the scientific, mathematical,

logistical, and applicable advantages of the VSF will be to complete cadaveric quantitation of the same surgical approaches specific to various STSs and to analyze the results. Specifically, three areas should be examined in detail when comparing this VSF methodology with previous methodologies: (1) the increase in accuracy of the measured area when measuring the area on a single plane versus on points in 3D space because of the measurement of only the perpendicular area; (2) the reduction in the variation in results because of the calculated probe length using the normalized unit of the VSF and how variations in probe length affect the calculated area or the VSF metric; and (3) further analysis of the limitations of Heron's formula, specifically regarding the choice of division of the bounded area of irregular shapes.

Our interdisciplinary research group also intends to replicate this experimental methodology with multiple neurosurgical approaches. We will then quantitatively analyze the benefits and disadvantages of different operative corridors to specific STSs, which will ultimately increase the body of reproducible, standardized, and comparable surgical freedom data and promote optimal surgical techniques and practices.

In regard to comparing the VSF with the previously used method, we predict that the quantitative results will correlate and will be approximately proportionate. It is important to highlight that the merits of the VSF are a result of two key features: the increased accuracy of this multifaceted biomedically orientated mathematical methodology and the ability to produce anatomically and spatially accurate 3D models. These two components have coalesced to produce an effective translational tool that

combines anatomical, clinical, and surgically pertinent principles for improved operative decision-making.

Although our report details the use of this methodology for neurosurgical operative corridors, this system can likely be used in its current form to quantitatively analyze and spatially visualize the surgical approaches of different surgical specialties. Doing so would require that they abide by the structural parameters of this measurement process: that the instrument freedom of the surgeon traverses from a region of larger maneuverability at the surgical entrance to a target apex of minimal maneuverability. As denoted when referencing skull base surgical concepts, it is in fixed domains of minimal freedom that knowledge and insight about the movement capabilities of an instrument are most important. Quantitation of spinal surgical corridors and specific STSs is certainly feasible using this methodology, and it is worthy of further investigation.

Our method for determining the VSF provides the surgeon with a diverse metric and a useful tool for improved surgical preoperative planning and decision-making. Current neurosurgical navigational systems plan surgical routes along a direct trajectory based on a linear display. These navigational approaches portray the trajectory line to the STSs in different views (e.g., axial, coronal, sagittal, and probe view), which is not always the optimal approach and does not incorporate any criteria relevant to surgical corridor analysis. These planning navigation systems also do not incorporate any modeling, which would elucidate or illustrate the degree of surgical freedom. By compiling a substantial body of data, we hope to develop standardized reproducible

surgical approach principles specific to operative corridors and STSs and thereby establish predictive surgical theory. Consequently, the integration of the VSF into intraoperative planning, as well as into surgical navigation software and systems, could prove to be a powerful tool for improving surgical decision-making and techniques, while ultimately minimizing surgical morbidity and mortality.

Conclusion

The VSF is a superior method of quantitative anatomical measurement. This innovative concept can be used to develop an actual geometric model of a surgical corridor that yields better assessment and prediction of the ability to manipulate surgical instruments. The VSF accounts for multiple inaccuracies in the practical and mathematical method of assessment, and it also enables the production of 3D models. For this reason, the VSF is a preferable and clinically applicable standard for the assessment of surgical freedom. This quantitative measurement can establish surgically attainable targets for specific approaches and also assess the suitability of a specific surgical approach compared to alternative operative options, thereby acting as a pivotal tool in the decision-making armamentarium of the neurosurgeon.

CHAPTER 6

The following chapter is in preparation for submission to the Journal of Neurosurgery.

CHAPTER 6

OPTIMAL ANTERO-LATERAL ACCESS CORRIDORS TO THE ANTERIOR SKULL BASE AND PARAMEDIAN VASCULATURE: QUANTITATIVE ANALYSIS OF UNILATERAL SUPRAORBITAL, TRANSORBITAL MICROSCOPIC AND TRANSORBITAL ENDOSCOPIC APPROACHES

Houlihan L.M, Loymak T., Abramov I, Jubran J.H., Staudinger Knoll A.J., Howshar J.T., Tran C., O'Sullivan M.G.J., Lawton M.T., Preul M.C.

Abstract

Objective: Use of the transorbital surgical corridor has increased. Transorbital neuroendoscopy (TONES) has established utility but has not been compared with an open craniotomy, which has a similar trajectory. The effect of visualization technology on surgical freedom has also not been analyzed.

Methods: Twenty specimens underwent supraorbital craniotomy (SOC), transorbital microscopic (TMS), and TONES dissections. Morphometric analysis included length of ipsilateral cranial nerves (CN) I, CN II, optic tract, A1, and contralateral CN II; area of exposure of the frontal lobe base; and craniocaudal and mediolateral angle of attack and volume of surgical freedom (VSF) of the paraclinoid internal carotid artery (ICA), terminal ICA, and anterior communicating artery (ACoA).

Results: All structures were accessible through an SOC. The full length of the contralateral CN II and ipsilateral A1 were reachable in 25% and 15% of cases,

respectively, with TMS and 35% and 15% of cases with TONES. TMS and TONES were hindered when accessing more distal vasculature. The mean (SD) frontal lobe base parenchymal exposures for SOC, TMS, and TONES were 955.4 (261.7) mm^2, 846.2 (249.9) mm^2, and 944.7 (158.8) mm^2, respectively (p=0.26 for all approaches). Multivariate analysis estimated that use of the SOC to access the paraclinoid ICA would result in an 11.17-mm^3 normalized volume (NV) increase compared to transorbital corridors (p<0.001). TMS resulted in a 3.5-mm^3 NV increase in volume compared to TONES (p=0.04). There was no difference between the 3 approaches for VSF of the ipsilateral terminal ICA (p=0.71). TMS provided increased access compared to TONES for the terminal ICA; TMS resulted in a 4.1-mm^3 NV increase in VSF (p=0.01). SOC produced the largest access corridor maneuverability to the ACoA (mean [SD] NV: 15.6 [5.6] mm^3 vs 13.7 [4.4] mm^3 for TMS vs 7.2 [3.5] mm^3 for TONES, p=0.01) and was confirmed with a 5.34-mm^3 NV increase in VSF of the ACoA for SOC compared to transorbital approaches (p=0.01).

Conclusion: Although the SOC provides superior surgical freedom for targets that require more lateral maneuverability, the transorbital corridor is an option to access the frontal lobe base and terminal ICA. This study also identifies quantifiable differences in instrument freedom between the microscope and endoscope. When using the transorbital corridor, a combined visualization strategy is optimal.

Introduction

Transorbital surgery has evolved substantially over the past 150 years. (L.M. Houlihan, Belykh, Zhao, O'Sullivan, & Preul, 2020) It was initially used exclusively by ophthalmologists and is now gaining significant momentum as a multidisciplinary minimally invasive surgical corridor. (L. M. Houlihan, Staudinger Knoll, et al., 2021b; Vural et al., 2021) The invention of the endoscope has opened many possibilities for less morbid surgical corridors, most prominently in skull base approaches, where abundant progress has been made in gaining midline and medial access and in using more straightforward operative trajectories. (Labib et al., 2019; Snyderman, Gardner, Wang, Fernandez-Miranda, & Valappil, 2021) It was with this possibility in mind that transorbital neuroendoscopic surgery (TONES) was developed. (Moe et al., 2010) Multiple anatomic feasibility and clinical publications have highlighted the significant advantages of this small corridor (Lim et al., 2020; Ramakrishna et al., 2016)—anterior skull base access without frontal sinus invasion, cosmetically attractive incision, short recovery, and minimal bony destruction of the skull base. TONES is currently being expertly executed by a small cohort of specialist skull base surgeons, but its use and awareness of the surgical corridor's benefits are increasing.

Although there is some literature about transorbital intracranial access with the endoscope as the method of visualization, no publications have investigated the feasibility of using the microscope or have quantitatively compared surgical approaches, specific to the visualization apparatus used by the surgeon. Although studies have looked

at complex skull base regions (Di Somma, Andaluz, Cavallo, Topczewski, et al., 2018; L. R. Lima et al., 2020) via a TONES approach, little substantial comparative quantification of the corridor and its surgical maneuverability has been completed. TONES has been used successfully in the clinical setting to access the anterior and middle cranial fossa for skull base repairs, as well as for tumor removal, (Park et al., 2020) but other than level IV evidence and expert surgeon accounts, minimal preclinical analysis has quantified the surgical freedom with a transorbital versus open cranial corridor. Furthermore, increased use of transorbital access corridors is based on the premise that they provide satisfactory visualization and surgical freedom and that the operative trajectory is equal or superior to open cranial corridors with respect to the region of interest. No open cranial approach with a comparable trajectory has been used as a test to elucidate the benefits and disadvantages of the transorbital route to the intracranial compartments for instrument maneuverability.

Our research group comprehensively analyzed the transorbital access corridor in comparison with an equivalent open craniotomy, the supraorbital craniotomy (SOC). We also investigated whether there was any difference in instrument maneuverability associated with the use of an endoscope versus microscope as the method of visualization.

Methods

Cadaveric Assessments

Ten cadaveric heads were obtained from an approved supplier and examined for anatomical elements outside the realm of biological variability. Heads were embalmed with a customized alcohol-based solution, and the arteries and veins were injected with red and blue silicone, respectively. All 10 heads underwent SOC, transorbital microscopic (TMS), and TONES approaches on the right and left sides, resulting in a total sample size of 20 specimens per approach. Institutional review board approval was not required for this cadaveric laboratory investigation.

Approaches

Supraorbital Craniotomy

The SOC was completed according to previously established anatomical parameters. (Cohen-Gadol, 2020; Martinez-Perez, Albonette-Felicio, Hardesty, & Prevedello, 2020) The head was positioned supine, turned, and with approximately 20° of backward tilt. The supraorbital notch was identified. An eyebrow incision measuring 4-6 cm was made. The supraorbital nerve, which was dissected and released, represented the medial boundary of the craniotomy. The frontalis branch of the facial nerve was preserved during soft-tissue dissection over the pterion. A burr hole was created at the keyhole. After dissection of the dura, a small craniotomy was fashioned with the aim of the inferior cut being flush with the fossa floor. After elevation of the bone flap,

sequential drilling of the fossa floor was completed, until the orbital roof was flattened as much as possible without infiltrating the orbital cavity to achieve maximal instrument access. The dura was opened in a crescent shape and secured inferiorly.

Transorbital Craniectomy

The TMS craniectomy was performed as described in detail (Chapter 4). In brief, the head was positioned along a trajectory similar to the trajectory for the SOC. A 4-5 cm superior lid crease incision was made along the natural crease in the upper eyelid. Sharp dissection along the preseptal plane was completed to identify the superior orbital rim. The supraorbital nerve was identified and released from the supraorbital canal. After the periosteum was incised at the orbital rim, subperiosteal dissection via a sweeping motion was completed with a dissector. The anterior and posterior ethmoidal arteries were cauterized and cut along the side of the periorbita. The craniectomy boundaries were the frontozygomatic suture to frontosphenoidal suture laterally, the frontal sinus anteriorly, and the junction of the frontal bone and cribriform plate of the ethmoid bone, the frontal sinus medially, and orbital rim laterally. The lamina papyracea, roof of the optic canal, frontal sinuses, and ethmoidal sinuses were preserved throughout. Durotomy was completed in a cruciate fashion.

Orbital and intracranial rigid endoscopy was performed using 4-mm 0°, 30°, and 45° endoscopes (Karl Storz Endoscopy America, Inc, El Segundo, California) as appropriate to maximize visualization. Once TMS measurements were completed, the

endoscope was inserted, and any enlargement or alteration to the transorbital craniectomy deemed to improve instrument access was completed, provided the lamina papyracea, roof of the optic canal, frontal sinuses, and ethmoidal sinuses were preserved.

Neuronavigation System

Each head was rigidly fixed in a Mayfield head holder (Integra Life Sciences Corporation, Cincinnati, Ohio) while measurements were obtained. A neuronavigation system (StealthStation S7 Surgical Navigation System; Medtronic, Dublin, Ireland) was used to acquire predetermined data points. Every point was regarded as a spatial point with 3 coordinates (i.e., x, y, and z; units were millimeters). All measurements have been rounded to the nearest 2 decimal places. All measurements were completed 3 times by 3 different neurosurgeons/neurosurgical residents, and the mean value was established to account for interrater and intrarater variability.

Coordinate Data Analysis

The Inchin neuroquantitative platform (inchin.org) was used to calculate the anatomical metrics. This standardized platform allows for storage of coordinate data for further review and analysis, and it produces standardized reproducible results.

Structure Lengths of Exposure

Ipsilateral cranial nerve (CN) I and II and the optic tract, A1, and contralateral CN II were examined with respect to all 3 approaches.

Parenchymal Area of Exposure

The ipsilateral frontal lobe base area of exposure (defined as the most anteromedial, anterolateral, posteromedial, and posterolateral extrema of the frontal lobe base) was examined with respect to all 3 approaches.

Angle of Attack

The maneuverability within each approach was evaluated with respect to various predetermined surgical target structures (STSs) that are of operative importance (ipsilateral paraclinoid internal carotid artery [ICA], terminal ICA, and anterior communicating artery [ACoA]). The craniocaudal and mediolateral angle of attack (AOA) specific to each STS was assessed. It was quantitatively measured as the maximum allowable AOA in the vertical and horizontal planes. The AOA was measured by moving the proximal end of a probe from an extreme superior or medial position to an extreme posterior or lateral position, with the distal end placed on the STS.

Volume of Surgical Freedom

The volume of surgical freedom (VSF) is defined as the maximal available working volume with respect to a specific surgical corridor and STS (L. M. Houlihan, Naughton, & Preul, 2021) and was developed to provide a 3-dimensional (3D) spatially and anatomically accurate quantitative and visual representation of a surgeon's instrument freedom. This standardized metric allowed for direct comparison of approach-specific and visualization-specific surgical maneuverability regardless of variability in data collection methodology. The VSF of the paraclinoid ICA, terminal ICA, and ACoA (measured in cubic millimeters of normalized volume [NV]) specific to the approach and visualization method was completed. Because the endoscope is situated within the surgical corridor, it was moved throughout extreme data coordinate collection to ensure maximal assessment of maneuverability and to best replicate the surgical scenario.

Statistical Analysis

IBM SPSS Statistics (version 26.0.0.1) was used for statistical analysis. Data are reported as mean (SD) as well as the proportion of inaccessible structures with respect to each approach unless noted otherwise. Kolmogorov-Smirnov with a Lilliefors significance correction tests and qnorm plots were employed to test for normality of the analysis of variance residuals, as well as a Bartlett test for equal variances. The one-way analysis of variance or Kruskal-Wallis test for mean differences for equality of proportions was completed for comparison between the SOC, TMS, and TONES

approaches. Univariate analysis between TMS and TONES (i.e., the Mann Whitney *U* nonparametric test) was conducted to allow for the violation of the assumption of normality. In this set of analysis, all variables exhibited nonnormality with either skew or kurtosis values greater than 2.0. Therefore, medians and interquartile ranges were reported except where noted. Ordinary least-squares regression modelling was used to estimate the effect of approach on selected dependent variables. All models were tested for multicollinearity among independent variables and heteroskedastic standard errors. Statistically significant difference was noted as a p-value at $\alpha=0.05$ or less.

3D Surgical Corridor Modelling

Images were photographed using the microscope or endoscope and displayed on a 19-inch high-definition monitor (Carl Zeiss Microscopy, LLC, White Plains, New York). Individual VSF datasets were used to produce 3D renderings of the surgical corridors using a student license for the 3D modelling software Solidworks 2020 (Dassault Systèmes, Vélizy-Villacoublay, France). The 3D models were also superimposed onto microscope and endoscope images of anatomical approaches to illustrate the surgical corridor specific to the STS.

Results

Morphometric Comparison of the SOC, TMS, and TONES Approaches

Accessibility of Structures

Within the cadaveric cohort of 20 specimens, 60% were male, and the mean age at death was 78.8 years. TMS and TONES approaches were more likely to have areas that were not accessible than the SOC approach (Figs. 6.1, 6.2). Although all structures were accessible through an SOC, the full length of the contralateral CN II and ipsilateral A1 was not always reachable via a TMS (25% [5/20] and 15% [3/20], respectively) or TONES (35% [7/20] and 15% [3/20], respectively) approach. In the surgical maneuverability analysis, access to distal vasculature was hindered in both TMS and TONES (inaccessible—ipsilateral paraclinoid ICA: 5% [TONES] 1/20, terminal ICA: 15% [TMS and TONES] 3/20, ACoA: 65% [TMS] 13/20 and 75% [TONES] 15/20).

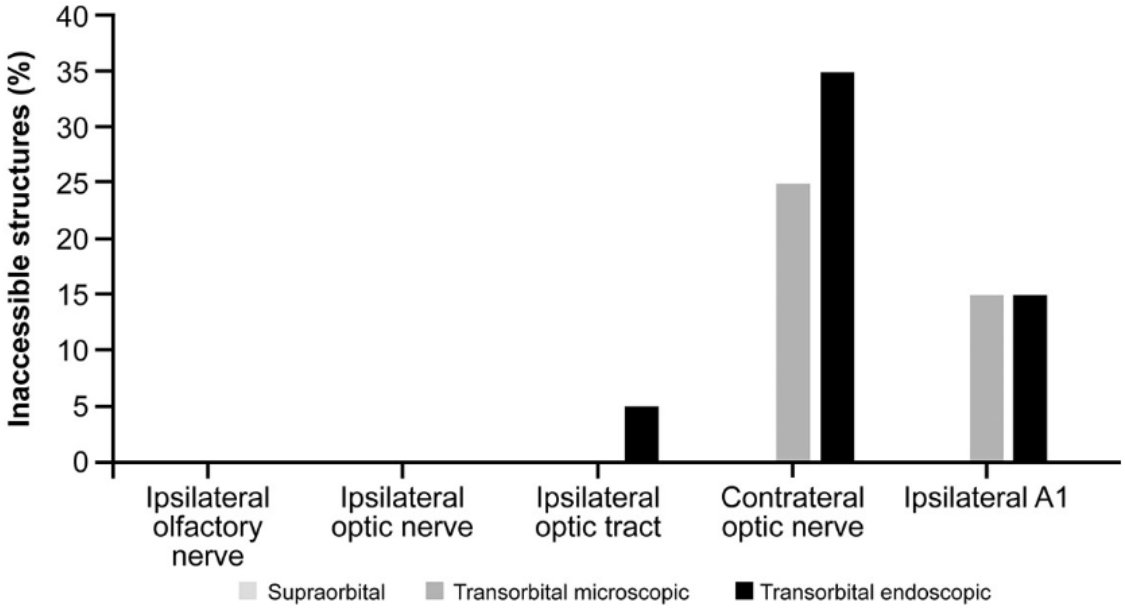

Figure 6.1. Percentage of surgical target structures in 10 cadaveric heads that were approached from 2 sides (n=20) that were inaccessible with the supraorbital, transorbital microscopic, and transorbital endoscopic approaches. Used with permission from Barrow Neurological Institute, Phoenix, Arizona.

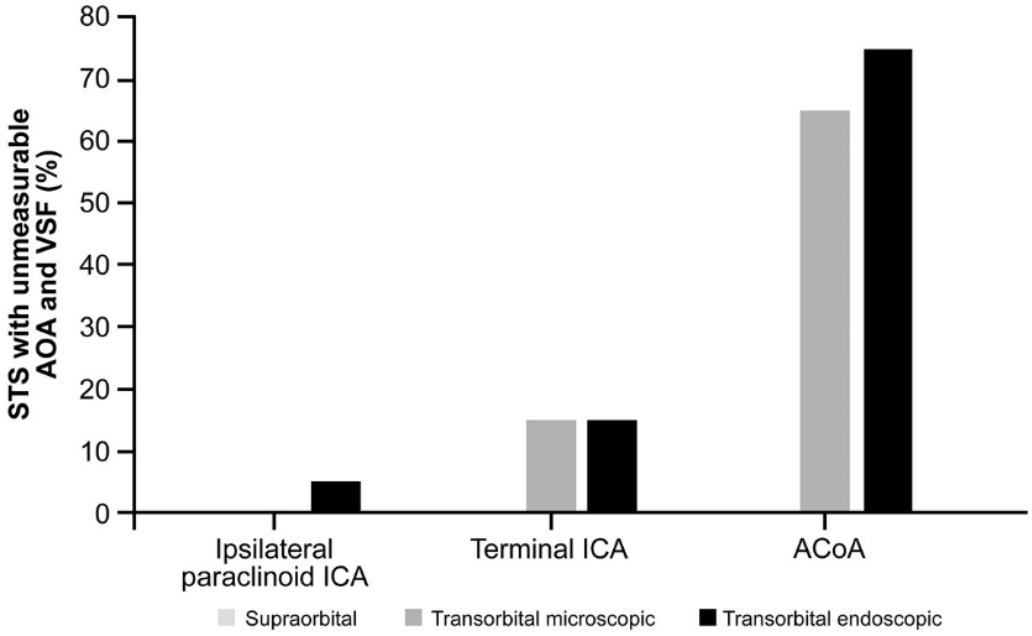

Figure 6.2. Percentage of surgical target structures in 10 cadaveric heads that were approached from 2 sides (n=20) with the supraorbital, transorbital microscopic, and transorbital endoscopic approaches in which assessment of angle of attack (AOA) and volume of surgical freedom (VSF) was not possible due to impaired instrument maneuverability. ACoA anterior communicating artery; ICA, internal carotid artery. Used with permission from Barrow Neurological Institute, Phoenix, Arizona.

Structure Lengths of Exposure

The results are summarized in Table 6.1. There were no significant differences between approaches in accessible length for the structures except for the ipsilateral CN II ($p<0.001$). However, in the ordinary least-squares regression model, the SOC was not

significantly correlated with a change in the length of the exposure for the ipsilateral optic nerve when compared to the other 2 approaches (p=0.51).

When comparing TMS and TONES, there is a difference in accessible structure length. Multivariate analysis showed that TMS had a more limited reach than TONES for the ipsilateral CN I (3.7 mm decrease, p=0.03) and ipsilateral CN II (4.8 mm decrease, p=0.002).

Table 6.1. Analysis of variance of accessible length of intracranial structures specific to the surgical approach

Structure of Interest	All Approaches, mm	Supraorbital, mm	Transorbital Microscopic, mm	Transorbital Endoscopic, mm	p-value
Ipsilateral olfactory nerve	16.6 (4.5)	16.5 (4.8)	15.1 (3.8)	18.2 (4.6)	0.09
Ipsilateral optic nerve	14.0 (4.1)	14.1 (2.7)	11.3 (3.0)	16.7 (4.5)	**<0.001**
Ipsilateral optic tract, median (IQR)	11.0 (9.4-13.3)	10.6 (9.3-13.7)	10.3 (8.6-12.9)	12.4 (10.1-14.0)	0.44*
Contralateral optic nerve	9.4 (3.2)	10.5 (3.2)	8.2 (2.7)	9.1 (3.5)	0.06^
Ipsilateral A1	16.0 (3.2)	17.0 (2.8)	15.1 (3.3)	15.5 (3.4)	0.16

Data are presented as mean (SD) unless otherwise indicated. IQR, interquartile range; SD, standard deviation.
* Model fails the assumption of equal variances. Kruskal-Wallis test p-values reported.
^ Model residuals fail the assumption of normality test, and the variable is transformed to natural log.

Frontal Lobe Base Parenchymal Exposure

The mean (SD) frontal lobe base parenchymal exposure for the SOC, TMS, and TONES was 955.4 (261.7) mm^2, 846.2 (249.9) mm^2, and 944.7 (158.8) mm^2, respectively. Univariate analysis did not show any statistically significant difference between all 3 approaches ($p=0.26$).

Angle of Attack

Both the craniocaudal and mediolateral AOA for the ipsilateral paraclinoid ICA were significantly larger via an SOC than with either of the transorbital approaches ($p<0.001$). Specifically, it was estimated that an SOC would provide a surgeon with a 3.84° increase in craniocaudal AOA and a 5.74° increase in mediolateral AOA to this STS ($p<0.001$) (Figure 6.3).

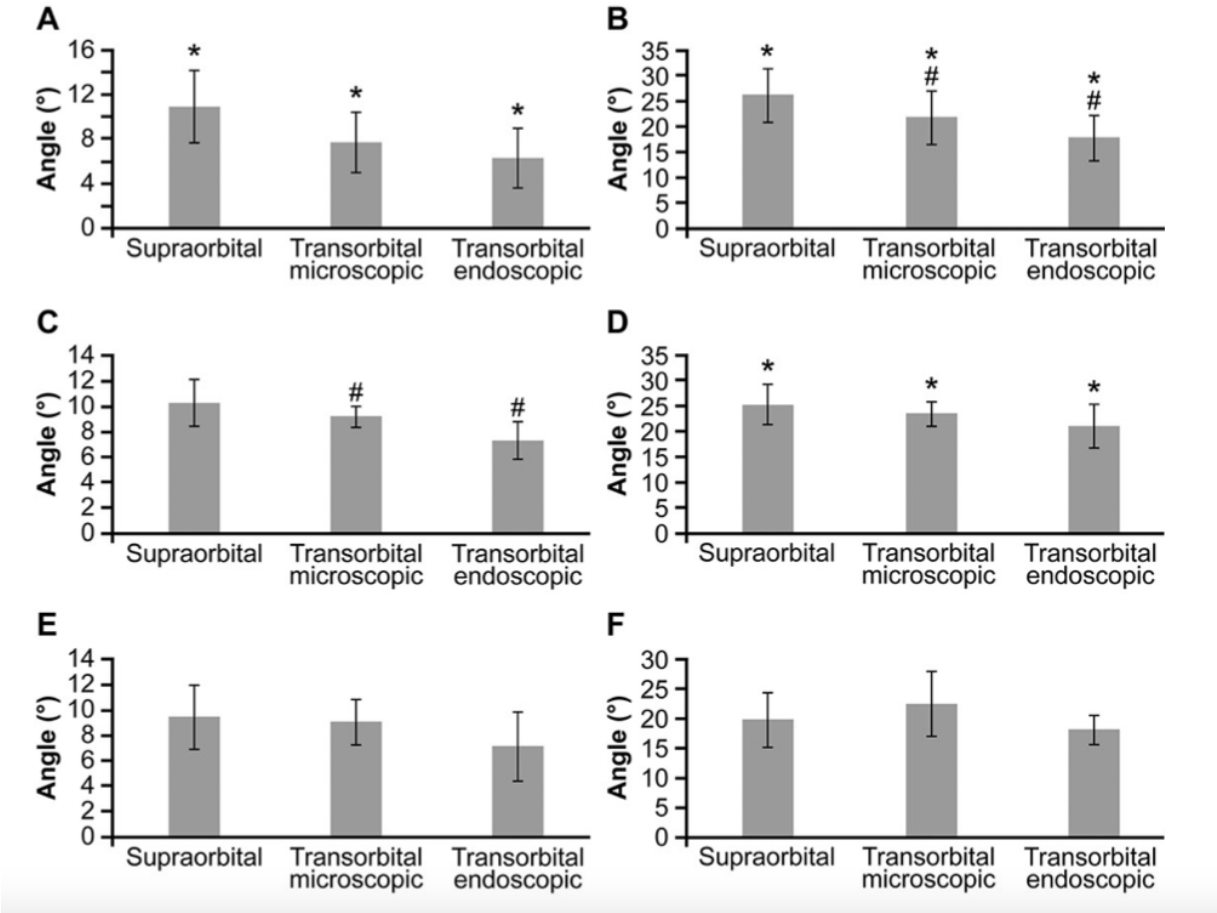

Figure 6.3. Quantitative comparison of the mediolateral and craniocaudal angles of attack (AOA) obtained in 10 cadaveric heads that were approached from 2 sides (n=20) with use of the supraorbital, transorbital microscopic, and transorbital neuroendoscopic surgery approaches, respectively. Values are mean or median; error bars represent standard deviation (SD) or interquartile range (IQR). (A) Craniocaudal ipsilateral paraclinoid internal carotid artery (ICA) mean (SD) AOA: 10.9° (3.3°), 7.7° (2.7°), 6.3° (2.7°). (B) Mediolateral ipsilateral paraclinoid ICA mean (SD) AOA: 26.1° (5.3°), 21.7° (5.2°), 17.7° (4.5°). (C) Craniocaudal ipsilateral terminal ICA median (IQR) AOA: 10.3° (8.4°-12.1°), 9.2° (8.6°-10.3°), 7.3° (6.5°-9.5°). (D) Mediolateral ipsilateral terminal ICA mean

(SD) AOA: 25.4° (4.0°), 23.6° (2.4°), 21.1° (4.3°). (E) Craniocaudal anterior communicating artery (ACoA) mean (SD) AOA: 9.4° (2.5°), 9.0° (1.8°), 7.1° (2.7°). (F) Mediolateral ACoA mean (SD) AOA: 19.8° (4.6°), 22.5° (5.5°), 18.1° (2.5°). * denotes statistically significant difference among approaches, according to ANOVA ($p<.05$). # denotes statistically significant difference between transorbital microscopic and transorbital neuroendoscopic approaches, according to Mann-Whitney U-test ($p<.05$). ACoA anterior communicating artery; ICA, internal carotid artery. Used with permission from Barrow Neurological Institute, Phoenix, Arizona.

When comparing TMS and TONES, there was no craniocaudal advantage with either technique; however, the mediolateral AOA was greater when using a TMS approach (median and interquartile range [IQR]: 21.0 (17.8-24.3) mm^3 NV vs 17.9 (16.3-20.9) mm^3 NV, p=0.03). Multivariate regression identified that a TMS approach would, on average, result in a 3.9° increase in mediolateral AOA to the paraclinoid ICA (p=0.02).

For the ipsilateral terminal ICA, there was no difference in the craniocaudal AOA between all 3 approaches (p=0.51, by Kruskal-Wallis test), but the mediolateral AOA difference was significant (p=0.004). The SOC is significantly correlated with an increase in the mediolateral AOA of the terminal ICA compared to both transorbital approaches, with a mean increase of 3.14° (p=0.01). It was confirmed on multivariate analysis that there was no statistically significant distinction between TMS and TONES.

When comparing SOC with transorbital approaches, no approach was superior with respect to craniocaudal (p=0.02) or mediolateral (p=0.44) AOA, or between TMS and TONES (craniocaudal [p=0.12] and mediolateral [p=0.09] AOA) for the ACoA.

Volume of Surgical Freedom

Initially, univariate analysis did not identify any difference in volume of surgical freedom (VSF) of the ipsilateral paraclinoid ICA between all 3 approaches (p=0.55, by Kruskal-Wallis test); however, multivariate analysis estimated that use of the SOC approach would result in an 11.17-mm^3 NV increase compared to transorbital corridors (p<0.001) (Figure 6.4). Furthermore, TMS was found to produce a larger VSF compared to TONES when accessing the ipsilateral paraclinoid ICA (p=0.02), which was confirmed in regression modelling, where TMS resulted in a 3.5-mm^3 NV increase in volume (p=0.04).

Upon review of the VSF of the ipsilateral terminal ICA, there was no difference seen between the 3 approaches (p=0.71, by Kruskal-Wallis test), and in modelling, the SOC approach nears, but does not confirm, significant correlation, or an increase in the terminal ICA VSF compared to the transorbital approaches (p=0.07). When comparing the 2 transorbital approaches, there is a substantial difference in the surgical freedom TMS provides compared to TONES when accessing the terminal ICA (median [IQR]: 15.2 [13.8-18.1] mm^3 NV vs 10.5 [7.8-14.9] mm^3 NV, p=0.08). This was confirmed in

modelling, where use of TMS was estimated to result in a 4.1 mm^3 NV increase in VSF compared to TONES (p=0.01).

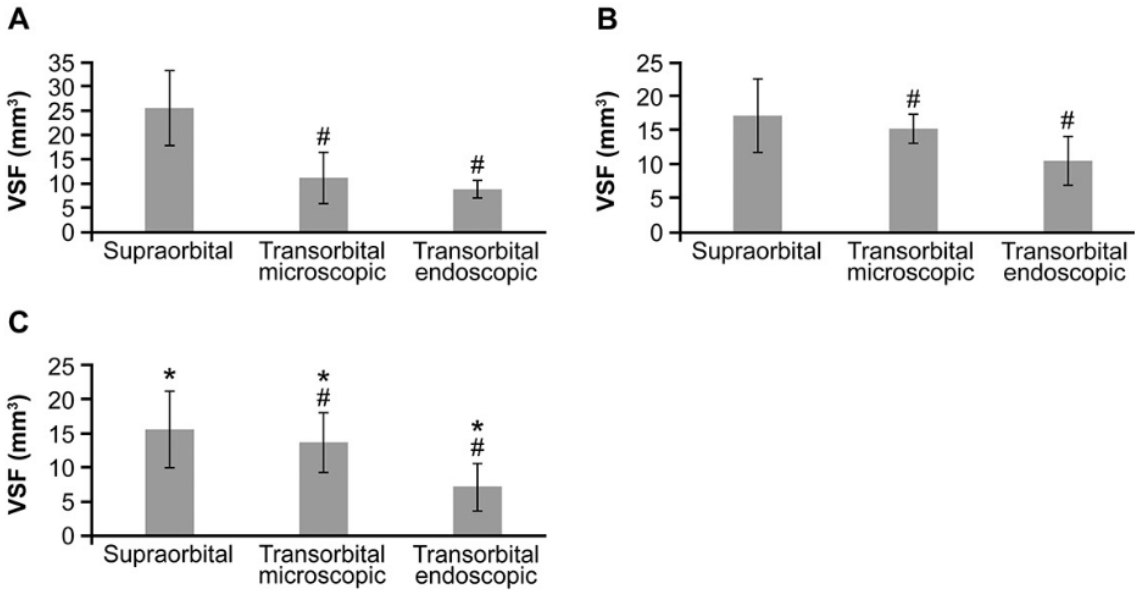

Figure 6.4. Quantitative comparison of the volume of surgical freedom (VSF) achieved in 10 cadaveric heads that were approached from 2 sides (n=20) with the supraorbital, transorbital microscopic, and transorbital neuroendoscopic surgery approaches, respectively. (A) Ipsilateral paraclinoid internal carotid artery (ICA) median and interquartile range (IQR) normalized volume (NV): 25.5 (13.5-28.9) mm^3, 11.2 (8.4-19.0) mm^3, 8.8 (6.5-10.2) mm^3. (B) Ipsilateral terminal ICA median (IQR) NV: 17.1 (11.5-22.4) mm^3, 15.2 (13.8-18.1) mm^3, 10.5 (7.8-14.9) mm^3. (C) Anterior communicating artery mean (SD) NV: 15.6 (5.6) mm^3, 13.7 (4.4) mm^3, 7.2 (3.5) mm^3. *

denotes statistically significant difference among approaches, according to ANOVA ($p<.05$). # denotes statistically significant difference between transorbital microscopic and transorbital neuroendoscopic approaches, according to Mann-Whitney U-test ($p<.05$). ACoA anterior communicating artery; ICA, internal carotid artery. Used with permission from Barrow Neurological Institute, Phoenix, Arizona.

The largest access corridor maneuverability to the ACoA was produced by the SOC (15.6 [5.6] mm^3 NV vs 13.7 [4.4] mm^3 NV for TMS vs 7.2 [3.5] mm^3 NV for TONES, p=0.01). This was confirmed with the SOC producing a 5.34-mm^3 NV increase in the VSF of the ACoA compared to the transorbital approaches (p=0.01). Additionally, the VSF produced by TMS was substantially greater than the VSF for TONES (median [IQR]: 12.3 [11.0-15.4] mm^3 NV vs 6.4 [6.3-7.9] mm^3 NV, p=0.03). Due to the small sample size (i.e., the small number of specimens wherein the ACoA could be accessed via a transorbital approach; n=12), modelling could not be completed.

Discussion

Approach-Specific Surgical Freedom

Selected Surgical Trajectory

The SOC is the most appropriate open craniotomy for comparison with a transorbital approach to the anterior cranial fossa. Although it may be argued that this craniotomy is, in itself, a minimally invasive approach, (Figueiredo et al., 2006) there are

no other skull base corridors that have a similar anterolateral trajectory. Publications have compared the TONES approach with open cranial corridors for access to the paramedian region. (Noiphithak et al., 2019a) Arguably, direct extrapolation of results is difficult, because the importance of the surgical trajectory is not taken into account. Furthermore, integrating the value of surgically applicable neuroanatomical quantitation into the decision-making process requires appreciation of the direction in which the surgeon wishes to approach the pathology. For this reason, when utilizing and assessing surgical metrics, incorporation of the trajectory and its influence on surgical freedom is paramount.

SOC vs the Transorbital Approach

The general assumption is that the larger the defect, the more maneuverability within the cranial cavity one has. However, there are other aspects that need to be considered. Regardless of the size of the craniotomy, access to the STS is influenced by traversing neurovascular and bony eminences along the path from superficial to deep. From a clinical perspective, larger surgical approaches are associated with greater morbidity and an increased risk of injury, infection, and general surgical complications. (Komotar, Starke, Raper, Anand, & Schwartz, 2013) Classification of a pathology as minimally invasive or aggressive can be subjective. Thus, objective analysis of surgical freedom is important in deciphering superiority of approach from a technical perspective.

The SOC has been used to manage lesions of the anterior cranial fossa (Ansari, Eisenberg, Rodriguez, Barkhoudarian, & Kelly, 2020; Seaman, Ali, Marincovich, Osorno-Cruz, & Greenlee, 2020) and to tackle paramedian lesions. (Eroglu et al., 2019; Kalani, Spetzler, & Wanebo, 2016; Xin et al., 2020) Considered one of the neurosurgeon's "workhorse" approaches, its benefits are well established in the literature. This study not only confirms where an SOC would be the preferable anterolateral access corridor, but also highlights that the transorbital route has comparable surgical parameters.

When considering lengths of imperative anatomy routinely appreciated during this approach, there was no difference in the accessible lengths of CN I, CN II, optic tract, A1, and contralateral CN II. Here lies the caveat with respect to contralateral CN II and the ipsilateral A1. At times, these were not accessible via a transorbital approach. Although a portion of the A1 is accessible if the terminal ICA focus is appreciable, greater access to this medial region as well as to the contralateral CN II is generally hindered in the transorbital approach due to the preserved lateral orbital rim. Additionally, in this scenario, the lamina papyracea is preserved to prevent invasion of the ethmoidal sinus and to decrease the risk of cerebrospinal fluid leak. These bony parameters limit the medial ipsilateral extent of the transorbital defect and make contralateral access unfeasible.

A striking result was the equivocal comparison of the area of exposure of the frontal lobe base (SOC: 955.4 [261.7] mm^2, TMS: 846.2 [249.9] mm^2, and TONES:

944.7 [158.8] mm^2, p=0.26). Although the SOC is known to be associated with minimal retraction injury, (Reisch & Perneczky, 2005) accessing the low frontal base to reach the lesion can result in inconvenient surgeon positioning or transgression of normal parenchyma. A transorbital access corridor provides not only a comparable area of exposure but also a superior trajectory, which results in no brain retraction, improved ergonomic surgeon positioning, and minimal invasion of normal brain to access a low frontal lesion.

When assessing surgical maneuverability specific to STS, this study has produced decisive results. Unequivocally, use of the SOC for access to the paraclinoid ICA provided the surgeons with considerably superior AOA and VSF. Although previous studies have highlighted larger surgical freedom compared to use of the SOC it has been used in clinical practice safely for vascular lesions. (Xin et al., 2020) Although the SOC did produce a mean increase of 3.14° in the mediolateral AOA on modelling for the terminal ICA, there was no significant difference in VSF noted between the SOC and TMS approaches (median [IQR] NV: 17.1 [11.5-22.4] mm^3 for SOC vs 15.2 [13.8-18.1] mm^3 for TMS vs 10.5 [7.8-14.9] mm^3 for TONES, p=0.71). This is a new insight into the potential use of a transorbital approach in accessing the terminal ICA from a surgical perspective, and it also highlights the prominent influence the surgical trajectory has on surgical freedom. As shown in Figure 6.5, looking up via a transorbital craniectomy allows for a favorable view of the terminal ICA along its long access, and our quantitative analysis has shown that this approach is a potentially feasible option.

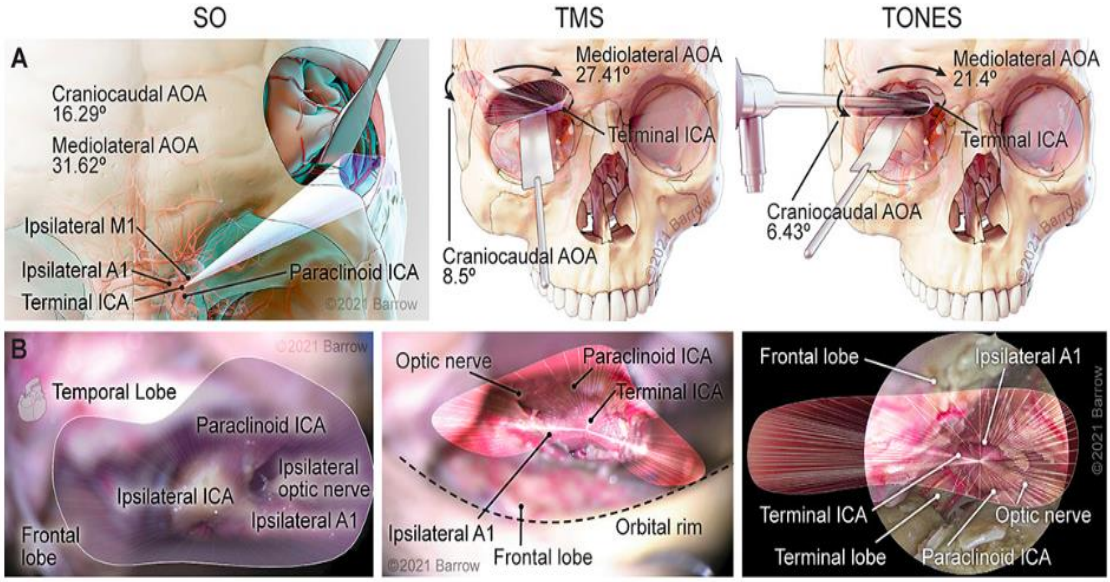

Figure 6.5. Illustration depicting 3-dimensional modelling of the surgical corridor to the terminal internal carotid artery (ICA) from supraorbital, transorbital microscopic (TMS), and transorbital neuroendoscopic surgery (TONES) approaches. (A) The anterior of the surgical corridor. (B) The surgical view of the cadaveric anatomy, which is in continuity with the surgical corridor model parameters (supraorbital: volume of surgical freedom [VSF] = 31.01 mm^3, craniocaudal angle of attack [AOA] = 16.29°, mediolateral AOA = 31.62°; TMS: VSF = 12.22 mm^3, craniocaudal AOA = 8.5°, mediolateral AOA = 27.41°; TONES: VSF = 12.5 mm^3, craniocaudal AOA = 6.43°, mediolateral AOA = 21.4°). AOA, angle of attack; ICA, internal carotid artery.

Initially, review of the ACoA metrics on AOA did not show any difference. This result is difficult to interpret in isolation, given that this STS was inaccessible in a sizeable number of specimens (TMS: 65% 13/20; TONES: 75% 15/20). Clarity and a definitive conclusion are obtained when this statistic is reviewed in combination with VSF, a metric that allows for evaluation of the corridor in 3D space. An SOC produces a 5.34-mm^3 NV increase in the VSF of the ACoA compared to the transorbital approaches ($p=0.01$), which is also in line with the anatomical parameters limiting the lateral extend of the transorbital approach, and is now conclusively quantified. Used with permission from Barrow Neurological Institute, Phoenix, Arizona.

Influence of Visualization Technology on Surgical Freedom

Although this investigation looked at the transorbital access corridor and a comparable cranial route, it is also important to assess whether visualization technology has any influence on maneuverability metrics. Preclinical and clinical attempts have been made to qualify and quantify this potential difference. (Catapano et al., 2006; Filipce & Ammirati, 2015; Filipce et al., 2009; Moller et al., 2020; Zhang et al., 2019) AOA in combination with VSF produces a robust means of completing a quantifiable feasibility analysis. The large specimen number as well as interrater and intrarater variability adds to the strength of conclusions produced in this study.

With respect to all 3 STS, TMS produced larger VSF compared to TONES. Regression models on both the paraclinoid ICA and terminal ICA showed an increase in

VSF (3.5 mm^3 NV and 4.1 mm^3 NV, respectively). Again, comparing AOA in isolation leads to more equivocal results and does not take into account the complete corridor produced. Both visualization methods were used through the same surgical corridor with the same anatomical parameters stipulated. Furthermore, the endoscope was moved throughout measurements to ensure maximal efforts were made to prevent hindrance of maneuverability (Figs. 6.5, 6.6, 6.7). Yet this metric still shows a statistically significant quantitative difference. Although there are undoubted advantages in visualization with use of the endoscope, these results suggest that, in certain circumstances, use of the microscope affords the surgeon superior instrument freedom. Crowding of the surgical corridor has been identified as an endoscope-associated issue. (Elhadi, Zaidi, et al., 2014) These results further affirm that this is an element that influences surgical freedom and should be taken into account in technique decision-making.

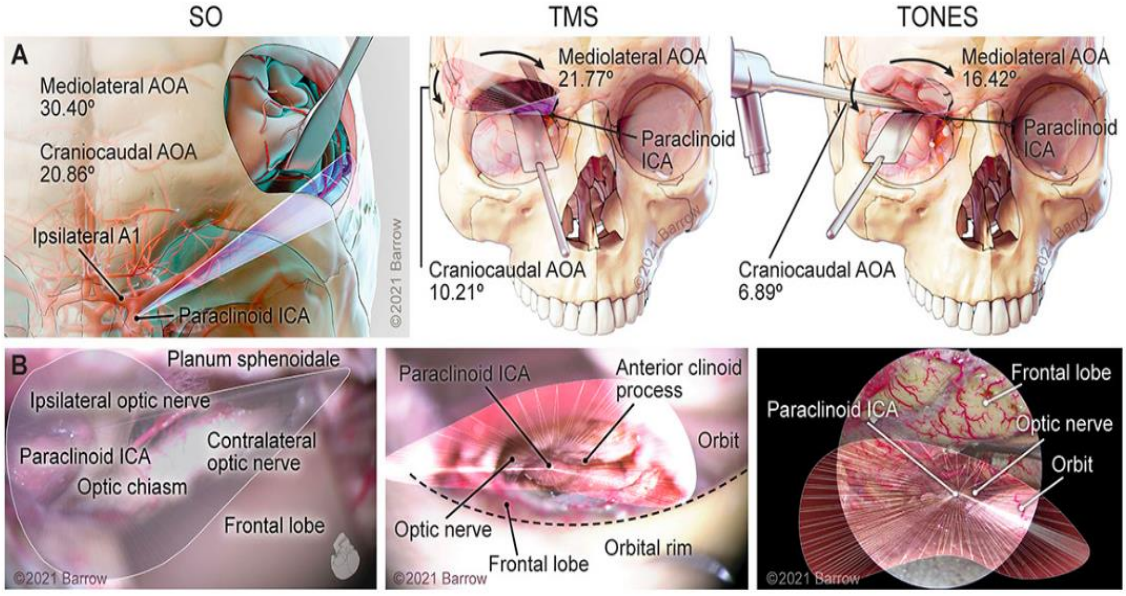

Figure 6.6. Illustration depicting 3-dimensional modelling of the surgical corridor to the paraclinoid internal carotid artery (ICA) from a supraorbital, transorbital microscopic (TMS), and transorbital neuroendoscopic surgery (TONES) approach. (A) The anterior of the surgical corridor. (B) The surgical view of the cadaveric anatomy, which is in continuity with the surgical corridor model parameters. Supraorbital: volume of surgical freedom (VSF) = 43.83 mm^3, craniocaudal angle of attack (AOA) = 20.86°, mediolateral AOA = 30.40°; TMS: VSF = 13.45 mm^3, craniocaudal AOA = 10.21°, mediolateral AOA = 21.77°; TONES: VSF = 9.71 mm^3, craniocaudal AOA = 6.89°, mediolateral AOA = 16.42°. AOA, angle of attack; ICA, internal carotid artery. Used with permission from Barrow Neurological Institute, Phoenix, Arizona.

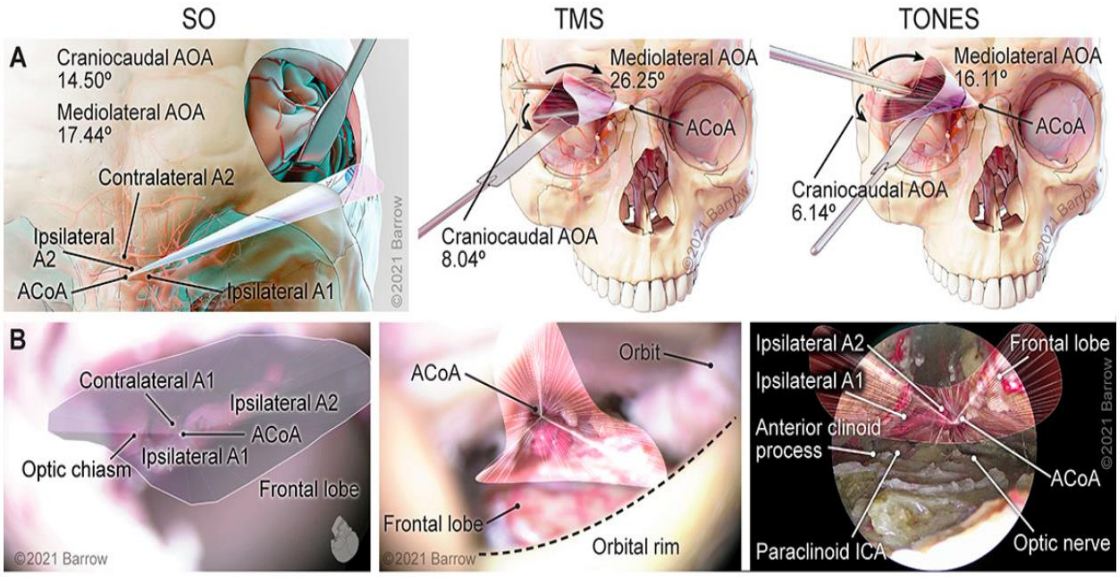

Figure 6.7. Illustration depicting 3-dimensional modelling of the surgical corridor to the anterior communicating artery from a supraorbital, transorbital microscopic (TMS), and transorbital neuroendoscopic surgery (TONES) approach. (A) The anterior of the surgical corridor. (B) The surgical view of the cadaveric anatomy, which is in continuity with the surgical corridor model parameters. Supraorbital: volume of surgical freedom (VSF) = 15.66 mm^3, craniocaudal angle of attack (AOA) = 14.50°, mediolateral AOA = 17.44°; TMS: VSF = 13.36 mm^3, craniocaudal AOA = 8.04°, mediolateral AOA = 26.25°; TONES: VSF = 9.36 mm^3, craniocaudal AOA = 6.14°, mediolateral AOA = 16.11°. AOA, angle of attack; ACoA, anterior communicating artery; ICA, internal carotid artery. Used with permission from Barrow Neurological Institute, Phoenix, Arizona.

Future Directions

Various technical aspects, such as site, size, and consistency, are evaluated by a surgeon when deciding how to approach a surgical lesion. Because of the nature of cranial anatomy, neurosurgeons and skull-base surgeons must consider these components as an intricate constellation, while taking into account inherent stereo-hindrance created by osteologic and neurovascular structures. Technology has substantially advanced our means of access by improving our visualization methods and instrumentation, allowing development of more nuanced surgical technique. Although these apparatuses provide operative advancement for all surgeons, there are nonetheless essential elements of the surgical decision-making process that are discretionary to the operating surgeon. Surgical trajectory and instrument maneuverability account for such intangible factors. Quantitative anatomy allows us to define these components and produces objective evidence to support the use of one approach or technology over another.

This is the first study, to our knowledge, that aimed to establish optimal surgical maneuverability specific to 3 trajectory- and plane-comparable approaches, while also considering not only the bony surgical corridor created but also the influence of visualization technology on a surgeon's instrument ability. What has yet to be established is what constitutes the required numerical parameters for each surgical freedom metric. It is likely that there is no universal answer and that such data need to be reviewed in the context of various patient- and pathology-specific scenarios. These results undoubtedly add to the body of knowledge on the feasibility of transorbital access, a minimally

invasive approach, and how it compares with open craniotomies. Although these results aim to guide the process of choosing an approach, the true value of these metrics can only be addressed when assimilated into clinical studies.

Study Limitations

Preserved tissue is known to be more rigid than live brain parenchyma. (Benet, Rincon-Torroella, Lawton, & Gonzalez Sanchez, 2014) This results in arguably negligible differences in the configuration and size of the intracranial structures and thus affects the area exposed. Nonetheless, results produced within these cadaveric feasibility studies are proportionate and reflect best estimations of the surgical anatomy, wherein the same corridor is fashioned in the same technical way by the surgeon. The metrics of surgical freedom act as a means of defining potential space specific to the approach, taking into account predetermined bony and neurovascular parameters, which are, in themselves, inherent to the surgical decision-making process.

Conclusion

The SOC provides superior surgical freedom when approaching the paraclinoid ICA and ACoA complex, but the transorbital corridor is a feasible alternative for accessing the frontal lobe base and terminal ICA. Although the endoscope provides outstanding intracranial visualization, this study suggests that, for particular STSs, instrument maneuverability is superior with use of the microscope. A combined

visualization strategy is likely the best way to use the minimally invasive transorbital approach.

CHAPTER 7

The following chapter is in preparation for submission to the Journal of Neurosurgery.

CHAPTER 7

EXPLORATORY ANALYSIS OF THE BIPORTAL TRANSORBITAL APPROACH; QUANTITATIVE COMPARISON OF ANTERIOR SUBFRONTAL CRANIOTOMY VERSUS BILATERAL TRANSORBITAL ENDOSCOPIC AND MICROSCOPIC APPROACHES TO THE ANTERIOR CRANIAL FOSSA AND PARAMEDIAN VASCULATURE

Houlihan L.M., Loymak T., Abramov I., Jubran J., Staudinger Knoll A.J., Howshar J.T., Farhadi D., Scherschinski L., O'Sullivan M.G.J., Lawton M.T., Preul M.C.

Abstract

Objective: As transorbital surgery grows in use and popularity, the body of evidence exploring its advantages and limitations needs to increase. The uni-portal transorbital approach has been used in clinical practice, as has the combined transorbital transnasal, but to date, no study has assessed the surgical use and applicability of a biportal bitransorbital approach.

Methods:10 specimens underwent an anterior subfrontal (A.Sub), bilateral transorbital microscopic (BTM) and bilateral transorbital neuroendoscopic (BTE) approaches. Morphometric analysis included: length of the bilateral cranial nerves (CN) I, II, optic tract and A1; the area of exposure of the anterior cranial fossa floor; cranio-caudal and medio-lateral angle of attack (AOA) and volume of surgical freedom (VSF) of

the bilateral paraclinoid internal carotid artery (ICA), bilateral terminal ICA and anterior communicating artery (ACoA), analysing whether the biportal approach promoted superiority in instrument freedom.

Results: BTM and BTE approaches had limited accessibility to the bilateral A1s, as well as the ACoA which was inaccessible in 30% (BTM) and 60% (BTE) respectively. The average total frontal lobe AOE was 1,648.4 mm^2 (1,516.6-1,958.8mm^2) 1,658.9 mm^2 (1,274.6-1,988.2 mm^2) and 1,914.9 mm^2 (1,834.2-2,014.2 mm^2) for the A.Sub, BTM and BTE respectively, with no statistically significant superiority between any of the 3 approaches (p=.276). It was estimated that the BTM and BTE are significantly correlated with a decrease of 8.71 mm^3 normalised volume (NV) (p=.005) and 14.34 mm^3 NV (p=.000) in the VSF of the right paraclinoid ICA compared with the A.Sub. No statistically significant difference in surgical freedom was noted between all 3 approaches when targeting the bilateral terminal ICA. BTE significantly correlated with a decrease of 105% in the (log)VSF of the ACoA compared with the A.Sub (p=.009).

Conclusion: While the concept of a biportal approach aims to improve the maneuvrability within these minimally invasive approaches, these results illustrate the pertinent issue of surgical corridor crowding as well as the importance of surgical trajectory planning. A biportal bi-transorbital approach provides improved visualisation, but it does not improve surgical freedom. Furthermore while it affords impressive ACF AOE, it is not suitable for addressing midline lesions due to limited lateral movement secondary to the preserved orbital rim. In such cases, a combined transorbital transnasal

route is preferable for minimising skull base destruction and maximising instrument access.

Introduction

Endoscopy has opened novel minimally invasive surgical corridors to the skull base, ventricular system, pituitary and suprasellar region (Cavallo et al., 2014; A. Li et al., 2017; Schwartz, Morgenstern, & Anand, 2019). Saying this, there are limitations associated with endoscopic access corridors. Crowding of the surgical corridor is the predominant issue faced by the multiple surgical disciplines which has taken advantage of this operative approach (Elhadi, Zaidi, et al., 2014; Kong et al., 2020). Biportal approaches have been proposed as the solution to impaired surgical freedom (Dallan, Castelnuovo, et al., 2015; Lim et al., 2020). This involves the fashioning of 2 endoscopic surgical corridors allowing for instrument access through one or both ports, as well as the utility of moving the endoscope to facilitate maximal maneuvrability. To date the most commonly cited biportal corridor when utilising the transorbital route is to accompany this with transnasal access (Alqahtani et al., 2015; Dallan, Castelnuovo, et al., 2015). This combination does have notable advantages. It incorporates a midline and paramedian corridor allowing for impressive breadth of instrument trajectory along the axial plane, with coplanar access to the skull base.

While the transnasal route provides excellent views of the infra-cranial and intracranial anatomy and pathologies, it is not without its potential issues (Borg,

Kirkman, & Choi, 2016). Nasal morbidity, CSF leaks, CSF fistulas, meningitis, incomplete resection and vascular injury are significant risks associated with endonasal surgical intervention (Conger et al., 2018; Romero et al., 2017; Schroeder, 2014). Although in its infancy transorbital neuroendoscopic surgery (TONES) has an increasing body of clinical evidence reporting innocuous, or low levels of risks (L. M. Houlihan, Staudinger Knoll, et al., 2021a; Vural et al., 2021). There have been no studies exploring the anatomical accessibility, or the surgically applicable benefits and disadvantages of a biportal bilateral transorbital approach. This study aimed to quantitatively scrutinise this bilateral transorbital route with an open craniotomy of comparable trajectory. Additionally, while the endoscope is the present primary method of visualisation used (TONES), we investigated the utility of a biportal transorbital microscopic surgical corridor (BTM). This study compares the anterior subfrontal (A.Sub), BTM and biportal TONES (BTE) and is designed to produce robust neuroquantitative metrics, analyse the approach's feasibility and determine whether a biportal bilateral TO approach is applicable to appropriate surgical pathologies.

Methods

Cadaveric Assessments

While biological variability is inherent to all life sciences (Higdon, 2013), cadaveric specimens were examined for anatomical irregularity prior to inclusion in study. A sample size of 10 heads were obtained from an approved supplier, embalmed,

and the arteries and veins injected respectively with red- and blue-coloured silicone. All 10 heads underwent an A.Sub, BTM and BTE approach for access to specific structures.

Institutional review board approval was not required for this cadaveric laboratory investigation.

Approaches

Anterior subfrontal craniotomy

Variations of the subfrontal approach are already established in the literature (Aftahy et al., 2020; Petraglia et al., 2011). The authors chose a modified anterior subfrontal approach (A.Sub) to access the midline, interhemispheric and subfrontal region. The rational here was to utilise an open cranial approach with similar planar trajectory and midline access that a transorbital corridor would have. The head was positioned supine with approximately 10 degrees extension. A bicoronal incision and flap was fashioned. The supraorbital nerves exiting the supraorbital canals were identified bilaterally. An approximate 6 X 5cm anterior frontal craniotomy was completed as low as possible with invasion into the frontal sinus. The orbital bar was preserved. The frontal sinus was cranialised, drilled until flush with the cranial floor and where necessary, bilaterally along the residual lateral walls of the frontal sinus. The superior sagittal sinus was ligated at 2 points and cut at the most anterior point possible within the curvilinear dural incision. The falx was cut along its inferior border to its most posterior margin. Parenchymal draining veins were preserved as much as possible.

Biportal TMS and TONES approaches

In this study, we utilised a biportal, bi-transorbital access corridor. The microscope (OPMI PENTERO 900) and 4-mm 0°, 30°, 45° endoscopes (Karl Storz Endoscopy America, Inc, El Segundo, California) were used to complete biportal TMS and TONES approach. The sequence of the operative steps were the same irrespective of visualisation technology and have respectively been previously described (Moe et al., 2010) (Chapter 4). The head was immobilised in a similar position as the A.Sub. In brief, bilateral 4-5 cm superior lid crease incisions along the natural crease in the upper eyelids was completed. Following sharp dissection along the preseptal plane, the bilateral supraorbital nerves were identified and released from the supraorbital canal. Subperiosteal dissection was completed with identification of the anterior and posterior ethmoidal arteries, cauterized and ligated along the side of the periorbita. The craniectomy boundaries were identified i.e. the frontozygomatic suture to frontosphenoidal suture laterally, the frontal sinus anteriorly and the junction of the frontal bone and cribriform plate of the ethmoid bone, the frontal sinus medially and orbital rim laterally. While completing each respective transorbital corridor, the head was turned 10-15 degrees as necessary to optimise the medial margin of the craniectomy as it was drilled and maximise the midline trajectory, while preserving the anatomical limitations namely, the lamina papyracea, roof of the optic canal, frontal, and ethmoidal sinuses. Durotomy was in a cruciate fashion.

Neuronavigation System

The heads were rigidly fixed in a Mayfield head holder (Integra Life Sciences Corporation, Cincinnati, Ohio)) during measurements. Stereotactic neuronavigation is a well-established method for measurement in quantitative neuroanatomy, (Seyit Kagan Başarslan, 2014) with each point regarded as a spatial point with 3 coordinates (i.e., x, y, and z; units were millimeters). Predetermined data points were obtained using a neuronavigation system (StealthStation S7 Surgical Navigation System; Medtronic, Dublin, Ireland). All measurements have been rounded to the nearest two decimal places. To account for inter and intra-rater variability all measurements were completed 3 times by 3 different neurosurgeons/neurosurgical residents and the average value calculated.

Co-ordinate data analysis

The Inchin neuroquantititative platform (inchin.org) was used to calculate the anatomical metrics, as it's methodology has been previously published and peer reviewed (Lena Mary Houlihan, 2021), allowing for adequate co-ordinate data storage, data mining when necessary and reproduction of metrics as required.

Structure lengths of exposure

Bilateral cranial nerves I, II, optic tract, and A1 were examined with respect to the A.Sub and both TO approaches.

Parenchymal area of exposure

Bilateral frontal lobe base areas of exposure (AOE) (defined as the most antero-medial, antero-lateral, postero-medial and postero-lateral extrema of the frontal lobe base) were assessed with the with respect to both approaches, distinguished as right, left and total cortical base AOE.

Angle of attack

Cranio-caudal and medio-lateral angles of attack (AOA) are defined as the maximum allowable AOA in the vertical and horizontal planes with respect to cranial orientation. The AOA was measured by moving the proximal end of a probe from an extreme superior or medial to an extreme posterior or lateral position, with the distal end placed on the surgical target structures (STS). The cranio-caudal and medio-lateral AOA of various predetermined STS with respect to the A.Sub and TO approaches were evaluated. These included the bilateral paraclinoid internal carotid artery (ICA), bilateral terminal ICA and anterior communicating artery (ACoA).

Volume of surgical freedom

The volume of surgical freedom (VSF) is defined as the maximal available working volume with respect to a specific surgical corridor and STS (Lena Mary Houlihan, 2021). It aims to produce a 3-dimensional spatially and anatomically accurate quantitative and visual representation of instrument freedom. It is a standardised metric,

measured at a perpendicular height of 10mm (regarded as the mm^3 normalised volume (NV). Because of this, it can directly compare approaches, as well as assess the influence different technologies have on surgical maneuvrability regardless of data collection methodology variability. The VSF of the bilateral paraclinoid ICA, bilateral terminal ICA and ACoA specific to the approach and visualisation method used was completed.

Statistical Analysis

Stata MP version 15 was used for the analyses. Tests for skew and kurtosis of the variables' distribution were conducted. When test values were greater than 2.0, the variable was considered skewed. As most variables were skewed, medians and inter-quartile ranges were predominantly reported instead of means and standard deviations, unless specified. The proportion of inaccessible structures with respect to each approach was also noted. Qnorm plots and Shapiro-Wilk tests were employed to test for normality of the ANOVA residuals. When the assumption of normality among the residuals of the ANOVA models was not met, the variables were log-transformed. Bartlett's test for equal variances was also completed. When the assumptions of normality and equal variance were met, one-way ANOVA tests for mean differences were completed. In cases where the assumption of equality of variance was not met, the test for differences among approaches was tested using the nonparametric Kruskal-Wallis test, that is robust to violations of the equality of variance assumption.

When univariate analyses indicated different lengths, AOE, AOA, or VSF among A.Sub and TO approaches, multivariate regression models were estimated to confirm the significant findings. Ordinary least-squares (OLS) regression was used to estimate the impact of the approaches on the dependent variables, after controlling for other factors (specimens' sex and age at death). The models were tested for multi-collinearity among independent variables and heteroskedastic standard errors. The control factor age at death was transformed to its natural log version to account for non-linearity. Statistically significant differences are reported when p-values are at $\alpha = .05$ or less.

3D surgical corridor modelling

Photographs were taken using the microscope and endoscope and displayed on a 19-inch high-definition monitor (Carl Zeiss Microscopy, LLC, White Plains, New York). Sample VSF datasets were used to produce 3D renderings of the surgical corridors using a student license for the 3D modelling software Solidworks 2020 (Dassault Systèmes, Vélizy-Villacoublay, France). The 3D models were also superimposed onto apparatus-images of anatomical approaches to illustrate the surgical corridor specific to the STS.

Results

Morphometric comparison of the A.Sub and bilateral TO approaches

Accessibility of structures

Within a sample size of 10, all structures were accessible through an A.Sub approach. Results for the BTM and BTE approaches were equivocal with 20% (2/10) and 10% (1/10) of the right and left respective A1s inaccessible (Figure 7.1). A.Sub allowed for surgical maueuvrability assessment in all STSs except for the ACoA in 10% (1/10) of specimens (Figure 7.2). Accessibility between the BTM and BTE was comparable except for access to the ACoA where the complex was not accessible in 60% (6/10) (BTE) compared to 30% (3/10) (BTM).

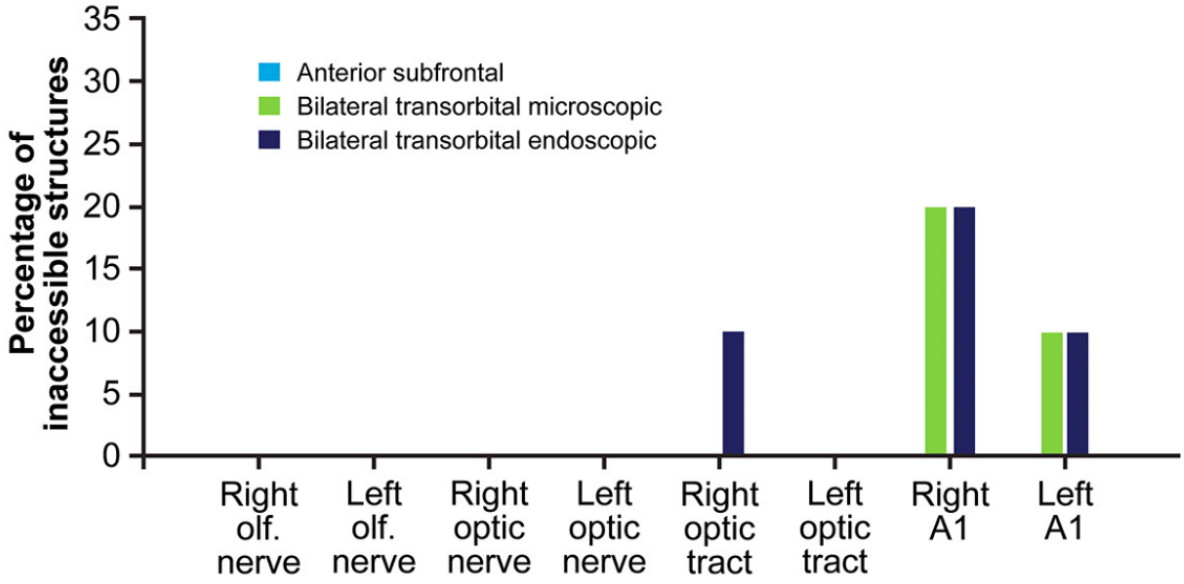

Figure 7.1. Percentage of surgical target structures in 10 cadaveric heads that were approached bilaterally (n=10) that were inaccessible with the anterior subfrontal, bilateral transorbital microscopic, and bilateral transorbital endoscopic approaches. Used with permission from Barrow Neurological Institute, Phoenix, Arizona.

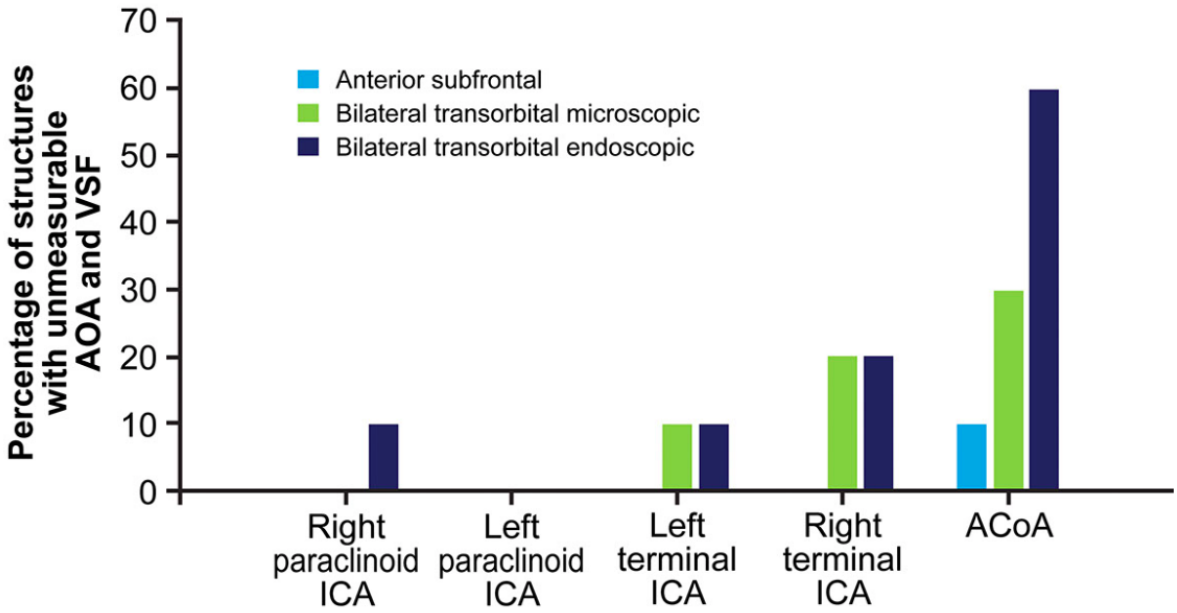

Figure 7.2. Percentage of surgical target structures in 10 cadaveric heads with the anterior subfrontal, bilateral transorbital microscopic, and bilateral transorbital endoscopic approaches in which assessment of angle of attack (AOA) and volume of surgical freedom (VSF) was not possible due to impaired instrument maneuverability. ACoA anterior communicating artery; ICA, internal carotid artery. Used with permission from Barrow Neurological Institute, Phoenix, Arizona.

Structure lengths of exposure

The results are summarised in Table 1. Univariate analyses showed no significant differences between approaches in relation to their respective accessible lengths except for the right and left CN I (p=.003 and 0.29 respectively). However, regression analysis showed no significant CN I length advantage between using BTE compared with A.Sub

(p=.067) while BTM was notably restricted. Use of BTM resulted in a 7.64 mm decrease in the length of the right CN I , as well as a 7.02mm decrease in the length of the left CN I as compared with the A.Sub (p=.009). Analysis of more distal midline structures were limited in both TO approaches. Use of the BTM and BTE resulted in a 4.45mm (p=.005) and 3.47 mm (p=.025) decrease in the length of right A1 respectively, on average when compared to an A.Sub approach.

Table 7.1. Analysis of variance of accessible length of intracranial structures specific to the surgical approach

Structure of Interest	All Approaches, mm	Anterior Subfrontal, mm	Bilateral Transorbital Microscopic, mm	Bilateral Transorbital Endoscopic, mm	p-value
Right olfactory nerve	19.0 (16.7–23.2)	23.3 (18.0-30.1)	16.3 (12.2-19.6)	19.0 (16.7-22.6)	**.003**
Left olfactory nerve	17.0 (14.0-20.3)	17.8 (15.7-25.5)	14.6 (10.9-17.3)	18.0 (13.8-20.3)	**.029**
Right optic nerve*	13.2 (11.1-15.1)	13.8 (12.8-15.7)	11.2 (10.3-11.4)	14.6 (13.0-19.2)	.465
Left optic nerve	13.1 (11.5-17.9)	12.8 (11.9-15.7)	11.6 (9.2-13.0)	17.5 (13.4-20.9)	**.011**
Right optic tract	11.2 (9.4-13.4)	11.2 (9.9-14.5)	9.8 (8.4-13.0)	13.3 (10.1-13.6)	.263
Left optic tract	11.9 (9.7-13.2)	12.2 (9.4-13.1)	10.9 (8.8-12.7)	12.0 (10.5-14.0)	.294
Right A1	16.0 (13.6-19.4)	18.7 (15.2-20.1)	15.0 (11.8-16.0)	15.7 (12.2-18.2)	**.034**
Left A1	16.3 (14.6-17.1)	15.7 (14.7-16.6)	16.3 (15.2-16.8)	16.5 (14.4-17.3)	.445

Data are presented as median (IQR) unless otherwise indicated. IQR, interquartile range.
* Model fails the assumption of equal variances. Kruskal-Wallis test p-values reported.

Frontal lobe base parenchymal exposure

Bilateral frontal lobe base AOE was accessible through both approaches. The average total frontal lobe area was 1,648.4 mm^2 (1,516.6-1,958.8mm^2) 1,658.9 mm^2 (1,274.6-1,988.2 mm^2) and 1,914.9 mm^2 (1,834.2-2,014.2 mm^2) for the A.Sub, BTM and BTE respectively. There was no statistically significant superiority between any of the 3 approaches (p=.276).

Angle of attack (AOA)

For both the right and left paraclinoid ICA craniocaudal and mediolateral AOA, the A.Sub was shown to be statistically superior ($p<0.05$) (Figure 7.3). This was evident in multivariate analysis where the A.Sub was estimated to significantly increase the craniocaudal AOA by 4.05 degrees (right) and 3.65 degrees (left) compared to the BTM (p= .004 and .005 respectively) and by 4.69 degrees (right) and 5.94 degrees (left) compared to the BTE (p=.001 and .000 respectively) . For the mediolateral AOA of the paraclinoid ICA the A.Sub significantly increases instrument access by 7.69 degrees (right) and 8.12 degrees (left) compared to the BTM (p= .001 and .001 respectively), as well as by 11.98 degrees (right) and 12.03 degrees (left) compared to the BTE (p= .000 and .000 respectively).

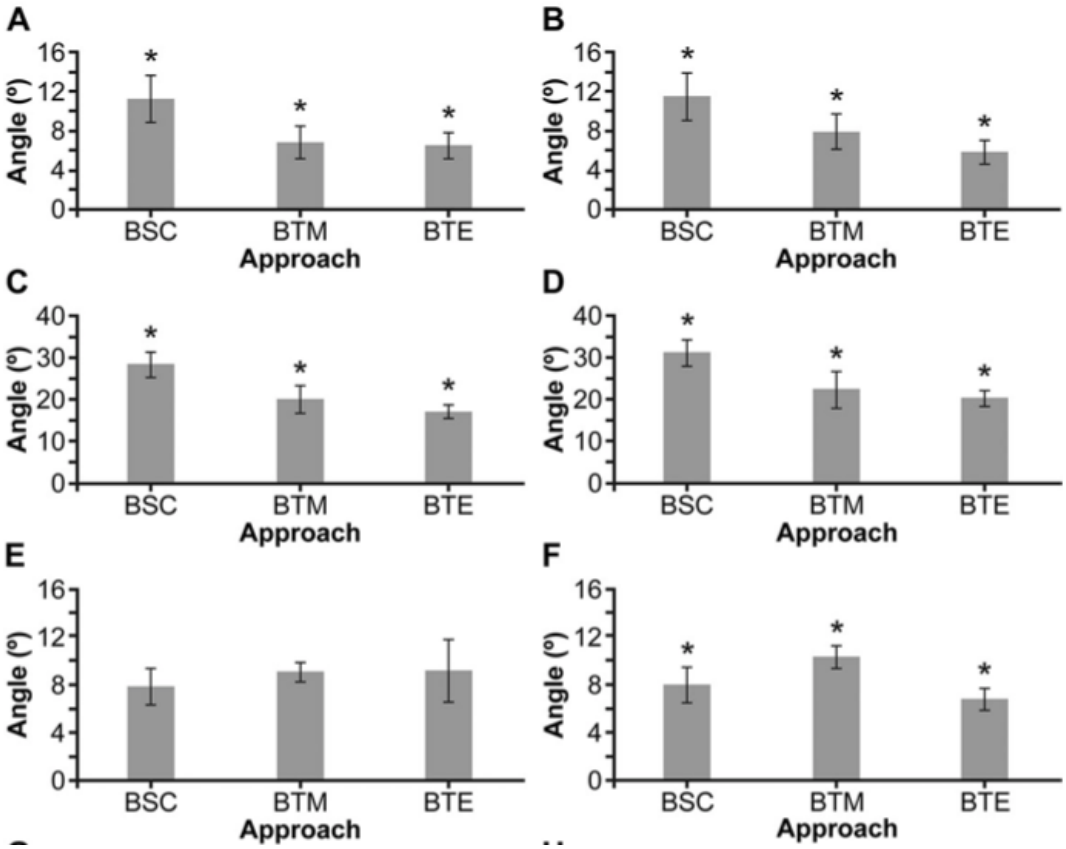

Figure 7.3. Quantitative comparison of the mediolateral and craniocaudal angles of attack (AOA) obtained in 10 cadaveric heads that were approached bilaterally (n=10) with use of the anterior subfrontal, bilateral transorbital microscopic, and bilateral transorbital neuroendoscopic surgery approaches, respectively. Values are median; error bars represent standard deviation interquartile range (IQR). (A) Craniocaudal right paraclinoid internal carotid artery (ICA) AOA: 11.3 (9.2-14.1) °, 6.8 (5.3-8.7) °, 6.5 (4.4-7.2) °. (B) Craniocaudal left paraclinoid ICA AOA: 11.5 (9.5-14.4) °, 7.9 (6.6-10.3) °, 5.8 [4.2-6.7] °. (C) Mediolateral right paraclinoid ICA AOA: 28.3 (25.0-31.1) °, 20.0 (17.0-23.6)°, 17.1 (14.7-17.9)°. (D) Mediolateral left paraclinoid ICA AOA: 31.2 (27.9-34.3)°, 22.4

(20.0-29.0)°, 20.3 (17.5-21) °. (E) Craniocaudal right terminal ICA AOA: 7.8 (5.4-8.4)°, 9.0 (7.7-9.4) °, 9.1 (6.9-12.1) °. (F) Craniocaudal left terminal ICA AOA: 8.0 (7.5-10.5) °, 10.3 (8.6-10.6) °, 6.8 (5.5-7.4) °). BSC, bilateral subfrontal/anterior subfrontal; BTM bilateral transorbital microscopic; BTE, bilateral transorbital neuroendoscopic. Used with permission from Barrow Neurological Institute, Phoenix, Arizona.

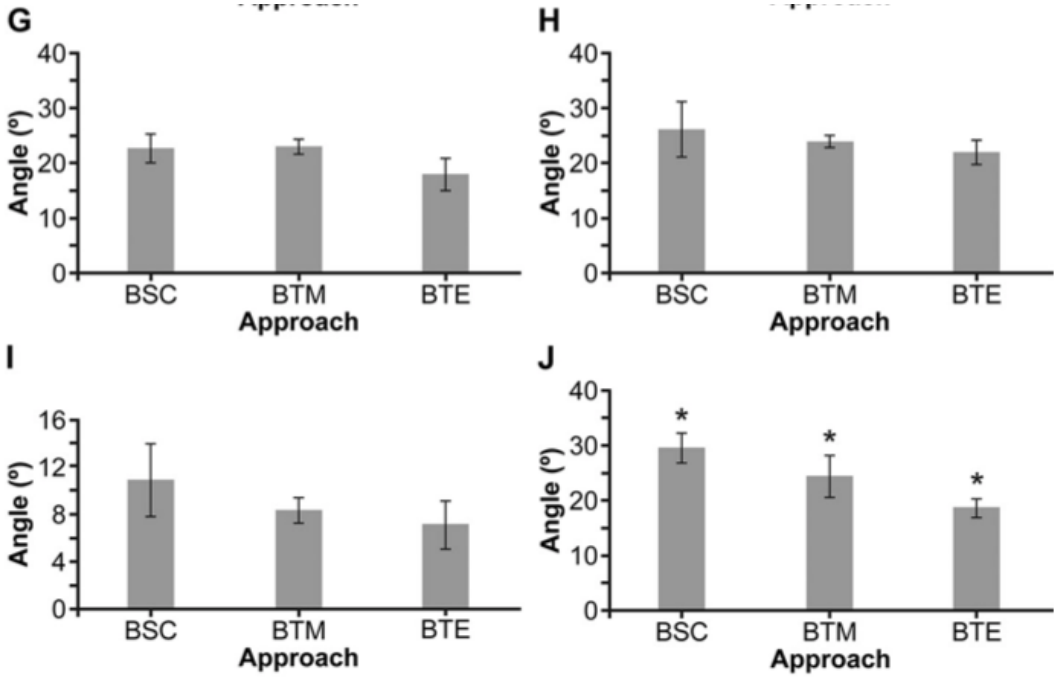

Figure 7.3. (continued) (G) Mediolateral right terminal ICA AOA: 22.6 (20.4-25.6) °, 22.9 (21.8-24.6) °, 17.9 (16.5-22.5) °. (H) Mediolateral left terminal ICA AOA: 26.0 (20.9-31.1) °, 23.8 (23.4-25.7) °, 21.8 (20.0-24.6)°. (I) Craniocaudal anterior communicating artery (ACoA) AOA: 10.9 (8.0-14.2) °, 8.3 (7.9-10.1) °, 7.1 (5.3-9.4) °. (J) Mediolateral ACoA AOA: 29.4 (24.8-30.3) °, 24.3 (19.2-26.9) °, 18.6 (17.1-20.6) °. BSC, bilateral subfrontal/anterior subfrontal; BTM bilateral transorbital microscopic;

BTE, bilateral transorbital neuroendoscopic. Used with permission from Barrow Neurological Institute, Phoenix, Arizona.

Although the A.Sub showed pronounced superiority compared to both TO approaches with respect to accessing the bilateral paraclinoid ICAs, the same could not be said for the bilateral terminal ICAs. Initial univariate analyses showed no significant difference between the approaches except in relation to the craniocaudal AOA of the left terminal ICA (p=0.005). Multi-variate analysis showed that BTE is significantly correlated with a decrease of 2.56 degrees in the craniocaudal AOA (p=.011) targeting the left terminal ICA craniocaudal AOA compared with the A.Sub approach after controlling for sex and age at death. There was no statistical superiority noted between the BTM and A.Sub (p=.439).

There was no difference between all 3 approaches for the craniocaudal AOA of the ACoA (p=.110), but the mediolateral AOA did show significance (p=.011). This was confirmed where regression modelling showed that BTE was significantly correlated with a decrease of 8.62 degrees in the mediolateral AOA compared with the A.Sub after controlling for sex and age at death (p=.010), while comparison with the BTM approached statistical significance (p=.057).

Volume of surgical freedom

While an ANOVA test showed statistical significance for the VSF of the right paraclinoid ICA (p=0.000), the same could not be said for the left paraclinoid ICA (Kruskal-Wallis: p=0.465) (Figure 7.4).

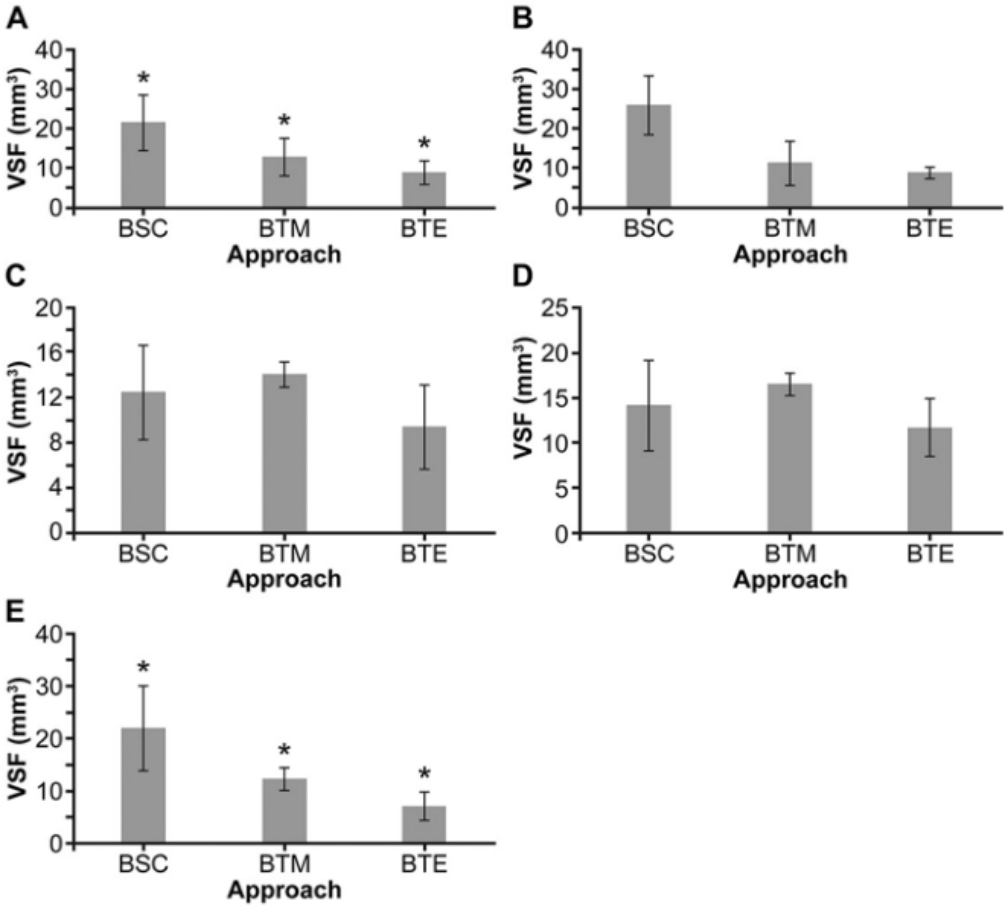

Figure 7.4. Quantitative comparison of the volume of surgical freedom (VSF) achieved in 10 cadaveric heads that were approached bilaterally (n=10) with the anterior subfrontal, bilateral transorbital microscopic, and bilateral transorbital neuroendoscopic surgery

approaches, respectively. Values are median; error bars represent standard deviation interquartile range (IQR). (A) Right paraclinoid internal carotid artery (ICA) normalized volume (NV): 21.5 (15.1-29.5) mm^3 12.7 (9.0-18.7) mm^3 8.8 (4.1-10.1) mm^3. (B) Left paraclinoid ICA NV: 25.9 (21.7-36.7) mm^3, 11.2 (8.2-19.4) mm^3, 8.8 (7.2-10.2) mm^3 (C) Right terminal ICA NV: 12.5 (8.2-16.6) mm^3, 14.1 (12.9-15.2) mm^3, 9.4 (7.9-15.3) mm^3. (D) Left terminal ICA NV: 14.2 (10.5-20.6) mm^3, 16.5 (16.1-18.6) mm^3, 11.7 (7.0-13.4) mm^3. (E) Anterior communicating artery NV: 22.0 (11.1-27.5) mm^3, 12.3 (11.0-15.4) mm^3, 7.1 (4.7-10.2) mm^3. BSC, bilateral subfrontal/anterior subfrontal; BTM bilateral transorbital microscopic; BTE, bilateral transorbital neuroendoscopic. Used with permission from Barrow Neurological Institute, Phoenix, Arizona.

On more detailed analysis, it was estimated that the BTM and BTE are significantly correlated with a decrease of 8.71 mm^3 NV (p=.005) and 14.34 mm^3 NV (p=.000) in the VSF of right paraclinoid ICA compared with the A.Sub after controlling for sex and age at death (Figure 7.5).

No statistically significant difference in surgical freedom was noted between all 3 approaches when targeting the right (log transformed) (p=.418) or left (p=.075) terminal ICA (Figure 7.6).

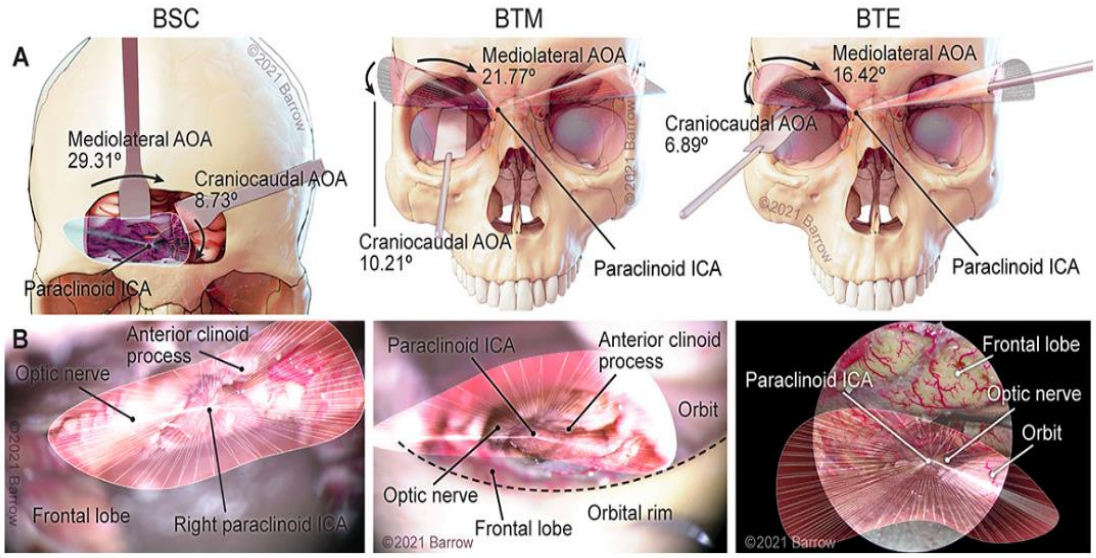

Figure 7.5. Illustration depicting 3-dimensional modelling of the surgical corridor to the right paraclinoid internal carotid artery (ICA) from an anterior subfrontal (BSC), bilateral transorbital microscopic (BTM), and bilateral transorbital neuroendoscopic surgery (BTE) approach. (A) The anterior of the surgical corridor. (B) The surgical view of the cadaveric anatomy, which is in continuity with the surgical corridor model parameters. anterior subfrontal: volume of surgical freedom (VSF) = 13.63mm^3, craniocaudal angle of attack = 8.73°, mediolateral angle of attack = 29.31°; BTM: VSF = 13.45 mm^3, craniocaudal AOA = 10.21°, mediolateral AOA = 21.77°; BTE: VSF = 9.71 mm^3, craniocaudal AOA = 6.89°, mediolateral AOA = 16.42°. Used with permission from Barrow Neurological Institute, Phoenix, Arizona.

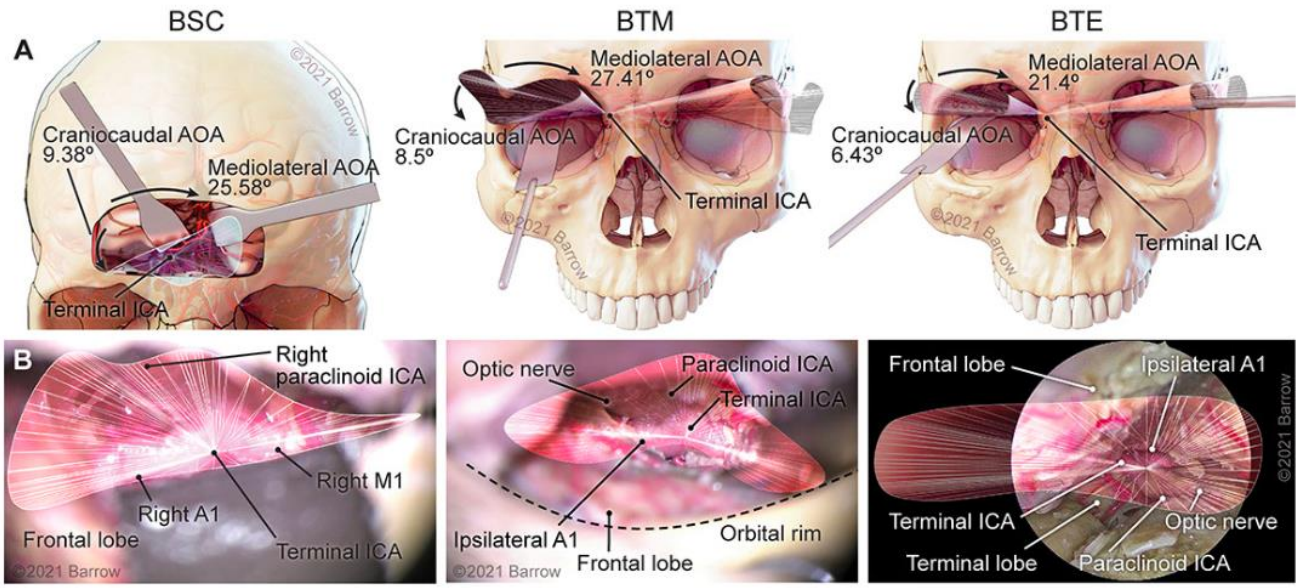

Figure 7.6. Illustration depicting 3-dimensional modelling of the surgical corridor to the right terminal internal carotid artery (ICA) from an anterior subfrontal (BSC), bilateral transorbital microscopic (BTM), and bilateral transorbital neuroendoscopic surgery (BTE) approach. (A) The anterior of the surgical corridor. (B) The surgical view of the cadaveric anatomy, which is in continuity with the surgical corridor model parameters. anterior subfrontal: volume of surgical freedom (VSF) = 11.92mm^3, craniocaudal angle of attack = 9.38°, mediolateral angle of attack = 25.58°; BTM: VSF = 12.22mm^3, craniocaudal angle of attack = 8.5°, mediolateral angle of attack = 27.41°; BTE: VSF = 12.5mm^3, craniocaudal angle of attack = 6.43°, mediolateral angle of attack = 21.4°. Used with permission from Barrow Neurological Institute, Phoenix, Arizona.

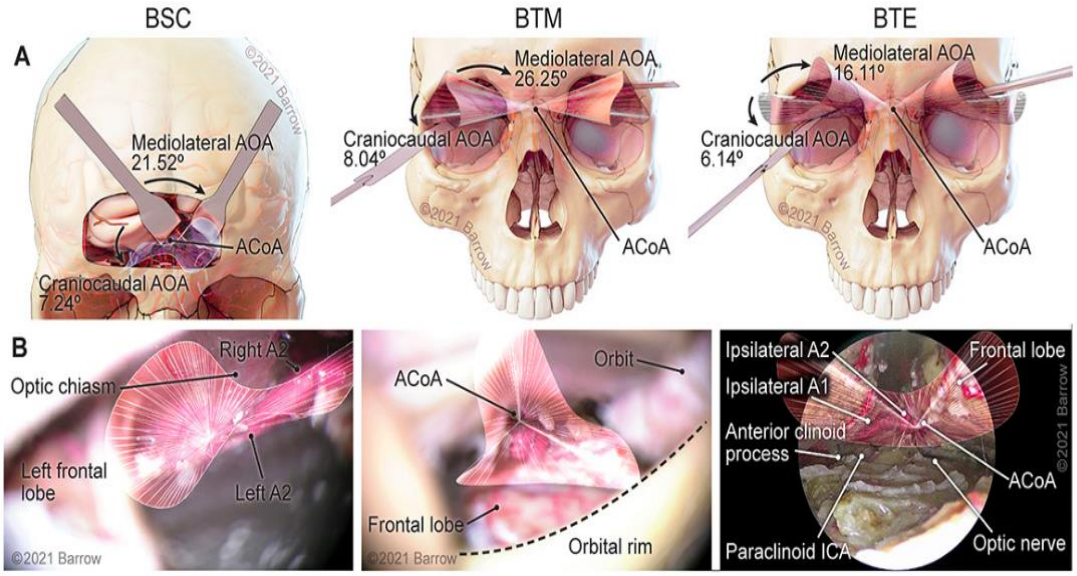

Figure 7.7. Illustration depicting 3-dimensional modelling of the surgical corridor to the anterior communicating artery (ACoA) from an anterior subfrontal (BSC), bilateral transorbital microscopic (BTM), and bilateral transorbital neuroendoscopic surgery (BTE) approach. (A) The anterior of the surgical corridor. (B) The surgical view of the cadaveric anatomy, which is in continuity with the surgical corridor model parameters. anterior subfrontal: volume of surgical freedom (VSF) = 8.25mm^3, craniocaudal angle of attack = 7.24°, mediolateral angle of attack = 21.52°): BTM: VSF = 13.36mm3, craniocaudal angle of attack = 8.04°, mediolateral angle of attack = 26.25°; BTE: VSF = 9.36mm^3, craniocaudal angle of attack = 6.14°, mediolateral angle of attack = 16.11°. Used with permission from Barrow Neurological Institute, Phoenix, Arizona.

A statistical difference was identified on assessment of the ACoA (log transformed) (p=.015). There was no significant difference noted between the (log transformed) ACoA VSF of the BTM and A.Sub (p=.227). However the BTE significantly correlated with a decrease of 105% in the (log) VSF of the ACoA compared with the A.Sub (p=.009) (Figure 7.7) .

Discussion

Comparative morphometric analysis of the A.Sub, BTM and BTE

Given the extent of the open craniotomy, the majority of surgical metrics were assumed to be larger for the A.Sub as compared to the minimally invasive TO approaches. This can be seen upon review of the accessibility to the various STSs of interest. The A.Sub purports complete accessibility to all STSs bar in 1 specimen where the ACoA was not reachable. This is far superior to the BTM and BTE where both approaches had limited midline access to the ACoA especially. Saying this, the discrepancy between STSs and regions of interest was not unequivocally superior for the open approach. When estimating the maximal accessible lengths, there was no statistically significant difference between the A.Sub and BTE for the bilateral CN I, II, optic tract and bilateral A1. The BTE had better accessibility to CN I compared to BTM. This is likely due to the angled capabilities of the endoscope and its ability to visualise more anterior along the ACF floor whereas, the microscope is limited in its straight line of view by the protuberance of the already retracted orbital contents.

Surgical corridor crowding

While crowding has been difficult to quantify, this study has substantial evidence to support the prevalence of this issue. In general although BTM had limited access to medial structures, BTE was even more significantly hindered (30% versus 60% to the ACoA).

As expected the AOA and VSF of the paraclinoid ICA obtained via an A.Sub was larger than via both TO approaches, where the BTM provided approximately 5 degrees more mediolateral AOA compared to BTE. Similarly the VSF garnered by BTM is approximately $5mm^3$ greater than BTE. Likewise, BTE was limited in its surgical freedom to the ACoA. This was prevalent in the mediolateral AOA to the ACoA when compared to both A.Sub and BTM, as well as the VSF where BTE significantly correlated with a 105% decrease in maneuvrability compared to the A.Sub. The BTM and A.Sub were comparable ($p=.227$), but again it must be noted that in general the ACoA was not always accessible through a TO approach.

The original idea behind a biportal approach was to address the issue of surgical instrument crowding and increase maneuvrability garnered with an endoscopic approach appropriate to the extent of the pathology. While BTE provides bilateral access for visualisation of STSs, the mediolateral AOA is still limited compared to a BTM. This could be due to the surgeon's preference of ipsilateral visualisation, or handedness while accessing the STS as visualisation along the same axis a one's hand is more organic and

direct. Biportal access does improve general 360 degree visualisation of any intracranial target which is a huge advantage of the endoscope, but this does not necessarily extrapolate to maximal instrument maneuvrability. This study highlights the importance of clarifying the surgical trajectory warranted for the STS as this will primarily determine not only the surgical approach and degree of freedom required, but also the optimal method of visualisation.

Surgical Applicability

When analysing the area of exposure of the ACF frontal lobe parenchyma, there was no statistically significant superiority noted between any of the 3 approaches (p=.276). The median AOE across all 3 approaches was 1,763.3 mm^2 (1,528.4-2,010.9mm^2). While this is a decent portion of low frontal base, it must also be taken into account the exact region of the ACF accessible. Midline accessibility is not possible through a TO approach because the lateral orbital rim prevents lateral movement of instruments. For this reason while the low frontal lobe is reachable and advantageous via a TO approach, the anterior 2/3rds of the falx is visible with an angled endoscope, but not surgically accessible. Furthermore medial deep STS accessibility was also hindered. This study confirms that due to preservation of the lateral orbital rim, a component inherent to the TO approach, the biportal bitransorbital surgical corridor is not appropriate for midline lesions. For midline lesions extending bilaterally, such as a falcine, olfactory groove meningioma or neuroesthesioblastoma, based on its location, a combined

transorbital, transnasal approach is a superior skull base option for such pathologies and has been utilised successfully in clinical practice (Dallan, Castelnuovo, et al., 2015). A transnasal corridor provides the midline maneuvrability required for such lesions and, in combination with an ipsilateral TO corridor, supplies the surgeon with substantial ipsilateral ACF access (917.2mm^2 [770.5-1,020.2mm^2]). This combined approach minimises the extent of skull base and sinus destruction, while also permitting potential preservation of the lamina papyracea. Undoubtedly an ipsilateral ACF extra-parenchymal or low frontal lesion would be suitable for surgical intervention through an ipsilateral TO approach, where exposure has been identified to be comparable with open cranial approaches (Chapter 6).

The access to the terminal ICA was equivocal where BTM was identified as similar to the A.Sub. On surgical freedom analysis there was no statistically significant difference noted between the A.Sub, BTM or BTE. While the A.Sub is not the standard craniotomy used to tackle the terminal ICA, it is encouraging to see similar instrument freedom between the TO minimally invasive approaches and an open craniotomy where CSF leak, sinus injury and suboptimal cosmesis are serious potential complications (Uwe Kehler * & Piek, 2013). From a vascular perspective, this study, as well as others completed (Chapter 6) have illustrated that the terminal ICA is feasibly accessible through a TO approach with consistently impressive instrument maneuvrability through a TMS corridor and therefore should be considered a potential surgical target in operative practice.

Both the microscope and endoscope have respective advantages. Crowding has always been an operative concern of the endoscopic corridor. A biportal approach is proposed as the solution to this. On comparative review, microscopic technique through the same TO corridor has superior surgical freedom, regardless of biportal visualisation and access. It is more ergonomic and intuitive for the line of sight to follow the surgeon's hands movements as opposed to at an alternate angle which requires additional spatial orientation. The biportal approach undoubtedly provides increased 360 visualisation, but surgical access is gained predominantly through the ipsilateral corridor. These concepts bring to the fore the importance of not only one's surgical trajectory to the lesion, but also the optimal trajectory of the viewing apparatus. It is here where the benefits of the exoscope may be beneficial (Herlan, Marquardt, Hirt, Tatagiba, & Ebner, 2019a). This visualisation method improves the surgeon's position, as well as facilitating the use of microsurgical technique combined with the endoscope's illumination and image quality (Ricciardi et al., 2019). Saying this, stereoscopy is consistently exclusive to the microscope alone. When analysing surgeon-based factors for selection of a surgical approach, expertise and experience with these visualisation technologies is a critical element of the decision-making process, which should be assimilated in conjunction with the approach corridor quantitative metrics.

Study Limitations

The deductions gleaned from this research are based on the measurement of cadavers, tissue which is usually more rigid than in vivo brain parenchyma (Benet et al., 2014). Slight differences in morphology and sizes of the structures can affect the area exposed. Cadaveric feasibility studies are the best model at our disposal for preclinical anatomical operative techniques analysis. The results garnered are also deemed grossly proportional, regardless of the discrepancies between in vivo and ex vivo treated tissue. This also gives us insight into the potential space reproducible specific to the surgical approach and circumferential anatomy producing a visually descriptive metric for operative planning.

The A.Sub is not the most common approach utilised for the STSs assessed in this study. Other publications have reviewed the surgical freedom of the anterior paramedian vasculature and compared it to approaches deemed more appropriate for tackling such pathologies (Chapter 6). The A.Sub in this study was used as a litmus test craniotomy with similar trajectory and planar view of the transorbital access corridor. It is meant to represent an open comparative of instrument maneuvrability specific to the STS and also provide context for extrapolation of the BTM and BTE results.

Conclusion

The biportal TO approach provides increased 360 degree visualisation of the paramedian vasculature, but is not useful in increasing surgical freedom to specific STSs.

This study also highlights the instrument maneuvrability limitations associated with the endoscope which are not, in this permutation, compensated by biportal access. While access to the ACF and terminal ICA is impressive and comparable with an open craniotomy, the biportal bi-TO approach is not a suitable operative corridor for midline lesions. Its only benefit is with regard to alternate trajectory visualisation along the paramedian region. For this reason a recommendation of use of the established combined transnasal, transorbital access corridor appears to be the optimal option for substantial midline and ipsilateral anterior skull base access.

CHAPTER 8

Portions of the following chapter are in preparation for submission to the journal Neurosurgical Review.

CHAPTER 8

DISCUSSION

Innovation

Establishing a new standard in neuroquantitative anatomy

There have always been discrepancies noted between the scientific and medical research produced and published in the literature. This is evident in various scoring platforms used to assess the 'utility', 'quality' and citation power of the literature. Furthermore the number of readers invested in specialist medical research areas is substantially smaller than scientific communities. The highest ranking neurosurgical journal – Journal of Neurosurgery - as per 2020 holds an impact factor value of 5.11(Neurosurgery, 2021), whereas Nature holds a value of 49.926 (Nature, 2021). These metrics underscore the disparity between the inherently integrated fields.

Scientific studies pride themselves on robust methodology, which is transparent, homogenous and reproducible so as to be fastidious and absolute in the results garnered. Medical research is inherently heterogenous. The human condition cannot be exactly reproduced because biological variability exists. The best model cannot account for every influence of genetic and acquired environmental factors. The facets of these two connected fields appear mutually exclusive and their research patterns have evolved in such a nature.

Basic science is predominantly experimental whereas medical research is rooted in observational studies and creates inferences for further experimental analysis through this pathway. Both areas have their respective advantages and disadvantages. It is through combining their strengths with acceptable levels of compromise that translational applicable advances can be established in an optimal setting.

This was one of the aims of this body of research. These studies evaluated a minimally invasive novel surgical corridor - the transorbital approach - its validity in neurosurgical practice, as well as both qualitatively and quantitatively assessing available technological advances in a robust experimental fashion. The field of quantitative neuroanatomy was previously primarily descriptive, however quantification is now integral to all assessment. The comparative studies provide increased knowledge on specifics relevant to neurosurgeons such as pathology location, involved anatomical structures, instrument maneuvrability and the advantages and disadvantages of distinct technologies. This is all with the intention of selecting the most suitable surgical approach and technology, specific to the patient, pathology and anatomy, so as to perform the best surgical procedure. These results were garnered with a methodology structured on the basis of powerful scientific principles by optimizing absolute and relative characteristics inherent to the nature of the research area. This research represents a new standard in quantitative analysis in neuroanatomy which is reproducible, substantive and incorporates the best applicable standards of scientific practice.

Variability is a key element which must account for in statistical experimental design in biological studies. It applied to multiple aspects of this research including specimens, time points, technical replication of experimental protocols and grouping of samples (Higdon, 2013). It is accepted that there are two categories for consideration in biological experimental design. These include:

1. Biological variability: variability due to subjects, organisms, and biological samples – Cadaveric specimens in this scenario
2. Technical variability: variability due to measurement, instrumentation, and sample preparation – Investigator bias and measurement procedure heterogeneity and paucity were relevant here

Robust design is integral to maximising informative analysis of the experimental data and requires a meticulous process of planning to ensure efficient statistical inference (Kreutz & Timmer, 2009). There are steps which can be taken (and were taken) to ameliorate the influence of biological variability and improve the quality of study results. Firstly from a general perspective experimentation and the process of planning is an iterative process (Moed, 2012). Prior knowledge about the system of interest based on the published literature is necessary for development of a comprehensive experimental model (Kreutz & Timmer, 2009). For neuroquantitative analysis, the determination of an optimal design specific to this research requires prior knowledge and competency in anatomy, neurosurgery, operative skills, instrumental and technological capabilities, as well as quantitative anatomical measurement. Having this skillset allows the researcher to

appropriately assimilate, critique and improve upon the published data and experimental methods previously used to scrutinize and explore the question posed – in this instance with respect to the transorbital approach (L. M. Houlihan, Belykh, et al., 2021; L. M. Houlihan, Staudinger Knoll, et al., 2021c).

Sampling refers to the process of the selection of experimental units relevant to the intervention or particular being assessed. The aim of an appropriate sampling is to avoid systematic errors and to minimize covariates in the measurements, due to inhomogeneities (Kreutz & Timmer, 2009). Therefore, having a substantial sample size is absolutely necessary and contributes to the credibility of the results as well as its generalisability.

While this principle was maximally incorporated in this research, what is practical and affordable also needs to be addressed. Cadaveric tissue is a coveted, rare and costly commodity. It presently stands as the best model at our disposal for analysing surgical technique and for training purposes. The donated tissue allows us to explore improvements in our operative strategy and technique in an environment where experimentation is safe. This further emphasises the necessity of the neurosurgical anatomical laboratory as a requisite to develop new approaches and improve surgical skills. With this in mind, maximising the utility of specimens is obligatory, while in turn, trying to embody the principle of substantive sampling.

There is acceptance amongst the surgical and anatomical community about general principles in human and neurological anatomy due to the countless exploratory efforts over the centuries (Rhoton, 2003; Vesalius, 1542). Admittedly there is variation in human anatomy, but the efforts behind present anatomical investigations in quantitative anatomy is to identify generalisable principles applicable to surgical intervention. This is the process of induction.

Even between cadavers there is heterogeneity in the anatomy. Arguably this is of benefit to the sampling set, because in humans undergoing surgery, there is also variability. This is reflective of the above comments on the differences between medical and scientific research. In medical science, we cannot account for all patient elements, but attempt to structure our studies in the most complete and reproducible way possible.

Such variability in inherent to the human condition and so it is appropriate that this is represented in our studies. Therefore any potential inductions which are made, are from a representative cohort. Regardless, throughout the data collection process all variables should be accounted for to ensure all potential inferences can be identified. Accounting and collecting this information also allows identification of over-representation of specific confounders if present.

Improvement in the knowledge based on first results is followed by the design and execution of new experiments, which are used to refine such knowledge (Kreutz & Timmer, 2009). This is an important factor in the refinement of the experimental process

and was incorporated in these studies. Initially we elucidated noteworthy anatomy and surgical boundaries, the breadth and limitations of the microscopic transorbital corridor, as well as the logistics of instrumentation. Subsequently, the best method of comprehensive quantitative assessment was created and validated. Finally comparative analysis on transorbital approach permutations and visualisation technology was completed.

When discussing quantitative studies, similar experimental challenges are posed and must be (and were) accounted for with respect to biological variability.

Replication

Replication is a key strategy to avoid unintended confounding (Kreutz & Timmer, 2009). Repeated measurements allow for the estimation in the variability of the data. This also allows for computation of error bars as a measure of confidence for each data point. In this research's experimental model replication and repetition of collection of the data points was strengthened by multiple attempts at measurement, at multiple time points, by multiple neurosurgeons knowledgeable of intracranial anatomy and the experimental process. This procedure improves the power of the analysis, as well as accounting for inter and intra-rater variability with the aim of calculating the most accurate quantitative result. Regardless all results are accompanied by a standard deviation or interquartile range, which in itself is a estimation of parameters and is representative of biological variability. Here, there is an assumption of normal distribution – although skew/kurtosis,

as seen in the datasets is inherent - in accordance with the central limit theorem of statistics (Kwak & Kim, 2017) and consequentially central tendency is taken into account. By this reasoning, the aim of the above interventions is to improve the precision of the results by increasing the number of experimental repetitions. It should also be noted that investigator bias is a prominent confounder in quantitative anatomical experimental design, more so than issues specific to the specimen.

Due to the fixed nature of the cadaveric tissue as well as it's rigid-frame positioning during data collection, confounding within the specimen is not a huge concern. What is pertinent however is the effect of repeated traction, force and manipulation of the tissues, as they can become damaged and depreciate in anatomical quality. For this reason, succinct planning of the data collection pathway is necessary to maximise quantitative gain while minimising investigator time, effort and specimen trauma.

A substantial sample size is a key component which is novel to these studies when compared to published quantitative anatomical literature. The sample sizes quoted in these experimental groups are far larger than present accepted samples sizes in quantitative publications (Alqahtani et al., 2015; E. Belykh et al., 2018; Sun et al., 2019). This biological replication leads to confidence intervals that appropriately reflect the inter-individual and inter-experimental variability. This will result in more general results and extends the scope of these studies (Kreutz & Timmer, 2009).

Randomisation

Randomisation is another strategy to avoid systematic errors (Kreutz & Timmer, 2009). This minimizes the risk of unintended confounding. A non-random assignment between experimental conditions and experimental units can introduce systematic errors, leading to distorted, or biased results (Fisher, 1992). This is a difficult element to incorporate into quantitative anatomical research. Attempts which should be made to minimise investigator bias, is multiple qualified neurosurgeons taking measurements independent of one another. The acquisition of cadaver specimens available is random due to their valuable and scarce nature. Admittedly the patient demographics are more likely to include older individuals who died with underlying health conditions and pathologies. There is no way to alter these cadaver specific variables and this remains an accepted element of biological variability within these studies.

Research novelty

An acknowledgement in the value of the transorbital corridor amongst the neurosurgical skull base community is evident. Similar in vein to the gradual integration of the orbitotomy into standard practice, neurosurgeons are expanding their scope to utilise transorbital endoscopy and with this, increasing multi-disciplinary affiliations are evolving. Amalgamating keyhole cranial interventions with transorbital endoscopic assistance, as well as hypothesising the use of this access point using microscopic technique as an accessory port is an exciting area of skull base surgery. Chapters 6 and 7

highlight the potential and pitfalls of the corridor compared to comparable open approaches as well as elucidating the benefits and disadvantages of our surgical technologies.

This surgical corridor possesses the principles of an optimal modern skull base technique; minimally invasive, minimal morbidity, with priority of patient satisfaction. Still a relatively small research area in neurosurgery, given the historical medical influences which tarnished its progression, this approach is at the modern forefront of maximally cosmetic, maximal result neurosurgery.

This body of work set out with 2 explicit aims; to establish the potential of the transorbital approach with use of the microscope and to quantitatively and qualitatively assess open approaches with technology specific transorbital access corridors.

Chapter 4 established the optimal neurosurgical set up for a transorbital microscopic surgical corridor, provided a detailed anatomical description of accessible structures and highlighted its limitations. Through completion of methodological exploratory examination with specimen numbers of statistical significance, I described in detail the anatomical targets from an extradural, intradural, parenchymal, vascular and cranial nerve perspective and compared that with present accepted standards in surgical care. This resulted in conclusions that are not only scientifically substantive, but also directly applicable for the targets and regions of interest in the operative setting.

The second research goal was to quantitively analyse the technology and surgical techniques at a neurosurgeon’s disposal for accessing the anterior cranial fossa via the

transorbital corridor. This included detailed evaluation of the endoscopic and microscopic approaches with respect to the predetermined surgical target structures. In addition while systematically reviewing the established transorbital approaches, this research assessed area of exposure, degree of instrument maneuvrability - with use of the novel metric 'volume of surgical freedom' established during this dissertation - and visibility in relation to pertinent technological advances. Direct comparison of the microscope and endoscope with respect to target structures is scant in the literature and the methodology inconsistent. These experiments are methodical, reproducible and propose surgically applicable conclusions which quantitatively confirm clinical and technical ideals. These studies elucidate the optimal transorbital surgical technique in relation to anatomical targets and optimal instrumentation. This ultimately provides evidence for the surgeon for operative planning and best patient care.

Limitations

Fixed cadaveric heads, a valuable commodity, is the type of specimen which is used in quantitative neuroanatomy. These specimens lack obvious components for perfect simulation of a surgical setting; the remainder of the body, blood flow, patient-specific co-morbidities which influence the operative setting, a competent cerebrospinal fluid system and in vivo tissue. This is an experimental restriction. They are however the best and closest representation/model of the in vivo subject available for experimental purposes.

Future work

Inchin neuroquantitative platform

Anatomical competency is of the utmost importance in surgical practice. (Aziz & Mansor, 2006; Burgess & Ramsey-Stewart, 2015) It is the cardinal infrastructure upon which the knowledge base for all surgeons is founded and subsequently evolves. (Selcuk et al., 2019) The surgeon must be aware of standardized structures and their spatial positioning, associated variations, and physiologic sequelae. The efforts and discoveries of anatomists have spurred pivotal breakthroughs in surgical and medical treatment (Iorio-Morin & Mathieu, 2020; Melly et al., 2018) as well as in the development of basic scientific progression and understanding of the disease process. (Barth & Ray, 2019)

Quantitative neuroanatomical studies are an accepted, safe, and objective means of gauging the feasibility and validity of different neurosurgical maneuvers. Quantitation of surgically related neuroanatomy has advanced substantially due to the use of neuronavigation systems, which allow for multi-faceted real-time analysis of operative approaches that prior to this, because of the nature of the small nuanced surgical corridors, would have been grossly inaccessible. Neurosurgery now works in an evolving but restricted world i.e. we work in distances and volumes which are millimetric. Our clinical imaging is held to an exacting standard. Navigation registration must be millimetric so as to guide us to the pathology. What our micro-instruments can achieve is dependent on multiple factors, on our visualization means for example, as confirmed and described in this body of work. However predicting the capability of our instruments

cannot be garnered from navigation, or any other tool. Neuroquantition is the only means of assessment. This technology is focused on the quantification of maneuvres. There are significant deficits, as described above, in our methods of quantitation.

The field of neuroanatomy requires a standardised measurement platform, as non-standard measurements are only as good as the single study that produced them. One of the barriers to this cooperation and standardisation is the individual implementations of calculation tools employed within neuroanatomical labs. Presently anatomical publications are accepted 'in good faith' with little scrutiny of the calculatory process for the neuroanatomical parameters. A study would have much more universal benefit and scientific credibility if its data could be directly compared to other studies. A greater degree of cooperation and standardisation, it is generally agreed, would be extremely useful in the field of quantitative neuroanatomy.

Because neurosurgical researchers are using personal calculators which they have either created, or received from laboratory colleagues, there is limited reproducibility, consistent methodology, and quality assurance as to the validity of their results. To advance the field of neuroanatomy, efforts towards standardisation of technique, production of large centralised data units and transparent collaboration of methodology and results must be established. While this dissertation's studies describe the application of scientific methodology to the field of surgical technique and technology, this issue requires a more global explanation.

The solution to the problem of a distributed problem is a centralised solution. In this case, that means a single, globally accessible tool for storing neuroanatomical data and calculating neuroanatomical metrics. The Inchin platform (inchin.org), developed during this dissertation, is a prototype web-based software tool which is designed to maintain a database of measurement records. The software will be accessed through a web-browser, providing a user-friendly interface for users to input data, recall data, and calculate neuroanatomical metrics from the data. The database will allow for recall and recalculation of all previously entered data. Neuroanatomical metrics include:

- Structure Length
- Angle of Attack
- Area of Exposure
- Volume of Surgical Freedom (VSF) (Lena Mary Houlihan, 2021)

We aim to establish the first ever interactive online quantitative neuroanatomy platform which would allow for a standardised quality assured quantitation system for anatomical parameters, allowing for clear secure data storage and analysis, as well as promote inter-institutional and interdisciplinary research development and evolution.

Transorbital surgery in clinical practice

Surgery may appear to be a coarse artform compared with modern pharmaceutical and interventional therapies, but surgery, and specifically neurosurgery in this example, is a crucial specialty in both preventative and therapeutic medicine. The goal is to

incorporate modern, technological developments with key surgical concepts to produce the best outcome for the patient; minimal morbidity, minimal mortality and maximised therapeutic result and quality of life.

These pre-clinical studies elucidate specific targets which are appropriate for transorbital access and also detail the optimal surgical adjuncts with which to approach localised pathologies. As is evident in the published literature, there is significant overlap in cadaveric and clinical goals and concepts, as well as studies which are produced by multi-disciplinary teams including neurosurgeons, otolaryngologists, craniofacial and ophthalmological surgeons. Determinants assessed in this body of work include degree of the attacking angle in specific axes, satisfactory visualisation for vessel interrogation and surgical maneuvrability i.e. volume of surgical freedom. The practical nature of this research permits direct translation into clinical practice. This information will enable neurosurgeons, otolaryngologists, craniofacial and ophthalmologic surgeons to maximise the multiple benefits of the transorbital corridor's parameters within the realm of the distinct pathology, technology, popular technique and medical setting. While transorbital neuroendoscopic surgery is in use within a select cohort of specialists, the next step with this research field is incorporation of the conclusions identified here into operative planning and surgical practice. These preclinical experiments are the basis upon which clinicians develop new and improved strategies of providing healthcare; by striving for methods, techniques and treatments

which produce optimal care and cure against a pathology, while simultaneously aspiring for zero risk or harm for the patient.

Conclusion

The research findings illustrated in this body of work are diverse, reproducible and applicable. Firstly, I describe through this robust methodological process the means by which surgical anatomical studies can be optimised as in scientific experimentation. This idea will be carried forward in the form of the Inchin neuroquantitative platform which aims to act as a standardised robust experimental tool for anatomical researchers and improve the value and quality of the work produced.

Transorbital surgery, its historical foundation, literature analysis, surgical advantages, disadvantages and pertinent nuances of operative technology has been analysed in depth. It is a surgical corridor with substantive potential for access to the anterior cranial fossa and specific surgical target structures. The neuroquantitative metrics investigated confirm the utility and benefit of endoscope and microscope as well as the most appropriate setting wherein a transorbital corridor should be utilised. The transorbital corridor has impressive potential, can utilise all our available technological advances, promotes multi-disciplinary co-operation and learning amongst clinicians and ultimately, is a means of improving our operative patient care.

REFERENCES

Abdel Aziz, K. M., Bhatia, S., Tantawy, M. H., Sekula, R., Keller, J. T., Froelich, S., & Happ, E. (2011). Minimally invasive transpalpebral "eyelid" approach to the anterior cranial base. *Neurosurgery, 69*(2 Suppl Operative), ons195-206; discussion 206-197. doi:10.1227/NEU.0b013e31821c3ea3

Acar, F., Naderi, S., Guvencer, M., Ture, U., & Arda, M. N. (2005). Herophilus of Chalcedon: a pioneer in neuroscience. *Neurosurgery, 56*(4), 861-867; discussion 861-867. doi:10.1227/01.neu.0000156791.97198.58

Almeida, J. P., Omay, S. B., Shetty, S. R., Chen, Y. N., Ruiz-Trevino, A. S., Liang, B., . . . Schwartz, T. H. (2018). Transorbital endoscopic eyelid approach for resection of sphenoorbital meningiomas with predominant hyperostosis: report of 2 cases. *J Neurosurg, 128*(6), 1885-1895. doi:10.3171/2017.3.JNS163110

Almeida, J. P., Ruiz-Trevino, A. S., Shetty, S. R., Omay, S. B., Anand, V. K., & Schwartz, T. H. (2017). Transorbital endoscopic approach for exposure of the sylvian fissure, middle cerebral artery and crural cistern: an anatomical study. *Acta Neurochir (Wien), 159*(10), 1893-1907. doi:10.1007/s00701-017-3296-8

Alqahtani, A., Padoan, G., Segnini, G., Lepera, D., Fortunato, S., Dallan, I., . . . Castelnuovo, P. (2015). Transorbital transnasal endoscopic combined approach to the anterior and middle skull base: a laboratory investigation. *Acta Otorhinolaryngol Ital, 35*(3), 173-179. Retrieved from https://www.ncbi.nlm.nih.gov/pubmed/26246661

Andaluz, N., Romano, A., Reddy, L. V., & Zuccarello, M. (2008). Eyelid approach to the anterior cranial base. *J Neurosurg, 109*(2), 341-346. doi:10.3171/JNS/2008/109/8/0341

Arraez-Aybar, L. A., Navia-Alvarez, P., Fuentes-Redondo, T., & Bueno-Lopez, J. L. (2015). Thomas Willis, a pioneer in translational research in anatomy (on the 350th anniversary of Cerebri anatome). *J Anat, 226*(3), 289-300. doi:10.1111/joa.12273

Aziz, N., & Mansor, O. (2006). The role of anatomists and surgeons in clinical anatomy instruction inside and outside the operating room. *Malays J Med Sci, 13*(1), 76-77. Retrieved from https://www.ncbi.nlm.nih.gov/pubmed/22589596

Balakrishnan, K., & Moe, K. S. (2011). Applications and outcomes of orbital and transorbital endoscopic surgery. *Otolaryngol Head Neck Surg, 144*(5), 815-820. doi:10.1177/0194599810397285

Barth, A. L., & Ray, A. (2019). Progressive circuit changes during learning and disease. *Neuron, 104*(1), 37-46. doi:10.1016/j.neuron.2019.09.032

Belykh, E. G., Zhao, X., Cavallo, C., Bohl, M. A., Yagmurlu, K., Aklinski, J. L., . . . Preul, M. C. (2018). Laboratory evaluation of a robotic operative microscope : visualization platform for neurosurgery. *Cureus, 10*(7), e3072. doi:10.7759/cureus.3072

Benedict, W. L. (1949). Surgical treatment of tumors and cysts of the orbit. *Am J Ophthalmol, Pt.1 32*(6), 763-773. doi:10.1016/s0002-9394(49)90001-x

Beretta, F., Andaluz, N., Chalaala, C., Bernucci, C., Salud, L., & Zuccarello, M. (2010). Image-guided anatomical and morphometric study of supraorbital and transorbital minicraniotomies to the sellar and perisellar regions: comparison with standard techniques. *J Neurosurg, 113*(5), 975-981. doi:10.3171/2009.10.JNS09435

Berke, R. N. (1954). A modified Kronlein operation. *AMA Arch Ophthalmol, 51*(5), 609-632. doi:10.1001/archopht.1954.00920040619006

Bly, R. A., Ramakrishna, R., Ferreira, M., & Moe, K. S. (2014). Lateral transorbital neuroendoscopic approach to the lateral cavernous sinus. *J Neurol Surg B Skull Base, 75*(1), 11-17. doi:10.1055/s-0033-1353363

Brock, M., & Dietz, H. (1978). The small frontolateral approach for the microsurgical treatment of intracranial aneurysms. *Neurochirurgia (Stuttg), 21*(6), 185-191. doi:10.1055/s-0028-1090343

Burgess, A. W., & Ramsey-Stewart, G. (2015). The importance of surgeons teaching anatomy, especially by whole-body dissection. *Med J Aust, 202*(1), 18-19. doi:10.5694/mja14.00410

Burns, J. A., Dodson, E. E., & Gross, C. W. (1996). Transnasal endoscopic repair of cranionasal fistulae: a refined technique with long-term follow-up. *Laryngoscope, 106*(9 Pt 1), 1080-1083. doi:10.1097/00005537-199609000-00007

Burns, P., Rohrich, R., & Chung, K. (2011). The levels of evidence and their role in evidence-based medicine. *Plast Reconstr Surg, 128*, 305-310. doi:10.1097/PRS.0b013e318219c171

Caruso, J. P., & Sheehan, J. P. (2017). Psychosurgery, ethics, and media: a history of Walter Freeman and the lobotomy. *Neurosurg Focus, 43*(3), E6. doi:10.3171/2017.6.FOCUS17257

Castelnuovo, P., Lepera, D., Turri-Zanoni, M., Battaglia, P., Bolzoni Villaret, A., Bignami, M., . . . Dallan, I. (2013). Quality of life following endoscopic endonasal resection of anterior skull base cancers. *J Neurosurg, 119*(6), 1401-1409. doi:10.3171/2013.8.JNS13296

Chen, H. I., Bohman, L. E., Emery, L., Martinez-Lage, M., Richardson, A. G., Davis, K. A., . . . Lucas, T. H. (2015). Lateral Transorbital Endoscopic Access to the Hippocampus, Amygdala, and Entorhinal Cortex: Initial Clinical Experience. *ORL J Otorhinolaryngol Relat Spec, 77*(6), 321-332. doi:10.1159/000438762

Chen, H. I., Bohman, L. E., Loevner, L. A., & Lucas, T. H. (2014). Transorbital endoscopic amygdalohippocampectomy: a feasibility investigation. *J Neurosurg, 120*(6), 1428-1436. doi:10.3171/2014.2.JNS131060

Choi, K. J., Jang, D. W., & Abi Hachem, R. (2018). Endoscopic endonasal approaches to the orbit. *Int Ophthalmol Clin, 58*(2), 85-99. doi:10.1097/IIO.0000000000000222

Ciporen, J. N., Moe, K. S., Ramanathan, D., Lopez, S., Ledesma, E., Rostomily, R., & Sekhar, L. N. (2010). Multiportal endoscopic approaches to the central skull base: a cadaveric study. *World Neurosurg, 73*(6), 705-712. doi:10.1016/j.wneu.2010.03.033

Cushing, H. (1912). *The Pituitary Body and its Disorders Clinical States Produced by Disorders of the Hypophysis Cerebri* Philadelphia, London, J.B. Lippincott company.

Dallan, I., Castelnuovo, P., Locatelli, D., Turri-Zanoni, M., AlQahtani, A., Battaglia, P., . . . Sellari-Franceschini, S. (2015). Multiportal combined transorbital transnasal endoscopic approach for the management of selected skull base lesions: preliminary experience. *World Neurosurg, 84*(1), 97-107. doi:10.1016/j.wneu.2015.02.034

Dallan, I., Locatelli, D., Turri-Zanoni, M., Battaglia, P., Lepera, D., Galante, N., . . . Castelnuovo, P. (2015). Transorbital endoscopic assisted resection of a superior orbital fissure cavernous haemangioma: a technical case report. *Eur Arch Otorhinolaryngol, 272*(12), 3851-3856. doi:10.1007/s00405-015-3556-2

Dandy, W. E. (1922). Prechiasmal intracranial tumors of the optic nerves. *Amer. J. Ophthalmol, 5*(3), 169-188.

Dandy, W. E. (1942). Orbital Tumors: Results Following the Transcranial Operative Attack. *London: H.K. Lewis & Co. Ltd*.

Dandy, W. E. (1945). *Surgery of the Brain, A monograph from Volume XII Lewis' Practice of Surgery*. Hagerstown: WF Prior Co.

Dare, A. O., Landi, M. K., Lopes, D. K., & Grand, W. (2001). Eyebrow incision for combined orbital osteotomy and supraorbital minicraniotomy: application to aneurysms of the anterior circulation. Technical note. *J Neurosurg, 95*(4), 714-718. doi:10.3171/jns.2001.95.4.0714

de la Torre, J. C., & Surgeon, J. W. (1976). Dexamethasone and DMSO in experimental transorbital cerebral infarction. *Stroke, 7*(6), 577-583. doi:10.1161/01.str.7.6.577

Delashaw, J. B., Jr., Tedeschi, H., & Rhoton, A. L. (1992). Modified supraorbital craniotomy: technical note. *Neurosurgery, 30*(6), 954-956. doi:10.1227/00006123-199206000-00028

Di Somma, A., Andaluz, N., Cavallo, L. M., Keller, J. T., Solari, D., Zimmer, L. A., . . . Cappabianca, P. (2018). Supraorbital vs Endo-Orbital Routes to the Lateral Skull Base: A Quantitative and Qualitative Anatomic Study. *Oper Neurosurg (Hagerstown), 15*(5), 567-576. doi:10.1093/ons/opx256

Di Somma, A., Langdon, C., de Notaris, M., Reyes, L., Ortiz-Perez, S., Alobid, I., & Ensenat, J. (2020). Combined and simultaneous endoscopic endonasal and transorbital surgery for a Meckel's cave schwannoma: technical nuances of a mini-invasive, multiportal approach. *J Neurosurg*, 1-10. doi:10.3171/2020.4.JNS20707

Draf, W. (1983). *Endoscopy of the Paranasal Sinuses: Technique, Typical Findings, Therapeutic Possibilities*: Springer-Verlag.

El-Hai, J. (2005). *The Lobotomist: A Maverick Medical Genius and His Tragic Quest to Rid the World of Mental Illness*: Wiley.

Elhadi, A. M., Almefty, K. K., Mendes, G. A., Kalani, M. Y., Nakaji, P., Dru, A., . . . Little, A. S. (2014). Comparison of surgical freedom and area of exposure in three endoscopic transmaxillary approaches to the anterolateral cranial base. *J Neurol Surg B Skull Base, 75*(5), 346-353. doi:10.1055/s-0034-1372467

Elhadi, A. M., Hardesty, D. A., Zaidi, H. A., Kalani, M. Y., Nakaji, P., White, W. L., . . . Little, A. S. (2015). Evaluation of surgical freedom for microscopic and endoscopic transsphenoidal approaches to the sella. *Neurosurgery, 11 Suppl 2,* 69-78; discussion 78-69. doi:10.1227/NEU.0000000000000601

Elhadi, A. M., Kalb, S., Perez-Orribo, L., Little, A. S., Spetzler, R. F., & Preul, M. C. (2012). The journey of discovering skull base anatomy in ancient Egypt and the special influence of Alexandria. *Neurosurg Focus, 33*(2), E2. doi:10.3171/2012.6.FOCUS12128

Ferrari, M., Schreiber, A., Mattavelli, D., Belotti, F., Rampinelli, V., Lancini, D., . . . Nicolai, P. (2016). The Inferolateral Transorbital Endoscopic Approach: A Preclinical Anatomic Study. *World Neurosurg, 90*, 403-413. doi:10.1016/j.wneu.2016.03.017

Fiamberti, A. M. (1937). Proposta di una tecnica operatoria modificata e semplificata per gli interventi alla Moniz sui lobi frontali in malati di mente. *Rassegna di Psichiatrici*(26), 797.

Frazier, C. H. (1913). I. An Approach to the Hypophysis through the Anterior Cranial Fossa. *Ann Surg, 57*(2), 145-150. doi:10.1097/00000658-191302000-00001

Freeman, W. (1948a). Transorbital leucotomy. *Lancet, 2*(6523), 371-373. doi:10.1016/s0140-6736(48)90947-7

Freeman, W. (1948b). Transorbital Lobotomy. *The American Journal of Psychiatry, 105,* 734-740.

Fries, G., & Perneczky, A. (1998). Endoscope-assisted brain surgery: part 2--analysis of 380 procedures. *Neurosurgery, 42*(2), 226-231; discussion 231-222. doi:10.1097/00006123-199802000-00008

Galbraith, J. E., & Sullivan, J. H. (1973). Decompression of the perioptic meninges for relief of papilledema. *Am J Ophthalmol, 76*(5), 687-692. doi:10.1016/0002-9394(73)90564-3

Guiot, G., Rougerie, J., Fourestier, M., Fournier, A., Comoy, C., & Vulmiere, J. (1963). Une nouvelle technique endoscopique: Explorations endoscopiques intracrâniennes. *Presse Med, 72*, 1225-1231.

Haab, O. (1905). *Atlas and Epitome of Operative Ophthalmology*. Philadephia: WB Saunders Co.

Hakuba, A., Liu, S., & Nishimura, S. (1986). The orbitozygomatic infratemporal approach: a new surgical technique. *Surg Neurol, 26*(3), 271-276. doi:10.1016/0090-3019(86)90161-8

Hakuba, A., Tanaka, K., Suzuki, T., & Nishimura, S. (1989). A combined orbitozygomatic infratemporal epidural and subdural approach for lesions involving the entire cavernous sinus. *J Neurosurg, 71*(5 Pt 1), 699-704. doi:10.3171/jns.1989.71.5.0699

Herlan, S., Marquardt, J. S., Hirt, B., Tatagiba, M., & Ebner, F. H. (2019). 3D exoscope system in neurosurgery: comparison of a standard operating microscope with a new 3D exoscope in the cadaver lab. *Oper Neurosurg (Hagerstown), 17*(5), 518-524. doi:10.1093/ons/opz081

Higdon, R. (2013). Experimental Design, Variability. In W. Dubitzky, O. Wolkenhauer, K.-H. Cho, & H. Yokota (Eds.), *Encyclopedia of Systems Biology* (pp. 704-705). New York, NY: Springer New York.

Horgan, M. A., Anderson, G. J., Kellogg, J. X., Schwartz, M. S., Spektor, S., McMenomey, S. O., & Delashaw, J. B. (2000). Classification and quantification of the petrosal approach to the petroclival region. *J Neurosurg, 93*(1), 108-112. doi:10.3171/jns.2000.93.1.0108

Houlihan, L. M., Belykh, E., Zhao, X., O'Sullivan, M. G. J., & Preul, M. C. (2021). From Kronlein, through madness, to a useful modern surgery: the journey of the transorbital corridor to enter the neurosurgical armamentarium. *J Neurosurg*, 1-10. doi:10.3171/2020.8.JNS201251

Houlihan, L. M., Staudinger Knoll, A. J., Kakodkar, P., Zhao, X., O'Sullivan, M., Lawton, M. T., & Preul, M. C. (2021a). Transorbital neuroendoscopic surgery as a mainstream neurosurgical corridor: a systematic review. *World Neurosurg*. doi:10.1016/j.wneu.2021.04.104

Houlihan, L. M., Staudinger Knoll, A. J., Kakodkar, P., Zhao, X., O'Sullivan, M. G. J., Lawton, M. T., & Preul, M. C. (2021b). Transorbital Neuroendoscopic Surgery as a Mainstream Neurosurgical Corridor: A Systematic Review. *World Neurosurg*. doi:10.1016/j.wneu.2021.04.104

Huang, J., Mocco, J., Choudhri, T. F., Poisik, A., Popilskis, S. J., Emerson, R., . . . Connolly, E. S., Jr. (2000). A modified transorbital baboon model of reperfused stroke. *Stroke, 31*(12), 3054-3063. doi:10.1161/01.str.31.12.3054

Hudgins, W. R., & Garcia, J. H. (1970). Transorbital approach to the middle cerebral artery of the squirrel monkey: a technique for experimental cerebral infarction applicable to ultrastructural studies. *Stroke, 1*(2), 107-111. doi:10.1161/01.str.1.2.107

Iaizzo, P. A., Anderson, R. H., & Hill, A. J. (2013). The importance of human cardiac anatomy for translational research. *J Cardiovasc Transl Res, 6*(2), 105-106. doi:10.1007/s12265-012-9419-y

Imola, M. J., Sciarretta, V., & Schramm, V. L. (2003). Skull base reconstruction. *Curr Opin Otolaryngol Head Neck Surg, 11*(4), 282-290. doi:10.1097/00020840-200308000-00012

Iorio-Morin, C., & Mathieu, D. (2020). Perspective on the homunculus, the history of cerebral localization, and evolving modes of data representation. *World Neurosurg, 135*, 42-47. doi:10.1016/j.wneu.2019.11.104

Ismail, A. S., Costantino, P. D., & Sen, C. (2007). Transnasal transsphenoidal endoscopic repair of CSF leakage using multilayer acellular dermis. *Skull Base, 17*(2), 125-132. doi:10.1055/s-2007-970556

Janakiram, T. N., Subramaniam, V., & Parekh, P. (2015). Endoscopic Endonasal Repair of Sphenoid Sinus Cerebrospinal Fluid Leaks: Our Experience. *Indian J Otolaryngol Head Neck Surg, 67*(4), 412-416. doi:10.1007/s12070-015-0924-6

Jane, J. A., Jr. (2013). Endoscopy versus microscopy. *J Neurosurg, 118*(3), 611; discussion 611-612. doi:10.3171/2012.7.JNS12632

Jane, J. A., Park, T. S., Pobereskin, L. H., Winn, H. R., & Butler, A. B. (1982). The supraorbital approach: technical note. *Neurosurgery, 11*(4), 537-542. Retrieved from https://www.ncbi.nlm.nih.gov/pubmed/7145070

Jho, H. D. (1997). Orbital roof craniotomy via an eyebrow incision: a simplified anterior skull base approach. *Minim Invasive Neurosurg, 40*(3), 91-97. doi:10.1055/s-2008-1053424

Kassam, A., Gardner, P., Snyderman, C., Mintz, A., & Carrau, R. (2005). Expanded endonasal approach: fully endoscopic, completely transnasal approach to the

middle third of the clivus, petrous bone, middle cranial fossa, and infratemporal fossa. *Neurosurg Focus, 19*(1), E6.

Knapp, H. (1874). A case of carcinoma of the outer sheath of the optic nerve, removed with preservation of the eyeball. *Arch Ophthalmol Otol, 4*, 323–354.

Knoop KJ, D. W. (2014). *Clinical Procedures in Emergency Medicine: Ophthalmologic procedures.* (J. Roberts Ed. 6th edition ed.). Philadelphia: Elsevier.

Kong, D. S., Kim, Y. H., & Hong, C. K. (2020). Optimal indications and limitations of endoscopic transorbital superior eyelid surgery for spheno-orbital meningiomas. *J Neurosurg*, 1-8. doi:10.3171/2020.3.JNS20297

Kreutz, C., & Timmer, J. (2009). Systems biology: experimental design. *FEBS J, 276*(4), 923-942. doi:10.1111/j.1742-4658.2008.06843.x

Kronlein, R. U. (1889). Zur Pathologie and operativen Behandlung der Dermoidcysten der Orbita. *Beitr z Klin Chir Tubing, 4*, 149–163.

Li, J., Wang, J., Jing, X., Zhang, W., Zhang, X., & Qiu, Y. (2008). Transsphenoidal optic nerve decompression: an endoscopic anatomic study. *J Craniofac Surg, 19*(6), 1670-1674. doi:10.1097/SCS.0b013e31818b4316

Lim, J., Roh, T. H., Kim, W., Kim, J. S., Hong, J. B., Sung, K. S., . . . Hong, C. K. (2020). Biportal endoscopic transorbital approach: a quantitative anatomical study and clinical application. *Acta Neurochir (Wien), 162*(9), 2119-2128. doi:10.1007/s00701-020-04339-0

Lima, L. R., Beer-Furlan, A., Prevedello, D. M., Carrau, R. L., Servian-Duarte, D. A., Galarce, M. G., . . . Giannetti, A. V. (2020). Minimally Invasive Approaches to the Lateral Cavernous Sinus and Meckel's Cave: Comparison of Transorbital and Subtemporal Endoscopic Techniques. *World Neurosurg*. doi:10.1016/j.wneu.2020.04.180

Lima, V., Burt, B., Leibovitch, I., Prabhakaran, V., Goldberg, R. A., & Selva, D. (2009). Orbital compartment syndrome: the ophthalmic surgical emergency. *Surv Ophthalmol, 54*(4), 441-449. doi:10.1016/j.survophthal.2009.04.005

Lin, B. J., Hong, K. T., Chung, T. T., Liu, W. H., Hueng, D. Y., Chen, Y. H., . . . Tang, C. T. (2019). Endoscopic transorbital transtentorial approach to middle incisural space: preclinical cadaveric study. *Acta Neurochir (Wien), 161*(4), 831-839. doi:10.1007/s00701-019-03831-6

Mariniello, G., Maiuri, F., de Divitiis, E., Bonavolonta, G., Tranfa, F., Iuliano, A., & Strianese, D. (2010). Lateral orbitotomy for removal of sphenoid wing meningiomas invading the orbit. *Neurosurgery, 66*(6 Suppl Operative), 287-292; discussion 292. doi:10.1227/01.NEU.0000369924.87437.0B

Maroon, J. C., & Kennerdel, J. S. (1976). Lateral microsurgical approach to intraorbital tumors. *J Neurosurg, 44*(5), 556-561. doi:10.3171/jns.1976.44.5.0556

Martin, P., & Cushing, H. (1923). Primary Tumors of the Chiasm and Optic Nerve in Their Intracranial Portion. *Arch. Ophth., 52*, 209.

Matsushima, T., Kobayashi, S., Inoue, T., Rhoton, A. S., Vlasak, A. L., & Oliveira, E. (2018). Albert L. Rhoton Jr., MD: his philosophy and education of neurosurgeons. *Neurol Med Chir (Tokyo), 58*(7), 279-289. doi:10.2176/nmc.ra.2018-0082

McMains, K. C., Gross, C. W., & Kountakis, S. E. (2004). Endoscopic management of cerebrospinal fluid rhinorrhea. *Laryngoscope, 114*(10), 1833-1837. doi:10.1097/00005537-200410000-00029

Melly, L., Torregrossa, G., Lee, T., Jansens, J. L., & Puskas, J. D. (2018). Fifty years of coronary artery bypass grafting. *J Thorac Dis, 10*(3), 1960-1967. doi:10.21037/jtd.2018.02.43

Moe, K. (2007). *Endoscopic orbital and transorbital-intracranial surgery.* Paper presented at the Pacific Coast Otolaryngology-Ophthalmology Society Annual Meeting, Oahu, HA.

Moe, K. S. (2003). The precaruncular approach to the medial orbit. *Arch Facial Plast Surg, 5*(6), 483-487. doi:10.1001/archfaci.5.6.483

Moe, K. S. (2007). *Endoscopic orbital and transorbital-intracranial surgery.* Paper presented at the Pacific Coast Otolaryngology-Ophthalmology Society Annual Meeting, Oahu, HA.

Moe, K. S., Bergeron, C. M., & Ellenbogen, R. G. (2010). Transorbital neuroendoscopic surgery. *Neurosurgery, 67*(3 Suppl Operative), ons16-28. doi:10.1227/01.NEU.0000373431.08464.43

Moe, K. S., Kim, L. J., & Bergeron, C. M. (2011). Transorbital endoscopic repair of cerebrospinal fluid leaks. *Laryngoscope, 121*(1), 13-30. doi:10.1002/lary.21280

Moher, D., Liberati, A., Tetzlaff, J., & Altman, D. (2009). Preferred reporting items for systematic reviews and meta-analyses: the PRISMA statement. *J Clin Epidemiol, 62*, 1006-1012. doi:10.1016/j.jclinepi.2009.06.005

Moniz, E. *Letter from Egas Moniz to Walter Freeman, June 24, 1936, in Walter Freeman and James Watts Collection, 1918-1988, Collection No. MS0803.UA*: George Washington University Special Collections Research Center.

Noiphithak, R., Yanez-Siller, J. C., Revuelta Barbero, J. M., Cho, R. I., Otto, B. A., Carrau, R. L., & Prevedello, D. M. (2019). Comparative Analysis of the Exposure and Surgical Freedom of the Endoscopic Extended Minipterional Craniotomy and the Transorbital Endoscopic Approach to the Anterior and Middle Cranial Fossae. *Oper Neurosurg (Hagerstown), 17*(2), 174-181. doi:10.1093/ons/opy309

Noiphithak, R., Yanez-Siller, J. C., Revuelta Barbero, J. M., Otto, B. A., Carrau, R. L., & Prevedello, D. M. (2018). Quantitative analysis of the surgical exposure and surgical freedom between transcranial and transorbital endoscopic anterior petrosectomies to the posterior fossa. *J Neurosurg, 131*(2), 569-577. doi:10.3171/2018.2.JNS172334

Norris, J. L., & Cleasby, G. W. (1981). Endoscopic orbital surgery. *Am J Ophthalmol, 91*(2), 249-252. doi:10.1016/0002-9394(81)90183-5

Nyquist, G. G., Anand, V. K., Mehra, S., Kacker, A., & Schwartz, T. H. (2010). Endoscopic endonasal repair of anterior skull base non-traumatic cerebrospinal fluid leaks, meningoceles, and encephaloceles. *J Neurosurg, 113*(5), 961-966. doi:10.3171/2009.10.JNS08986

Park, H. H., Hong, S. D., Kim, Y. H., Hong, C. K., Woo, K. I., Yun, I. S., & Kong, D. S. (2019). Endoscopic transorbital and endonasal approach for trigeminal schwannomas: a retrospective multicenter analysis (KOSEN-005). *J Neurosurg*, 1-10. doi:10.3171/2019.3.JNS19492

Park, H. H., Yoo, J., Yun, I. S., & Hong, C. K. (2020). Comparative Analysis of Endoscopic Transorbital Approach and Extended Mini-Pterional Approach for Sphenoid Wing Meningiomas with Osseous Involvement: Preliminary Surgical Results. *World Neurosurg, 139*, e1-e12. doi:10.1016/j.wneu.2020.01.115

Perneczky, A., & Fries, G. (1998). Endoscope-assisted brain surgery: part 1--evolution, basic concept, and current technique. *Neurosurgery, 42*(2), 219-224; discussion 224-215. doi:10.1097/00006123-199802000-00001

Pillai, P., Baig, M. N., Karas, C. S., & Ammirati, M. (2009). Endoscopic image-guided transoral approach to the craniovertebral junction: an anatomic study comparing surgical exposure and surgical freedom obtained with the endoscope and the operating microscope. *Neurosurgery, 64*(5 Suppl 2), 437-442; discussion 442-434. doi:10.1227/01.NEU.0000334050.45750.C9

Priddy, B. H., Nunes, C. F., Beer-Furlan, A., Carrau, R., Dallan, I., & Prevedello, D. M. (2017). A Side Door to Meckel's Cave: Anatomic Feasibility Study for the Lateral Transorbital Approach. *Oper Neurosurg (Hagerstown), 13*(5), 614-621. doi:10.1093/ons/opx042

Ramakrishna, R., Kim, L. J., Bly, R. A., Moe, K., & Ferreira, M., Jr. (2016). Transorbital neuroendoscopic surgery for the treatment of skull base lesions. *J Clin Neurosci, 24*, 99-104. doi:10.1016/j.jocn.2015.07.021

Raza, S. M., Quinones-Hinojosa, A., Lim, M., & Boahene, K. D. (2013). The transconjunctival transorbital approach: a keyhole approach to the midline anterior skull base. *World Neurosurg, 80*(6), 864-871. doi:10.1016/j.wneu.2012.06.027

Reinard, K., Basheer, A., Jones, L., Standring, R., Lee, I., & Rock, J. (2015). Surgical technique for repair of complex anterior skull base defects. *Surg Neurol Int, 6*, 20. doi:10.4103/2152-7806.151259

Saraceno, G., Agosti, E., Qiu, J., Buffoli, B., Ferrari, M., Raffetti, E., . . . Doglietto, F. (2019). Quantitative Anatomical Comparison of Anterior, Anterolateral and Lateral, Microsurgical and Endoscopic Approaches to the Middle Cranial Fossa. *World Neurosurg*. doi:10.1016/j.wneu.2019.10.178

Schaberg, M., Murchison, A. P., Rosen, M. R., Evans, J. J., & Bilyk, J. R. (2011). Transorbital and transnasal endoscopic repair of a meningoencephalocele. *Orbit, 30*(5), 221-225. doi:10.3109/01676830.2011.579686

Selcuk, I., Tatar, I., & Huri, E. (2019). Cadaveric anatomy and dissection in surgical training. *Turk J Obstet Gynecol, 16*(1), 72-75. doi:10.4274/tjod.galenos.2018.15931

Seyit Kagan Başarslan, C. G. (2014). Neuronavigation: a revolutionary step of neurosurgery and its education. *Derleme\review*. doi:10.17944/mkutfd.15885

Shimanskaya, V. E., Wagenmakers, M., Bartels, R., Boogaarts, H. D., Grotenhuis, J. A., Hermus, A., . . . van Lindert, E. J. (2018). Toward Shorter Hospitalization After

Endoscopic Transsphenoidal Pituitary Surgery: Day-by-Day Analysis of Early Postoperative Complications and Interventions. *World Neurosurg, 111*, e871-e879. doi:10.1016/j.wneu.2017.12.174

Spektor, S., Anderson, G. J., McMenomey, S. O., Horgan, M. A., Kellogg, J. X., & Delashaw, J. B., Jr. (2000). Quantitative description of the far-lateral transcondylar transtubercular approach to the foramen magnum and clivus. *J Neurosurg, 92*(5), 824-831. doi:10.3171/jns.2000.92.5.0824

Stallard, H. B. (1947). A plea for lateral orbitotomy (Kronlein's operation). *Br Med J, 1*(4499), 408. doi:10.1136/bmj.1.4499.408

Stallard, H. B. (1960). A Plea for Lateral Orbitotomy: With Certain Modifications. *Br J Ophthalmol, 44*(12), 718-723. doi:10.1136/bjo.44.12.718

Stippler, M., Gardner, P. A., Snyderman, C. H., Carrau, R. L., Prevedello, D. M., & Kassam, A. B. (2009). Endoscopic endonasal approach for clival chordomas. *Neurosurgery, 64*(2), 268-277; discussion 277-268. doi:10.1227/01.NEU.0000338071.01241.E2

Tham, T., Costantino, P., Bruni, M., Langer, D., Boockvar, J., & Singh, P. (2015). Multiportal Combined Transorbital and Transnasal Endoscopic Resection of Fibrous Dysplasia. *J Neurol Surg Rep, 76*(2), e291-296. doi:10.1055/s-0035-1566126

Topczewski, T. E., Di Somma, A., Pineda, J., Ferres, A., Torales, J., Reyes, L., . . . Prats-Galino, A. (2020). Endoscopic endonasal and transorbital routes to the petrous apex: anatomic comparative study of two pathways. *Acta Neurochir (Wien), 162*(9), 2097-2109. doi:10.1007/s00701-020-04451-1

Tosun, F., Carrau, R. L., Snyderman, C. H., Kassam, A., Celin, S., & Schaitkin, B. (2003). Endonasal endoscopic repair of cerebrospinal fluid leaks of the sphenoid sinus. *Arch Otolaryngol Head Neck Surg, 129*(5), 576-580. doi:10.1001/archotol.129.5.576

Ulutas, M., Cinar, K., Dogan, I., Secer, M., Isik, S., & Aksoy, K. (2019). Lateral transorbital approach: an alternative microsurgical route for supratentorial cerebral aneurysms. *J Neurosurg*, 1-12. doi:10.3171/2019.9.JNS191683

van Lindert, E., Perneczky, A., Fries, G., & Pierangeli, E. (1998). The supraorbital keyhole approach to supratentorial aneurysms: concept and technique. *Surg Neurol, 49*(5), 481-489; discussion 489-490. doi:10.1016/s0090-3019(96)00539-3

Vijayalakshmi, P. (2007). The precaruncular approach to the medial orbit. *J AAPOS, 11*(2), 208. doi:10.1016/j.jaapos.2007.02.003

Wada, T., & Toyota, M. (1951). Transorbital brain-ventricle puncture or a new method for pneumoventriculography. *Tohoku J Exp Med, 54*(3), 223-226. doi:10.1620/tjem.54.223

Wax, M. K., Ramadan, H. H., Ortiz, O., & Wetmore, S. J. (1997). Contemporary management of cerebrospinal fluid rhinorrhea. *Otolaryngol Head Neck Surg, 116*(4), 442-449. doi:10.1016/s0194-5998(97)70292-4

Weisstein, E. W. Heron's formula. *MathWorld - A Wolfram Web Resource.* Retrieved from https://mathworld.wolfram.com/HeronsFormula.html

Weisstein, E. W. Polygon area. *MathWorld-A Wolfram Web Resource.* Retrieved from https://mathworld.wolfram.com/PolygonArea.html

Wilson, D. H. (1971). Limited exposure in cerebral surgery. Technical note. *J Neurosurg, 34*(1), 102-106. doi:10.3171/jns.1971.34.1.0102

Winterton, J. V., Patel, K., & Mizen, K. D. (2007). Review of management options for a retrobulbar hemorrhage. *J Oral Maxillofac Surg, 65*(2), 296-299. doi:10.1016/j.joms.2005.11.089

Wormald, P. J., & McDonogh, M. (1997). 'Bath-plug' technique for the endoscopic management of cerebrospinal fluid leaks. *J Laryngol Otol, 111*(11), 1042-1046. doi:10.1017/s0022215100139295

Yasargil, M. G., Fox, J. L., & Ray, M. W. (1975). *The operative approach to aneurysms of the anterior communicating artery.* : Springer-Verlag.

Zweig, J. L., Carrau, R. L., Celin, S. E., Schaitkin, B. M., Pollice, P. A., Snyderman, C. H., . . . Hegazy, H. (2000). Endoscopic repair of cerebrospinal fluid leaks to the sinonasal tract: predictors of success. *Otolaryngol Head Neck Surg, 123*(3), 195-201. doi:10.1067/mhn.2000.107452

APPENDICES

APPENDIX A

LIST OF PUBLICATIONS

The following is a list of papers which make up this body of work. It details the papers which are published, those under review for publication and those which are in preparation for submission.

Published manuscripts

1. Houlihan L.M., Belykh E., Zhao X., & O'Sullivan M.G.J., P. M. C. (2020). From Krönlein, through madness, to a useful modern surgery: the journey of the transorbital corridor to enter the neurosurgical armamentarium.
2. Houlihan, L. M., Staudinger Knoll, A. J., Kakodkar, P., Zhao, X., O'Sullivan, M., Lawton, M. T., & Preul, M. C. (2021). Transorbital neuroendoscopic surgery as a mainstream neurosurgical corridor: a systematic review. *World Neurosurg*. doi:10.1016/j.wneu.2021.04.104
3. Lena Mary Houlihan, D. N., Mark C. Preul. (2021). Volume of surgical freedom:the most applicable anatomical measurement for surgical assessment and 3-dimensionalmodeling. *Frontiers in BIomedical Engineering and Biotechnology, Volume 9*. doi:10.3389/fbioe.2021.628797

Manuscripts in preparation

1. Lena Mary Houlihan. Thanapong Loymak, Irakliy Abramov, Mohamed A. Labib, Michael G.J. O'Sullivan, Michael T. Lawton, Mark C. Preul. Transorbital microsurgery: the most minimally invasive corridor to the anterior cranial fossa

and paramedian structures. *In preparation for submission to Journal of Neurosurgery*

2. Lena Mary Houlihan. Thanapong Loymak, Irakliy Abramov, Jubran H. Jubran, Ann J. Staudinger Knoll, Jacob T. Howshar, Chelsea Tran, Michael G.J. O'Sullivan, Michael T. Lawton, Mark C. Preul. Optimal antero-lateral access corridors to the anterior skull base and paramedian vasculature: quantitative analysis of unilateral supraorbital, transorbital microscopic and transorbital endoscopic approaches. *In preparation for submission to Journal of Neurosurgery*
3. Lena Mary Houlihan. Thanapong Loymak, Irakliy Abramov, Jubran H. Jubran, Ann J. Staudinger Knoll, Jacob T. Howshar, Dara Farhadi, Lea Scherschinski, Michael G.J. O'Sullivan, Michael T. Lawton, Mark C. Preul. Exploratory analysis of the biportal transorbital approach; quantitative comparison of anterior subfrontal craniotomy versus bilateral transorbital endoscopic and microscopic approaches to the anterior cranial fossa and paramedian vasculature *In preparation for submission to Journal of Neurosurgery*

APPENDIX B

CHAPTER 3 SEARCH PROTOCOL

Section 1: Administrative Information

1. Title: Transorbital interventions in skull base surgery: a protocol for a systemic review

2. Registration: Our systematic review protocol was submitted to the International Prospective Register of Systematic Reviews (PROSPERO) on 15 November 2019 (registration number 158756).

Corresponding author: Mark C. Preul, MD

mark.preul@dignityhealth.org

Author Affiliations:

Barrow Neurological Institute, 350 W. Thomas Drive, Phoenix, AZ 85013

3b. Contributions: LMH and ASK completed the systematic review protocol. LMH, ASK, PK, and XZ completed the acquisition, analysis, and interpretation of data. LMH and ASK drafted the original article. MCP provided critical revision of the article. MCP provided final approval of the version to be published.

4. Amendments: Should there be a need for amendments to the protocol, the date of each amendment, a description of the change, and the rationale will be given/noted.

Amendment changes were not made to the protocol.

5a. Support: This study was supported by funds from the Newsome Chair in Neurosurgery Research held by Mark C. Preul, MD, and from the Barrow Neurological Foundation, St. Joseph's Hospital and Medical Center, Phoenix, Arizona.

5b. Sponsor: This review does not have any specific sponsoring agent.

5c. Role of the Sponsor in Protocol Development: This research is being completed in the Neurosurgical Anatomy Laboratory of Barrow Neurological Institute. Barrow Neurological Institute is not involved in any aspect of the project, such as the design of the project's protocol and analysis plan, the collection, and the analyses.

Section 2: Introduction

6. Rationale: Transorbital surgery that accessed the cranial compartment was developed and used by neurosurgeons and psychiatrists beginning in the 1930s to conduct transorbital prefrontal lobotomy procedures in patients with schizophrenia and psychoses[1-3] via perforation of the orbital plate without danger to the structures in the orbit or the large intracranial vessels.[4-6] With this minimally invasive procedure, there were only minor postoperative complications noted (minor subscleral hemorrhage, transient swelling, and ecchymosis).[4-6] The inappropriate use of lobotomies seems to

have contributed to a negative view of the transorbital approach, at least in the neurosurgical realm.

Beginning in the 1800s, surgeons and ophthalmologists were the most prominent group to apply transorbital approaches via orbitotomies to gain access to orbital or circumferential extraorbital structures. Transorbital approaches for tumor and foreign body removal and orbital decompression[7-9] were minimally invasive and had satisfactory surgical outcomes. Superior eyelid/eyebrow or transconjunctival/inferior eyelid incisions allowed for an anterior orbitotomy approach for the surgical treatment of optic sheath carcinoma.[10] Medial transconjunctival orbitotomy was used for optic nerve decompression because of impingement by periorbital meninges and anterior and medial intraconal lesions.[11] Orbital decompression via the manipulation of the surrounding bony orbital construct was conducted using orbital roof removal during a frontal craniotomy with satisfactory results[12] or the removal of the orbital floor and entire ethmoidal complex was performed for decompression of the inferior anatomy.[13] Temporary retraction of the orbital contents was possible, allowing for direct access to deep intracranial anatomical structures, neurovascular bundles, the orbital apex, and the anterior and middle cranial fossae.[14] Orbital pathology extending into the cranial compartment was approached via cranial routes developed by neurosurgeons, but initiation through an orbital corridor was not promoted.

The microsurgical technique helped propel transorbital approaches into the modern neurosurgical scope of practice, although there were still varying opinions among the

members of the neurosurgical and ophthalmological specialties on the applications of this approach. As the surgical preferences trend toward noninvasive procedures with maximal intracranial exposure, recognition of the anatomical boundaries of the orbit for skull base pathologies of the anterior and middle cranial fossae remains difficult,[15] which has led to the incorporation of the transorbital approach in an attempt to overcome the orbital roof and gain intracranial and intraorbital access. The supraorbital approach[16] provides access to supraorbital lesions and deeper neurovascular structures, allowing for wide intracranial exposure for extended, bilaterally situated, deep intracranial areas[17] with limited exposure of the cerebral surfaces and minimal brain retraction.[18] The orbitozygomatic infratemporal approach extended the craniotomy for visualization of the parasellar region and interpeduncular fossa, with minimal brain retraction, excellent exposure, and safe manipulation.[19] The combination of orbitotomy and craniotomy allowed for minimally invasive access to the skull base corridor with superior cosmetic results compared to the transcranial or craniofacial approaches previously used.

The innovation of endoscopy expanded the possibilities of transorbital approaches, allowing for direct access to the sphenoid bone, orbital apex, and anterior and middle cranial fossae, with temporary retraction of the eyeball.[20] Neurosurgeons incorporated endoscopic transorbital approaches for midline intracranial interventions, while otorhinolaryngologists excelled at the extracranial skull base and transnasal endoscopic approaches to access the anterior and middle cranial fossae.[21] Intracranial endoscopy allowed for improved illumination, magnification, and visualization, in addition to the

ability to enter previously obscure microscopic surgical corridors, although its use was still restricted by the orbital roof curvature and neurovascular structures around the supraorbital fissure and optic canal.[22] Endonasal endoscopy only provided narrow midline access.[23] In the 2000s, transorbital neuroendoscopic surgery (TONES) allowed for a surgical pathway through the orbit via a craniotomy in one of the four orbital walls, providing optimal visualization and magnification.[24,25,26] Four approaches were classified to access a specific compartment: precaruncular, superior eyelid crease, lateral retrocanthal, and preseptal lower eyelid.[26] A 2016 study determined that the TONES procedures were useful to treat cerebrospinal fluid (CSF) leaks, inflammatory and tumor interventions, fractures, meningoencephaloceles, abscesses, and hematomas.[27]

As technology advanced and surgeons became more accustomed to transorbital approaches, the multiport endoscopic skull base approaches gained popularity, which allowed better visualization and facilitated dissection with a two-handed microsurgical technique. Transnasal and transorbital endoscopic techniques for meningoencephalocele repair,[28] transnasal transorbital techniques for intraorbital optic nerve biopsy,[29] and multiport endoscopic approaches for tension pneumocephalus after endoscopic sinus surgery[30] were reported. The disadvantages of multiport techniques included few orbit-specific tools for the potential depth of intracranial work and instrument crowding.[31]

The development of transorbital approaches, from their use by ophthalmologists, neurosurgeons, and psychiatrists to the current use of these approaches in neurosurgical procedures, has emphasized the use of transorbital approaches as a minimally invasive

surgical technique that allows for extensive visualization in a variety of applications. Further investigation to conduct a systematic review of the medical literature is warranted to better understand what pathologies are being treated with transorbital approaches and what approach is used most commonly. A review of operative outcomes and common complications and an assessment of the present body of evidence currently available are necessary for understanding the risks and benefits associated with transorbital approaches.

7. Objectives: The objectives of this systematic review are as follows:

1. For what pathologies is the transorbital approach being used?
2. What approach is most commonly used: precaruncular, superior lid crease, or lateral orbit?
3. What are the most common complications associated with specific transorbital approaches, including, but not limited to, failure of operative intervention, recurrence or necessity for retreatment, poor cosmetic results, infection, pain, hemorrhage, cranial nerve or neurological deficit, diplopia, or blindness?
4. If necessary, what is the retreatment?
5. Who is using transorbital approaches most often for skull base pathologies: otorhinolaryngologists, ophthalmologists, or neurosurgeons?
6. What region of the skull base or anatomy is most commonly reached via the transorbital approach?

7. What types of studies are available on transorbital approaches in the realms of clinical and anatomical studies?
8. What level of evidence is available for the transorbital approach?
9. What types of transorbital approaches are being used to get to the skull base?
10. What is the length of patient follow-up?

Section 3: Methods

8. Eligibility Criteria: Studies will be selected according to the criteria outlined below.

Study Design

We included all studies that have been published from all institutions that included human subjects. We excluded unpublished studies.

Participants

We included studies examining male and female adult humans (18 years and older) who have undergone transorbital surgery. We excluded studies with patients less than 18 years of age.

Interventions

We included only studies of operative intervention via the transorbital approach for skull base pathologies. In our review of the literature, we defined the transorbital approach as

an endoscopic surgical intervention through which intracranial access is established with the preservation of the orbital ring and lateral orbital ridge.

Outcomes

We examined the outcomes of the approach with the best outcomes for skull base pathologies and the most common complications associated with specific transorbital approaches, including, but not limited to, failure of the operative intervention, recurrence or necessity for retreatment, poor cosmetic results, infection, pain, hemorrhage, cranial nerve or neurological deficit, diplopia, and blindness. Outcomes were collected, as reported. We extracted the data outcomes in all data forms, as reported in the included studies.

Timing

There are no restrictions on the length of follow-up.

Setting

There are no restrictions on the setting.

Language

We included only articles reported in English. A list of possibly relevant titles in other languages will be provided as appropriate.

9. Information Sources: We searched the PubMed, Cochrane Library, Ovid MEDLINE, and EMBASE databases. The search was developed by LMH and was performed by LMH, ASK, PK, and XZ under the supervision of MCP.

10. Search Strategy: We identified all relevant studies with no limits on study design, date, or setting, although only studies reported in English and those with participants 18 years of age or older were included. The PubMed, Cochrane Library, Ovid MEDLINE, and EMBASE databases were searched. The search operative strategy was developed by a health sciences librarian with expertise in systematic review searching. The DATABASE Search Strategy is included as Appendix C.

11a. Data Management: Literature search results were uploaded to a data extraction spreadsheet, which allowed us to create a Preferred Reporting Items for Systematic Reviews and Meta-Analysis (PRISMA) flow diagram once the analysis was complete.

11b. Selection Process: The review authors independently screened the titles and abstracts generated by the inclusion criteria with screening questions and criteria for selection. We obtained the full reports of all studies that appeared to meet the inclusion criteria. LMH and ASK then screened the full-text reports and decided whether they meet the inclusion criteria. We resolved disagreements through discussion or, when required,

through consultation with a third review author. We recorded the reasons for excluding trials. None of the review authors were blind to the journal titles, study authors, or institutions.

11c. Data Collection Process: Data extracted included authors, publication year, number of participants, age range, study design, country of research, outcomes, and numbers of included and excluded participants. LMH, ASK, PK, and XZ reviewed the full-text reports to extract the data. We resolved disagreements through discussion or, when required, through consultation with a third review author. We contacted the authors for additional information, if needed, to determine the study eligibility.

12. Data Items: The pathologies for transorbital skull base approach include iatrogenic, postoperative, or traumatic CSF leak; trauma resulting in epidural hematoma, acute subdural hematoma, or intraparenchymal hematoma; tumors that are either intrinsic lesions (from gliomas or metastases) or extrinsic lesions (from meningiomas); and vascular pathologies, including aneurysm, arteriovenous malformation, fistula, and cavernous malformation. The transorbital skull base approach is also used to access cranial nerves. The target location is defined as the frontal lobe (superior, middle, or inferior) or the skull base. Skull base targets may include the anterior cranial fossa (supraorbital, medial orbit, lateral orbit, cribriform plate, planum sphenoidale, crista galli, or lesser wing of the sphenoid), middle cranial fossa (greater wing of the sphenoid,

anterior clinoid process, posterior clinoid process, tuberculum sellae, hypophyseal fossa, or dorsum sellae), and interhemispheric region. The approaches were defined as the superior lid crease, precaruncular, and lateral orbit. Outcomes were defined as successes or failures. Successful outcomes included no recurrence of a CSF leak; treatment of or removal of a lesion (trauma, tumor, or vascular pathology); or no necessity for further operative intervention. Failure outcomes included recurrence of a CSF leak; failure of treatment or failure to remove a lesion (trauma, tumor, or vascular pathology); or the necessity for further operative intervention. Complications were defined as adverse events associated with the operative intervention, including failure of the operative intervention, recurrence or necessity for retreatment, poor cosmetic results, infection, pain, hemorrhage, cranial nerve or neurological deficit, diplopia, or blindness.

13. Outcomes and Prioritization:

Primary Outcome

The primary outcome for which data are sought is the identification of the approach that has the best outcomes for skull base pathologies accessed via TONES. Outcomes are defined as success or failure. Successful outcomes include no recurrence of a CSF leak; treatment of or removal of a lesion (trauma, tumor, or vascular pathology); or no necessity for further operative intervention. Failure outcomes include recurrence of a CSF leak; failure of treatment or failure to remove a lesion (trauma, tumor, or vascular pathology); or the necessity for further operative intervention.

Secondary Outcome

The secondary outcome for which data were sought is the identification of the most common complications associated with specific transorbital approaches, including adverse events associated with the operative intervention, such as the failure of the operative intervention, recurrence or necessity for retreatment, poor cosmetic results, infection, pain, hemorrhage, cranial nerve or neurological deficit, diplopia, or blindness.

14a. Criteria of Quantitative Synthesis (Data Synthesis): We will conduct a meta-analysis if studies are sufficiently similar.

14b. Proposed Additional Analyses (Data Synthesis): None.

14c. Type of Summary Planned if Quantitative Synthesis is Not Appropriate (Data Synthesis): If a quantitative analysis of data is deemed inappropriate, we will present information in tables and text to summarize study characteristics and findings.

References

1. Fiamberti AM. [The original method of transorbital leukotomy]. *Med Hyg (Geneve).* 1952;10(218):195.

2. Fiamberti AM. Proposta di una tecnicaoperatoriamodificata e semplificata per gli interventialla Moniz sui lobi frontali in malati di mente. *Rassegna di Psichiatrici.* 1937(26):797.
3. Fiamberti AM. Considerazionisullaleucotomiaprefrontale con il metodotransorbitario. *Giornale di Psichiatria e Neuropatologia.* 1939(67):291-3.
4. Freeman W, Watts JW. Prefrontal lobotomy: the surgical relief of mental pain. *Bull N Y Acad Med.* 1942;18(12):794-812.
5. Freeman W. Transorbital leucotomy. *Lancet.* 1948;2(6523):371-3.
6. Freeman W. Transorbital lobotomy. *Am J Psychiatry*. 1948;105:734-40.
7. Anderson RL, Linberg JV. Transorbital approach to decompression in Graves' disease. *Arch Ophthalmol.* 1981;99(1):120-4.
8. Linberg JV, Anderson RL. Transorbital decompression. Indications and results. *Arch Ophthalmol.* 1981;99(1):113-9.
9. Stokken J, Gumber D, Antisdel J, Sindwani R. Endoscopic surgery of the orbital apex: outcomes and emerging techniques. *Laryngoscope.* 2016;126(1):20-4.
10. H K. A case of carcinoma of the outer sheath of the optic nerve, removed with preservation of the eyeball. 323–354. *Arch Ophthalmol Otol.* 1874;4: 323–54.
11. Galbraith JE, Sullivan JH. Decompression of the perioptic meninges for relief of papilledema. *Am J Ophthalmol.* 1973;76(5):687-92.
12. Naffziger HC. Progressive exophthalmos following thyroidectomy; its pathology and treatment. *Ann Surg.* 1931;94(4):582-6.

13. Rootman DB. Orbital decompression for thyroid eye disease. *SurvOphthalmol.* 2018;63(1):86-104.
14. Norris JL, Cleasby GW. Endoscopic orbital surgery. *Am J Ophthalmol*. 1981;91(2):249-52.
15. Moe KS, Kim LJ, Bergeron CM. Transorbital endoscopic repair of cerebrospinal fluid leaks. *Laryngoscope.* 2011;121(1):13-30.
16. Jane JA, Park TS, Pobereskin LH, Winn HR, Butler AB. The supraorbital approach: technical note. *Neurosurgery.* 1982;11(4):537-42.
17. Reisch R, Perneczky A. Ten-year experience with the supraorbital subfrontal approach through an eyebrow skin incision. *Neurosurgery*. 2005;57(4 Suppl):242-55; discussion -55.
18. Cutney C, Bernardino CR, Buono LM, Goldman WH, Maus M. Transorbital craniotomy through a suprabrow approach: a case series. *Orbit.* 2001;20(2):107-17.
19. Hakuba A, Liu S, Nishimura S. The orbitozygomatic infratemporal approach: a new surgical technique. *Surg Neurol.* 1986;26(3):271-6.
20. Norris JL, Cleasby GW. Endoscopic orbital surgery. *Am J Ophthalmol.* 1981;91(2):249-52.
21. Draf W. *Endoscopy of the Paranasal Sinuses: Technique, Typical Findings, Therapeutic Possibilities*. Springer-Verlag; 1983.

22. Balakrishnan K, Moe KS. Applications and outcomes of orbital and transorbital endoscopic surgery. *Otolaryngol Head Neck Surg.* 2011;144(5):815-20.
23. Stippler M, Gardner PA, Snyderman CH, Carrau RL, Prevedello DM, Kassam AB. Endoscopic endonasal approach for clival chordomas. *Neurosurgery.* 2009;64(2):268-77; discussion 77-8.
24. Moe KS, Bergeron CM, Ellenbogen RG. Transorbital neuroendoscopic surgery. *Neurosurgery.* 2010;67(3 Suppl Operative):ons16-28.
25. Moe K, ed. Endoscopic orbital and transorbital-intracranial surgery. Pacific Coast Otolaryngology-Ophthalmology Society Annual Meeting; 2007; Oahu, HI.
26. Moe KS, Kim LJ, Bergeron CM. Transorbital endoscopic repair of cerebrospinal fluid leaks. *Laryngoscope.* 2011;121(1):13-30.
27. Ramakrishna R, Kim LJ, Bly RA, Moe K, Ferreira M, Jr. Transorbital neuroendoscopic surgery for the treatment of skull base lesions. *J Clin Neurosci.* 2016;24:99-104.
28. Schaberg M, Murchison AP, Rosen MR, Evans JJ, Bilyk JR. Transorbital and transnasal endoscopic repair of a meningoencephalocele. *Orbit.* 2011;30(5):221-5.
29. Koutourousiou M, Gardner PA, Stefko ST, Paluzzi A, Fernandez-Miranda JC, Snyderman CH, et al. Combined endoscopic endonasal transorbital approach with transconjunctival-medial orbitotomy for excisional biopsy of the optic nerve: technical note. *J Neurol Surg Rep.* 2012;73(1):52-6.

30. Bly RA, Morton RP, Kim LJ, Moe KS. Tension pneumocephalus after endoscopic sinus surgery: a technical report of multiportal endoscopic skull base repair. *Otolaryngol Head Neck Surg.* 2014;151(6):1081-3.
31. Priddy BH, Nunes CF, Beer-Furlan A, Carrau R, Dallan I, Prevedello DM. A side door to Meckel's cave: anatomic feasibility study for the lateral transorbital approach. *OperNeurosurg (Hagerstown).* 2017;13(5):614-21.

APPENDIX C

CHAPTER 3 DATABASE SEARCH STRATEGY

1. Trans orbital or transorbital
2. Precaruncular trans orbital approach
3. Superior lid crease trans orbital approach
4. Lateral orbit trans orbital approach
5. Endoscopic trans orbital approach
6. Microscopic trans orbital approach
7. Endoscopic trans orbital open combined approach
8. Endoscopic trans orbital transnasal combined approach

APPENDIX D

CHAPTER 6 DETAILED STATISTICAL ANALYSIS

Table 1. Means and Standard Deviations of Lengths, Volumes, and Angles by Approach Type

	All	Supraorbital	Transorbital Microscopic	Transorbital Endoscopic
Sample Size	60 (100%)	20(33.3%)	20(33.3%)	20(33.3%)
Female	24 (40%)	8 (40%)	8 (40%)	8 (40%)
Age at Death (SD)	78.8 (7.4)	78.8 (7.5)	78.8 (7.5)	78.8 (7.5)
Controls:				
Ipsilateral Approach Frontal Lobe Area	915.5 (229.7)	955.4 (261.7)	846.2 (249.9)	944.7 (158.8)
Approach Lengths:				
Ipsilateral Olfactory Nerve	16.6 (4.5)	16.5 (4.8)	15.1 (3.8)	18.2 (4.6)
Ipsilateral Optic Nerve	14.0 (4.1)	14.1 (2.7)	11.3 (3.0)	16.7 (4.5)
Ipsilateral Optic Tract, Median (IQR)	11.0 (9.4-13.3)	10.6 (9.3-13.7)	10.3 (8.6-12.9)	12.4 (10.1-14.0)
Contralateral Optic Nerve	9.4 (3.2)	10.5 (3.2)	8.2 (2.7)	9.1 (3.5)
Ipsilateral A1	16.0 (3.2)	17.0 (2.8)	15.1 (3.3)	15.5 (3.4)
Angles of Attack:				
Ipsilateral Paraclinoid ICA CC	8.3 (3.5)	10.9 (3.3)	7.7 (2.7)	6.3 (2.7)
Ipsilateral Paraclinoid ICA ML	21.9 (6.0)	26.1 (5.3)	21.7 (5.2)	17.7 (4.5)
Ipsilateral Terminal ICA CC, Median (IQR)	9.1 (7.3-10.6)	10.3 (8.4-12.1)	9.2 (8.6-10.3)	7.3 (6.5-9.5)
Terminal ICA ML	23.5 (4.0)	25.4 (4.0)	23.6 (2.4)	21.1 (4.3)
ACoA CC	9.0 (2.5)	9.4 (2.5)	9.0 (1.8)	7.1 (2.7)
ACoA ML	20.1 (4.6)	19.8 (4.6)	22.5 (5.5)	18.1 (2.5)
Volumes of Surgical Freedom:				
Ipsilateral Paraclinoid ICA NU, Median (IQR)	11.8 (8.5-20.8)	25.5 (13.5-28.9)	11.2 (8.4-19.0)	8.8 (6.5-10.2)

Terminal ICA ML, Median (IQR)	14.6 (10.9-18.1)	17.1 (11.5-22.4)	15.2 (13.8-18.1)	10.5 (7.8-14.9)
ACoA NU	13.9 (5.8)	15.6 (5.6)	13.7 (4.4)	7.2 (3.5)

SD = Standard Deviation. IQR = interquartile range.

Assessment of assumptions of normality and equal variance

ANOVA tests reveal that at times statistically significant differences (p-value at α=.05 or less) exist according to approach.

The assumption of normality among the residuals of the ANOVA models is met for all but two of the variables (contralateral optic nerve length and ACoA ML angle), as evidenced by the K-S tests. These two variables were log-transformed for inclusion in the ANOVA model.

The assumption of equality of variance among the ANOVA models is met for all models except for six: Ipsilateral Optic Tract Length; Ipsilateral Terminal ICA CC Angle, Ipsilateral Paraclinoid ICA NU Volume; Terminal ICA ML Volume. For these six models, the test for differences among approaches was tested with a Kruskal-Wallis test.

Table 2. Results of Univariate Analyses comparing all Approaches.

	ANOVA or Kruskal-Wallis *p*-value	**K-S / Lilliefors *p*-value**	**Equality of Variance *p*-value**
Controls:			
Ipsilateral Approach Frontal Lobe Area	.257	.200	.083
Approach Lengths:			
Ipsilateral Olfactory Nerve	.087	.200	.576
Ipsilateral Optic Nerve	.000	.200	.072
Ipsilateral Optic Tract *	.438	.200	.043
(log) Contralateral Optic Nerve ^	.060	.006	.624
Ipsilateral A1	.162	.064	.705
Angles of Attack:			
Ipsilateral Paraclinoid ICA CC	.000	.055	.601
Ipsilateral Paraclinoid ICA ML	.000	.200	.758
Ipsilateral Terminal ICA CC *	.508	.068	.003
Terminal ICA ML	.004	.200	.082
ACoA CC	.191	.080	.628
(log) ACoA ML ^	.439	.013	.297
Volumes of Surgical Freedom:			
Ipsilateral Paraclinoid ICA NU *	.549	.200	.000
Terminal ICA ML *	.705	.200	.001
ACoA NU	.011	.200	.501

Means = ANOVA;
* Model fails the assumption of equal variances. Kruskal-Wallis test p-values reported.
^ Model residuals fail the assumption of normality test and variable is transformed to natural log.

Illustrative Q-Qnorm plot

Ipsilateral Approach Frontal Lobe Area:

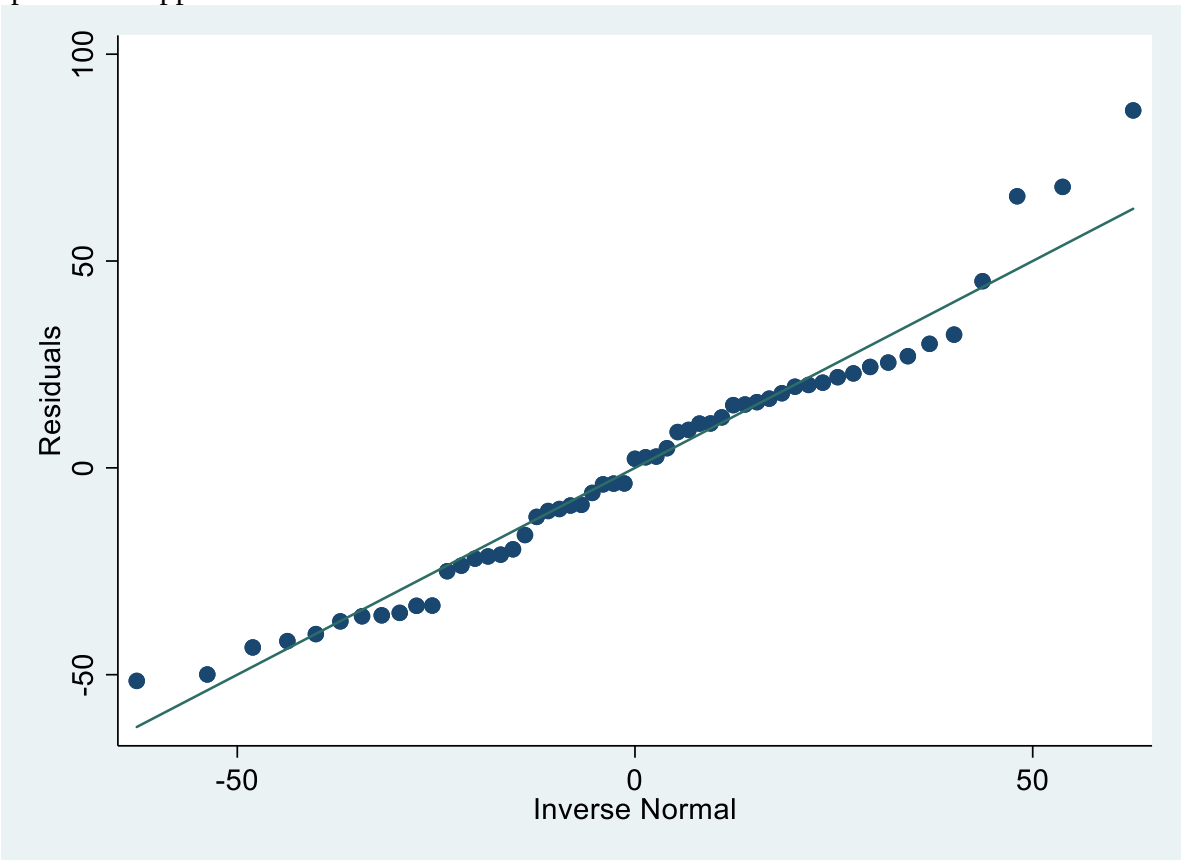

Table 3. Proportion of Not Accessible Areas by Category and Approach Type

	All	Supraorbital	Transorbital Microscopic	Transorbital Endoscopic
Approach Lengths:				
Ipsilateral Olfactory Nerve	0%	0%	0%	0%
Ipsilateral Optic Nerve	0%	0%	0%	0%
Ipsilateral Optic Tract	1.6%	0%	0%	5%
Contralateral Optic Nerve	20%	0%	25%	35%
Ipsilateral A1	10%	0%	15%	15%
Angles of Attack:				
Ipsilateral Paraclinoid ICA CC	1.6%	0%	0%	5%
Ipsilateral Paraclinoid ICA ML	1.6%	0%	0%	5%
Ipsilateral Terminal ICA CC	10%	0%	15%	15%
Terminal ICA ML	10%	0%	15%	15%
ACoA CC	46.7%	0%	65%	75%
ACoA ML	46.7%	0%	65%	75%
Volumes of Surgical Freedom:				
Ipsilateral Paraclinoid ICA NU	1.6%	0%	0	5%
Terminal ICA ML	10%	0%	15%	15%
ACoA NU	46.7%	0%	65%	75%

Results of multivariate analysis comparing the supraorbital approach to the transorbital approaches

Regression specifics follow:

Model 1

	Coefficient	95% Confidence Interval	*p*-value
Model 1: Predicting Angle of attack ipsilateral paraclinoid ICA CC			
Supraorbital dummy	3.84	2.17 – 5.5	.000
Female	.78	-.87 – 2.42	.345
Ln Age	2.97	-5.5 – 11.5	.700
Ipsilateral Approach Frontal Lobe Area	-.002	-.006 - 0	.141
Approach Planum Sphenoidale	.019	-.007 - .046	.149
R-squared	.370		

n=54.

Model 2

	Coefficient	95% Confidence Interval	*p*-value
Model 2: Predicting Angle of attack ipsilateral paraclinoid ICA ML			
Supraorbital dummy	5.74	2.79 – 8.69	.000
Female	1.35	-1.54 – 4.25	.354
Ln Age	-5.28	-20.25 – 9.69	.482
Ipsilateral Approach Frontal Lobe Area	.000	-.005 - .006	.907
Approach Planum Sphenoidale	.022	-.024 - .068	.346
R-squared	..307		

n=54.

Model 3

	Coefficient	95% Confidence Interval	*p*-value
Model 3: Predicting Volume of surgical freedom ipsilateral Paraclinoid ICA NU			
Supraorbital dummy	11.17	7.5 – 14.83	.000
Female	2.4	-1.19 – 5.99	.186
Ln Age	-1.29	-19.86 – 17.26	.889
Ipsilateral Approach Frontal Lobe Area	.003	-.004 - .01	.365
Approach Planum Sphenoidale	.097	.04 - .16	.001

R-squared	.588

n=54.

Model 4

	Coefficient	95% Confidence Interval	*p*-value
Model 4: Predicting Angle of attack ipsilateral terminal ICA CC			
Supraorbital dummy	1.42	-.300 – 3.14	.103
Female	-.083	-1.74 – 1.57	.919
Ln Age	4.89	-4.57 – 14.36	.302
Ipsilateral Approach Frontal Lobe Area	-.001	-.004 - .002	.544
Approach Planum Sphenoidale	.019	-.009 - .048	.182
R-squared	.139		

n=49.

Model 5

	Coefficient	95% Confidence Interval	*p*-value
Model 5: Predicting Angle of attack terminal ICA ML			
Supraorbital dummy	3.14	.80 – 5.48	.010
Female	1.51	-.74 – 3.78	.182
Ln Age	5.9	-6.97 – 18.78	.36
Ipsilateral Approach Frontal Lobe Area	.001	-.003 - .006	.509
Approach Planum Sphenoidale	-.01	-.049 - .028	.584
R-squared	.189		

n=49.

Model 6

	Coefficient	95% Confidence Interval	*p*-value
Model 6: Predicting Volume of surgical freedom terminal ICA NU			
Supraorbital dummy	3.38	-.249 – 7.01	.067
Female	.63	-2.8 – 4.07	.716
Ln Age	4.08	-17.97 – 26.13	.711
Ipsilateral Approach Frontal Lobe Area	-.002	-.008 - .003	.300
Approach Planum Sphenoidale	.056	-.037 - .15	.234
R-squared	.192		

n=49.

Model 7

	Coefficient	95% Confidence Interval	*p*-value
Model 7: Predicting Volume of surgical freedom ACoA NU			
Supraorbital dummy	5.34	1.22 – 9.45	.013
Female	-2.09	-6.37 – 2.18	.323
Ln Age	3.11	-18.26 – 24.48	.767
Ipsilateral Approach Frontal Lobe Area	-.003	-.012 - .004	.313
Approach Planum Sphenoidale	.054	-.009 - .117	.089
R-squared	.298		

n=32.

Model 8

	Coefficient	95% Confidence Interval	*p*-value
Model 8: Predicting Length of ipsilateral optic nerve			
Supraorbital dummy	-.76	-3.04 – 1.53	.506
Female	-.85	-3.08-1.38	.446
Ln Age	-4.66	-16.26-6.94	.424
Ipsilateral Approach Frontal Lobe Area	.00	-.00-.01	.279
Approach Planum Sphenoidale	.03	-.01-.06	.162
R-squared	.078		

n=55.

Table 4. Medians and Interquartile ranges of Lengths, Volumes, and Angles by Transorbital Approach Type.

	All	Transorbital Microscopic	Transorbital Endoscopic
Sample Size	40 (100%)	20(33.3%)	20(33.3%)
Female	16 (40%)	8 (40%)	8 (40%)
Age at Death, Mean (SD)	78.8 (7.4)	78.8 (7.5)	78.8 (7.5)
Controls:			
Ipsilateral Approach Frontal Lobe Area	919.6 (747.9-1,032.4)	849.3 (690.4-1,005.4)	952.4 (818.7-1,058.7)
Approach Lengths:			
Ipsilateral Olfactory Nerve	17.2 (14.2-20.0)	15.1 (11.1-18.5)	18.6 (16.2-20.8)
Ipsilateral Optic Nerve	13.0 (11.0-17.2)	11.2 (10.0-12.6)	16.1 (13.2-20.2)
Ipsilateral Optic Tract	11.5 (9.4-13.3)	10.3 (8.6-12.9)	12.4 (10.1-14.0)
Contralateral Optic Nerve	7.8 (6.8-10.0)	7.7 (6.2-8.9)	8.5 (7.1-10.5)
Ipsilateral A1	16.1 (12.6-17.0)	15.8 (12.0-16.5)	16.5 (13.6-17.3)
Angles of Attack:			
Ipsilateral Paraclinoid ICA CC	6.7 (5.3-8.3)	7.3 (6.1-9.0)	6.4 (4.2-7.1)
Ipsilateral Paraclinoid ICA ML	20.0 (17.0-22.7)	21.0 (17.8-24.3)	17.9 (16.3-20.9)
Ipsilateral Terminal ICA CC	8.6 (6.8-10.1)	9.2 (8.6-10.3)	7.3 (6.5-9.5)
Terminal ICA ML	22.9 (19.8-25.7)	23.4 (22.5-25.7)	20.0 (17.8-24.6)
ACoA CC	7.9 (6.6-10.0)	8.3 (7.9-10.1)	6.8 (6.5-7.5)
ACoA ML	20.6 (17.1-24.4)	24.3 (19.2-26.9)	17.7 (16.6-19.6)
Volumes of Surgical Freedom:			
Ipsilateral Paraclinoid ICA NU	9.6 (7.6-14.3)	11.2 (8.4-18.9)	8.8 (6.5-10.2)
Terminal ICA NU	13.4 (9.0-16.1)	15.2 (13.8-18.1)	10.5 (7.8-14.9)
ACoA NU	11.4 (7.1-13.9)	12.3 (11.0-15.4)	6.4 (6.3-7.9)

Table 5. Results of Univariate Analyses comparing Transorbital Microscopic Approach to the Transorbital Endoscopic Approach.

	Mann-Whitney U test *p*-value	**Equality of Variance *p*-value**
Controls:		
Ipsilateral Approach Frontal Lobe Area	.137	.055
Lengths:		
Ipsilateral Olfactory Nerve	.011	.406
Ipsilateral Optic Nerve	.000	.107
Ipsilateral Optic Tract	.019	.991
Contralateral Optic Nerve	.475	.326
Angles of Attack:		
Ipsilateral Paraclinoid ICA CC	.062	.933
Ipsilateral Paraclinoid ICA ML	.031	.537
Ipsilateral Terminal ICA CC *	.048	.002
Terminal ICA ML *	.082	.032
ACoA CC	.122	.391
ACoA ML	.088	.139
Volumes of Surgical Freedom:		
Ipsilateral Paraclinoid ICA NU	.017	.061
Terminal ICA NU	.008	.160
ACOM NU	.028	.620

* Violates the assumption of equal variances.

Results of multivariate analysis comparing the transorbital microscopic and transorbital endoscopic approaches

Regression specifics follow:

Model 1

	Coefficient	95% Confidence Interval	*p*-value
Model 1: Predicting Length of the ipsilateral olfactory nerve			
Transorbital microscopic dummy	-3.67	-6.8 - -.45	.027
Female	.09	-3.1 – 3.3	.952
Ln Age	11.1	-6.1 – 28.3	.196
Ipsilateral Approach Frontal Lobe Area	-.00	-.01 - .00	.448
Approach Planum Sphenoidale	-.02	-.08 - .04	.509
R-squared	.370		

n=35.

Model 2

	Coefficient	95% Confidence Interval	*p*-value
Model 2: Predicting Length of the ipsilateral optic nerve			
Transorbital microscopic dummy	-4.78	-7.6 - -2.0	.002
Female	-.36	-3.2 – 2.4	.798
Ln Age	1.72	-13.4 – 16.8	.818
Ipsilateral Approach Frontal Lobe Area	.00	-.01 - .01	.779
Approach Planum Sphenoidale	.03	-.03 - .08	.336
R-squared	.354		

n=35.

Model 3

	Coefficient	95% Confidence Interval	*p*-value
Model 3: Predicting Length of the ipsilateral optic tract			
Transorbital microscopic dummy	-1.1	-2.8 - .7	.207
Female	-.40	-2.2 – 1.3	.641
Ln Age	6.7	-2.5 – 16.0	.146

Ipsilateral Approach Frontal Lobe Area	.00	-.00 - .01	.107
Approach Planum Sphenoidale	-.02	-.05 - .02	.279
R-squared	.288		

n=34.

Model 4

	Coefficient	95% Confidence Interval	*p*-value
Model 4: Predicting angle of attack ipsilateral Paraclinoid ICA ML			
Transorbital microscopic dummy	3.95	.62 – 7.3	.022
Female	-.98	-4.3 – 2.4	.557
Ln Age	-12.4	-30.2 – 5.4	.165
Ipsilateral Approach Frontal Lobe Area	.00	-.00 - .01	.253
Approach Planum Sphenoidale	.03	-.03 - .10	.299
R-squared	.239		

n=34.

Model 5

	Coefficient	95% Confidence Interval	*p*-value
Model 5: Predicting angle of attack ipsilateral terminal ICA CC			
Transorbital microscopic dummy	.50	-1.4 – 2.4	.592
Female	-.53	-2.4 – 1.3	.565
Ln Age	8.5	-3.4 – 20.4	.156
Ipsilateral Approach Frontal Lobe Area	-.00	-.01 - .00	.279
Approach Planum Sphenoidale	-.00	-.05 - .03	.668
R-squared	.174		

n=29.

Model 6

	Coefficient	95% Confidence Interval	*p*-value
Model 6: Predicting volume of surgical freedom ipsilateral Paraclinoid ICA NU			
Transorbital microscopic dummy	3.54	.16 – 6.9	.041
Female	.10	-3.3 – 3.5	.951

Ln Age	-7.96	-26.1 – 10.1	.375
Ipsilateral Approach Frontal Lobe Area	-.00	-.01 - .01	.617
Approach Planum Sphenoidale	.05	-.01 - .12	.105
R-squared	.252		

n=34.

Model 7

	Coefficient	95% Confidence Interval	*p*-value
Model 7: Predicting volume of surgical freedom terminal ICA NU			
Transorbital microscopic dummy	4.05	.99 – 7.11	.012
Female	.55	-2.4 – 3.6	.712
Ln Age	-2.64	-22.7 – 17.5	.789
Ipsilateral Approach Frontal Lobe Area	-.00	-.01 - .01	.754
Approach Planum Sphenoidale	.01	-.05 - .08	.733
R-squared	.283		

n=29.

APPENDIX E

CHAPTER 7 DETAILED STATISTICAL ANALYSIS

Table 1. Means and Standard Deviations of Lengths, Areas of Exposure, Angles, and Volumes of Surgical Approach by Approach Type

	All	Bilateral subfrontal Craniotomy	Bilateral Transorbital Microscopic	Bilateral Transorbital Endoscopic
Sample Size	30 (100%)	10(33.3%)	10(33.3%)	10(33.3%)
Female	12 (40%)	8 (40%)	8 (40%)	8 (40%)
Age at Death (Mean, SD)	78.8 (7.4)	78.8 (7.4)	78.8 (7.4)	78.8 (7.4)
Lengths:				
Right olfactory nerve	19.0 (16.7–23.2)	23.3 (18.0-30.1)	16.3 (12.2-19.6)	19.0 (16.7-22.6)
Left olfactory nerve	17.0 (14.0-20.3)	17.8 (15.7-25.5)	14.6 (10.9-17.3)	18.0 (13.8-20.3)
Right optic nerve	13.2 (11.1-15.1)	13.8 (12.8-15.7)	11.2 (10.3-11.4)	14.6 (13.0-19.2)
Left optic nerve	13.1 (11.5-17.9)	12.8 (11.9-15.7)	11.6 (9.2-13.0)	17.5 (13.4-20.9)
Right optic tract	11.2 (9.4-13.4)	11.2 (9.9-14.5)	9.8 (8.4-13.0)	13.3 (10.1-13.6)
Left optic tract	11.9 (9.7-13.2)	12.2 (9.4-13.1)	10.9 (8.8-12.7)	12.0 (10.5-14.0)
Right A1	16.0 (13.6-19.4)	18.7 (15.2-20.1)	15.0 (11.8-16.0)	15.7 (12.2-18.2)
Left A1	16.3 (14.6-17.1)	15.7 (14.7-16.6)	16.3 (15.2-16.8)	16.5 (14.4-17.3)
Areas of Exposure:				
Intradural right cortical (Mean, SD)	857.0 (189.0)	813.5 (186.1)	890.1 (243.1)	867.5 (134.1)
Intradural left cortical	917.2 (770.5-1,020.2)	900.0 (795.9-932.9)	793.9 (686.0-915.88)	1,032.4 (971.8-1,101.4)

Total frontal cortical	1,763.3 (1,528.4-2,010.9)	1,648.4 (1,516.6-1,958.8)	1,658.9 (1,274.6-1,988.2)	1,914.9 (1,834.2-2,014.2)
Angles of Attack:				
Right paraclinoid ICA CC	7.6 (6.5-11.1)	11.3 (9.2-14.1)	6.8 (5.3-8.7)	6.5 (4.4-7.2)
Right paraclinoid ICA ML	20.1 (17.1-25.1)	28.3 (25.0-31.1)	20.0 (17.0-23.6)	17.1 (14.7-17.9)
Left paraclinoid ICA CC	8.2 (6.4-11.1)	11.5 (9.5-14.4)	7.9 (6.6-10.3)	5.8 (4.2-6.7)
Left paraclinoid ICA ML	22.4 (20.2-30.9)	31.2 (27.9-34.3)	22.4 (20.0-29.0)	20.3 (17.5-21.6)
Right terminal ICA CC	8.5 (6.7-9.6)	7.8 (5.4-8.4)	9.0 (7.7-9.4)	9.1 (6.9-12.1)
Right terminal ICA ML	22.0 (18.6-25.6)	22.6 (20.4-25.6)	22.9 (21.8-24.6)	17.9 (16.5-22.5)
Left terminal ICA CC	8.0 (7.1-10.3)	8.0 (7.5-10.5)	10.3 (8.6-10.6)	6.8 (5.5-7.4)
Left terminal ICA ML	23.9 (20.9-27.0)	26.0 (20.9-31.1)	23.8 (23.4-25.7)	21.8 (20.0-24.6)
ACoA CC	8.2 (7.5-11.6)	10.9 (8.0-14.2)	8.3 (7.9-10.1)	7.1 (5.3-9.4)
ACoA ML	24.5 (19.7-28.4)	29.4 (24.8-30.3)	24.3 (19.2-26.9)	18.6 (17.1-20.6)
Volumes of Surgical Freedom:				
Right paraclinoid ICA	12.7 (9.0-20.2)	21.5 (15.1-29.5)	12.7 (9.0-18.7)	8.8 (4.1-10.1)
Left paraclinoid ICA	12.0 (8.3-22.3)	25.9 (21.7-36.7)	11.2 (8.2-19.4)	8.8 (7.2-10.2)
Left terminal ICA	14.9 (11.0-18.4)	14.2 (10.5-20.6)	16.5 (16.1-18.6)	11.7 (7.0-13.4)
Right terminal ICA	13.5 (8.2-15.6)	12.5 (8.2-16.6)	14.1 (12.9-15.2)	9.4 (7.9-15.3)
ACoA	12.5 (9.6-22.0)	22.0 (11.1-27.5)	12.3 (11.0-15.4)	7.1 (4.7-10.2)

SD = Standard Deviation.

Testing the assumptions of normality and equal variance

The assumption of normality among the residuals of the ANOVA models is met for all but four of the variables as evidenced by the Shapiro-Wilk tests. These variables were log-transformed for inclusion in the ANOVA model.

The assumption of equality of variance among the ANOVA models is met for all models except for four models. For these four models, the test for differences among approaches was tested with a Kruskal-Wallis test.

Table 2. Results of Univariate Analyses comparing all Approaches.

	ANOVA or Kruskal-Wallis *p*-value	**Shapiro-Wilk *p*-value**	**Equality of Variance *p*-value**
Lengths:			
Right olfactory nerve	.003	.292	.454
Left olfactory nerve	.029	.496	.118
Right optic nerve *	.465	.571	.007
Left optic nerve	.011	.393	.638
Right optic tract	.263	.222	.084
Left optic tract	.294	.634	.950
Right A1	.034	.466	.447
Left A1 *	.445	.361	.014
Areas of Exposure:			
Intradural right cortical	.664	.658	.234
Intradural left cortical	.042	.147	.070
Total frontal cortical	.276	.357	.100
Angles of Attack:			
Right paraclinoid ICA CC	.003	.150	.892
Right paraclinoid ICA ML	.000	.831	.710
Left paraclinoid ICA CC	.000	.303	.931
Left paraclinoid ICA ML	.000	.895	.399
Right terminal ICA CC *	.462	.304	.025
Right terminal ICA ML	.165	.303	.173
Left terminal ICA CC	.005	.720	.291
Left terminal ICA ML	.234	.274	.133
(log) ACoA CC ^	.110	.001	.102
ACoA ML	.011	.205	.323
Volumes of Surgical Freedom:			
Right paraclinoid ICA	.000	.592	.317
Left paraclinoid ICA *	.465	.280	.003
Left terminal ICA	.075	.586	.057
(log) Right terminal ICA ^	.418	.008	.227
(log) ACoA ^	.015	.006	.236

Means = ANOVA;
* Model fails the assumption of equal variances. Kruskal-Wallis test p-values reported.
^ Model residuals fail the assumption of normality test and variable is transformed to natural log.

Example of Q-Q norm plot for assessment of normality

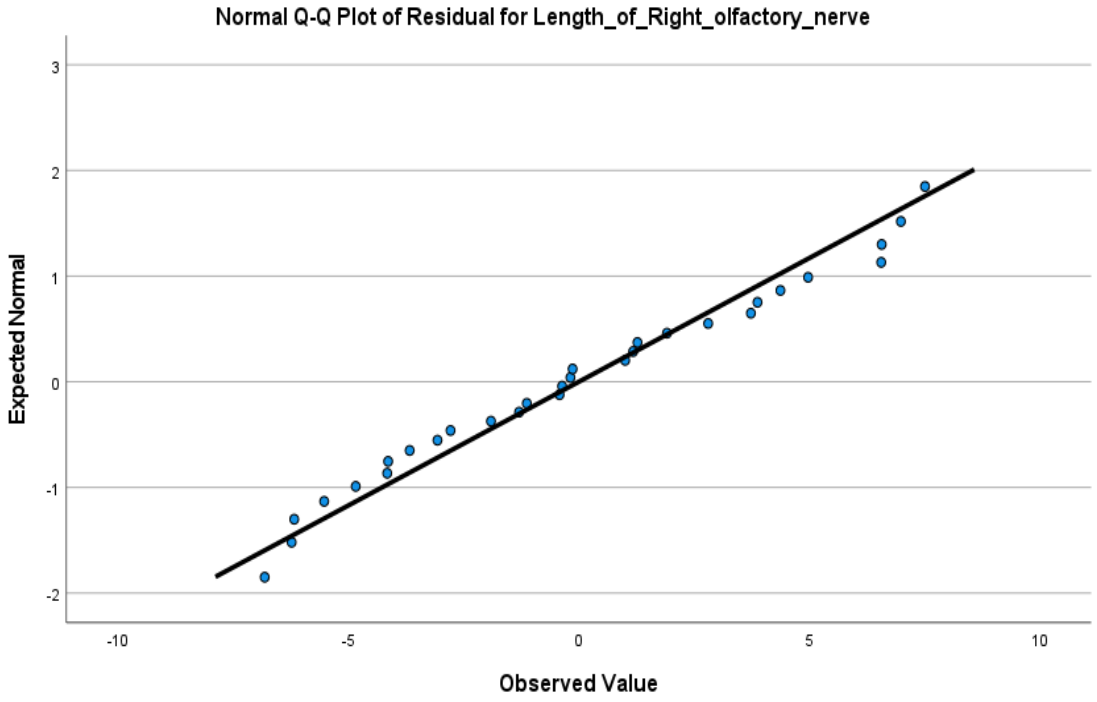

Table 3. Proportion of Missing Data by Category and Approach Type

	All (n=30)	Bilateral subfrontal Craniotomy (n=10)	Bilateral Transorbital Microscopic (n=10)	Bilateral Transorbital Endoscopic (n=10)
Lengths:				
Right olfactory nerve	0%	0%	0%	0%
Left olfactory nerve	0%	0%	0%	0%
Right optic nerve	0%	0%	0%	0%
Left optic nerve	0%	0%	0%	0%
Right optic tract	3%	0%	0%	10%
Left optic tract	0%	0%	0%	0%
Right A1	13%	0%	20%	20%
Left A1	7%	0%	10%	10%
Areas of Exposure:				
Intradural right cortical	0%	0%	0%	0%
Intradural left cortical	0%	0%	0%	0%
Total frontal cortical	0%	0%	0%	0%
Angles of Attack:				
Right paraclinoid ICA CC	3%	0%	0%	10%
Right paraclinoid ICA ML	3%	0%	0%	10%
Left paraclinoid ICA CC	0%	0%	0%	0%
Left paraclinoid ICA ML	0%	0%	0%	0%
Right terminal ICA CC	13%	0%	20%	20%
Right terminal ICA ML	13%	0%	20%	20%
Left terminal ICA CC	7%	0%	10%	10%
Left terminal ICA ML	7%	0%	10%	10%
ACoA CC	33%	10%	30%	60%
ACoA ML	33%	10%	30%	60%
Volumes of Surgical Freedom:				
Right paraclinoid ICA	3%	0%	0%	10%
Left paraclinoid ICA	0%	0%	0%	0%
Left terminal ICA	7%	0%	10%	10%
Right terminal ICA	13%	0%	20%	20%
ACoA	33%	10%	30%	60%

Results of multivariate analysis comparing the anterior subfrontal/bilateral subfrontal approach to the transorbital approaches

Regression specifics follow:

Model 1

	Coefficient	95% Confidence Interval	*p*-value
Model 1: Predicting Length of right olfactory nerve			
Bilateral transorbital microscopic dummy	-7.64	-11.69 - -3.59	.001
Bilateral transorbital endoscopic dummy	-3.78	-7.83 - .276	.067
Female	-.59	-4.05 – 2.85	.725
Ln Age	11.84	-5.94 – 29.61	.182
R-squared	.316		

n=30.

Model 2

	Coefficient	95% Confidence Interval	*p*-value
Model 2: Predicting Length of left olfactory nerve			
Bilateral transorbital microscopic dummy	-7.02	-12.11 - -1.93	.009
Bilateral transorbital endoscopic dummy	-4.58	-9.67 - .51	.076
Female	-2.00	-6.34 – 2.33	.350
Ln Age	12.76	-9.57 – 35.08	.250
R-squared	.199		

n=30.

Model 3

	Coefficient	95% Confidence Interval	*p*-value
Model 3: Predicting Length of right A1			
Bilateral transorbital microscopic dummy	-4.45	-7.43 - -1.47	.005

Bilateral transorbital endoscopic dummy	-3.47	-6.46 - -.49	.025
Female	-.93	-3.47 – 1.60	.453
Ln Age	20.18	5.93 – 34.44	.008
R-squared	.384		

n=26.

Model 4

	Coefficient	95% Confidence Interval	*p*-value
Model 4: Predicting angle of attack targeting right paraclinoid ICA CC			
Bilateral transorbital microscopic dummy	-4.05	-6.64 - -1.46	.004
Bilateral transorbital endoscopic dummy	-4.69	-7.36 - -2.03	.001
Female	.77	-1.47 – 3.01	.484
Ln Age	9.60	-1.81 – 21.01	.095
R-squared	.345		

n=29.

Model 5

	Coefficient	95% Confidence Interval	*p*-value
Model 5: Predicting angle of attack targeting right paraclinoid ICA ML			
Bilateral transorbital microscopic dummy	-7.69	-11.73 - -3.52	.001
Bilateral transorbital endoscopic dummy	-11.98	-16.20 - -7.76	.000
Female	1.93	-1.61 – 5.48	.272
Ln Age	8.16	-9.93 – 26.25	.361
R-squared	.540		

n=29.

Model 6

	Coefficient	95% Confidence Interval	*p*-value
Model 6: Predicting angle of attack targeting left paraclinoid ICA CC			
Bilateral transorbital microscopic dummy	-3.65	-6.11 - -1.19	.005
Bilateral transorbital endoscopic dummy	-5.94	-8.39 - -3.47	.000
Female	.17	-1.92 – 2.27	.865
Ln Age	4.71	-6.09 – 15.51	.378
R-squared	.430		

n=30.

Model 7

	Coefficient	95% Confidence Interval	*p*-value
Model 7: Predicting angle of attack targeting left paraclinoid ICA ML			
Bilateral transorbital microscopic dummy	-8.12	-12.63 - -3.61	.001
Bilateral transorbital endoscopic dummy	-12.03	-16.54 - -7.53	.000
Female	.03	-3.80 – 3.87	.986
Ln Age	-.91	-20.69 – 18.86	.925
R-squared	.486		

n=30.

Model 8

	Coefficient	95% Confidence Interval	*p*-value
Model 8: Predicting angle of attack targeting left terminal ICA CC			
Bilateral transorbital microscopic dummy	.73	-1.19 – 2.65	.439
Bilateral transorbital endoscopic dummy	-2.56	-4.47 - -.63	.011
Female	.48	-1.17 – 2.12	.553

Ln Age	6.15	-2.81 – 15.11	.169
R-squared	.298		

n=28.

Model 9

	Coefficient	95% Confidence Interval	*p*-value
Model 9: Predicting angle of attack targeting ACoA ML			
Bilateral transorbital microscopic dummy	-5.08	-10.34 - .17	.057
Bilateral transorbital endoscopic dummy	-8.62	-14.90 - -2.34	.010
Female	2.05	-2.99 – 7.09	.401
Ln Age	-2.37	-27.37 – 22.63	.842
R-squared	.299		

n=20.

Model 10

	Coefficient	95% Confidence Interval	*p*-value
Model 10: Predicting volume of right paraclinoid ICA			
Bilateral transorbital microscopic dummy	-8.71	-14.49 - -2.93	.005
Bilateral transorbital endoscopic dummy	-14.34	-20.28 - -8.39	.000
Female	1.52	-3.48 – 6.51	.537
Ln Age	-.49	-25.96 – 24.97	.968
R-squared	.436		

n=29.

Model 11

	Coefficient	95% Confidence Interval	*p*-value
Model 11: Predicting (log) volume ACoA			
Bilateral transorbital microscopic dummy	-.37	-.99 - .25	.227
Bilateral transorbital endoscopic dummy	-1.05	-1.79 - -.31	.009
Female	.16	-.43 - .76	.573
Ln Age	.40	-2.55 – 3.35	.777
R-squared	.246		

n=20.